AD NUMBER

AD-136 057

CLASSIFICATION CHANGES

TO **UNCLASSIFIED**

FROM **SECRET**

AUTHORITY

OCA; Aug 31, 1987

19990317077

BRASS BELL

ON[illegible]ISSANCE AIRCRAFT WEAPON SYSTEM

Bell Aerospace CORPORATION

REPORT NO. D143-945-055

FC

CONTRACT AF 18 (600)-1607
SUPPLEMENTAL AGREEMENT NO. 4

BRASS BELL

This document contains a Title Page, Frontispiece, pages i through viii, pages 1 through 130 and 16 separator pages.

PREPARED BY TECHNICAL PUBLICATIONS

31 AUGUST 1957

BELL Aircraft CORPORATION

SECRET

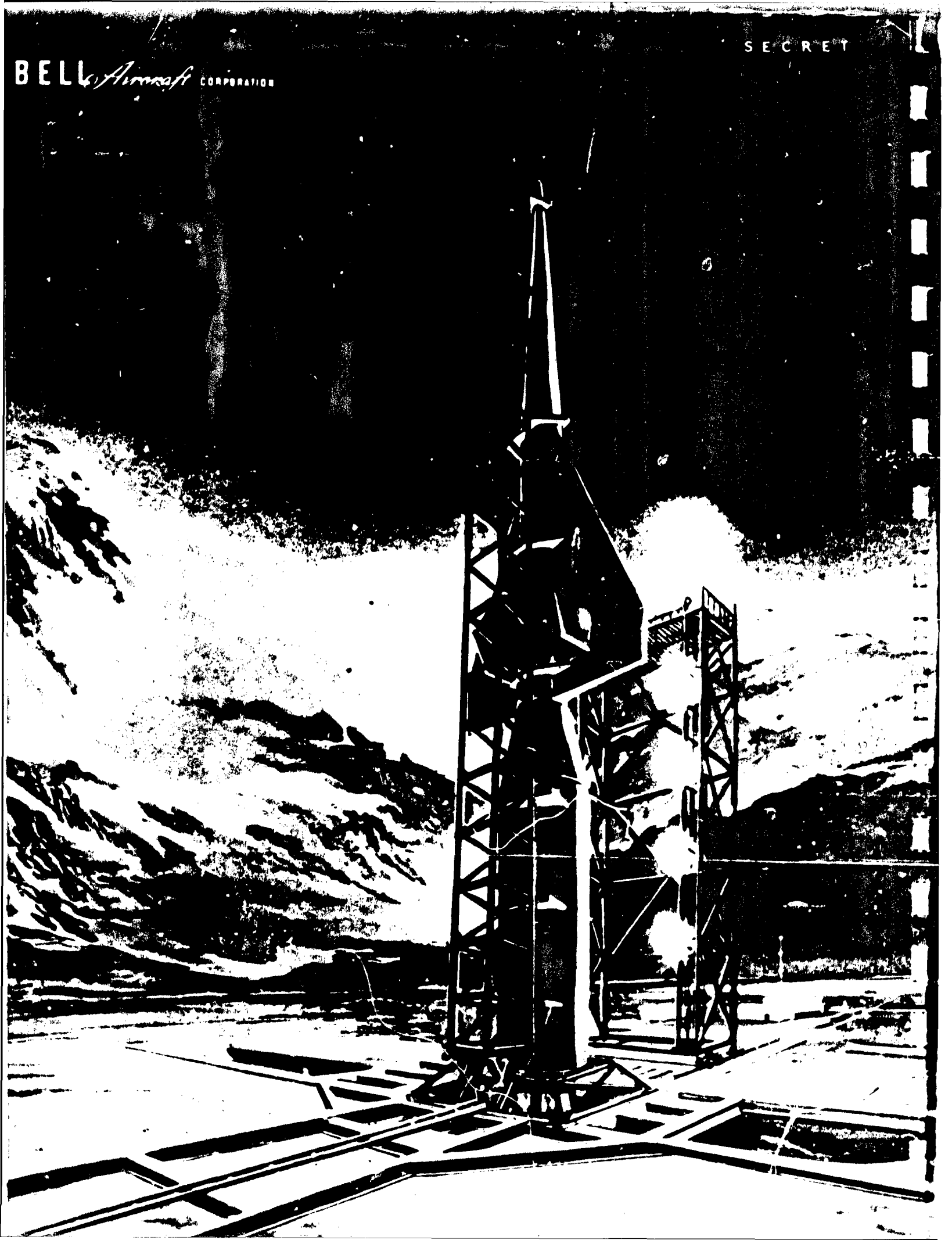

BELL

THE ATTACHED DOCUMENT CONTAINS

SECRET INFORMATION AND AS SUCH IT MUST BE

RECORDED—On a Classified Document Register and Marked with the assigned Bell Identification number when you originate, reproduce or receive a classified document See Bell Aircraft Corporation Security Manual

STORED—Minimum requirements call for a steel file cabinet equipped with a steel bar and three-position combination dial type padlock

TRANSMITTED—In double sealed opaque containers The classified information shall be protected from direct contact with the inner cover by a sheet or by folding inward Only the inner container shall indicate the classification Both the inner and outer cover shall indicate the addressee and addressor

By U S registered mail air or surface, by appropriately cleared messenger designated by the company or by protected commercial express, air or surface, under billing which assures the highest degree of protective handling

RECEIPTED FOR—Classified Document Receipt, Form G6-32, must be enclosed within the inner wrapper for all SECRET matter dispatched outside Bell Aircraft Corporation Niagara Frontier Division facilities Hand Receipt, Form G6-42, must be used for all transmittals of SECRET matter between individuals or by company mail service within Bell Aircraft Corporation Niagara Frontier Division facilities

ADDITIONAL SECURITY INFORMATION

(1) Bound documents—Classified books or pamphlets, the pages of which are permanently and securely bound together so that the pages thereof cannot be removed without damage or mutilation, shall be marked with the classification assigned to the document at the top and bottom on the outside of the front cover and back cover, title, first and last pages and all printed, typed or written pages which contain classified information, including the reverse side, if used

(2) Correspondence and unbound documents—Correspondence and other documentary material not permanently and securely bound together shall be marked with the appropriate classification at the top and bottom of each page which contains classified information, including the cover page, if used The marking shall be placed so that it will not be hidden from view when the pages are clipped or stapled together

(3) Letters of Transmittal—A letter transmitting defense information shall be marked with a classification at least as high as the highest classified enclosure Letters of Transmittal, when appropriate, shall indicate that upon removal of classified enclosures such letters will be downgraded or declassified

(4) National Defense Stamp—Documents containing classified defense information furnished authorized persons other than those in or in the employ of, agencies of the Department of Defense shall bear a notation substantially as follows "

This document contains information affecting the national defense of the United States, within the meaning of the Espionage Laws Title 18, U S C, Sections 793 and 794, the transmission or revelation of which in any manner to an unauthorized person is prohibited by law "

(5) "Restricted Data"—In addition to the markings prescribed above "Restricted Data" will be marked in capital letters, Restricted Data—Atomic Energy 1954" not less than 1/4 inch in height

FOREWORD

During the period from 22 March 1956 to 30 September 1956 the Bell Aircraft Corporation conducted an investigation of a weapon system incorporating a manned, rocket-boosted, hypersonic glide, reconnaissance airplane under Air Force contract. Upon completion of this work, the contract was extended to 31 August 1957. This work has been performed under contract with the Intelligence and Reconnaissance Systems Division, RDZPI, Air Research and Development Command, Contract Number AF 18(600)-1607. The work extension was accomplished under Supplemental Agreement No. 4 (57-19) to this contract. The effort during this program has included design studies, system analyses, and test programs (with emphasis on the latter.)

The work accomplished under Supplemental Agreement No. 4 is reported in the following series of Bell Aircraft Corporation reports of which this report is a part:

Number	Title
D143-945-049	Aerodynamics
D143-945-050	Structures
D143-945-051	Flight Control
D143-945-052	Radar
D143-945-053	Photographic System
D143-945-054	Weapon System
D143-945-055	Summary Report

The results of the navigation system investigation which was subcontracted to the General Electric Company are reported in their report, R57 APS83, which is also a part of this series of reports.

In addition to these reports, a series of test data reports covering specific experiments conducted under this contract have also been prepared and are being submitted in accordance with the terms of the contract.

CONTENTS

CONTENTS (cont.)

CONTENTS (cont.)

CONTENTS (cont)

TABLES

ILLUSTRATIONS

ILLUSTRATIONS (cont.)

ILLUSTRATIONS (cont.)

I Abstract

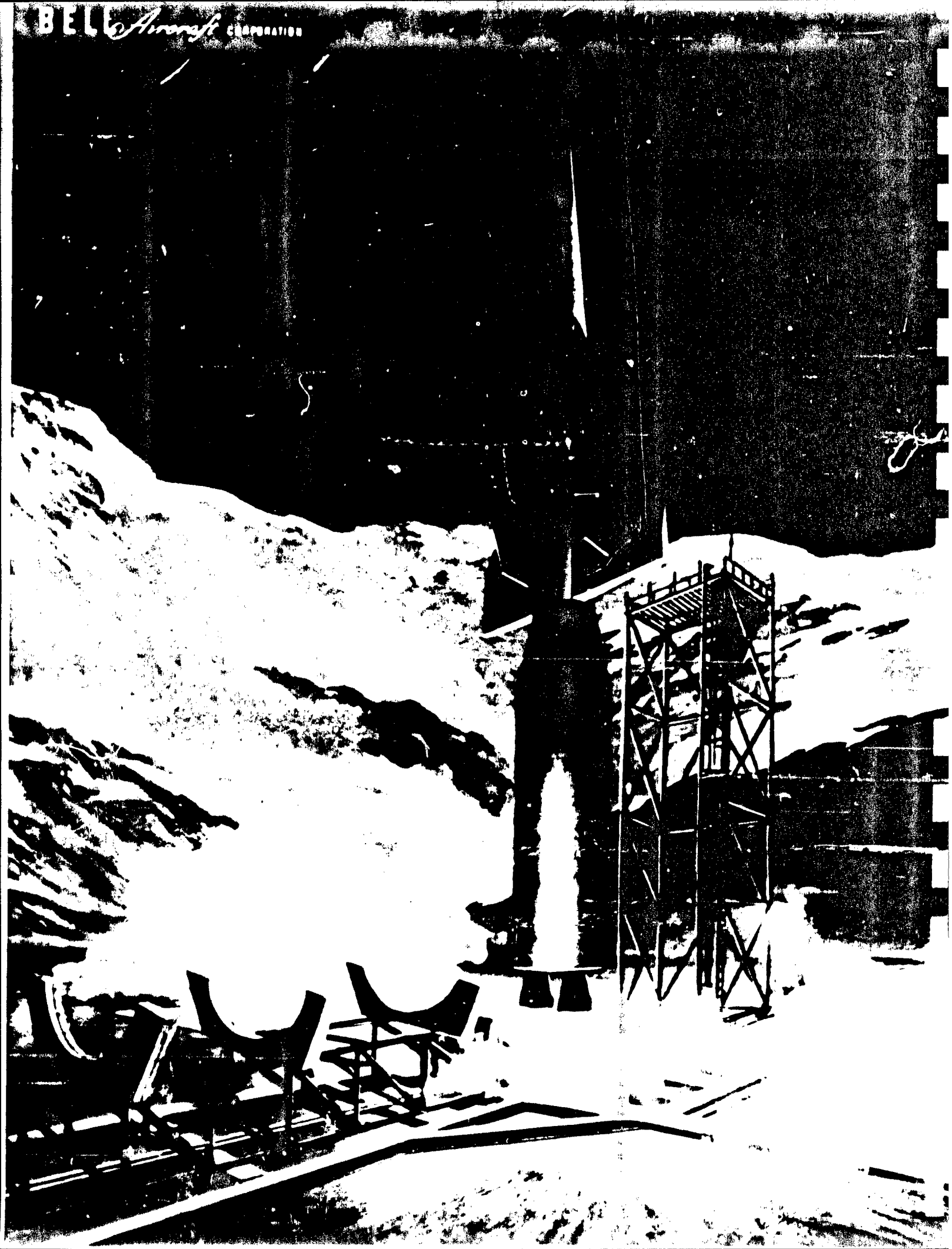
BELL Aircraft CORPORATION

This report summarizes the work accomplished in the design studies, system analyses, and test programs associated with the application of the rocket-boosted glide aircraft principle to a reconnaissance function. The latter function includes radar, ferret, and photographic capabilities. Two basic configurations utilizing two stages of boost are recommended for further study. One configuration consists of an expendable first-stage booster and a second stage which is a glide airplane containing the second-stage boost motors and tanks. The other configuration also consists of an expendable first-stage booster, but in this case the second boost stage (motors and tanks) is also expendable. The glide aircraft in this case is considerably smaller, since it does not have to carry these expendable components during cruise. Analyses of both liquid and solid propellant combinations have been conducted from both a cost and installation standpoint. Typical configurations using both types of propellants are presented. Other design areas considered include side-by-side crew seating, vertical fin size and location, and leading edge designs (cooled and heat-sustaining).

Structural design investigations have resulted in improved methods of double-wall panel construction, sealing, and attachment. The construction improvement includes design, structural materials, and insulation. Tests have been conducted which indicate the feasibility of this type of structure for thermal, load-carrying, and flutter considerations. Studies and tests with respect to "hot-spot" areas (nose and leading edge) indicate feasibility of both liquid-metal and heat-sustaining techniques. Preliminary studies of the use of pressurized hydrogen as a coolant for both these and the primary cooling areas indicate that further investigation is warranted.

Aerodynamic analyses and experimental programs which better define the environment resulting from high-speed and high-altitude flight have been conducted. The results of these programs are compared with existing theories and techniques used to compute Brass Bell parameters. In general, no major modifications of techniques used are necessary, and especially good correlation was obtained in the case of the heat transfer methods.

Studies of the navigation system indicate that the use of a radar altimeter for vertical channel instrumentation is both necessary and practical. The effects of cross-coupling between channels, which occurs when the true coordinate system and the coordinates indicated by the navigation system are not coincident, are shown to be negligible. The application of digital techniques to this system is shown to be satisfactory.

Reaction controls are shown to be unnecessary for the flight conditions encountered. The use of a constant angle of attack as a means of control for approximating the maximum glide range is recommended.

A multifrequency coherent Doppler system has been shown to be marginal for the radar reconnaissance of the required resolution. A number of other types of systems have been studied, and the design compromises necessary for obtaining the desired performance have been established.

It now appears that the ferret system capability can be extended down to the 100-megacycle frequency by modifying the systems previously proposed and providing additional antennas. Additional ferret capsules will not be required.

The desired photographic capabilities can be achieved, even for low-contrast objects, through the use of photographic emulsion techniques presently known and the use of focal

lengths compatible with the space available in the aircraft.

The advantages and problems associated with displaying the radar, map, and optical information on a single display medium are discussed.

Operational and ground support areas which involve unusual or significant developments are discussed. Depending upon the design adopted, these will include such areas as rocket test facilities, propellant manufacture and storage facilities, coolant manufacture and storage, and subsystem checkout facilities.

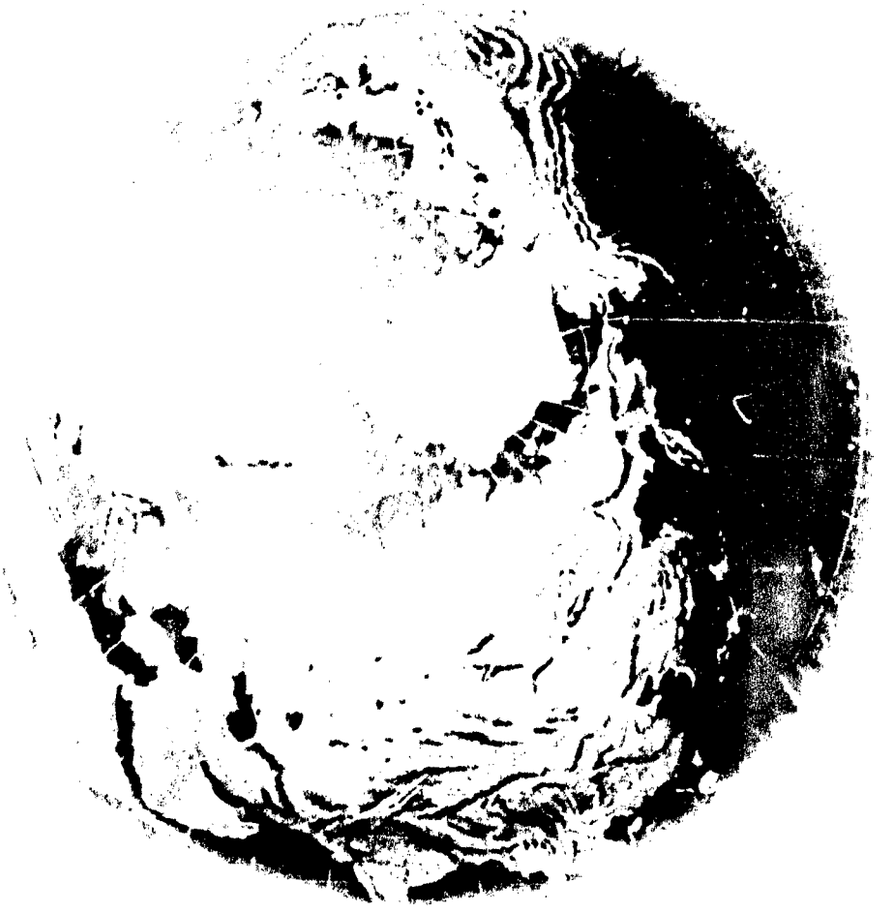

II Introduction

The feasibility of utilizing a manned, rocket-boosted, hypersonic, glide vehicle with intercontinental range to perform various military missions was explored by the Bell Aircraft Corporation as early as 1951. This work was expanded until, in April of 1954, a contract was negotiated with the Air Force under which Bell Aircraft was to conduct an analysis of the technical problems involved in the design of such a vehicle for use in a strategic bombardment/reconnaissance weapon system. As this contract neared completion, it was extended to include analytical investigations and design studies of a weapon system which adapted the rocket bomber concept either to satisfy or exceed the criteria for a reconnaissance weapon system as presented in Development Requirements, System No. 118P.

On the basis of the preceding studies which indicated the feasibility and reconnaissance value of an aircraft capable of such performance, Air Force Contract 18(600)-1607 was awarded to the Bell Aircraft Corporation. The objective of the work under this contract was to conduct design studies, system analyses, and test programs of such a vehicle for reconnaissance purposes.

Upon completion of the work required by the initial contract, the contract was extended by Supplemental Agreement No. 4. Under this agreement, the general objectives of the contract remained the same. The only major changes were in the capabilities desired of the reconnaissance sensors. The new capabilities are enumerated in Section III.

One of the major recommendations with respect to any future effort, which resulted from the work done initially under this contract stated, "The program should continue to emphasize the experimental aspects of the necessary investigations. Further verification of much of the theoretical work can be obtained only by means of experimental confirmation." This recommendation is the keynote to the work performed under Supplemental Agreement No. 4. The major effort was devoted to experimental work in the fields of structures and aerodynamics. Design study effort was limited to that required to guide and interpret work in other phases of the program. A relatively small amount of effort was devoted to the analysis of subsystems.

Many of the experimental programs were conducted in outside facilities, either under subcontract or in Government facilities using Government funds. In the latter cases, the only expense to the contract is the model. Wherever the experimental work has been completed, the results have been incorporated into the current series of reports. In some cases it was necessary to schedule tests beyond the original contract completion date because of facility scheduling and equipment procurement. The work accomplished on these tests will be reported upon completion of the tests.

The only subsystem study program subcontracted during the present phase of the contract concerned the Navigation System. This work, which was performed by the General Electric Company, was an extension of the work they had initiated during the previous study period.

Two types of reports have been prepared for submission in this series: general technical reports covering certain technical areas (as listed in the Foreword) and test data reports covering specific tests. All reports submitted are listed in Appendix I.

This report summarizes the work accomplished during this program period, and wherever possible indicates the effects of experimental results upon weapon system design. It also includes specific recommendations as to how future efforts may best be expended in the development of a hypersonic boost glide weapon system. Recommendations for future work are presented in detail in a program planning report (Reference 1) which was also prepared under this Contract.

III Weapon System Concept

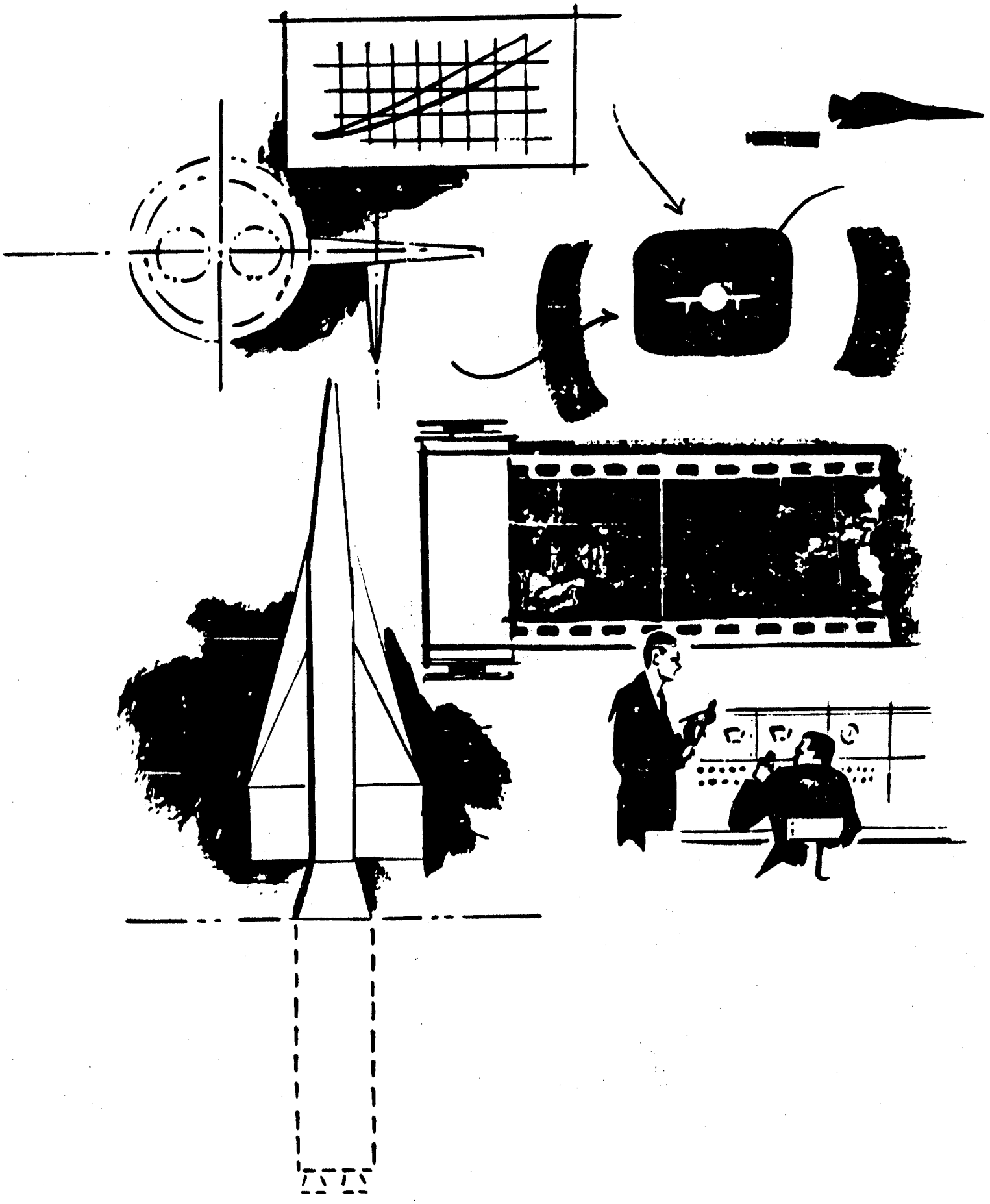

A. REQUIREMENTS

The military requirements of this reconnaissance aircraft weapon system, as defined in the contractual work statement, are as follows:

1. PERFORMANCE OBJECTIVES

a. The Air Force has a long-range requirement for a reconnaissance weapon system capable of intercontinental range. However, an urgent intermediate requirement exists for a vehicle with a minimum range of 5500 nautical miles.

b. Operational altitudes in excess of 100,000 feet at hypersonic flight speeds are required.

2. OPERATIONAL FEATURES

The system is desired to have the following operational capabilities:

a. Pioneer and surveillance reconnaissance consisting of the following:

(1) Photographic coverage, both search and detail targeting. Resolvable surface dimensions will be no greater than 20 feet and 5 feet respectively. Resolvable surface dimensions of one (1) foot are desirable. (These requirements have been interpreted as corresponding respectively to the "Terrain", "Operational" and "Technical" objective reconnaissance requirements of Reference 2.)

(2) Ferret surveillance from 1000 mc to 40,000 mc. Ferret surveillance from 100 mc to 1000 mc is desirable.

(3) Radar surveillance using high-resolution techniques. Resolvable ground dimensions will be no greater than 100 feet.

(4) Auxiliary data is to be recorded concurrently with the recording of basic reconnaissance data.

(5) A ground data handling system compatible with Project 438L.

b. The navigation accuracy shall be consistent with the needs of the reconnaissance subsystems.

B. SYSTEM DESCRIPTION

The Brass Bell weapon system concept centers about the use of a manned, hypersonic, glide vehicle which is rocket-boosted to the velocity (18,000 feet per second) and altitude (170,000 feet) necessary to obtain the required glide range (5500 nautical miles). The boost and cruise portions of the flight are shown in Figures 1 and 2, respectively. Although the design of a configuration has not been emphasized in this phase of the program, two typical configurations have been included in this report to illustrate the trends indicated by the results of this period of study. (Refer to Figures 3, 4, and 6.) Both liquid and solid-propellant rocket engines have been considered, and a typical configuration using each type of engine is presented. The liquid propellant configuration uses lox-JP-4 in the first stage and fluorine-ammonia in the second stage. The solid propellant configuration uses solid fuel in the first stage boost only and fluorine-ammonia in the second stage.

In addition to the propellant investigation, two different boosting configurations have been considered, one using two expendable booster stages, the other using a single expendable stage but retaining the second stage motor in the airplane. Both configurations shown here have two expendable stages. It is reiterated that the configurations shown are typical and do not constitute a recommendation at this time.

In order to provide control during the first stage of boost, the thrust nozzles are gimballed such that they can be deflected in the same direction for azimuth and longitudinal control and differentially for roll control. During the second

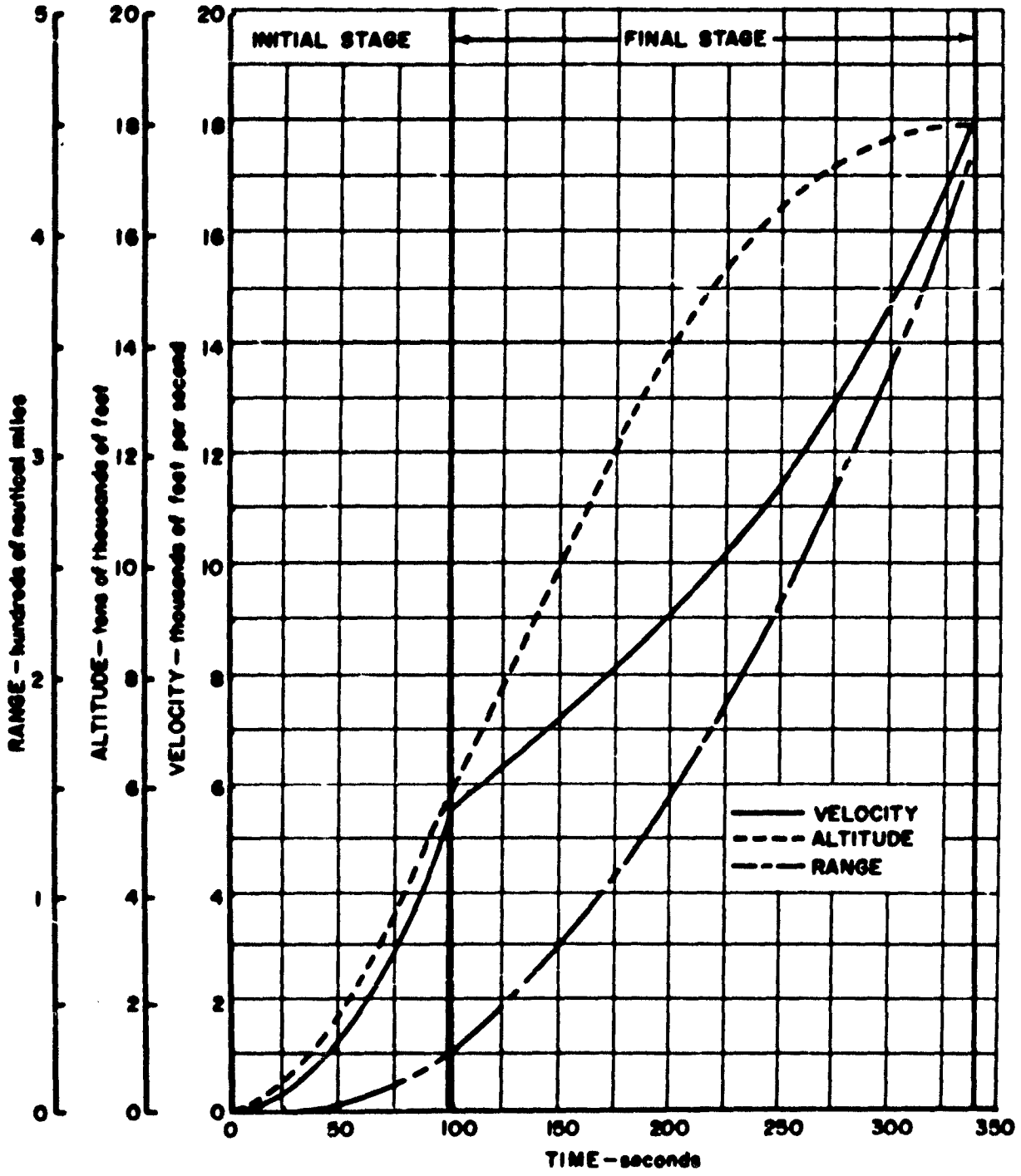

Figure 1. Typical Flight Profile – Boost Phase

stage of boost, control is also provided by gimballed thrust chambers for the configurations shown.

The vehicle is launched vertically, and, while vertical, is rolled into the correct azimuth angle. As it climbs along this azimuth, it is deflected through a programmed attitude sequence which provides zero attitude change at boost separation and places the airplane in the proper attitude for glide at maximum lift-to-drag ratio at the end of burning. During the

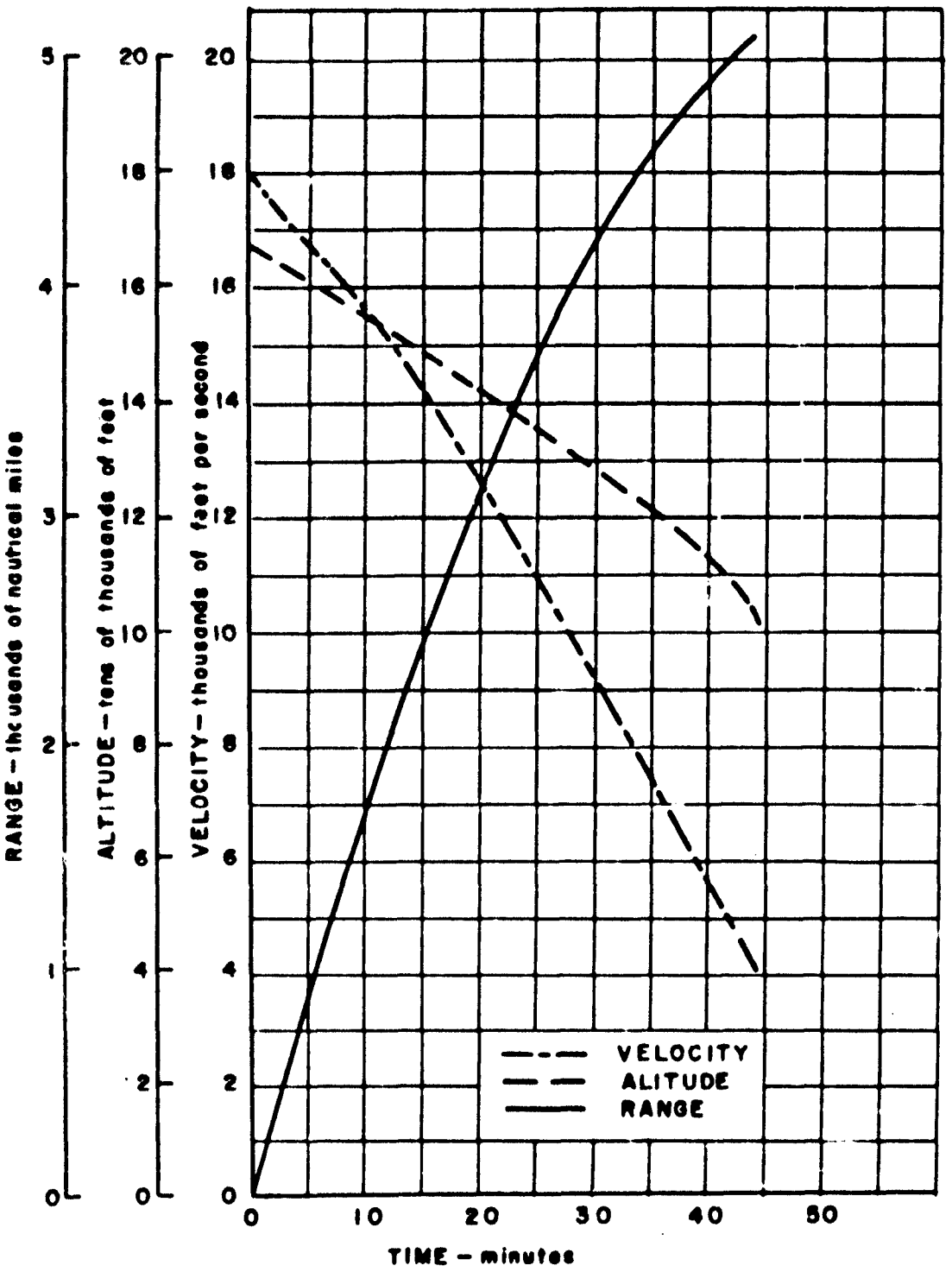

Figure 2. Typical Flight Profile – Glide Phase

first stage of boost, the attitude is programmed as a function of time; during the second stage of boost, it is programmed as a function of altitude.

Once the vehicle is at the proper angle of attack for maximum L/D (at the end of boost), it is maintained in this attitude throughout the flight. It is presently contemplated that this

attitude will be controlled by maintaining constant angle of attack which very closely approximates the maximum L/D condition.

The navigation system is designed around an inertial platform which provides the basic reference information. This navigation system utilizes an arbitrary coordinate system. The desired course is programmed into the navigation system with latitude as a function of longitude (in the system coordinates), and the vehicle is maintained on course automatically. The course followed is a straight line in space — hence, curved with respect to the earth. This path is previously computed and laid out in order that the vehicle will not have to bank during its flight to compensate for Coriolis forces. The flight path can include maneuvers if desired, either to reach specific areas of interest or to confuse any enemy attempt to predict the flight path for counteractivities.

The navigation system presently under study will have the capability of directing the vehicle to the desired area with an error in indicated position corresponding to a CEP of approximately 10,000 feet at a range of 5000 nautical miles. At all intermediate ranges, the error in indicated position will be less. To this error must be added any errors in the known location of the "target" area, since these errors will be incorporated into the flight path programmed into the navigation system prior to take-off. As a result of the new requirements for the capability of resolving a surface dimension of one foot, it may be necessary to increase the accuracy of the navigation system. The extreme focal length required to obtain this capability limits coverage of the camera involved to a very small area. Unless some technique such as the use of a large format is utilized, increased navigational accuracy will be required. This limitation has not yet been established; hence, the navigation system requirements stated above have been retained.

The weapon system will have provisions for three types of reconnaissance: ferret, photographic, and radar. Other reconnaissance systems are not required by the contract. However, the use of infrared and other electromagnetic systems (such as passive microwave) have been considered for use with this weapon system.

It is planned to utilize the reconnaissance radar as a means of navigational checking during normal flight and as a primary navigational aid in emergencies. Hence, it will be included on all flights. Only one of the other types of reconnaissance systems will be included on any specific flight, as their size precludes the use of more than one at a time. Three different photographic installations are required, i.e., one each for the terrain, operational, and technical objective data. Similarly, two ferret installations are required, one for radar order of battle and one for technical intelligence data. In all five cases, the size of the equipment involved dictates that only one set of equipment can be carried on any given flight. Hence, there are, in effect, five different sets of equipment which can be carried one at a time with the radar. The other types of reconnaissance equipment have been examined only with respect to feasibility and no installation estimates have been prepared.

The reconnaissance data will be recorded by the particular sensor involved. The navigational and other supplementary data required for interpretation of the reconnaissance data will be recorded on a central recorder which can be used with all the sensors. The tie-in with the reconnaissance data will be made by means of a time-index. All reconnaissance and recording equipment will be started, controlled, and stopped automatically in normal operation.

After completion of the data-gathering portion of the flight, the vehicle continues to glide on to the landing area. The system is designed such that the required range (5500 nautical miles) is achieved at the time the vehicle has decelerated to a velocity of 4000 feet per second and an altitude of approximately 100,000 feet. With this residual energy, the vehicle has the capability of flying approximately 300 miles if no turns are required or of reaching the landing site if it is within approximately 120 miles of either side of the vehicle's course and less than 150 miles ahead of the vehicle's

present position. Several types of ground equipment are available for landing aids. Systems which provide a maximum of aid with a minimum of airborne equipment are preferred.

After the vehicle has landed, the reconnaissance data are removed and fed into the 438L ground data processing equipment. The methods of airborne data recording have been coordinated with work underway on project 438L.

The vehicle itself must be picked up and loaded on a dolly for transportation either to the site for return flight, or to the equipment to transport it back to the original launching site.

The function of the crew throughout the flight is to perform the tasks which check progress of the flight or operation of the entire system, and either to supplement or take over for the automatic equipment whenever deemed necessary. By this means the crew increases the system reliability and provides it with the capabilities of judgment, decision, and flexibility.

During the system development, initial low-speed flights of the final stage can be made using a B-36 as a mother airplane. This procedure would have the advantage of pilot familiarization during low-speed flights and landing, and would permit high-speed flights up to a velocity of 12,000 feet per second. Valuable flight information and control characteristics could thus be obtained prior to utilization of the first-stage booster with the vehicle in the vertical take-off attitude. Also, in this type of flight program, the operational capability of all subsystems could be determined under conditions similar to those over the enemy area.

IV Configuration Design

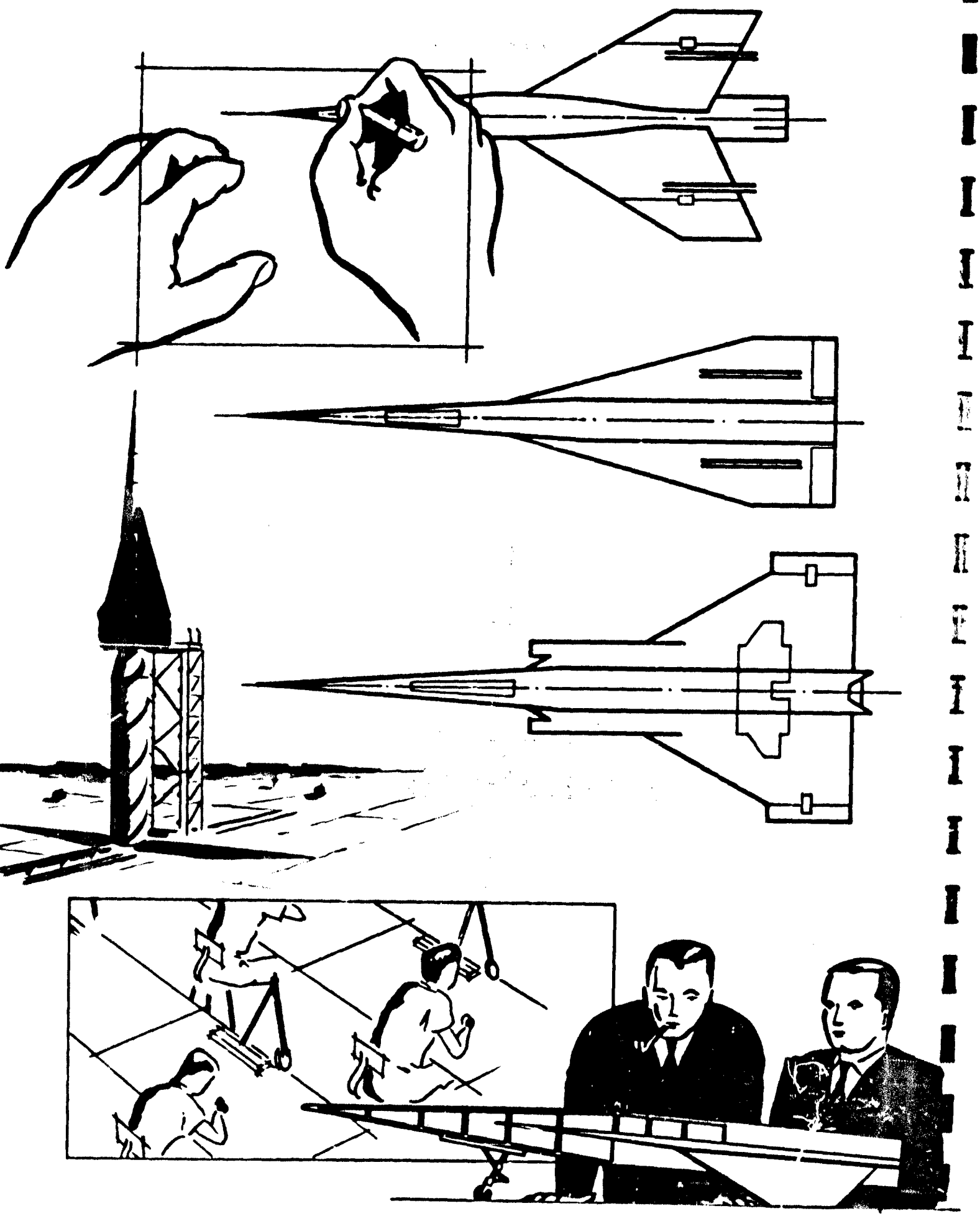

A. GENERAL

The design study effort during this period (Reference 3) was limited largely to that required to guide and interpret work in other phases of the program and to provide data for future optimization of the two basic Brass Bell configurations considered during previous studies. Both of these two configurations utilize two stages of boost, but differ in that the second stage of boost is integral with the airplane in one configuration and expendable in the other. Details of these configurations are presented in Reference 30. The selection of a single configuration on which to base future design studies is planned during the early stages of the next phase of the Brass Bell study.

A summary of the various configuration studies is presented as well as two types of thermal protection systems. The characteristics of a number of propellant combinations are discussed. A brief analysis of the cost per flight of the expendable hardware items is also presented, and details of the electrical system are discussed briefly.

B. CONFIGURATION

Configuration studies were conducted to evaluate the effects of changing various parameters and their over-all effect on vehicle size and weight. A number of propellant combinations were investigated, including solid propellants, and configurations established for each of these combinations. A side-by-side seating arrangement for the crew was incorporated into the configuration utilizing two expendable booster stages, instead of the tandem seating arrangement previously considered. This was believed to be advantageous from an instrumentation and human factors standpoint. A revised vertical fin arrangement was studied to provide greater directional stability. As a result, the upper vertical fin was eliminated and the two lower vertical fins were increased in area. Figure 3 shows all stages of a typical configuration which incorporates these changes, and Figure 4 shows the final stage of this configuration. In this particular configuration, both stages of boost are expendable. Liquid propellants are used for both stages; lox-JP for the first stage and fluorine-ammonia for the second stage.

Thermal protection methods, including a hydrogen cooling system and heat-sustaining leading edges were also investigated.

1. EFFECT OF VARIOUS PROPELLANT COMBINATIONS

The effects of various propellant combinations on over-all vehicle size and weight were studied to provide comparative data for evaluation purposes. Although these studies were conducted on a configuration which did not incorporate the latest design improvements, the results are applicable to the current configurations. Isolde solid propellant, fluorine-ammonia, and fluorine-hydrazine liquid propellants were investigated for both stages of boost. The latter propellant combination resulted in the lowest vehicle gross weight. A comparison of these vehicles is shown in Figure 5, while a comparison of the performance values of the propellants studied is shown on Table I. Advances in the solid-propellant rocket field made the use of a solid propellant for the first-stage booster competitive with lox-JP as shown in this figure. Layouts were made of a configuration utilizing a solid-propellant first stage and a liquid-propellant (fluorine-hydrazine) second stage. A typical configuration using these propellants is shown in Figure 6.

2. SIDE-BY-SIDE CREW ARRANGEMENT

The configuration with two expendable booster stages was revised to provide side-by-side seating instead of the original tandem seating arrangement in order to simplify the cockpit display and to provide better communications between the two crew members, thus improving their efficiency. This rearrangement required an increase in fuselage diameter from 60 to 72 inches and the relocation of various equipment items. As a result, an inboard profile drawing was prepared and is shown in Figure 7. The components for the primary

TAKE-OFF

TOTAL PROPELLANTS

DESIGN THRUST AT TAKE-OFF

STAGE I

PROPELLANTS (O + JP-4)

POWER PLANT 2 AT 168,500 LI

STAGE II

PROPELLANTS (F_2 + NH_3)

POWER PLANT 2 AT 34,000 LI

GLIDER

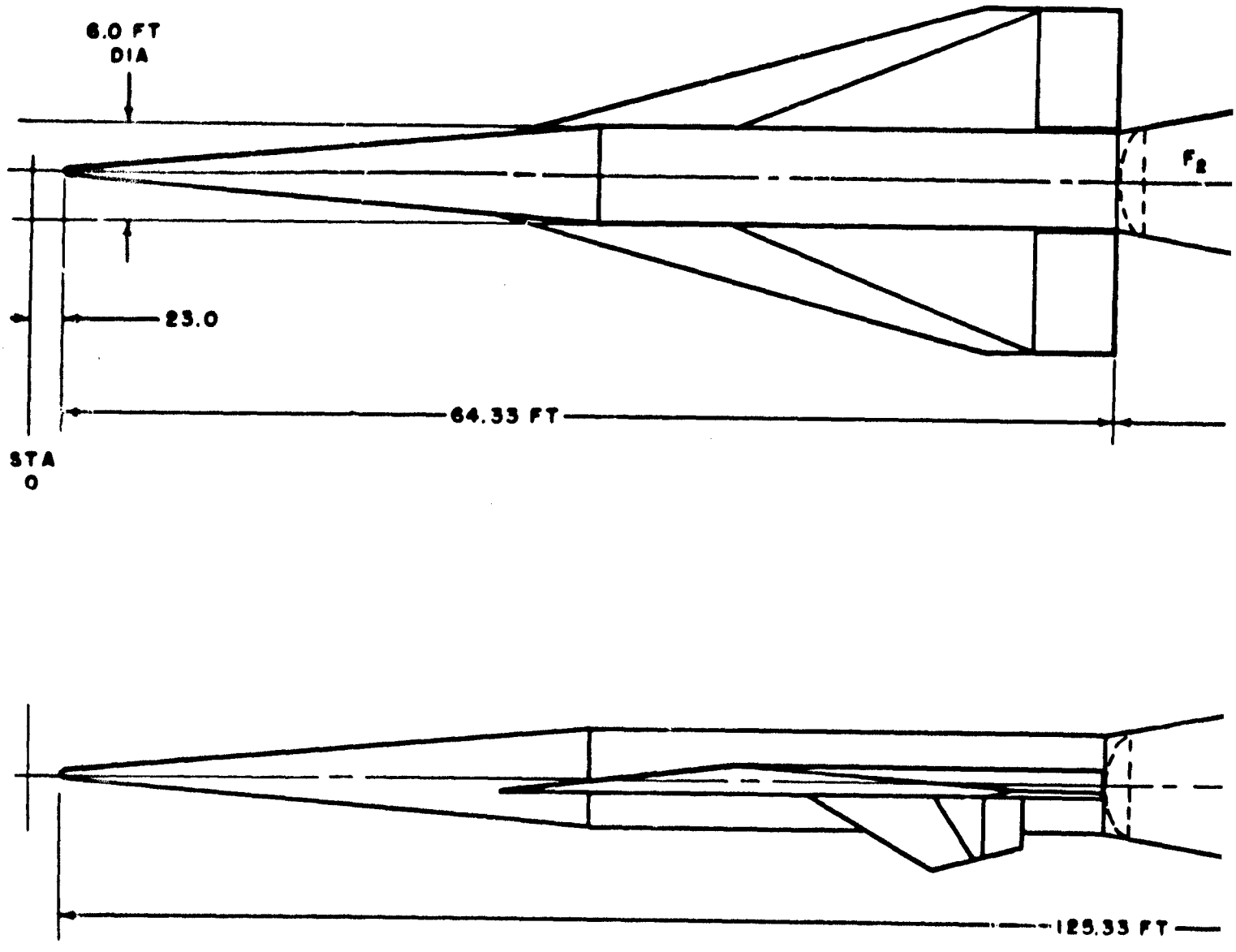

Figure 7. Configuration w

GROSS WEIGHT	192,649 LB
	162,734 LB
	337,000 LB
GROSS WEIGHT	124,676 LB
	113,917 LB

$A_e/A_t = 8$

GROSS WEIGHT	52,565 LB
	48,817 LB

$A_e/A_t = 20$

GROSS WEIGHT	15,408 LB

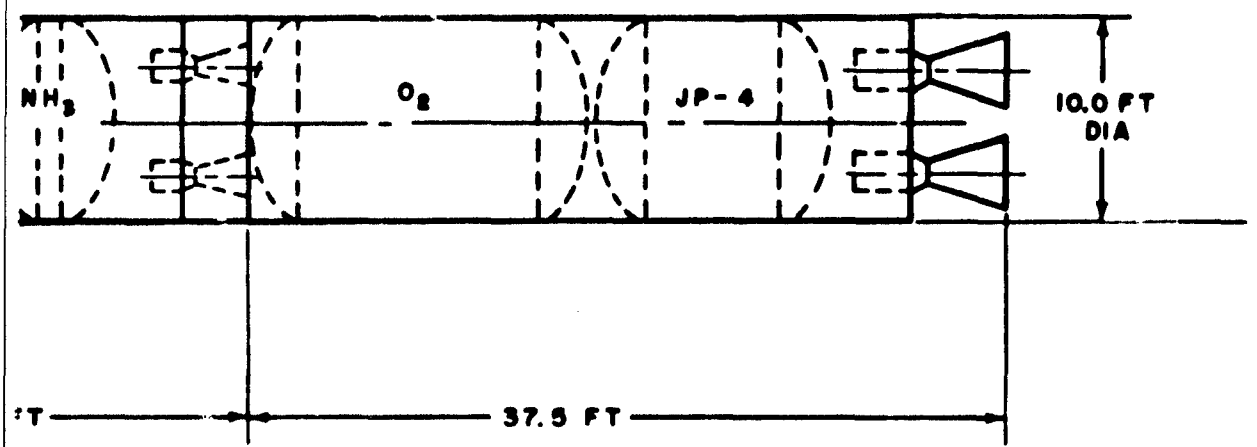

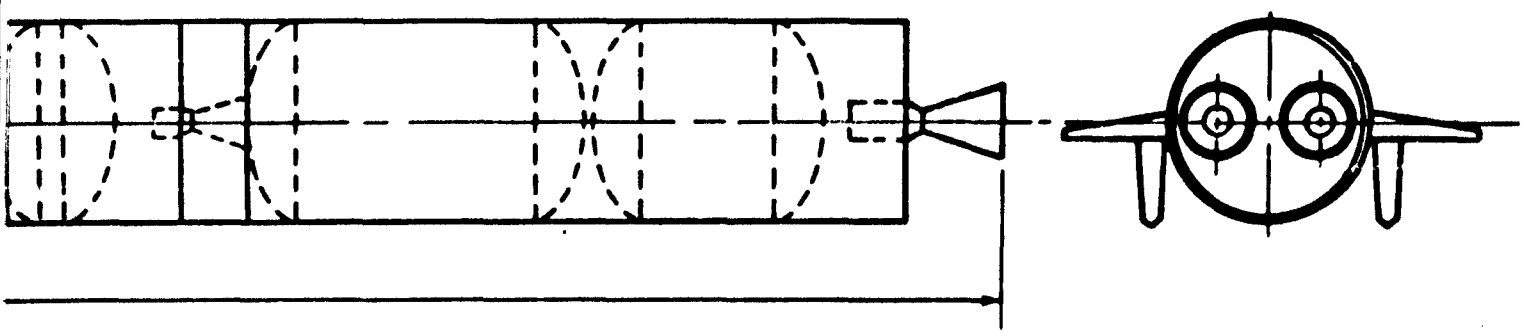

xpendable Stage II Booster

DIMENSIONS

WING SPAN	250.0 IN
AIRCRAFT LENGTH	772.0 IN
AIRCRAFT HEIGHT	110.0 IN
LANDING GEAR TREAD	94.0 IN

WEIGHTS

EMPTY WEIGHT	13182 LB
USEFUL LOAD	2458 LB
DESIGN GROSS	15640 LB
LANDING WEIGHT	13804 LB

CENTER OF GRAVITY

DESIGN GROSS WEIGHT	STA 520.42
EXTREME FORWARD	STA 520.42
EXTREME AFT	STA 539.44
LANDING	STA 539.44

WING

AREA (EXPOSED)	325 SQ FT
AIRFOIL SECTION	MODIFIED WEDGE
INCIDENCE	0
SWEEPBACK (L.E.)	75°
ASPECT RATIO (SUBSONIC)	0.875
CATHEDRAL	4°57'

TAIL

FIN AND RUDDER AREA (EACH)	38.5 SQ FT
AIRFOIL SECTION	MODIFIED DOUBLE WEDGE
SWEEPBACK (L.E.)	60°

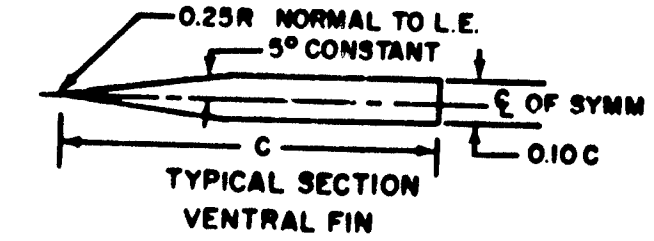

TYPICAL SECTION
VENTRAL FIN

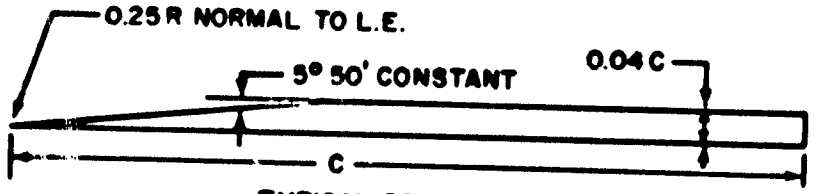

TYPICAL SECTION–WING

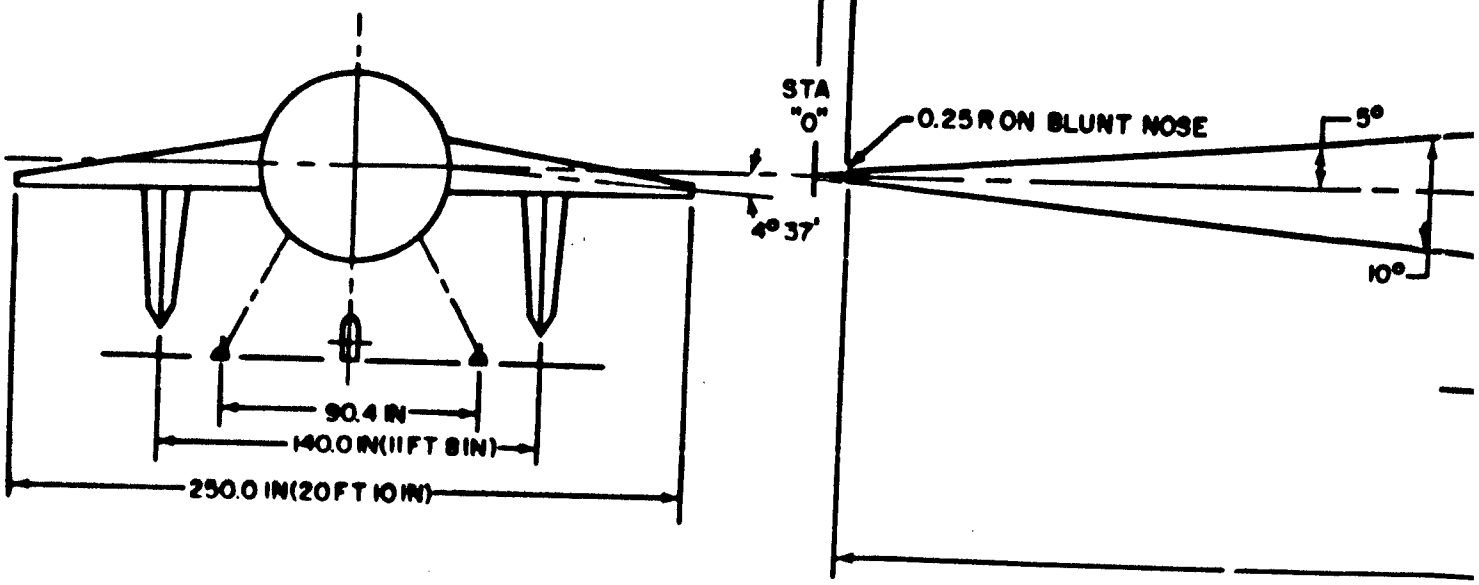

Figure 4. Fina

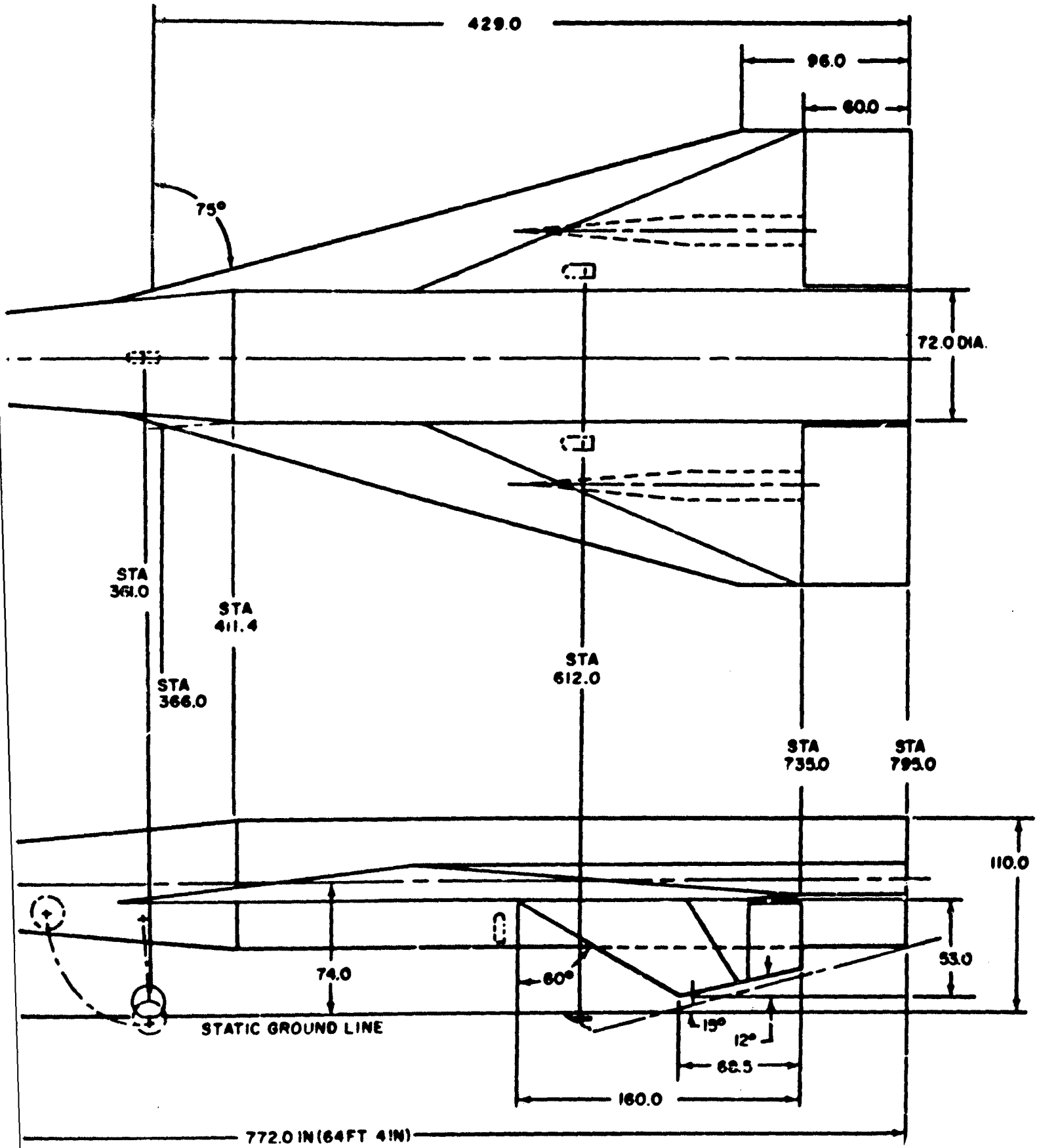
429.0
96.0
60.0
75°
72.0 DIA.
STA 361.0
STA 411.4
STA 366.0
STA 612.0
STA 735.0
STA 795.0
110.0
53.0
74.0
60°
19°
12°
68.5
160.0
STATIC GROUND LINE
772.0 IN (64FT 4IN)

age

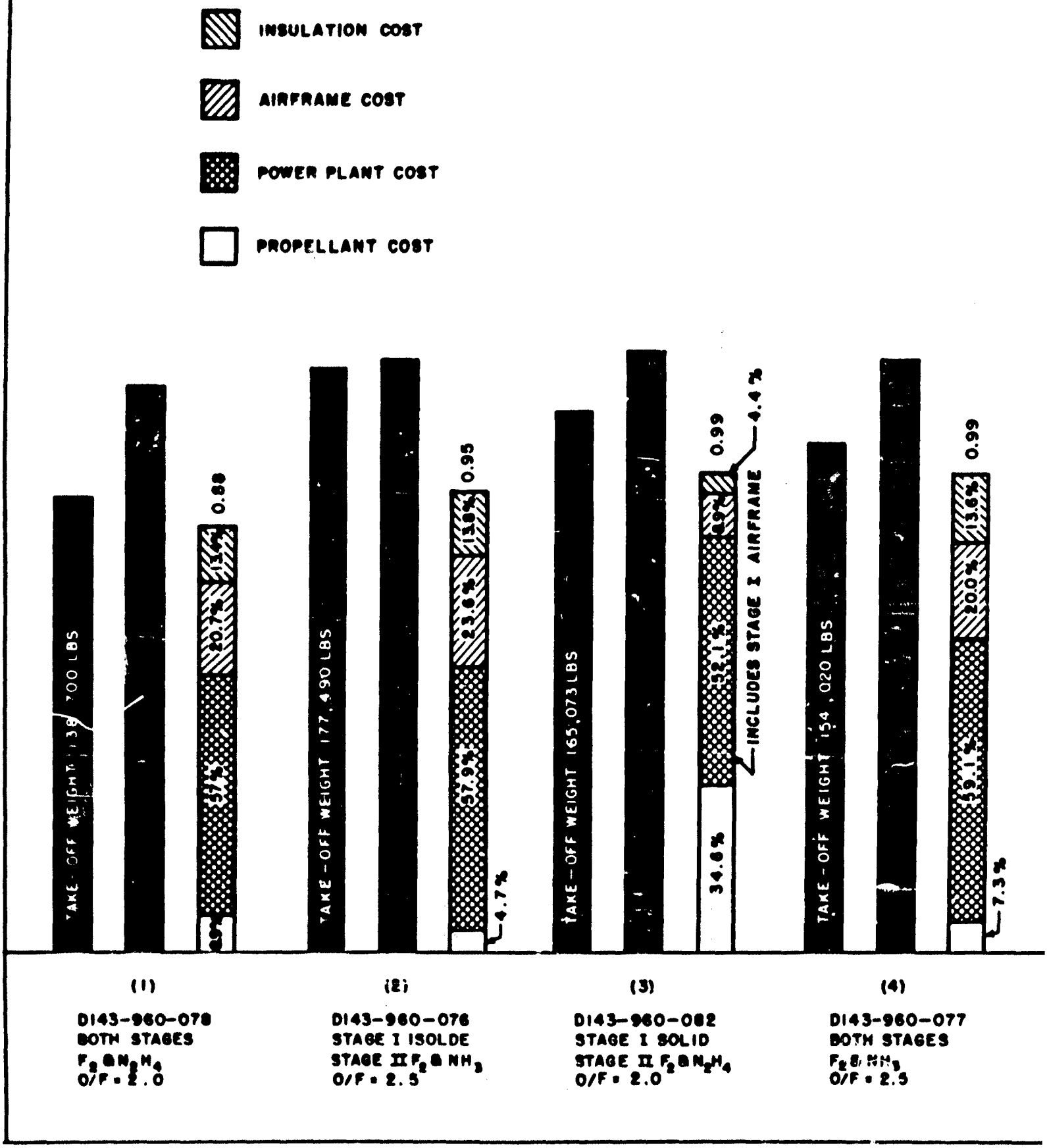
INSULATION COST
AIRFRAME COST
POWER PLANT COST
PROPELLANT COST
TAKE-OFF WEIGHT 177,490 LBS
0.88
20.7%
13.6%
0.95
23.6%
13.6%
57.9%
4.7%
TAKE-OFF WEIGHT 165,073 LBS
0.99
4.4%
32.1%
29.6%
34.6%
INCLUDES STAGE I AIRFRAME
TAKE-OFF WEIGHT 154,020 LBS
0.99
20.0%
13.6%
59.1%
7.3%
(1)
D143-960-078
BOTH STAGES
F2 & N2H4
O/F = 2.0
(2)
D143-960-076
STAGE I ISOLDE
STAGE II F2 & NH3
O/F = 2.5
(3)
D143-960-082
STAGE I SOLID
STAGE II F2 & N2H4
O/F = 2.0
(4)
D143-960-077
BOTH STAGES
F2 & NH3
O/F = 2.5

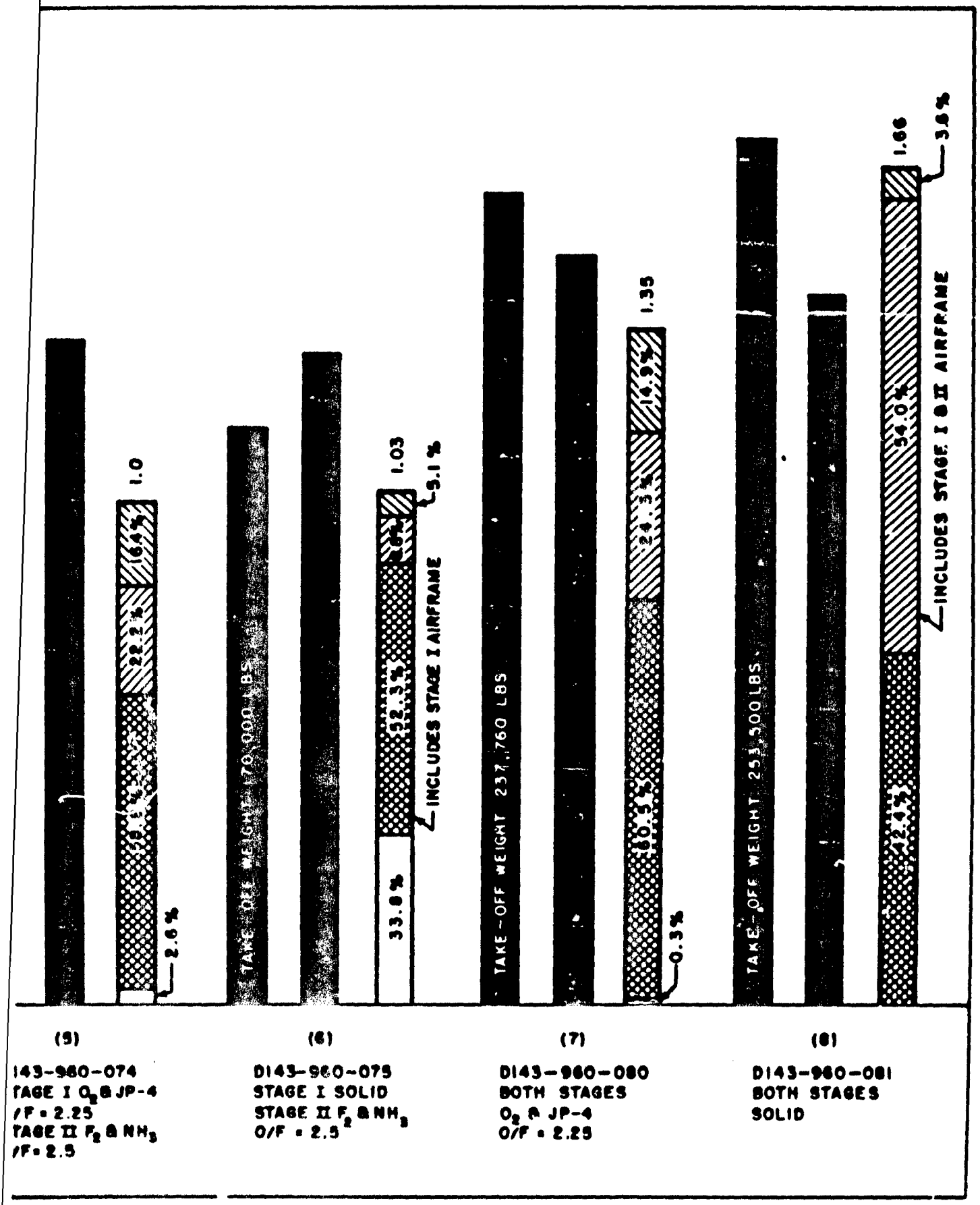

Figure 5. Propellant Evaluation

TAKE-OFF

TOTAL PROPELLANTS

DESIGN THRUST AT TAKE-

STAGE I

PROPELLANT (SOLID)

POWER PLANT 2 AT 162,

STAGE II

PROPELLANTS ($F_2 + N_2 H_4$

POWER PLANT 2 AT 33,

GLIDER

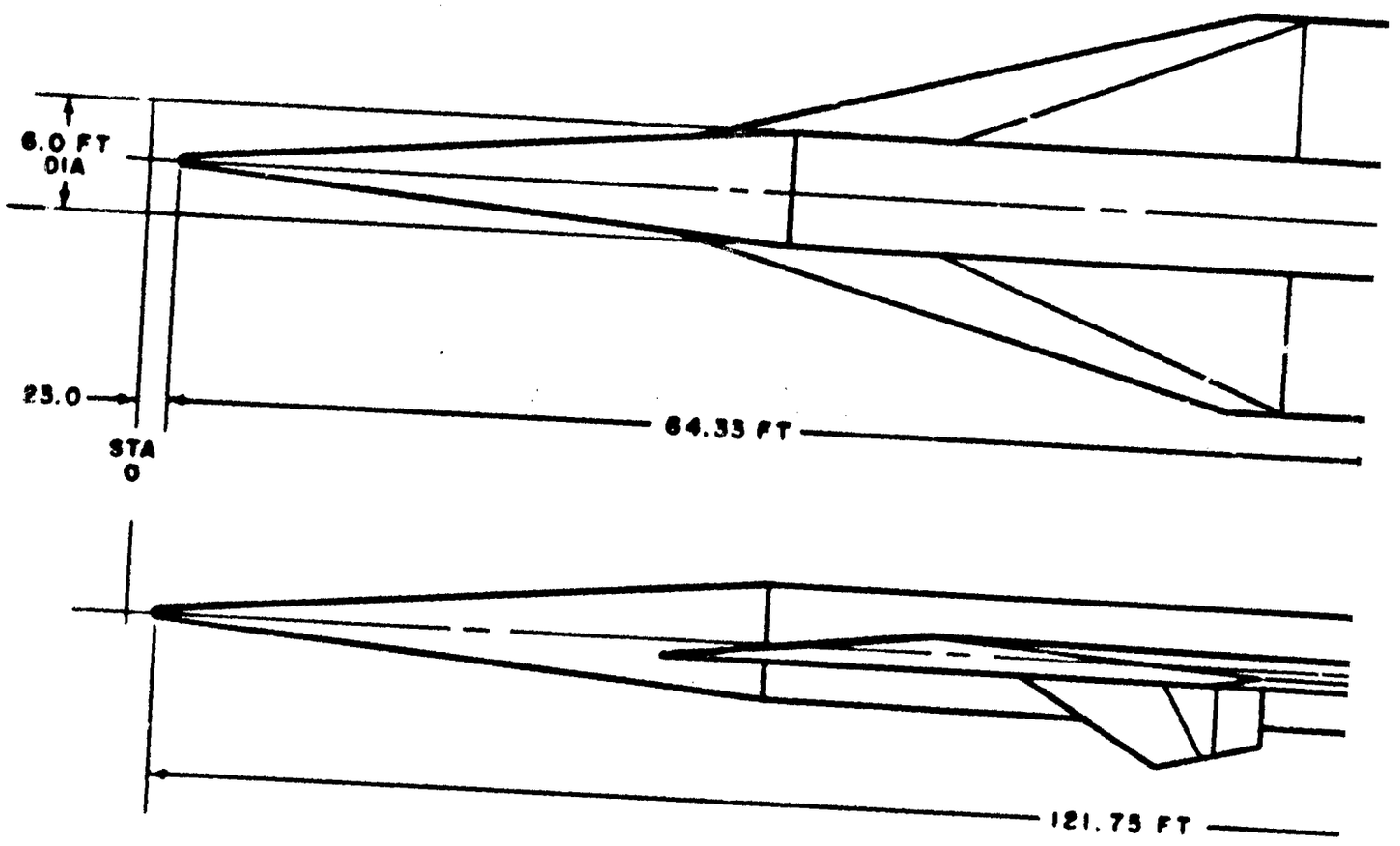

Figure 6. Typical Configuration

GROSS WT 185,461 LB
153,411 LB
324,600 LB

GROSS WT 119,130 LB
107,217 LB

AT $A_e/A_t = 8$

GROSS WT 50,923 LB
46,194 LB

AT $A_e/A_t = 20$

GROSS WT 15,408 LB

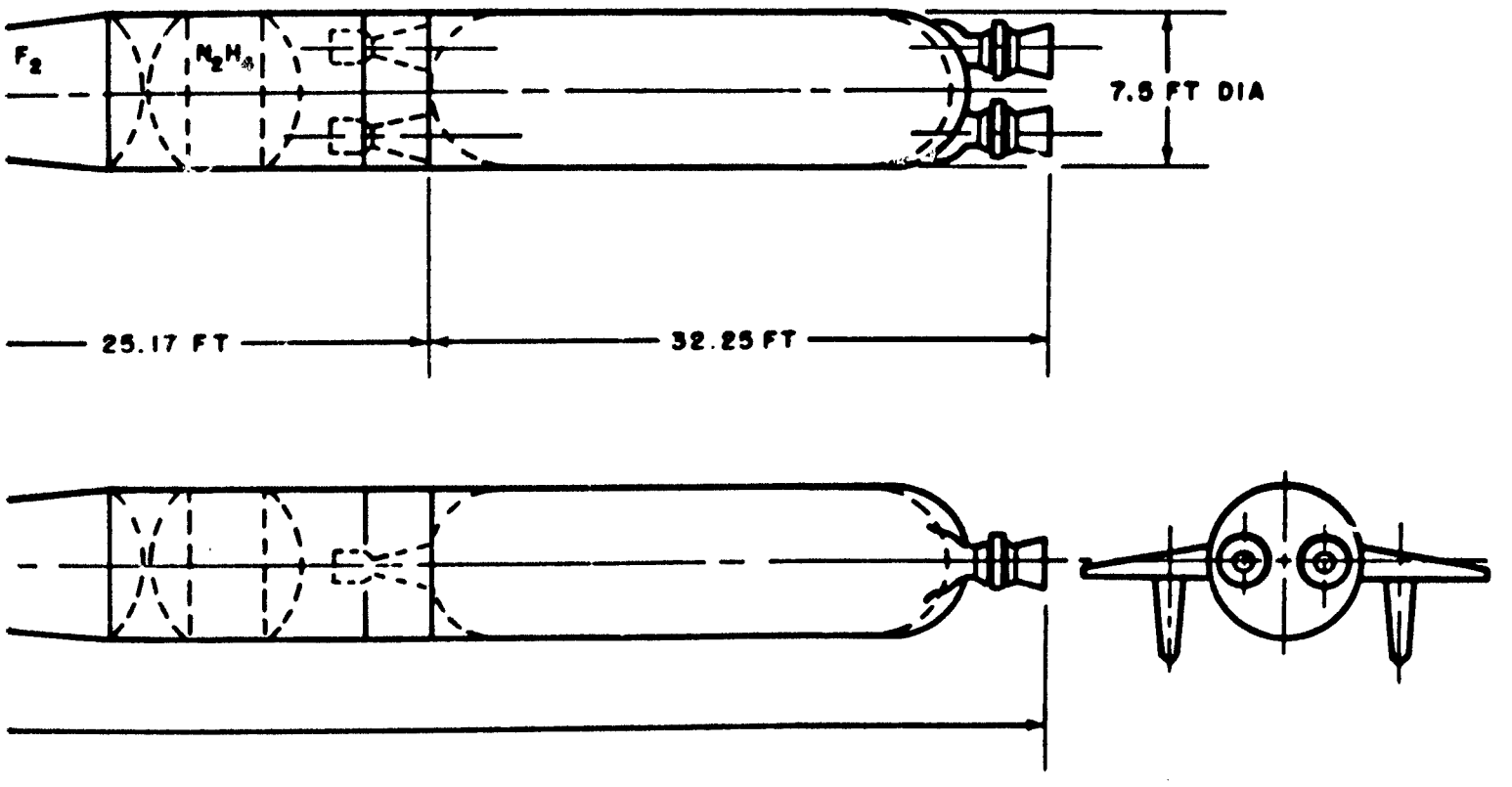

ting Solid Propellant for First Boost Stage

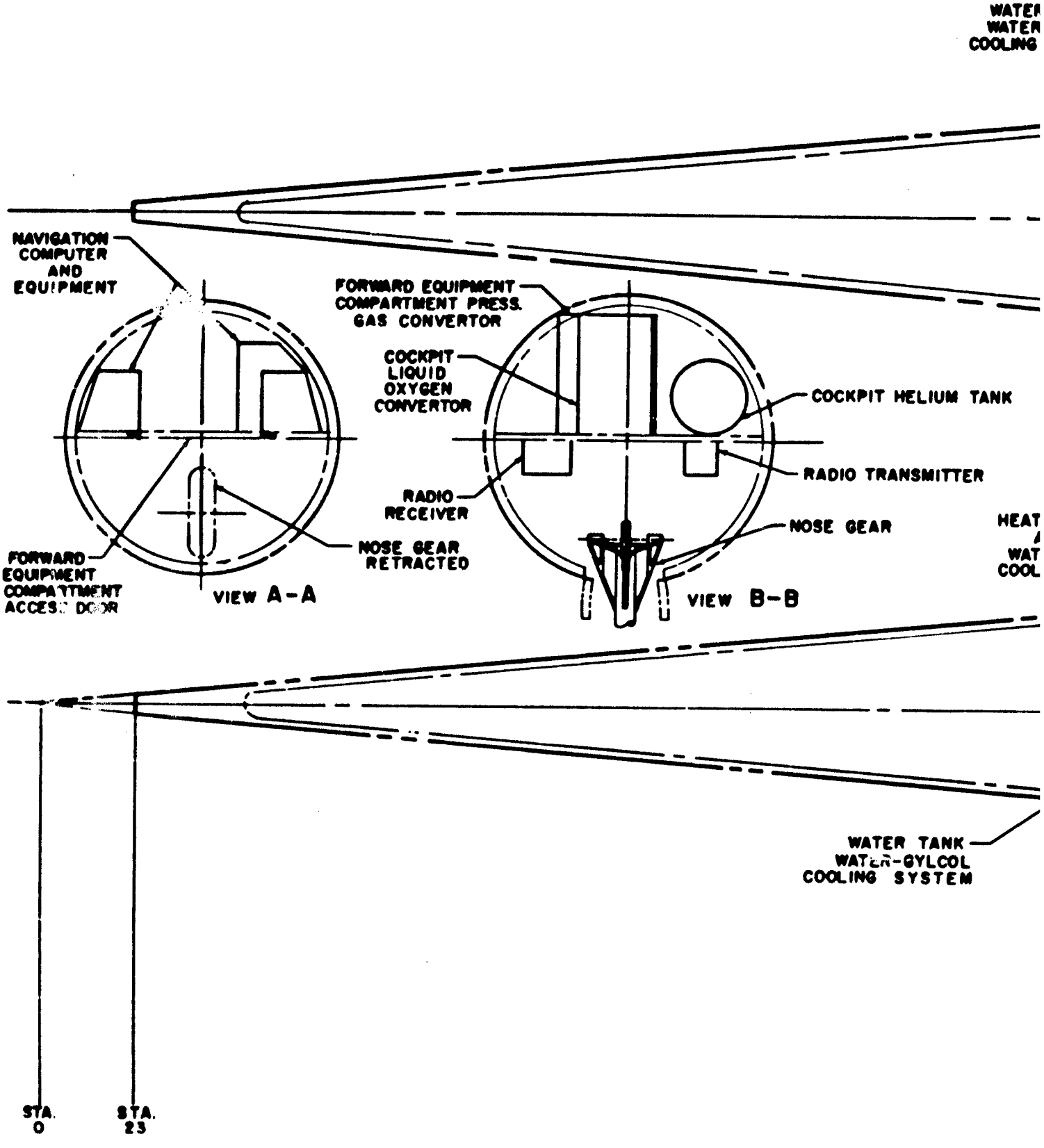
WATER
WATER
COOLING
NAVIGATION COMPUTER AND EQUIPMENT
FORWARD EQUIPMENT COMPARTMENT PRESS. GAS CONVERTOR
COCKPIT LIQUID OXYGEN CONVERTOR
COCKPIT HELIUM TANK
RADIO TRANSMITTER
RADIO RECEIVER
NOSE GEAR
NOSE GEAR RETRACTED
FORWARD EQUIPMENT COMPARTMENT ACCESS DOOR
VIEW A-A
VIEW B-B
HEAT
WAT
COOL
WATER TANK
WATER-GYLCOL COOLING SYSTEM
STA. 0
STA. 23

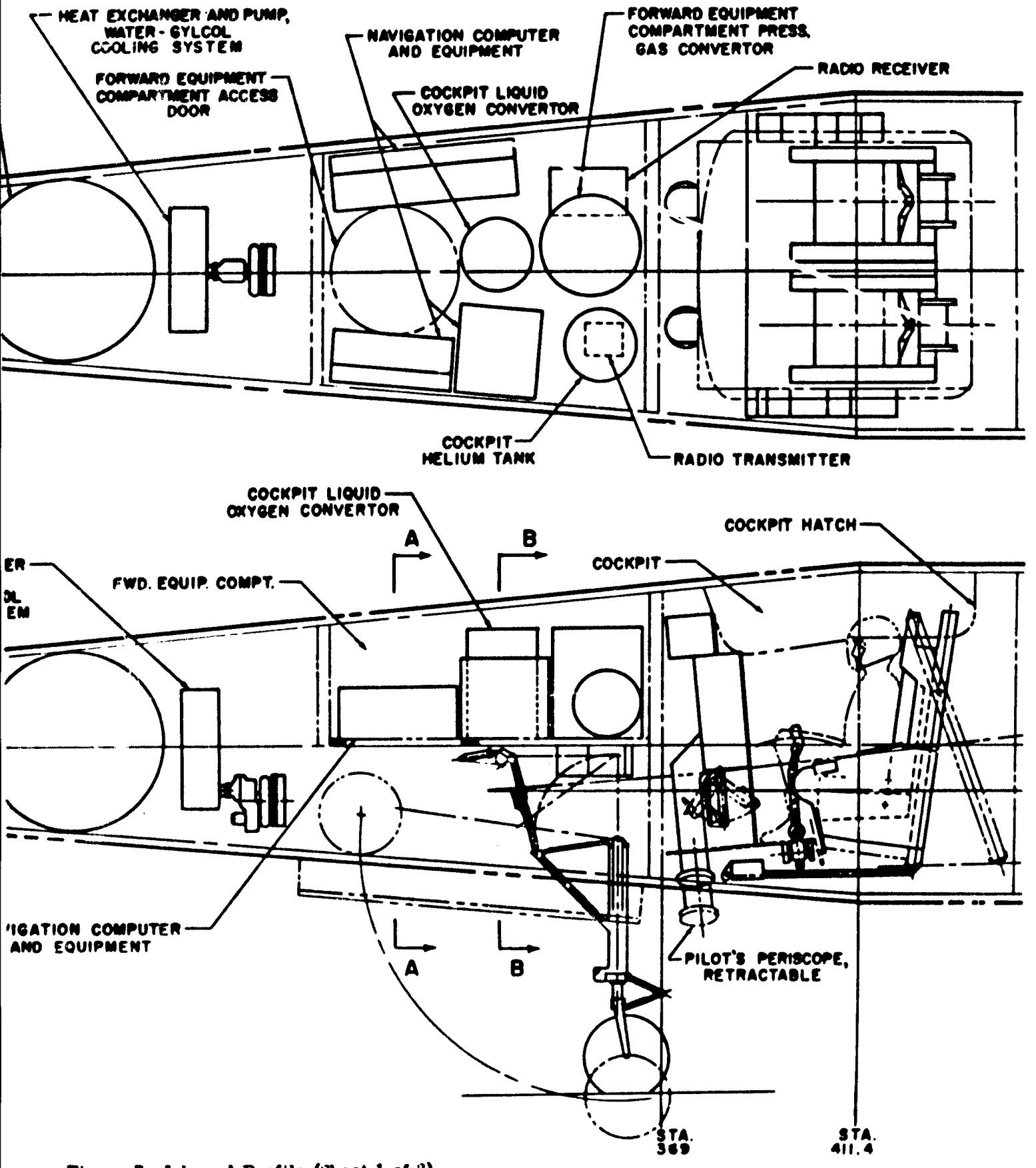

Figure 7. Inboard Profile (Sheet 1 of 2)

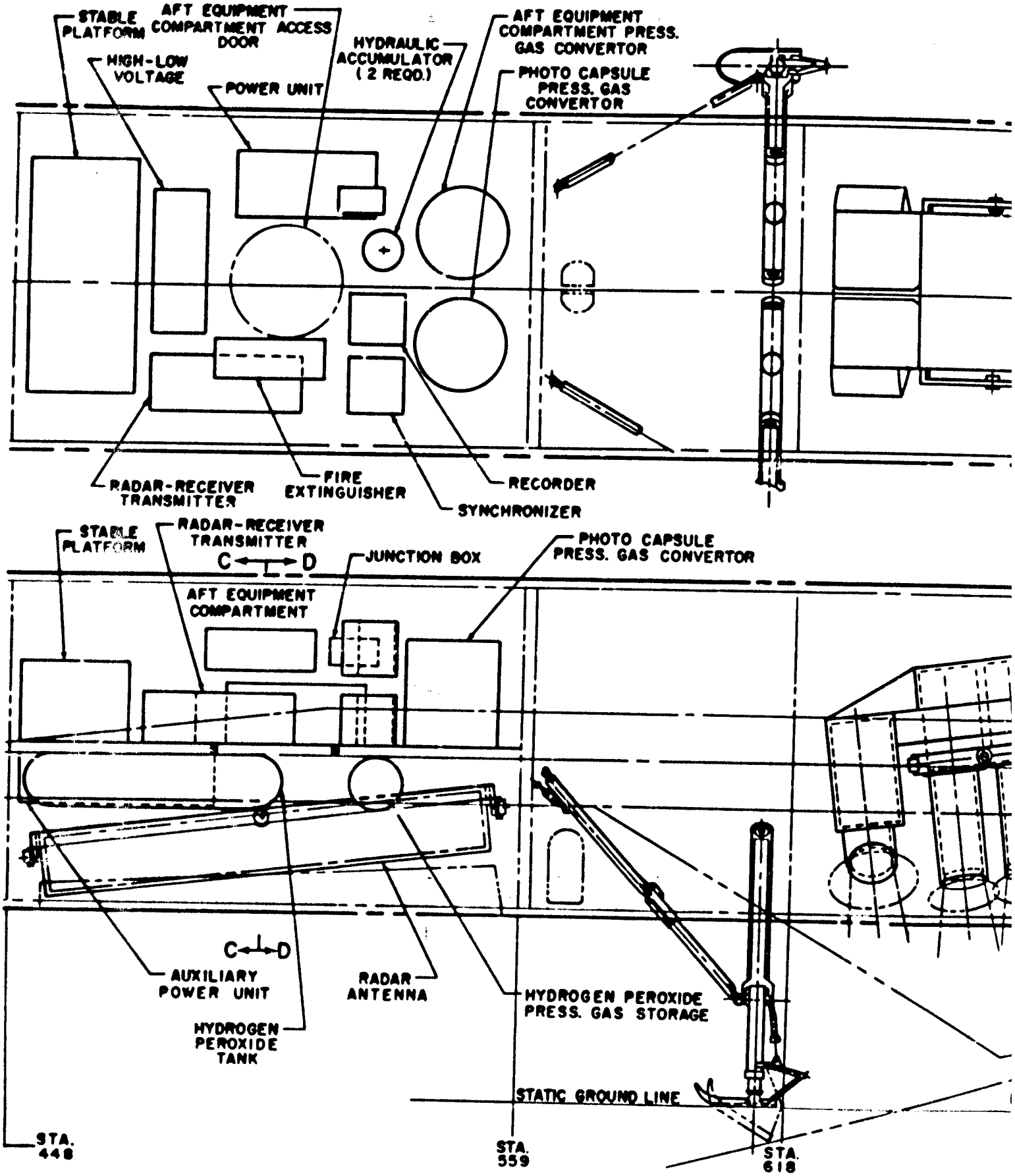

Figure 7. Inboard

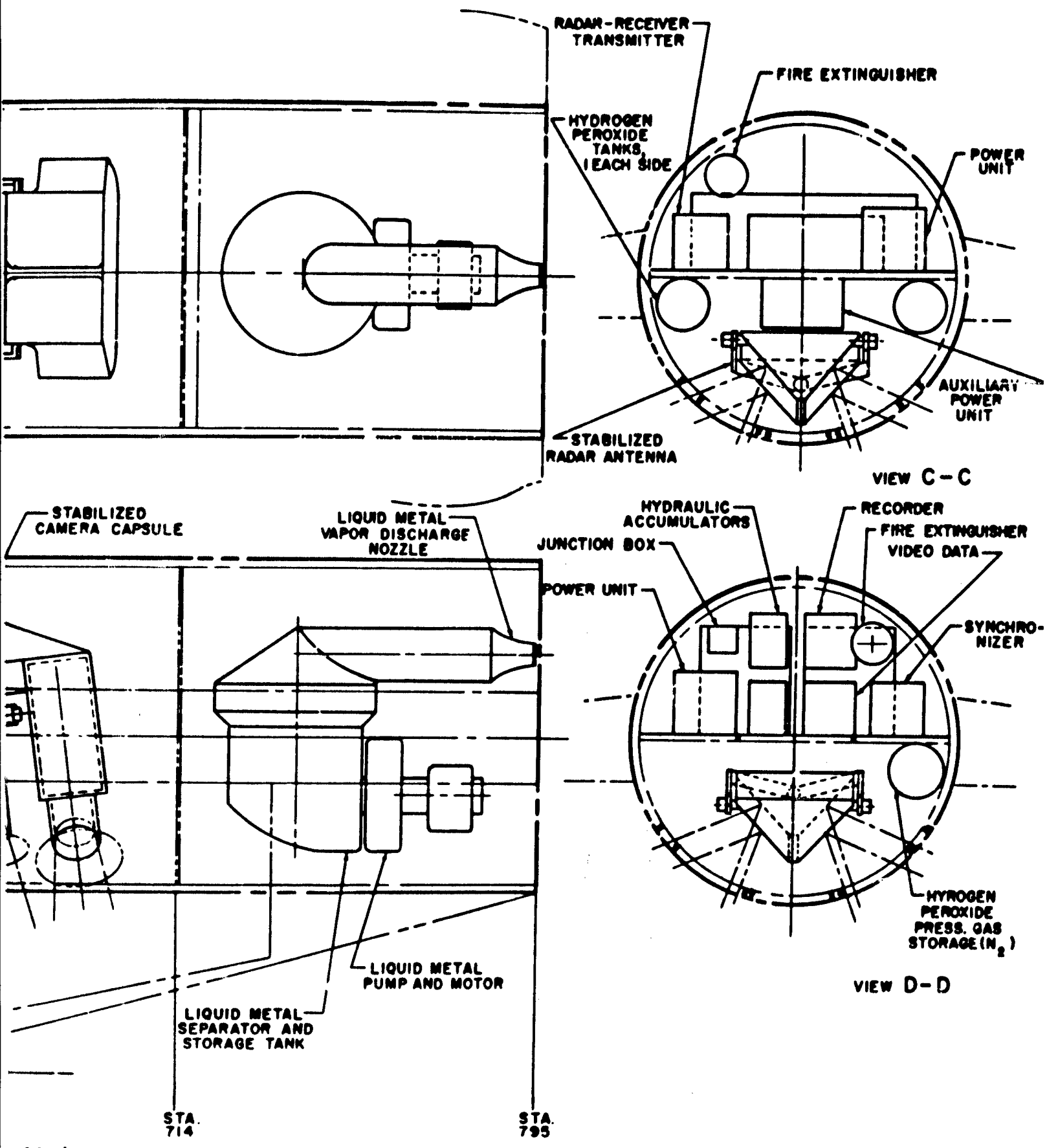

rofile (Sheet 2 of 2)

TABLE I

Propellant Performance Values — I_{sp}

	Sea Level	60,000 Ft	Remarks
Lox-JP	254	297	O/F = 2.25
Fluorine-Ammonia	275	344	O/F = 2.5 P_c = 300
Fluorine-Hydrazine	302	356*	O/F = 2.0
Isolde	230	272*	
Solid	250	270*	P_c = 1000

*50,000 ft

structure water-glycol cooling system are located in the nose of the airplane. Just aft of these items is the pressurized forward equipment compartment for electrical and electronic equipment. The nose gear is stowed below this compartment. The cockpit is supplied with an atmosphere of 3.1 psi oxygen and 2.4 psi helium from containers which maintain these elements in the liquid state. These containers and their associated converters are located in the forward equipment compartment. The crew members are provided with periscopes for external vision. Two eight-foot-long radar antennas with provisions for space stabilization are provided aft of the crew compartment. Above these antennas is an aft equipment compartment, which is pressurized and houses the components for the inertial guidance system and other electronic gear. The main landing gear is located forward of the reconnaissance equipment compartment. A skid is used to minimize stowage space and to eliminate the requirement for brakes. Since the airplane takes off in a vertical attitude, the gear is used only for landing. The reconnaissance equipment compartment is designed to accommodate any one of the five reconnaissance capsules.

The liquid metal storage tank, separator, and pump are located in the base of the fuselage. These components are used for cooling the leading edge surfaces and nose of the body by circulating a sodium-potassium (NaK) liquid through the heated areas in a closed loop arrangement and then utilizing the heat of vaporization of lithium to cool this loop in the separator. Exhaust gases are vented overboard.

3. REVISED VERTICAL FINS

Aerodynamic studies of the directional stability of the final airplane stage indicated that the effective upper vertical fin area combined with the two lower vertical fins was inadequate. The lower fins, which are more effective at hypersonic speeds, were therefore increased in area which permitted complete removal of the upper vertical fin as shown in Figure 3. In addition to this change, the fins were moved forward to clear the wing trailing edge control surfaces so that adequate elevator area could be provided. As a result of these changes it was necessary to move the main landing gear from the wing to the fuselage, which was accomplished with only a slight increase in fuselage length.

4. HYDROGEN COOLING SYSTEM FOR LEADING EDGES

Liquid metal cooling systems utilizing the heat of vaporization of lithium are being considered for cooling the leading edges of the wings and fins as well as the nose of the body. Another potential cooling system utilizes hydrogen for cooling these areas. In order to

investigate the over-all effects of this type of cooling system, an airplane configuration was established. It was found that, with a slight increase in fuselage length, the required amount of liquid hydrogen can be stored. A weight and balance analysis indicated that a weight reduction of the glider stage, as compared to the lithium system, was significant enough to warrant additional studies of the hydrogen systems.

C. THERMAL PROTECTION

1. HYDROGEN COOLING

The use of hydrogen gas, unique among the gases because of its high specific heat, as a coolant for the leading edges is under investigation. There are several systems which appear promising. In the system used for an airplane configurational study to evaluate the use of hydrogen, the gas is used first as a coolant in the heat exchanger for the primary structure skin cooling system, then ducted through the leading edges of the flight surfaces, and then, as a relatively hot gas, used to drive the turbine of the Auxiliary Power Unit. When so used, the hydrogen exhaust gas reduces the quantity of hydrogen peroxide normally required by the APU by about 50 per cent. In another system, the hydrogen gas, having served as a coolant in the primary skin cooling system heat exchanger, is then used in a similar manner in a heat exchanger with a relatively easy to handle liquid metal, such as sodium-potassium as the heat transfer medium. Section V describes this approach in more detail. Power recovery by means of a turbine is also possible in this system.

2. HEAT-SUSTAINING SYSTEMS

The direct approach to thermal protection of leading edges by means of heat-sustaining materials and favorable nose shapes was studied. A leading edge design consisting of shaped blocks of silicon carbide attached to the wing structure by a connecting section of "pyroceram" has been investigated. Weight calculations of such a design indicate an airplane weight reduction of 1400 pounds, when compared to the lithium-cooled liquid metal system.

"Pyroceram" was selected in this study as the material connecting the hot leading edge to the relatively cool wing structure because of its high temperature strength and its low thermal conductivity. There is now evidence that resistance of pyroceram to thermal shock may be better than first reported, and therefore more acceptable. Unfortunately, pyroceram, according to present information, has an emissivity ranging between 0.4 to 0.6. The desired emissivity for temperature relief for this material should be about 0.9. Further investigation of this material is required to determine whether the required emissivity can be obtained.

Pyroceram was also investigated as a material for the outer wall panels of the double-wall type of construction. In this application, the low coefficient of expansion of this material reduces the differential expansion between the inner structural wall and the outer thermal protective paneling, and so makes attachment and closure problems simpler.

Analysis indicates that 0.05-inch-thick outer wall panels with reinforcing waffle-type webs will satisfy the structural requirements. Such panels would compete, weight-wise, with present designs in metal. The required emissivity factor for pyroceram in this application is also about 0.90.

D. PROPULSION

1. PROPELLANTS

The studies conducted on Brass Bell to date have indicated the desirability of using high-energy propellants for the second-stage booster. Fluorine in combination with ammonia is one of the more promising combinations, although hydrazine is being investigated, and may result in an increase in performance. The use of high-energy propellants for the first-stage booster is not as critical as for the second stage. This fact will permit the use of propellants such as lox-JP, for which large thrust

motors are now being developed. (First-stage thrust is approximately 300,000 pounds and second-stage thrust is about 60,000 pounds.) Experimental work is being conducted by the Rocket Division of Bell Aircraft on fluorine-ammonia propellants. A 35,000-pound-thrust motor has been successfully fired for a duration of about 10 seconds. Regenerative cooling with ammonia or hydrazine must still be investigated. Considerable effort is required in this area.

Because of the hypergolic qualities of fluorine with almost any fuel, the rocket motor system can be simplified appreciably. This is reflected in extremely smooth starting characteristics, and has been repeatedly demonstrated experimentally. To date no turbine-driven fluorine pump development work has been undertaken by rocket manufacturers, although some work has been done on pump seals for fluorine.

A great deal of concern has been expressed concerning area contamination due to fluorine rocket motor exhaust. Recently, samples have been taken approximately 3000 feet downwind of a large horizontally fired fluorine motor. Samples have been taken under varying atmospheric conditions and indicate not more than two parts per million of hydrogen fluoride in the air. This condition may be compared against an allowable human exposure of three parts per million for an eight-hour period. Of particular interest is the fact that the exhaust gases from these tests were not neutralized in any fashion.

a. Isolde Monopropellant

A recently developed monopropellant, Isolde, has been theoretically and experimentally investigated. This propellant theoretically exhibits a specific impulse in the neighborhood of 230 seconds at sea-level conditions. It possesses a high bulk density and is a quiescent propellant as compared to liquified gases. Indications are, however, that it is susceptible to detonation under certain conditions, and difficulty has also been encountered in sustaining combustion with Isolde subsequent to initial ignition with unsymmetrical dimethyl hydrazine. It appears that considerable work with experimental motor test and propellant property determination must be done before this monopropellant can be used operationally.

b. Solid Propellants

The solid propellant rocket field has shown great progress in the past year. Up to this time, various characteristics such as low specific impulse and temperature limitations have precluded solid propellants from considerations for use on Brass Bell. However, specific impulse values of 246 seconds at sea level have recently been obtained experimentally. Motors 70 inches in diameter with a gross weight of over 20,000 pounds have been successfully fired. Considerable experimental work is now under way on the feasibility of gimballing solid propellant motor nozzles. Durations as long as 90 seconds have been successfully fired. A survey indicates that the Brass Bell vehicle could, within two years, have a solid-propellant first-stage booster of 30 million pound-seconds total impulse and exhibit a specific impulse of 250 seconds at sea level.

c. Lox-JP

In the field of liquid oxygen-JP propellants, one manufacturer has now successfully fired a single thrust chamber at a 300,000 pound thrust level. Also, a successful starting technique has been established. A turbine pump for this motor is now under construction. A motor such as this, with a single pump and thrust chamber, provides both safety and reliability. It is estimated that an operational motor could be developed from this experimental work within two to three years' time.

2. COST ANALYSIS

a. General

In the evaluation of the relative merit of various propellant combinations, primary emphasis is usually given to the effects on over-all size and weight of the complete weapon system. However, in a boost-glide type of vehicle, wherein the propulsion systems are not recovered, a very important factor is the

cost of the expendable materials. A brief cost analysis was therefore prepared analyzing the cost per flight of vehicles using different propellant combinations.

b. Conditions and Assumptions

The cost analysis is based upon the following conditions and assumptions:

(1) All configurations use two stages of boost which are expendable.

(2) Propellant combinations included lox-JP-4, fluorine-ammonia, fluorine-hydrazine, the monopropellant Isolde, and solid propellant.

(3) This analysis groups the cost into four major elements: propellants, rocket engine system, airframe, and airframe heat protection.

(4) In the case of the "solid" propellants, the cost of the airframe and engine are combined and insulation is not necessary. The unit costs of these items are summarized in Table II.

(5) The cost figures presented do not include any Research and Development expenditures (e.g., the cost of engine development and test for new propellant combinations). Furthermore, the cost of ground facilities (such as a fluorine production plant) and support equipment have not been considered.

(6) The hardware costs of the recoverable portions (the glide airplane) have not been included.

(7) All the examples provide the same altitude, speed and flight range performance.

TABLE II. UNIT COSTS

Propellants	Dollars
Liquid Oxygen	0.035/lb
(1) Liquid Fluorine	1.20/lb
Liquid Ammonia	0.044/lb
(2) Liquid Hydrazine	0.75/lb
JP-4 (RP-1)	0.021/lb
(3) Isolde	0.30/lb
(4) Solid	5.00/lb
Hardware	
(5) Airframe	35.00/lb
(6) Rocket Engine System	200.00/lb
(7) Insulation	141.00/sq ft
(8) Booster Control System	24,500/flight
Solid Propellant Inert Hardware	55.00/lb

(1) The General Chemical Division of the Allied Chemical and Dye Corporation estimated that, with a fluorine production rate of 4.5 tons per day, the cost will be $1.20 per pound. If the output is increased to 10 tons per day, the cost would be $0.77 per pound.

(2) The present cost of hydrazine is $3.00 per pound in drum lots. The projected cost at very high rates of production of $0.40 per pound. The cost of $0.75 per pound is consistent with the cost of $1.20 per pound used for fluorine.

(3) The present cost of isolde is $0.82 per pound in small quantities. The projected cost of $0.30 per pound used in this estimate is based on a discussion with Dr. Clark of NARTS concerning high quantity production.

(4) The cost of $5.00 per pound assigned to solid propellants represents the projected cost of propellant material plus loading and curring of advanced propellant formulations of the size required for Brass Bell capable of producing an over-all specific impulse of 250 seconds.

(5) The airframe consists primarily of tanks of conventional construction. The cost per pound is based upon current charges for similar tanks and associated structure.

(6) The rocket engine system (thrust chamber, gas generator, and turbine pump) cost is based upon data on a few actual engine systems modified where necessary by cost estimates from new engine proposals.

(7) The thermodynamic insulation protects the basic tank structure from the effects of aerodynamic heating. The cost figure per square foot includes the outer wall material, associated brackets, and fibrous insulation between the outer wall and tank structure.

(8) This item refers to actuators for the gimballed rocket motors as well as any special control system elements in the boosters (such as rate gyros).

c. Discussion of Results

Figure 5 presents the results of this brief analysis based on a cost per flight of the system. Eight configurations were analyzed. The desirability of the use of high-energy propellants in the second stage of boost is clearly indicated. The use of solids or lox-JP in the second stage increases the cost in the order of 50% over those vehicles utilizing high-energy propellants in the second stage. This study also indicates that from the cost standpoint, the type of propellant used for the first stage of boost has little effect. In spite of the relatively high cost of the fluorine-hydrazine propellant combination, their high energy combined with their high density results in the cheapest firing cost of any vehicle studies. Indications are that solids compare very closely in cost to that of liquid propellants of the lox-JP type. If, however, boil-off losses with liquified gases are included, indications are that solid propellant boosters would be cheaper. One advantage of a solid first-stage booster is the elimination of insulation to protect against aerodynamic heating. This insulation as known today is a costly item.

When sizes of the vehicles are considered in this comparison, no really significant difference in length is apparent unless low-energy propellants are used in the second stage. Fluorine-hydrazine in both stages results in the lightest take-off weight of all vehicles studied. However, here again, as in the case of the length variations, weight differences among the various configurations are negligible unless low-energy propellants are considered for the second stage. However, a solid first-stage booster is approximately 30 inches smaller in diameter than any liquid first-stage booster studied.

E. ELECTRICAL SYSTEM

Operation of an electrical system at the altitudes and environmental conditions experienced by Brass Bell will be somewhat simplified by locating most of this system in pressurized compartments under a controlled temperature environment. Equipment located outside of pressurized compartments can utilize self-contained pressurization systems. Power for the electrical system will be generated by two 75-horsepower hydrogen peroxide-driven auxiliary power units each driving a 15 KVA alternator. In the event of a failure of one APU, the other unit will supply the necessary power to safely continue the flight of the airplane under emergency conditions.

V Structures

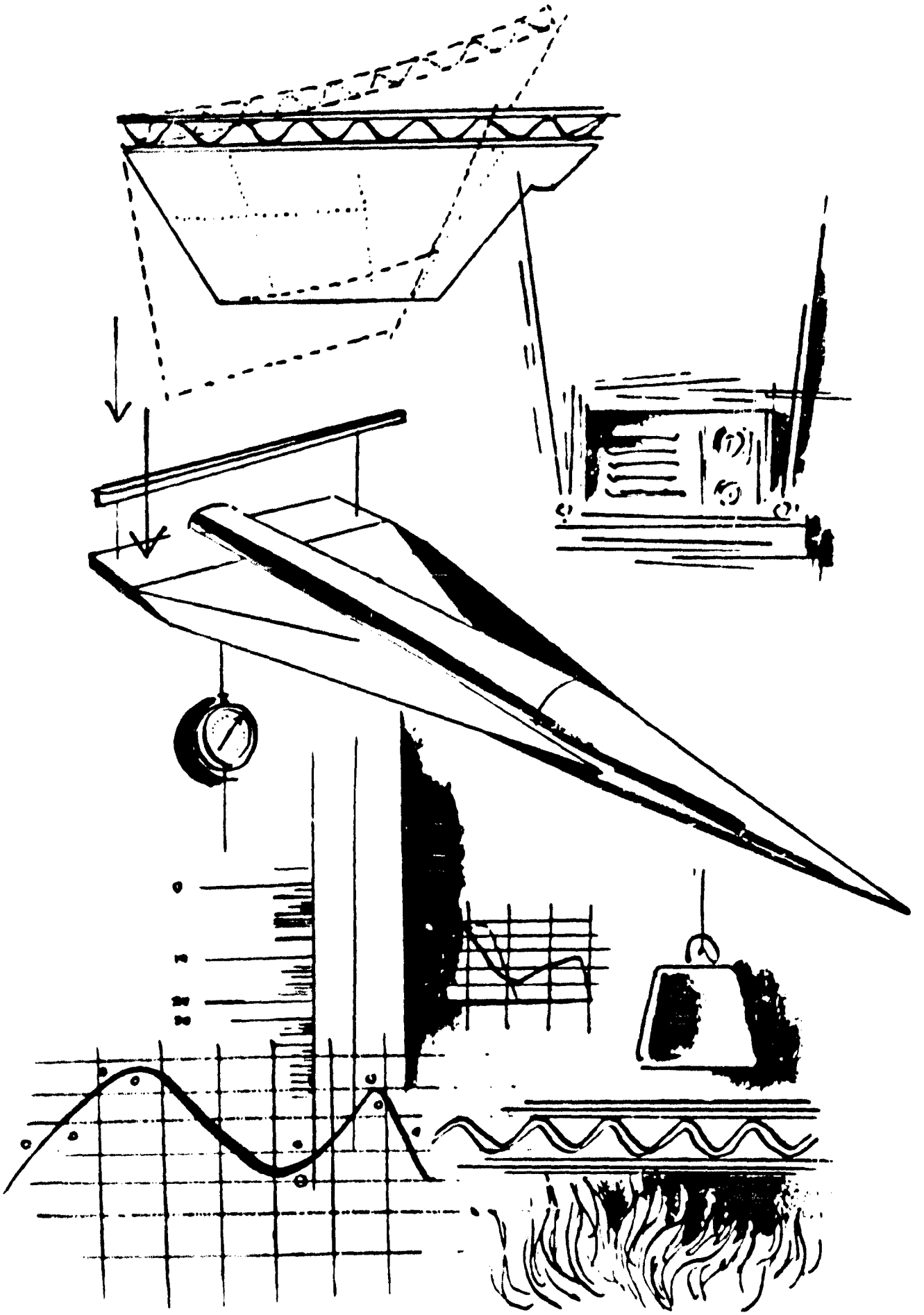

A. GENERAL

Previous studies of the airframe construction, summarized in References 4 and 5, encompassed the pertinent areas of both the final stage and the boosters. New structural approaches were evolved for areas subjected to a high thermal environment, and a sound engineering basis was achieved by supplementary wind tunnel and laboratory tests and by analysis of the vehicle.

The most efficient arrangement for most of the final stage structure was found to be an insulated and cooled light alloy structure. The evaporation of water supplied the cooling capacity. The insulating system consisted of an outer wall of small temperature-resistant panels surrounding a layer of fibrous insulation. By division of this outer wall into small panels, freedom for thermal expansion was attained. For the wing leading edges and the fuselage nose, where heating intensities exceed the resistance of the outer wall, two approaches have been evolved: cooling by the evaporation of liquid sodium or lithium, and a "heat-sustaining" structure of refractory material. Booster structure has been optimized, resulting in the use of insulated aluminum.

In the past, effort was concentrated on the development of Double-Wall, as the combination of an outer wall and an insulated light alloy structure has been termed, and the two systems for "hot-spot" areas. Panel elements for the outer wall were designed, fabricated, and successfully tested for strength, reaction to transient heating, and susceptibility to flutter. Supporting materials testing involved the oxidation resistance and strength of coated and uncoated materials at elevated temperatures. An evaporative liquid metal cooling system, representative of one approach to the leading edge problem, was operated successfully, and oxidation-resistance testing of refractory materials supported the other approach.

In accomplishing this work, laboratory equipment to simulate the aerodynamic, thermal, and loading conditions was designed and built. Considerable assistance was obtained from the NACA in planning wind tunnel tests and in conducting such tests in their facilities.

The work accomplished in the present period is summarized in Reference 6, and has included design studies, experimental investigations, and investigations of special equipment required for future tests. Attention has been concentrated upon the continued development of double-wall construction and the two approaches to hot-spot areas. Other areas of investigation have included studies of various types of booster structure and a computation of structural stiffnesses. The latter information was used for preliminary checks of control system characteristics. Emphasis has been placed on experimental programs and, in particular, on the demonstration of the practicability of double-wall construction.

B. DESIGN STUDIES

The design studies, which are summarized below, have included improved outer wall designs and insulation arrangements, and an analysis of panel flutter. Structural designs have been developed for both the cooled and heat-sustaining leading edges. Further studies of all structural cooling systems have concentrated on the use of hydrogen as the heat sink. Various types of booster structure were compared, and a successful correlation was made between temperatures calculated by the methods used throughout this work, and the results of recent flight tests. A review of the test results has formed part of the design studies.

1. OUTER WALL PANELS AND INSULANTS

In the previous period two outer wall panel designs were developed, the corrugated panel (Figure 8b) and the sandwich panel (Figure 8c). Both types were fabricated from 0.005-inch Inconel X sheet, with a honeycomb cell core of 0.002-inch material in the sandwich panel. Each panel had a span of 8 inches and a depth of approximately 0.3 inch. Continuous

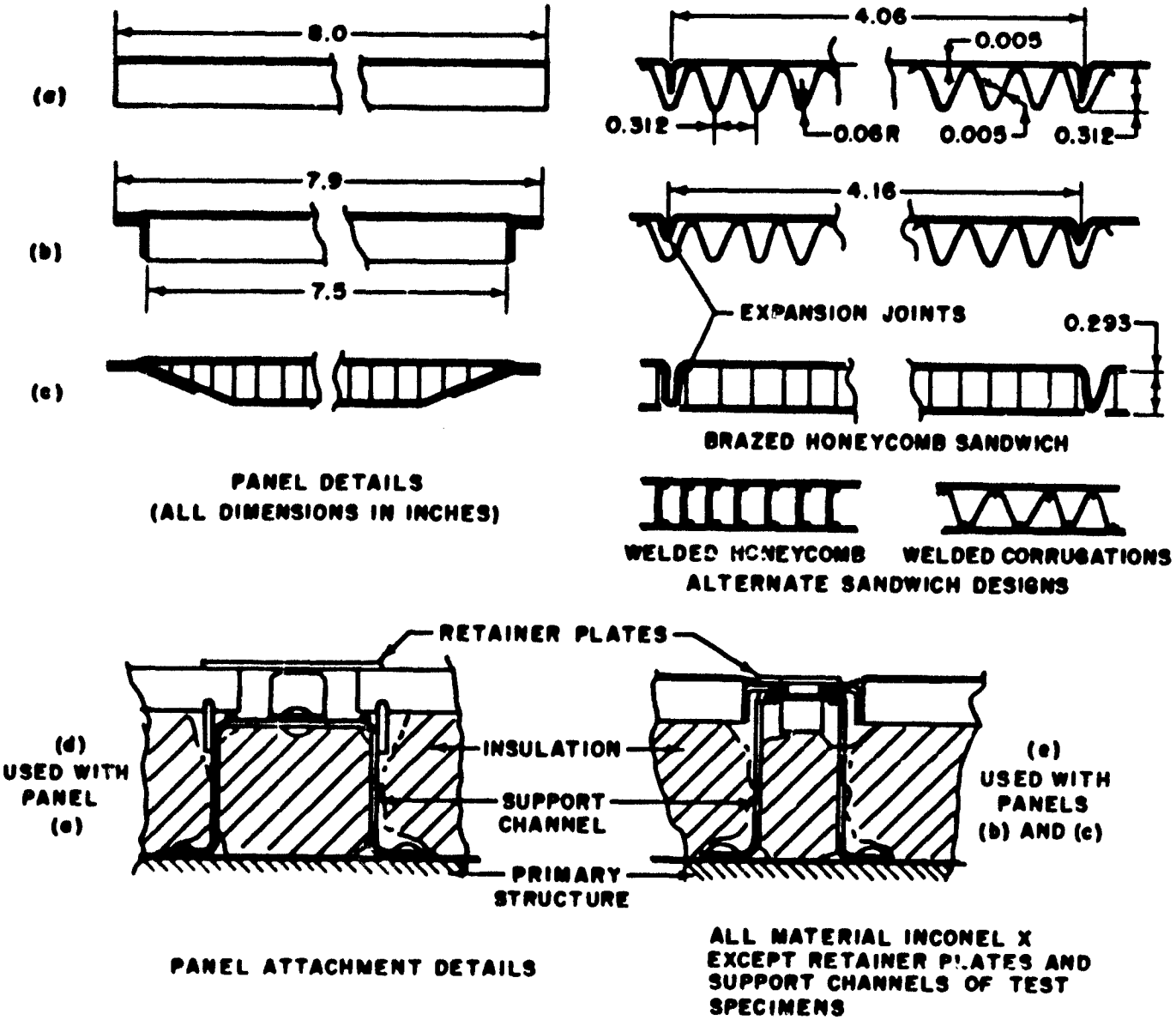

Figure 8. Outer Wall Panel Details

spotwelding was used to fabricate the corrugated panel, while the sandwich panel was brazed. Both types of panels were supported, with freedom to expand spanwise, by using small edge angles, and external retainer strips. Expansion joints were also provided in the skin by Vee-grooves at 4-inch chordwise spacing. Tests in this previous period were conducted only on the corrugated panel. From these tests, together with supporting analysis, objectives for the work of the present period were established.

a. Improved outer wall designs to give better edge sealing, a smoother surface, a minimum of close-tolerance fabrication, and provision for the use of coated and nonmetallic materials.

b. Continued theoretical and experimental investigations of panel flutter; to include transonic conditions and additional panel designs.

c. Wind tunnel tests to investigate panel edge leakage, internal airflow, panel loads, and outer wall drag.

d. Continued transient heating and strength tests, including sandwich panels.

e. Outer wall panels exposed to a stream having high stagnation temperature to check for local high-intensity heating.

f. Panels exposed to representative engine and boundary layer noise.

g. Continued oxidation and strength tests of coated and uncoated materials to extend outer wall usefulness above the limitations imposed by Inconel X.

h. Continued development of low-density ceramic panels for use in the 1700-2500° F temperature range.

i. Continued insulation development to improve resistance to heat and vibration.

Following these objectives, a large number of new outer wall designs were evolved. These designs included:

a. Modifications of the original attachment by removing the retainer strips and attaching the panel directly, using floating nuts.

b. The use of various forms of deep sandwich panels to combine insulating properties and resistance to aerodynamic forces.

c. Sandwich panels with localized attachments depending on support flexibility to absorb panel expansions.

d. Similar to c. but with attachments free to slide and rotate.

e. Sandwich panels attached by links.

In the above designs using sandwich panels with point attachments, an attempt was made to reduce the weight and number of attachments and the thermal leakage path through the insulation, by exploiting the multidirectional stiffness properties of the sandwich panel. All of these designs were based on the use of separate square panels having four attachment points. Two designs which most satisfactorily fulfill all requirements are shown in Figure 9.

In the first of these two designs, the panel is supported by four posts which have freedom to slide and rotate in order to eliminate all restraint against thermal deformations. The sliding surfaces are adjacent to the cool aluminum structure to avoid binding due to oxidation, thermal warpage, etc. The posts are accessible on the outside of the panel to simplify assembly, and are screwed into a high-temperature self-locking insert brazed into the panel. This locking arrangement is patented by The Delron Company, Inc.

In the second design, links are used to obtain complete freedom without relying on sliding surfaces. Edge channels are used to distribute the concentrated loads into the low-strength core material. This is an alternative to the use of inserts and is efficient if the edge member is a necessary part of the panel sealing arrangement. Both the edge member and the insert introduce thermal stresses.

The weights of these improved designs, including the panel, attachment and insulation are 1.59 pounds per square foot and 1.32 pounds per square foot, respectively, which compare with 1.46 pounds per square foot for the designs of Figure 8.

All the attachment designs using localized supports have a common problem of sealing the panel edges. Many seal designs have been evolved on the basis of certain principles which past experimental experience have shown to be important. These include:

a. Minimizing of mass concentration.

b. Avoidance of free edges in thin sheet.

c. No dependence on "spring" in hot areas because of creep effects.

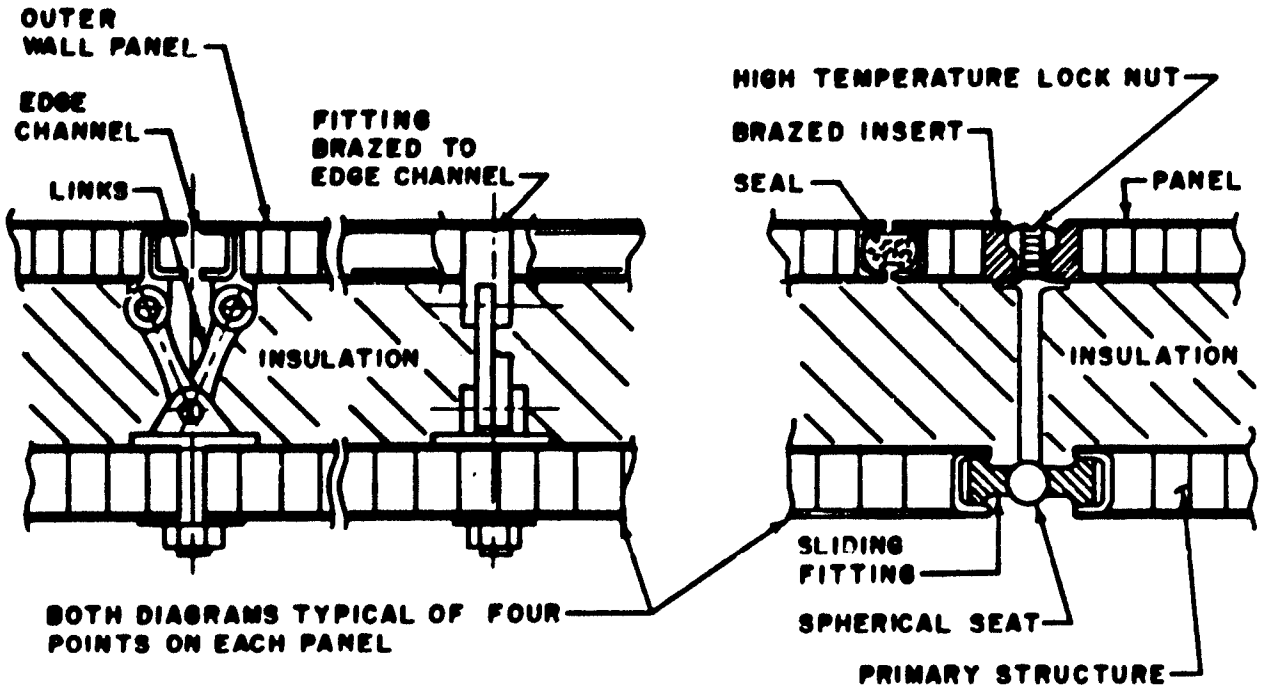

Figure 9. Improved Outer Wall Attachment Designs

d. Avoidance of close tolerance fabrication.

The most promising seal is shown in Figure 9. It consists of a "rope" type material made of very fine fibers of silica or aluminum oxide, either of which have good temperature resistance and freedom from oxidation. These materials are normally very brittle, but by using them in fibrous form, the resilience necessary for a good seal can be obtained.

Studies to improve the resistance of fibrous insulation to mechanical forces such as vibration has led to the experiment of packing the insulation in "bags" of woven "Refrasil". This material is also a high-temperature insulant, but is available only in a fabric form. The result has satisfactory mechanical properties, but is heavy. The use of an open mesh of Refrasil is proposed in order to reduce this weight.

Because theoretical and experimental work on panel flutter is limited and is generally inapplicable to the outer wall panels, an analytical method which utilizes experimental structural influence coefficients was developed and applied to the corrugated panel. The experimental influence coefficients together with "box" aerodynamic coefficients accounted for non-isotropic stiffness, aspect ratio, and edge restraints. These analyses predicted panel stability throughout the range M = 1.2 to M = 4. No analyses were performed for other Mach numbers.

Details of structural tests, and the data obtained, are given in Section C "Test Results". From these test results the following design implications are drawn:

a. The wind tunnel flutter checks show that both corrugated and sandwich panels have satisfactory flutter resistance for flight conditions over the speed range from M = 0.8 to M = 2.5. Tests to M = 4 were not complete at the time this report was prepared. Dynamic pressures considerably in excess of those expected during flight were applied in the theoretically critical speed range around M = 1.4. This suggests that the use of local rather than continuous panel supports will be

satisfactory for sandwich panels, or, alternatively, that the panel stiffness may be reduced.

b. Internal airflow tests demonstrated that the degree of panel sealing which it is expected will be achieved by improved design, is not sufficient to impose excessive loads on the panels. At the same time, the measured quantity of internal airflow was insufficient to disturb the insulation or to significantly increase cooling requirements.

c. Tests on a large model in the NACA Ames Unitary Plan Tunnel demonstrated the feasibility of double-wall construction in supersonic flow at high dynamic pressure. No disturbance of outer wall panels or insulation was observed; panel loads were very small; and internal airflow was insignificant. Drag data have not been reduced at the time of report preparation. This test also shows that no internal airflow problems will arise when better edge sealing is attained with improved designs. The possibility that improvements may increase panel loads has been checked in c. above.

d. Thermal tests on both types of panels showed satisfactory resistance to the transient heating occurring during boost. The corrugated panels were marginal in this respect, emphasizing the importance of avoiding mass concentration, long conduction paths, and thermal shielding in panel and attachment design. Temperature gradients were greater than predicted, suggesting a need for increased emissivity of internal metal surfaces. Strength tests on panel elements showed a much smaller strength reduction with temperature than the reduction of design loads. Excessive strength reduction in the sandwich panels suggests either that the fabrication process must be improved to reduce penetration of the face material by braze, or that a braze material having better strength above 1600°F must be developed.

e. Elevated temperature tests of 0.005-inch foil stock showed Inconel 702 to have great promise as an outer-wall material up to a temperature of 1800°F. Chromalloy Type SA gives adequate protection for Inconel X against oxidation at 2000°F, but when tested at room temperature the material shows brittleness, the cause of which is unknown. Materials investigations of sandwich ceramic outer wall panels are too elementary to state whether this method of reducing the weight of ceramic panels is feasible.

f. Thermoflex RF-300 fibrous insulation, having a nominal density of 3 pounds per cubic foot, shows, from tests conducted to date, to be an adequate material up to 2000°F.

g. Tests of an element of double-wall construction in the Ethylene Jet of the NACA Wallops Island facility, in which the specimen was subjected to Mach 2.0 airflow, showed that the construction can withstand equilibrium temperatures of approximately 1600°F without developing significant hot-spots. The need for reducing outer-wall roughness, therefore, should not be dictated by the occurrence of hot-spot areas.

2. WING LEADING EDGE AND FUSELAGE NOSE

Previous studies of hot-spot areas in the wing leading edge and the fuselage nose were concerned with system analysis for the cooled approach, and material investigations for the heat-sustaining approach. In the present period, structural aspects have been investigated and preliminary designs developed for both approaches. Designs for a cooled leading edge have assumed the use of a sodium system, although this involves a considerable weight penalty, because of the present lack of suitable materials for use with lithium.

For a sodium-cooled leading edge, maximum temperatures are approximately 1400°F, and Inconel X is a suitable material. The principal problems are concerned with accommodating thermal expansion and minimizing temperature gradients and thermal stresses.

The most promising design is shown in Figure 10. It consists of sections 8-1/2 feet long, each supported by six links to permit

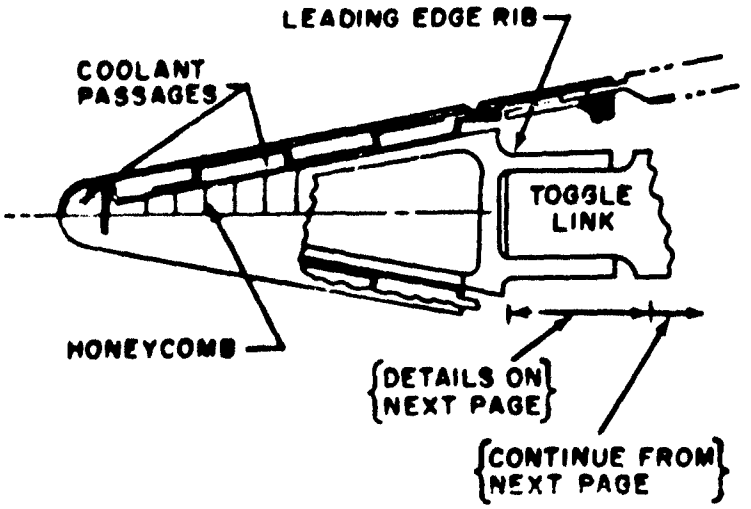

Figure 10. Leading Edge Design

expansion. The leading edge consists of a brazed sandwich structure of light gage material in which the skins are "expanded" in thickness to form thin-walled coolant passages. Supporting ribs are provided at each link, and spanwise beams and an external plate close the gap between the leading edge and the outer wall panels.

This structure is segmented and provided with lightening holes to minimize thermal stresses. Spaces where boundary layer air might enter are filled with fibrous insulation to act as a flow restriction. To minimize chordwise temperature gradients, all coolant flow is in parallel, with one pass along the leading edge section, and return by a separate manifold. Satisfactory checks of airload, pressure, and thermal stresses have been made.

Studies of the cooling system have shown that expansion of lines should be accommodated by flexible double-bellows sections. Expansion loops and sliding joints were found unacceptable because of weight, space, and sealing problems.

Thermal analysis of graphite and silicon carbide shapes, for the heat-sustaining leading edge, has shown that maximum temperatures can be reduced to approximately 3000°F by using a flat, rather than hemispherical, leading edge shape, and by also considering internal conduction. Oxidation tests conducted on a number of coated and uncoated refractory materials (see Section D, Test Results — Hot-Spot Areas) have shown the superiority of silicon carbide or compounds of this material, but no data have been obtained to indicate that it can be used for prolonged time periods at temperatures above 2800°F.

Due to low material strength and large chordwise temperature gradients, thermal stresses introduce another important problem in the design of a heat-sustaining leading edge. Figure 11 shows a typical design in silicon carbide, which has adequate strength for aerodynamic loads. Small sections, and a single attachment stud in each, are used to minimize thermal stresses.

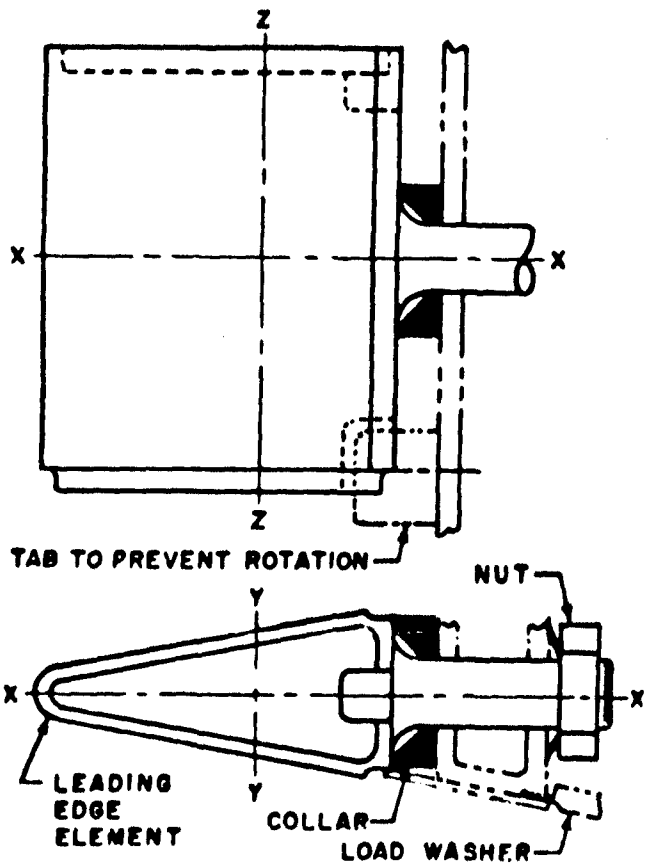

Figure 11. Heat-Sustaining Silicon Carbide Leading Edge

The preliminary studies discussed above have shown promise for the heat-sustaining leading edge, but not feasibility. Many more combinations of material, leading edge shape, internal shape, and method of attachment remain to be examined.

3. STRUCTURAL COOLING SYSTEMS

In previous studies (Reference 5) of the water cooling system for the final stage primary structure, open and closed systems were examined, analytical methods were developed for system optimization, and methods of incorporating cooling tubes into the structure were studied. Experimental work checked cooling tube spacing and thermal gradients between tubes. Weight studies were made of various liquid metal cooling systems for the wing leading edge, together with an analysis of operating conditions for sodium and lithium systems. An experimental evaporative sodium loop was constructed under subcontract by the MSA Research Corporation (previously Callery Chemical Company) and placed in operation.

Tests conducted during the present period on the primary cooling system (Section D) have shown difficulties with resin bonding of cooling tubes to the structure due to low conductivity of the adhesive. A small percentage of aluminum powder was included in the resin, but proved insufficient to improve conductivity. At a later date, a commercially available resin was found in which good conductivity was achieved by the introduction of large quantities of aluminum. Calculations show that this conductivity should be sufficient. No cooling system tests were conducted with this material but strength tests revealed good room temperature shear values despite the large proportion of metal; however, this strength is seriously reduced at operating temperatures.

More successful were tests with tubes clipped to the structure and the fillets filled with an oil-based colloidal copper. Conductivity is good, and tubes can be easily replaced or changed in position, but the oil base gives little control over the placement of material. Other materials have been evolved for future experimentation.

Another test of the cooling system has demonstrated the feasibility of the complete structural unit of outer wall, insulation, aluminum structure and cooling system, by operating continuously and satisfactorily under full-intensity heating. It was found that the heat conducted through the double wall to the primary cooling system agrees well with theory, and that the heat transmitted through the "short-circuits" (outer wall support structure) can be reduced to negligible values by adding insulation between the primary and outer wall support structure.

During this period the evaporative sodium-cooling loop was tested by the MSA Research Corporation (Section C). Objectives of this testing were to show system feasibility and to check operation of a vapor-liquid separator, an expansion valve, and the vapor exhaust nozzle. Apart from initial difficulties with instrumentation and some pump cavitation, all elements of the system functioned satisfactorily. As a result of these tests the following conclusions were drawn:

a. The danger of equipment failure due to air entry is nil, provided that the vapor exhaust system does not plug.

b. The air entry did not complicate cleaning operations.

c. The sodium vapor exhausted will produce dense white smoke and in some cases a yellow flame.

d. Air entry is not considered a serious problem.

Both "open" and "closed" types of systems have been considered. Reference 7 contains an explanation of these systems; a summary of the weight studies is given in Table III.

At the beginning of the present study period, it was considered that lithium would eventually be used as the heat-sink material

TABLE III. EVAPORATIVE LIQUID METAL COOLING SYSTEM WEIGHT COMPARISON

System Type	Open Cycle		Closed Cycle				
Coolant	Sodium	Lithium	Sodium	Sodium	Lithium	Lithium	Lithium
Circulating Fluid	Sodium	Lithium	NaK	Sodium	NaK	Sodium	Lithium
Maximum Leading Edge Temp (°F)	1600	2040	1632	1632	2072	2072	2072
Tank, (lb)	103	52	102	105	54	54	52
Separator mesh and transition (lb)	150	152	150	150	152	152	152
Nozzle (lb)	16	22	16	16	22	22	22
Evap. Coolant (lb)	1068	217	1012	1068	205	209	217
Heat exchanger (lb)	-	-	110	105	103	99	86
Heating elements (lb)	36	36	-	36	-	36	36
Expansion tank (lb)	-	-	17	17	17	17	17
Pump (lb)	440	176	480	400	480	400	160
Total (lb)	1813	655	1887	1897	1033	989	742

for a leading edge cooling system, because of its large heat capacity. Data on lithium are generally meager and, accordingly, a literature survey was conducted by the MSA Research Corporation. Contacts were made with the AEC to obtain the most recent experimental data. Vapor properties and pool boiling characteristics were found to be completely lacking, but corrosion is generally accepted as the most serious problem of lithium systems. The corrosion mechanism is not understood, but may be due to impurities. Corrosion studies are being conducted for the AEC by Nuclear Development Associates. These include the preparation of pure lithium.

The most important advance in structural cooling systems for Brass Bell was made during the present period, with the study and analysis of a system utilizing the sensible heat of hydrogen gas. Gaseous cooling systems were considered in the past, but were discarded because of the large ducts and blowers required, the handling and storage difficulties, and the small rates of heat transfer. These problems are resolved, however, by storage and pumping the coolant as a liquid and by using high pressure (1000 psi) when the coolant is in the gaseous form.

The large heat capacity of hydrogen is due to its specific heat, rather than heat of vaporization, so that temperature rise is important. When heated from liquid to a gas at 1100°F, hydrogen has a capacity which is half that of lithium, but five times that of water. By using it to cool the entire structure, therefore, a net weight saving is possible. The exhaust of high-temperature, high-pressure gas is also available for generation of auxiliary power, with a saving of fuel weight.

Two system arrangements have been considered and are shown diagrammatically in Figures 12 and 13. In both systems, liquid hydrogen is stored in a well-insulated aluminum tank at moderate pressure. After being pumped to 1000 psi in the liquid state, vaporization and temperature rise takes place in a heat exchanger, fed by heat from the cooling system of the primary structure. This heat is absorbed from the structure by the circulation of a water-glycol mixture through a closed circuit. Hydrogen temperature at this point is -60°F, so that there is no difficulty maintaining the aluminum structure at any reasonable temperature.

In the first system considered, the gaseous hydrogen then enters another heat

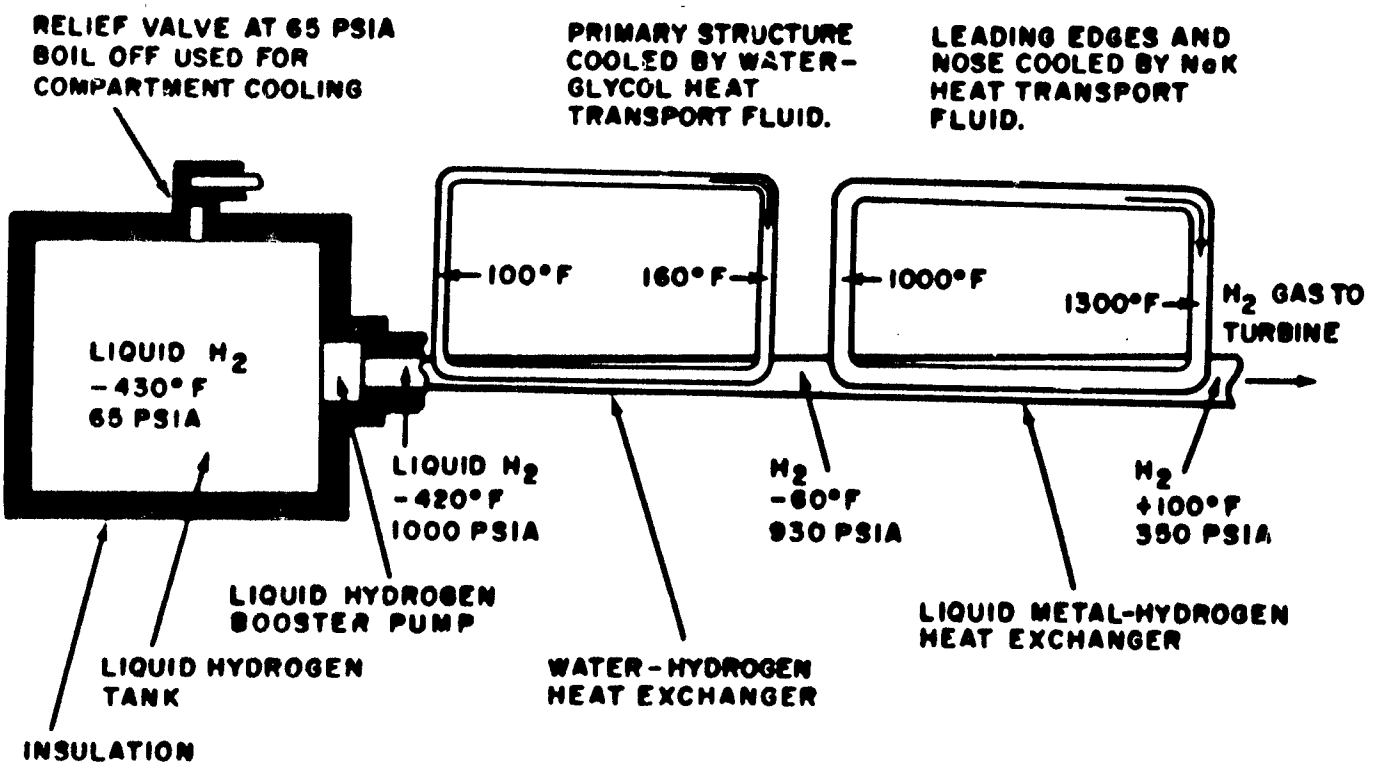

Figure 12. Schematic of Indirect Hydrogen Cooling System

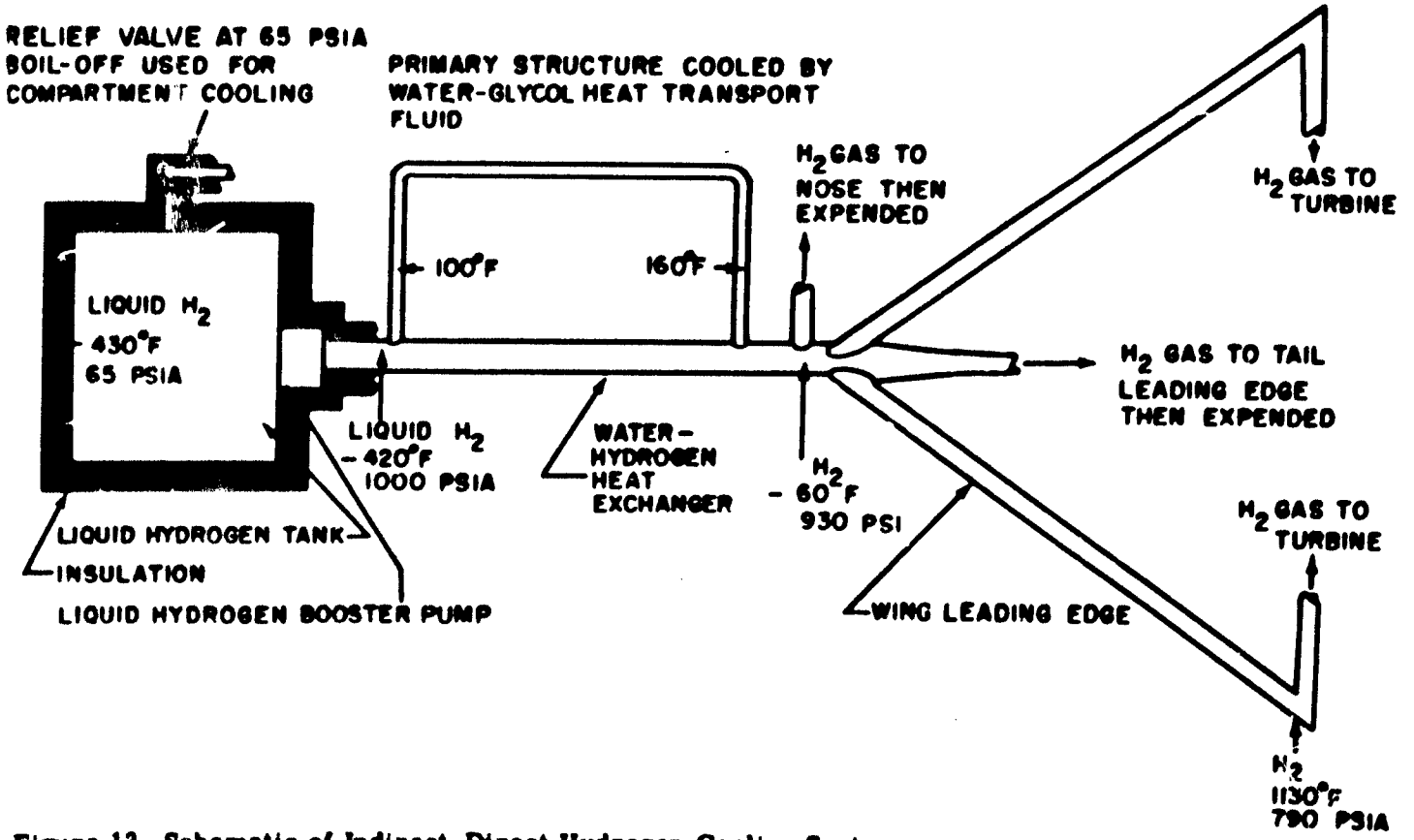

Figure 13. Schematic of Indirect-Direct Hydrogen Cooling System

TABLE IV. COMPARISON OF HYDROGEN COOLING SYSTEMS

Coolant	Hydrogen	Hydrogen
Circulating Fluid — Primary Structure	Water-Glycol	Water-Glycol
— Leading Edge	NaK	Hydrogen
Coolant Weights (pounds)		
Hydrogen	710*	710*
Water-Glycol	85	85
NaK	100	0
Component Weights (pounds) +		
Hydrogen Tank++	295	295
H_2O-H_2 Exchanger ++	15	15
NaK — H_2 Exchanger ++	33	0
Hydrogen Pump	75	75
H_2O Pump	25	25
NaK Pump	125	0
Total (pounds)	1463	1205
System Temperatures (°F)		
Hydrogen, Tank	-430	-430
Hydrogen, H_2O-H_2 exchanger	- 60	- 60
Hydrogen, outlet	1100	1100
Leading Edge, maximum	1400	1375
System Pressures (psia)x		
Hydrogen, tank	65	65
Hydrogen, pump outlet	1000	1000

* Includes 20% for in-flight boil-off and reserve.

\+ Leading edge and piping weights assumed the same and are not included.

++ Includes insulation.

x Pressure drop in distribution lines has been neglected.

exchanger where its temperature is raised to 1100°F by leading edge heat transported by a closed loop through which NaK is circulated. In the second system, the gaseous hydrogen is ducted directly to the nose and leading edges where it absorbs heat. Table IV shows typical characteristics of these two systems from which the weight advantage of the second system is evident. The principal disadvantage of this system is the possible danger of circulating gaseous hydrogen through a hot structure.

From Table IV, the maximum leading edge temperature using hydrogen systems is

1400°F. This is a particularly important advantage when compared with the evaporative, lithium systems because structural materials are available which have adequate strength, oxidation resistance, and other properties at this temperature. Both hydrogen systems are entirely feasible and are not dependent upon any materials development. Considerable experience is also available with circulating NaK loops similar to that used in the first of the two hydrogen systems described above. From a study of complete systems, including evaporated coolant, the use of hydrogen offers a 200-pound weight saving when compared with lithium. This saving can be increased by approximately 250 pounds if some APU fuel is saved by generating power from the exhaust hydrogen. It is expected, however, that this latter benefit will be offset by a slightly increased fuselage length, due to the large volume required for liquid hydrogen.

4. BOOSTER STRUCTURE

Because the structure of the first-stage booster represents a significant portion of the total structural weight of the vehicle, strength-weight studies of various portions of the booster structure have been conducted in previous study periods. These studies have included the analysis of various head configurations, and the study of the cylindrical portion of the booster. It was found that an insulated, ring-stiffened aluminum alloy construction would weigh less and possess other advantages over an unprotected booster of the same construction, but made of heat-resistant material. More efficient constructions of steel, in which the cylindrical shell has greater longitudinal stiffness, such as sandwich or longitudinally-stiffened construction, were not considered suitable because of the high degree of thermal stress which would be present and which would appreciably reduce the compressive strength. The aluminum construction was considered to be insulated with the same outer wall panels as used in the final-stage vehicle.

In the present study period, the previous work on the cylindrical portion of the booster was reviewed, considering the reduced thermal environment associated with a zero-lift type of flight plan, in order to provide weight data by which to optimize, at a later date, the final vehicle flight plan. In addition, the significance of the method of vehicle support and design loading conditions was estimated in terms of structural weight.

It was found that unprotected booster skin temperatures were appreciably reduced from those computed for the lift flight plan; however, the resulting thermal stresses in the area of propellants at subatmospheric temperature were still too high for either steel or uninsulated aluminum construction.

Protected forms of aluminum alloy construction, other than the ring-stiffened 6061-T6 shell construction previously proposed, were investigated. These were sandwich construction, which proved to be the lightest, and ring and longitudinally-stiffened construction which fell between the weight of the sandwich and ring-stiffened shell constructions. Thermal stresses, arising when the tank is filled with extremely low-temperature propellants (like liquid oxygen) were considered large enough to fracture resin bonds which are quite brittle at these temperatures. For these temperatures, therefore, ring and longitudinally-stiffened shell construction can best be used.

Further optimization information should soon be made available from work performed by Bell Aircraft under Contract AF 33(616)-5268 to the Aircraft Laboratory, WADC/WCLSJ, entitled "Investigation and Design Study for Fuel Stowage in High-Performance Aircraft".

It seems reasonable to believe, for the short flight time of the booster, that a less costly and lighter form of insulation than outer-wall panels can be developed. Expendable insulants for this and other applications are currently under study by Bell Aircraft under Contract AF 33(616)-5306 to the Aircraft Laboratory WADC/WCLSS-2, entitled "Insulation of Airframes Subject to Aerodynamic Heating".

In the study of other loading conditions for the booster, it was found that the lower

50 feet is designed by a ground wind condition which introduces large bending moments, the reduction of which by other launching support techniques would result in an appreciable weight saving. A further reduction in weight would be possible (on the order of 500 to 1000 pounds) if the portion of the cylindrical shell which shrouds the engine compartment could be eliminated by, perhaps, making this structure part of the ground installation.

5. CORRELATION OF HEAT TRANSFER DATA

Because of the importance of aerodynamic heating to the structural design and the need for extrapolating heat transfer calculation methods to very high speeds, it is necessary to correlate these methods with all applicable free-flight test data.

Free-flight test information has been provided primarily by the Pilotless Aircraft Research Division of the NACA. The information was obtained from three different vehicles with maximum velocities of 5400, 10,400 and 13,300 feet per second, respectively. Temperature measurements were made both at the nose and aft end of the body, where small pressure gradients exist. As a result, they provide experimental checks on both the stagnation point and the flat plate viscous heating theories used at Bell Aircraft.

Comparison of data with the T' Reference Temperature method (Reference 8) showed excellent agreement for all flights for regions behind the stagnation point. For the stagnation regions, a preliminary comparison of methods developed at Bell Aircraft (Reference 9), including recent modifications (Reference 6), has shown agreement of heat flux predictions within 20 per cent. Since equilibrium temperature varies as the fourth root of the heat flux, correlation with equilibrium temperatures is within 5 per cent. This latter value is important to the study of the temperature-resistant leading edge, since feasibility is critically related to temperature. Heat flux is important in the design of the cooled leading edge, but only weight is involved if flux predictions change.

C. TEST RESULTS - DOUBLE-WALL CONSTRUCTION

As noted previously, major effort was directed toward tests demonstrating the feasibility of double-wall construction, and for the development of elements of the construction, including the raising of the surface temperature limits in which the construction can be used. This work includes a functional test of the construction at the NACA Ames Laboratory, flutter-check and hot-jet tests at the NACA Langley Laboratory, and general structural evaluation of the materials and components of the outer wall panel fibrous insulation and water-cooling system at the Bell Aircraft Research Division Laboratories. The flutter-check and hot-jet test programs were planned with the assistance of the Structural Research Division, NACA Langley Aeronautical Laboratory.

The purpose and objectives of the tests and the design implications of the results are contained in Section B. Contained in this section are brief descriptions of the test specimens and setups, the equipment, instrumentation, and test procedures employed, and pertinent results.

1. WIND TUNNEL FLUTTER CHECKS

Previous wind tunnel flutter checks were conducted at the NACA Wallops Island facility at Mach 1.4, atmospheric density, and at elevated temperatures up to 950°F (Reference 7). Flutter occurred in almost all panels tested, with the exception of configuration shown in Figure 8b. However, it was possible to run only one test of the successful configuration. More experimental flutter tests were indicated, particularly at transonic and high supersonic speeds, and at dynamic pressures equal or greater than those which would be encountered by the Brass Bell vehicle.

In the present period, tests were conducted at the NACA Langley Aeronautical Laboratory, Transonic Dynamics Branch, 9 x 12-

inch transonic blowdown tunnel on elements of double-wall construction at speeds between Mach 0.8 and 2.5. The recent completion of these tests permits only the reporting of observations made during the tests, without benefit of the analysis of recorded data. Similar tests at Mach 3.0 and 4.0 at the Gas Dynamics Branch are scheduled for completion late in August 1957.

Two outer wall panel configurations, corresponding to those shown in Figures 8a and 8b were tested. Each specimen consisted of three continuously attached 4 x 8-inch panels held in place by the previously described retainer plates in a specially-built fixture which replaced the floor of the tunnel. There was insufficient room to mount the specimens on outer-wall support structure; however, vibration tests conducted at Bell Aircraft previous to the test, in which the specimens formed a part of a total double-wall element, showed very good agreement in the first natural frequency with the panels subsequently vibrated in the wind-tunnel fixture at the NACA.

The 8-inch panel dimension was aligned normal to the direction of the airflow. The specimens were instrumented with strain gages with which to determine panel frequencies and amplitudes. Figure 14 shows the panel installed in the bed-plate of the tunnel with top and nozzle blocks removed.

The specimens were subjected to the following values of Mach number and dynamic pressure. A transonic nozzle block provided continuously variable Mach numbers from 0.8 to 1.30 with corresponding maximum values of dynamic pressure from 2000 to 3080 pounds per square foot. Supersonic nozzle blocks provided maximum dynamic pressures of 1850 pounds per square foot at Mach 1.41, 3390 pounds per square foot at Mach 1.62, and 2060 pounds per square foot at Mach 2.5.

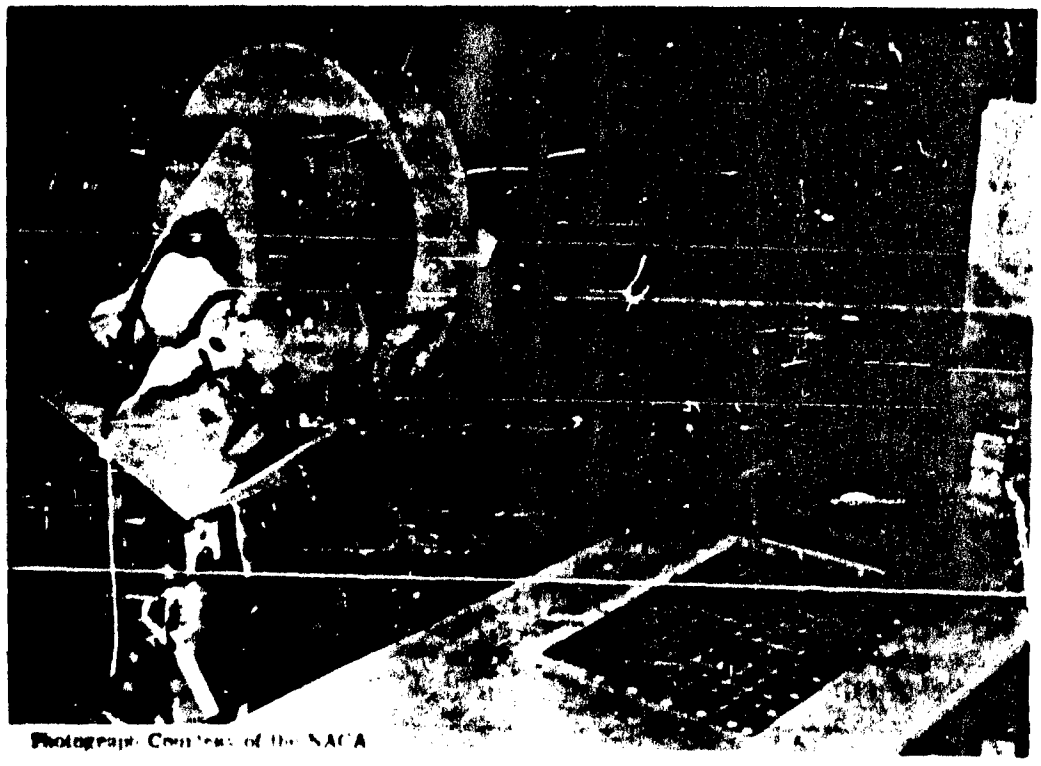

Photograph Courtesy of the NACA

Figure 14. Outer Wall Panels Installed in Floor of NACA-Langley Transonic Wind Tunnel

From observation of the action of the panels, and the strain gage readings on an oscilloscope during the tests, there was no model response that could be identified or suspected as being flutter. Though some motions of the panels were visible at high Mach numbers and dynamic pressures, as determined by strain-gage response, it is expected that the subsequent study of the data will show these motions to directly match the static pressure fluctuations in the tunnel. Examination of the panels after test showed no visible signs of damage.

2. INTERNAL AIRFLOW

An additional series of exploratory-type tests were conducted in the Bell-constructed test fixture described in Reference 7. The fixture accommodates a large element of double-wall construction and permits studying the effects of the leakage area in the outer wall on outer-wall pressure loads, mass rate of internal airflow between the walls, and the effects of this airflow on the fibrous insulation.

The outer wall panel specimen used was of the type shown in Figures 8b and 8e. Though this design should permit less leakage than the previous design tested, it was believed that the difference was insignificant. For this reason, all points of leakage were almost completely sealed with neoprene rubber, and for identification purposes, it was known as Seal no. 1. For some tests, every effort was made to effect a perfect seal (no. 2), using additional strips of rubber over the outer-wall retainer strips and held in place with bolted plates as shown in Figure 15. In one group of tests, no insulation was employed, while in the second group, the insulation was "packaged" in Refrasil bags. Though the Refrasil cloth was relatively heavy and not considered suitable for this application, it was the principle which was being explored. In installing the insulation for the second group of tests, it was necessary to remove the outer wall and replace the sealing, since, as subsequently learned from an analysis of the tests results, it was not possible to duplicate the degree of sealing. The seal types nos. 1 and 2 were reidentified as nos. 3 and 4, respectively.

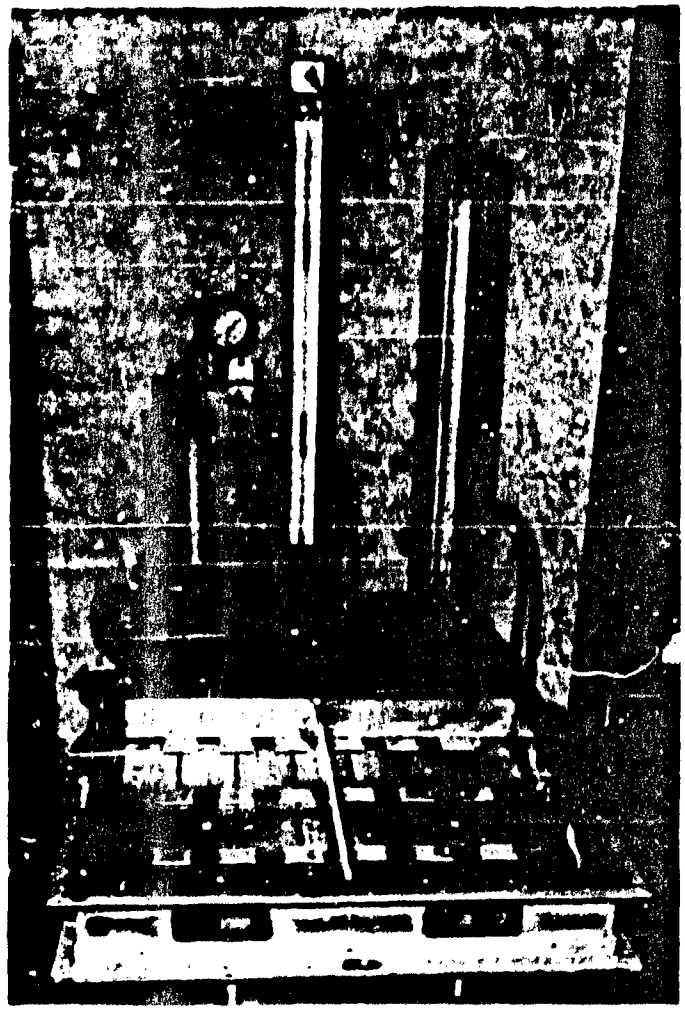

Figure 15. Double-Wall Test Assembly with Special Outer Wall Seal

Pressurized air introduced in the floor of the test fixture simulating the inner wall, or primary structure, which was then expelled through the outer wall (flow type A) (Figure 15), showed more leakage per unit area with the insulation installed than without, signifying the greater importance of the degree of sealing than the presence of insulation. No appreciable difference was found in the leakage when the air was forced through one portion of panels from the outside, made to travel between walls, and expelled in an adjacent area of outer wall

panels (flow type B). This flow is graphically shown in Figure 16, where the airflow through a unit area of outer wall is plotted against the pressure differentials applied.

An additional test was performed to determine the effect of a high degree of outer wall sealing on panel pressure loads which would be incurred during the ascent phase of the vehicle. In this test, Seal no. 2 (smallest leakage area) was used. The test fixture was sealed with ambient air and the portion above the double-wall specimen was vented to an altitude chamber evacuated to one psi. By means of a valve control, the pressure history of the critical ascent path for the vehicle was duplicated as closely as possible. Maximum pressure differential occurred during the initial portion of the ascent period and was measured to be 0.2 psi.

In all tests conducted, the packaged insulation showed no indication of movement or breakdown.

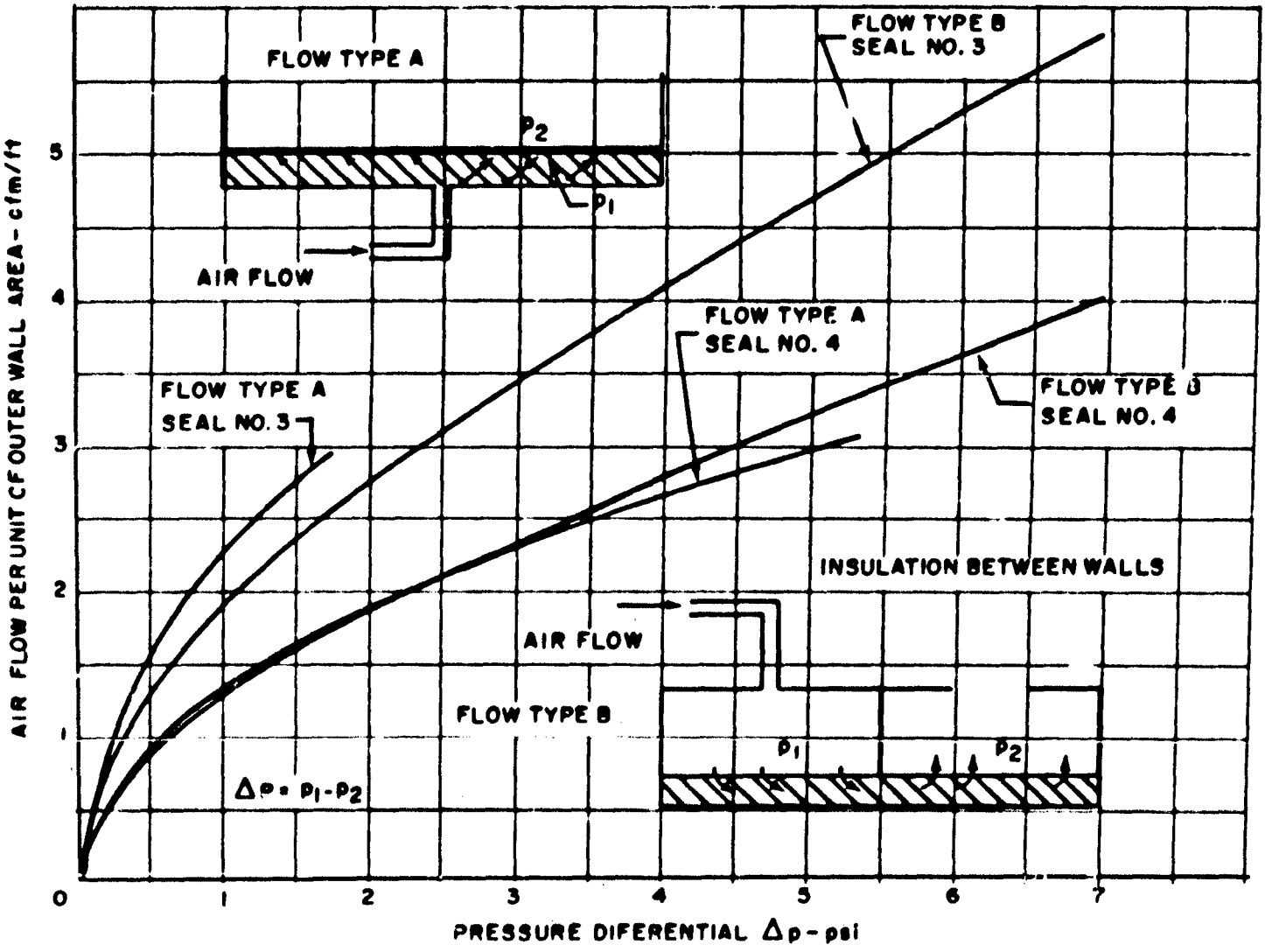

Figure 16. Measured Air Flow Through Outer Wall Panels

3. LOAD AND FLOW CHECKS

The test of a large model containing a full-scale section of double-wall construction in supersonic flow has been considered to be the major test by which feasibility of this novel form of construction can be demonstrated. This test, like the flutter tests previously described, was completed late in this study period, and only observations made during the test can be reported. It was conducted in the 8 x 7-foot Unitary Plan Wind Tunnel of the NACA Ames Aeronautical Laboratory at steady-state Mach numbers ranging from 2.4 to 3.5.

As more fully described in References 5 and 6, the prinicipal objectives of the test program were to explore the general behavior of the construction in supersonic flow, and particularly the effects of outer wall venting on outer wall panel loads, internal airflow between walls, and the action of this flow on the insulation. Aerodynamic heating conditions were not reproduced in this test, and a dynamic pressure of only 700 psf was obtained in comparison with a maximum flight dynamic pressure of 1700 psf, but this dissimilarity is not considered to be significant in evaluating the action of the construction.

The model, as shown in Figure 17, contained a surface area of double-wall construction of 6.6 square feet located on one surface of the model. The design of outer wall panels used and their support structure was that as shown in Figures 8b and 8e. No additional sealing of these panels was made. The one-inch space between the outer wall and the portion of the model representing the primary structure was filled with fibrous insulation. Each of the 24 outer wall panel elements was instrumented with strain gages to measure static and dynamic panel loads. Differential pressure pickups were located within the primary structural element in addition to 24 pressure orifices.

Tests were conducted with the model at angles of attack between ±14.65° for five intervals of Mach number. During the starting condition, the model was buffeted by subsonic and turbulent flow which increased in severity until supersonic flow was established. Loose pieces of the fibrous insulation were observed to bounce around between the walls in that portion of the model visible through the Plexiglas end panel of the model. Appreciable fluctuating panel loads were observed. After supersonic flow was established, the fluctuating pressure loads disappeared. Tufts mounted at the edge of the model behind the Plexiglas end panel showed no indication of flow within the panel. This condition was confirmed by the almost uniform pressures recorded on the inner wall. At large negative angles of attack (with respect to the outer wall panels), however, the Schlieren system indicated a large number of small shock waves originating from the test panel area.

In order to determine the drag effects of the particular outer wall design tested and the supersonic pressure distributions on the model, the outer walls were replaced by a smooth panel containing pressure orifices. All test conditions were repeated with this configuration. These effects will be analyzed as soon as the detailed test data are available.

4. STRENGTH, THERMAL, VIBRATION, AND NOISE TESTS

General structural evaluation tests were conducted on elements of double-wall construction to aid in design-development and to verify methods of analysis. These are continuing-type tests, some of which have been initiated in previous study periods.

a. Strength

Data were obtained on the elevated temperature yield and ultimate strengths, bending modulus, and on the creep characteristics of the corrugated panel configurations shown in Figure 8a. The specimens were approximately 2 x 8 inches, with the corrugations running along the long dimension. After exposure of the specimens to 10 and 100 hours at 1600°F, tests were run at both room and elevated temperatures up to 1600°F. Strength values of the skin or corrugation in compression gave

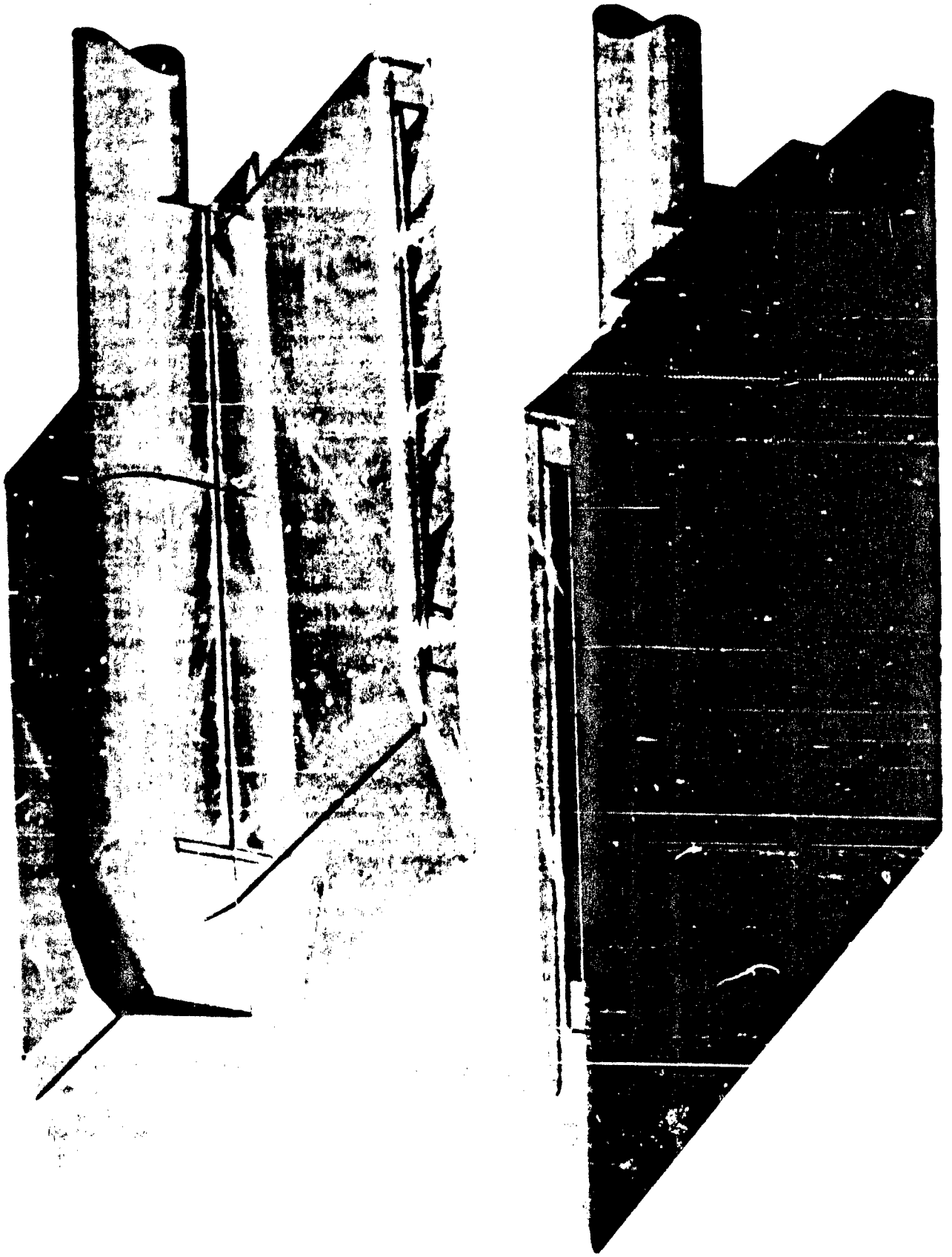

Figure 17. NACA-Ames Wind Tunnel Model

approximately the same values. The yield strength of the panels was defined as the stress at which buckling initiated; the ultimate strength was about 50 per cent higher. Stiffnesses and yield strength, as a function of temperature and in terms of equivalent panel loading, in pounds per square inch, are shown in Figure 18.

Limited creep data were obtained at 1600°F after a 10-hour exposure of the specimens at the same temperature. In one test, a linear creep rate (in terms of center deflection of an 8-inch beam) for a period of two hours, with the panel having a constant applied moment of 20 inch-pounds per inch (equivalent uniform load of 2.5 pounds per square inch), was observed to be 0.00095 inch per minute. In another test, a linear rate corresponding to a moment of 35 inch-pounds per inch was observed to be 0.0098 inch per minute for a period of one hour.

At this writing, the brazed honeycomb sandwich specimens were tested to only a limited degree. Before exposure of the panels for 10 and 100 hours at 1600°F, these specimens exhibited approximately the same strength as the corrugated specimens; however, after these temperature-soaking periods, the honeycomb panels lost a disproportionately large percentage of their strength, and failure occurred in skin wrinkling or tension fracture.

b. Thermal

The initial thermal tests described in the previous study period (Reference 7), were conducted at the NACA, and showed that the original outer wall design was not completely satisfactory. Though the panels, as described in Figure 8a, did not buckle permanently when subjected to initial heating rates as high as 100°F per second, objectionable permanent wrinkling occurred when the panel reached temperatures beyond 1400°F. Thermal tests during this period, therefore, were conducted principally on new, improved panel designs developed in the present and past study periods (illustrated in Figures 8b and 8c).

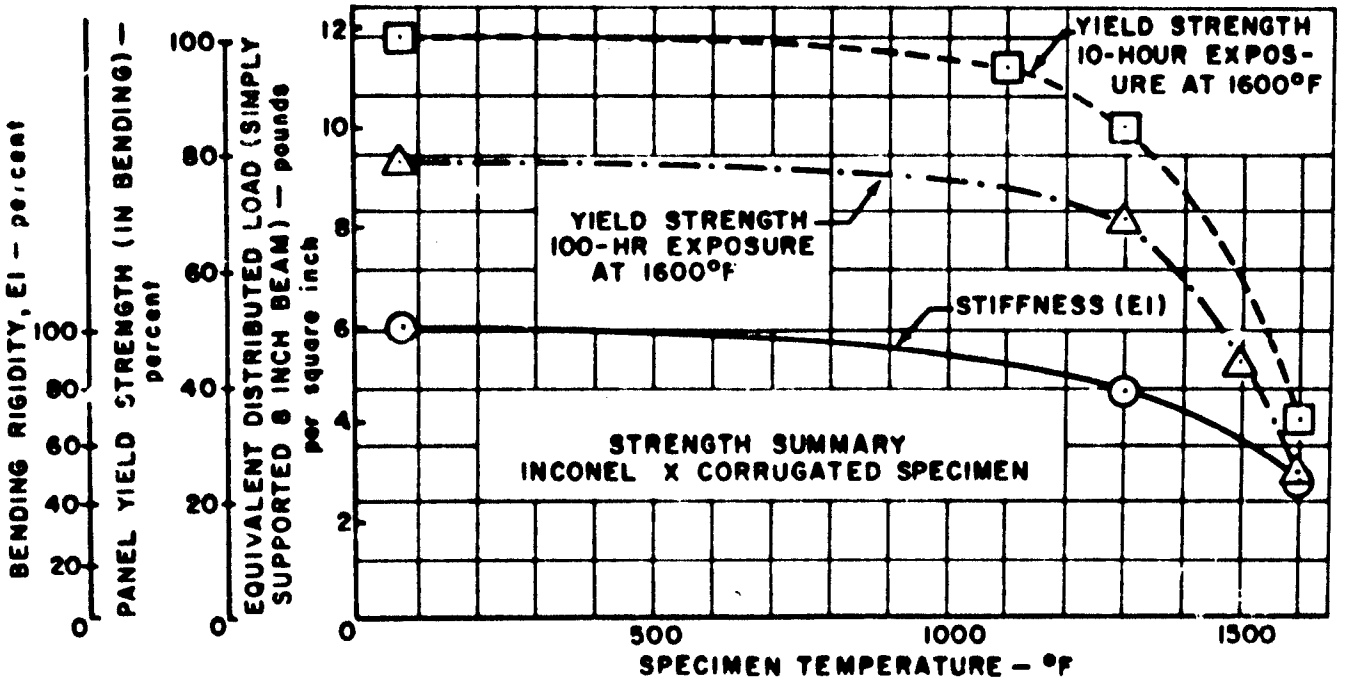

Figure 18. Outer Wall Panel Yield Strengths at Room and Elevated Temperatures after Exposure to 1600 F for 10 and 100 Hours

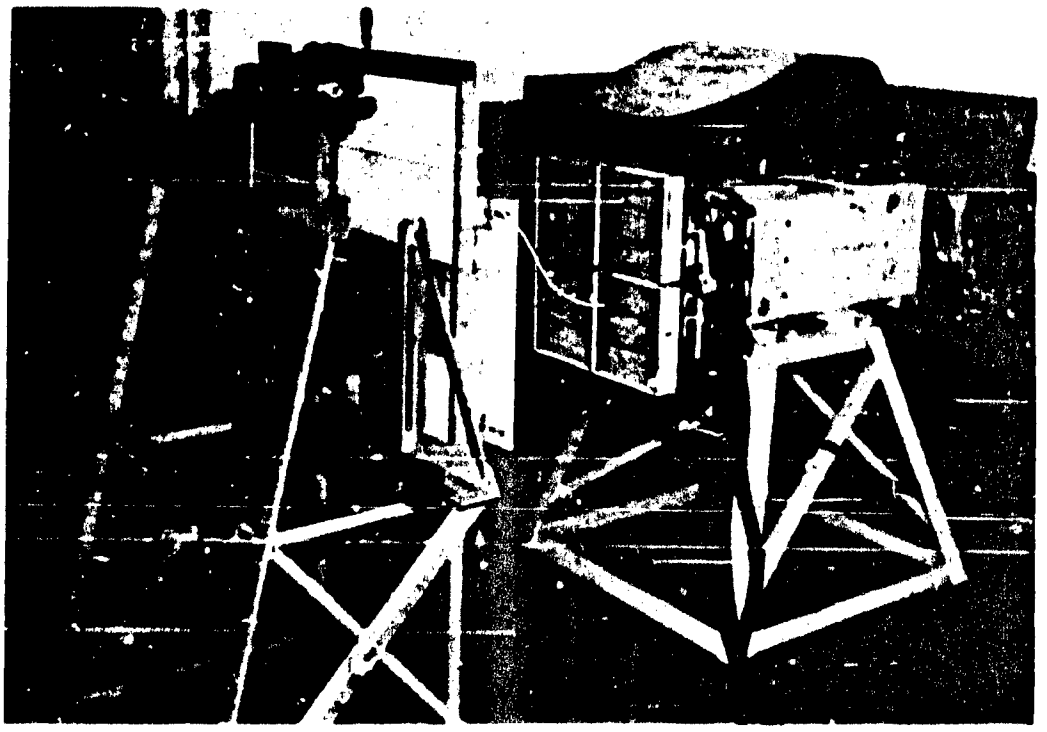

Figure 19. Radiant Heating Facility and Thermal Test Set-Up

These tests involved subjecting elements of double-wall construction to various heating rates and temperatures. Some tests were conducted on special 8 x 8-inch specimens in order to more fully understand the panel wrinkling which occurred in previous tests.

The specimens were three 4 x 8-inch panels, continuously attached by expansion joints, and mounted in a frame simulating the outer wall support structure and retaining plates; fibrous insulation was installed in all test specimens. The panels were radiantly heated by a Bell-constructed tubular quartz lamp facility, approximately 2 feet square, made in accordance with drawings supplied by the NACA Langley Aeronautical Laboratory (Figure 19). Temperature distributions throughout the surface of the specimens and through their depth were measured, along with time-variable deflections of the panel surfaces. In all tests, the maximum temperature of 1600°F was never exceeded. Panel heating rates, reproducing critical and twice critical values which would be experienced by the Brass Bell vehicle in the boost phase, were applied by varying the distance between the specimen and the radiant heater while monitoring panel skin temperature. In order to produce panel failures, high initial and gradually decreasing heating rates were also applied by maintaining a constant distance between specimen and heater.

It was found that the temperature gradient through the thickness in both panel types was approximately 500°F for the heating rates corresponding to the Brass Bell flight path. This gradient produced a maximum center deflection of the panel of 0.125 inch. The gradient was found to be extremely nonlinear. Two types of outer skin buckling occurred in the corrugated-type design. The first, due to the nonlinear temperature gradient, produced small, permanent plate buckles between the corrugations. Figure 20 shows the degree of panel deformation under an initial heating rate of 160°F per second. The second

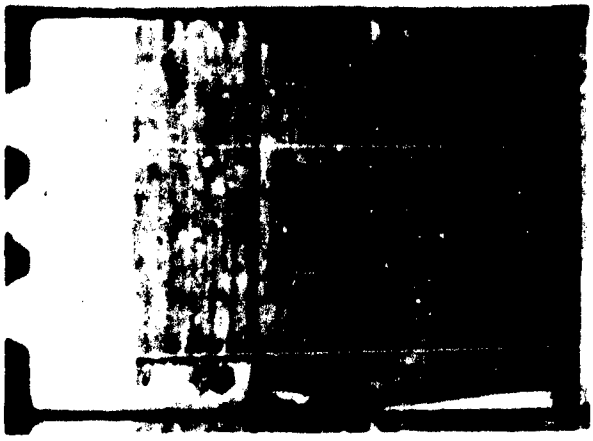

Figure 20. Corrugated Outer Wall Panel Undergoing High Heating Rate Test

type produced permanent wrinkling parallel to the corrugations, concentrated mainly in the two outside panel sections. From much experimentation with these and other panels which were unmounted, it appeared that the wrinkling was due to the nonuniform temperature distribution across the panel face. This gradient (from panel center to panel edge, 1/2-inch from retainer plates) measured as high as 250°F, and was obviously due to the heat capacity of the panel edging and panel supporting structure. It was found that cutting the chordwise edges relieved, but did not eliminate, wrinkling.

Though the honeycomb panel experienced approximately the same temperature gradients through its depth and across its face, no such wrinkling occurred, even though the edging was uncut. Permanent buckling of the skin did occur in individual honeycomb cells adjacent to the corners and edges of the panel. These were first observed at twice the Brass Bell heating rate.

c. Influence Coefficients

The load-deflection characteristics, or influence coefficients, were experimentally determined for the outer wall panel design described in Figure 8b. These coefficients were later used in the flutter analysis performed and are discussed in Section B.

The test specimen consisted of three 4 x 8-inch outer wall panels mounted in a frame simulating the outer wall support and retaining structure shown in Figure 8e. Concentrated loads were applied in increments at 27 stations on the panel's upper surface. Panel deflections at these stations were measured by means of dial gages. Test data were presented in the form of a compliance matrix which, when combined with the mass matrix, yielded fundamental, natural loads and frequencies.

d. Vibration

In order to supply additional data in the study of potential flutter and vibration problems, a test program was carried out to determine the vibration characteristics of the model used in the influence coefficient tests just described. These data were also found to be of value in evaluating the response of the panel in the acoustic test program described below.

The specimen was excited by an electromagnetic shaker which was operated to give a constant inertia loading to the specimen at all frequencies. Static-load calibrated strain gages, mounted on the panel, were used to measure stresses as a function of frequency. Direct measurement of panel amplitudes was accomplished by the use of a "Starrett" depth gage and a crystal phonograph pickup. The instrumentation disclosed a resonance at 525 cps, with the greatest amplitude occurring in the center panel.

e. Noise

Exploratory noise tests, employing discrete frequency acoustic inputs, were conducted on outer wall panel assemblies to determine their response characteristics prior to future, fatigue-life testing of complete double-wall assemblies.

The tests were conducted in the Bell Aircraft Resonant Sound Chamber. Outer

wall panels of the configurations shown in Figures 8b and 8c were frame-mounted, and the frame shock-mounted to an end wall of the chamber (Figure 21). The space between the wall and panel assembly was vented to minimize vacuum loads and was filled with fibrous insulation. The instrumentation consisted of electric strain gages located on the panels, and microphones placed near the specimen to measure sound pressure levels.

The chamber was operated by varying the distance between the driver (shown in Figure 21) and the specimen until resonance of the air column was established. Panel natural frequencies were determined by sweeping through the frequency spectrum at a constant sound pressure level until the response of the strain gages indicated a resonance. Identification of the modes of vibration at predominant resonances was guided by information obtained in the vibration tests previously described. The first panel natural frequency was observed at 560 cps for the corrugated panel, and 600 cps for the honeycomb panel; however, maximum stress levels in the panel were the same for both.

5. OUTER WALL MATERIALS

It was found in the previous study period (Reference 5), that Inconel X foil may be considered to be a suitable structural material for outer wall panels for use at 2000°F and exposure periods up to 24 hours if it could be protected from oxidative deterioration.

Investigations during the current study period were focused on three simultaneous approaches: oxidation-resistant alloys, oxidation protective coatings for alloys having suitable high-temperature strength characteristics but inadequate oxidation resistance, and low-density, high-temperature stable ceramic sandwiches. Major emphasis was placed on the first two approaches.

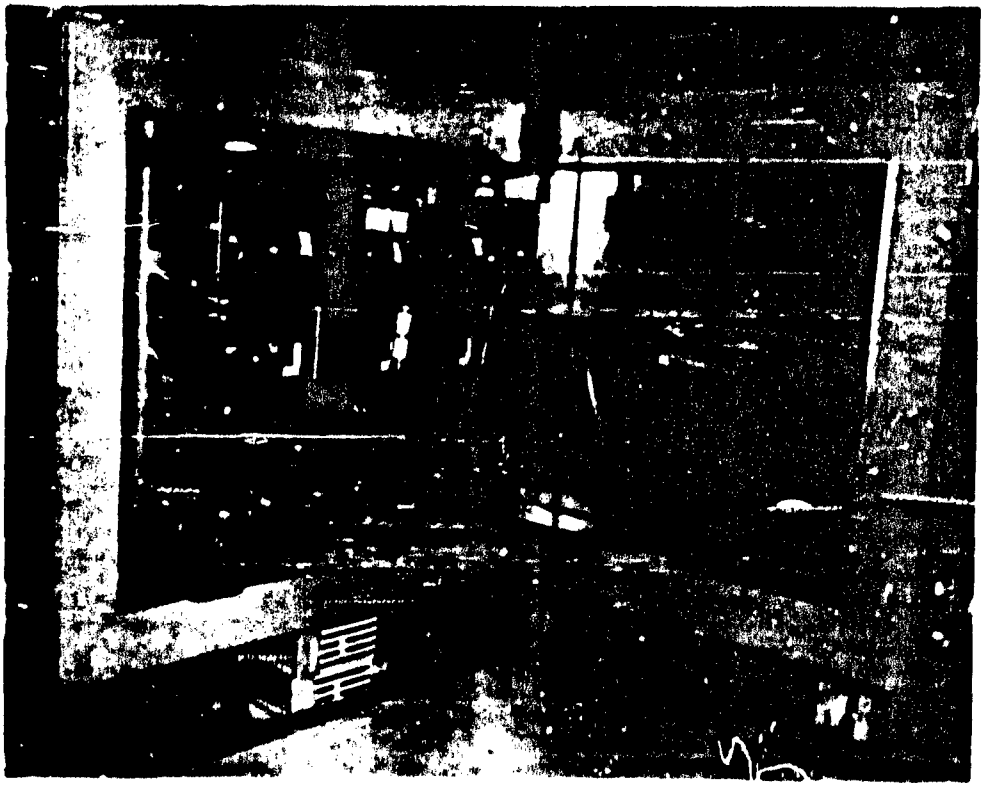

Figure 21. Outer Wall Panel Installed in Bell Aircraft Acoustic Sound Chamber

a. Metals

Published data indicated that bar and sheet stock of Inconel 702, Hastelloy R-235, and Haynes Alloy 25 have oxidative resistance superior to Inconel X. Experimental studies were performed to determine the separate and combined effects of temperature and oxidation on some of the mechanical properties of 5-mil-thick samples of these alloys. The samples were tested at the Bell Aircraft Research Division Laboratories over a temperature range of 1600° to 2000°F for exposure times of 1 to 100 hours.

The studies on Inconel 702 and Hastelloy R-235 expanded the knowledge of the behavior of nickel alloy systems other than Inconel and Inconel X, while the studies on Haynes Alloy 25 enabled comparison of the merits of one of the best-known cobalt alloys with the nickel alloys.

Inconel 702 showed immunity to intergranular oxidation up to 1800°F for periods of time up to 100 hours, and up to 2000°F for periods up to 24 hours. Both Hastelloy R-235 and Haynes Alloy 25 showed substantial intergranular oxidation at temperatures over 1600°F for all test periods (1 to 100 hours). Typical data are presented in Figure 22.

Because metallurgical changes take place within these alloys because of the effect of temperature and not oxidation, the strength of a given cross-sectional area is not neces-

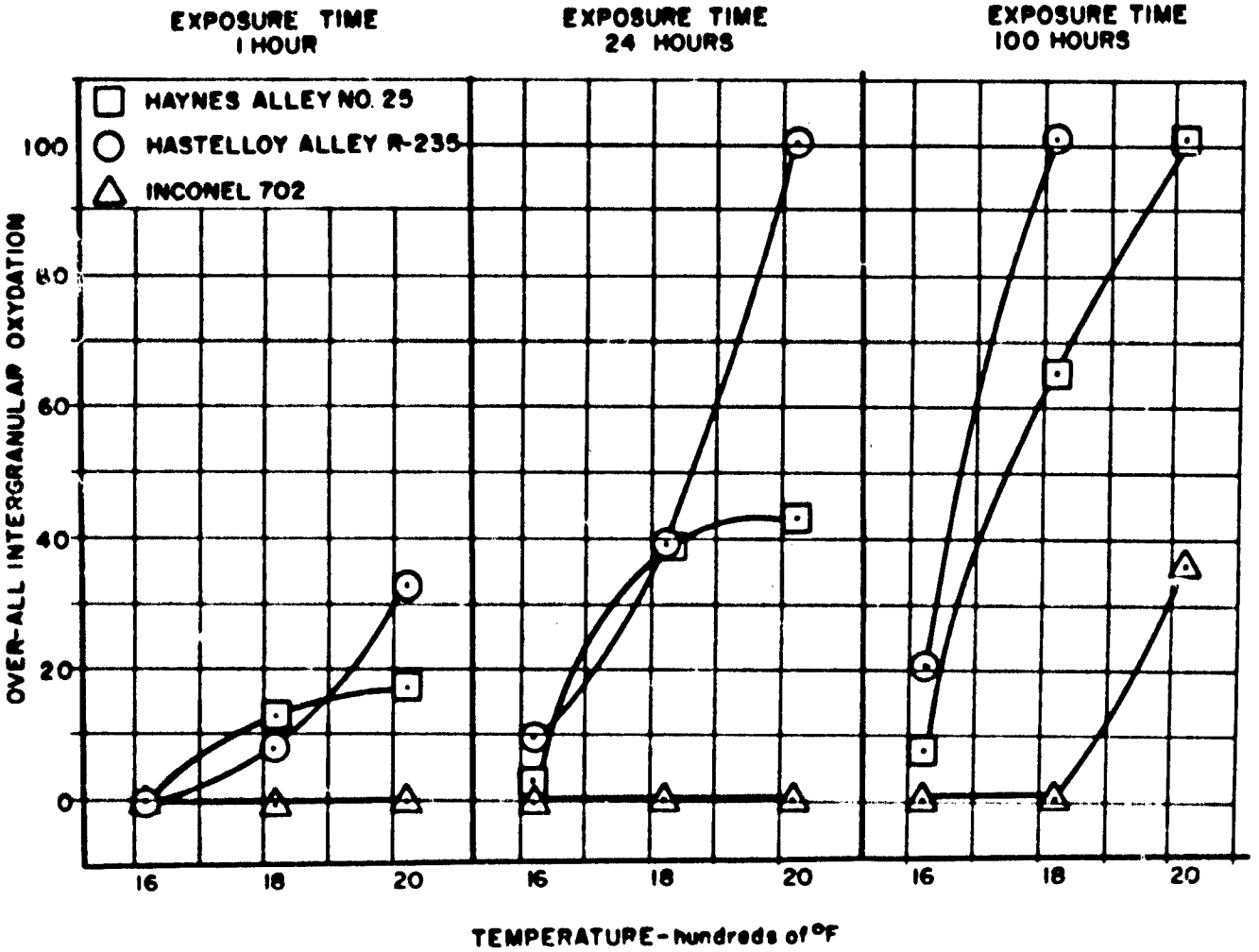

Figure 22. Percent Intergranular Oxidation vs Temperature

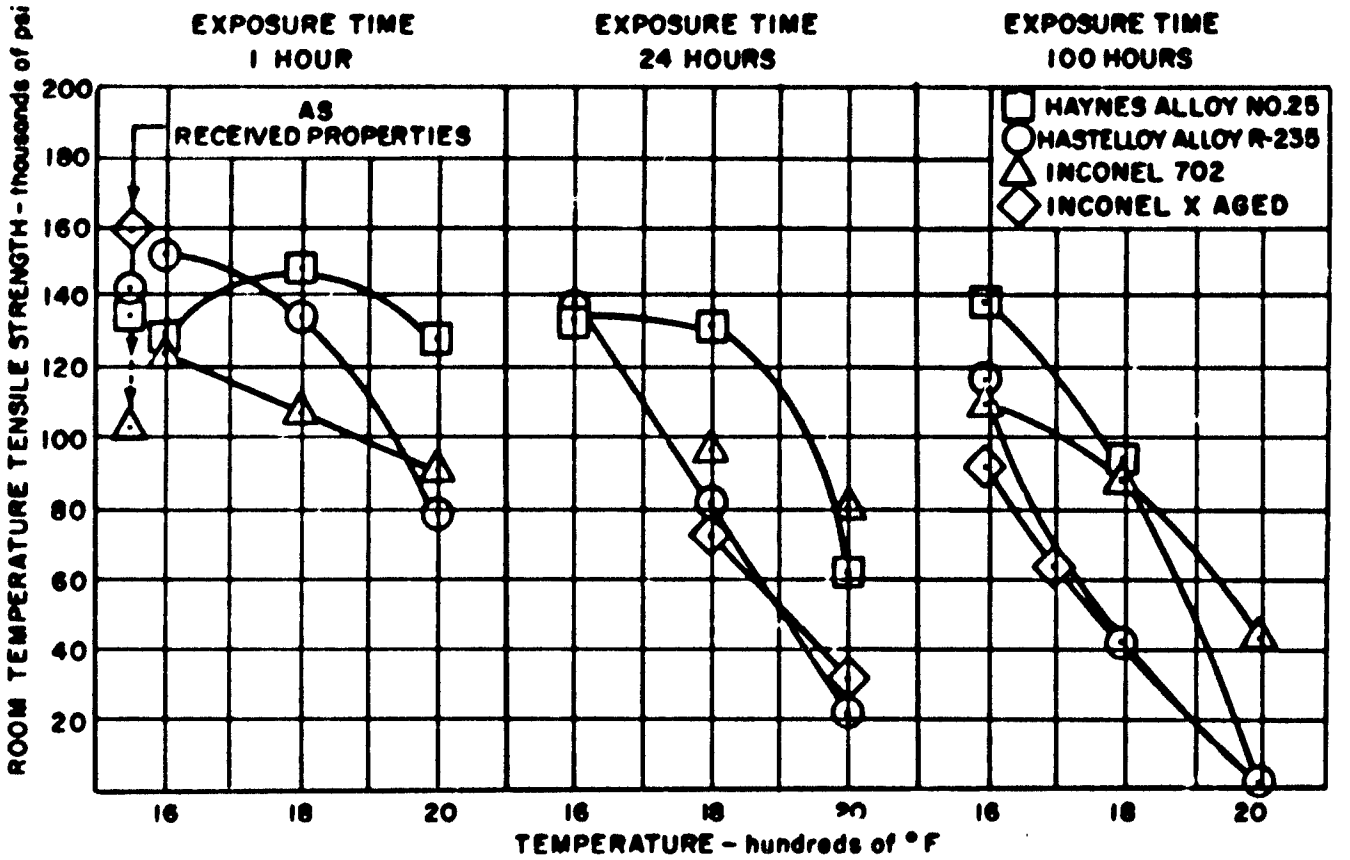

Figure 23. Room Temperature Tensile Strenght vs. Temperature for Various Exposure Times — Air Atmosphere

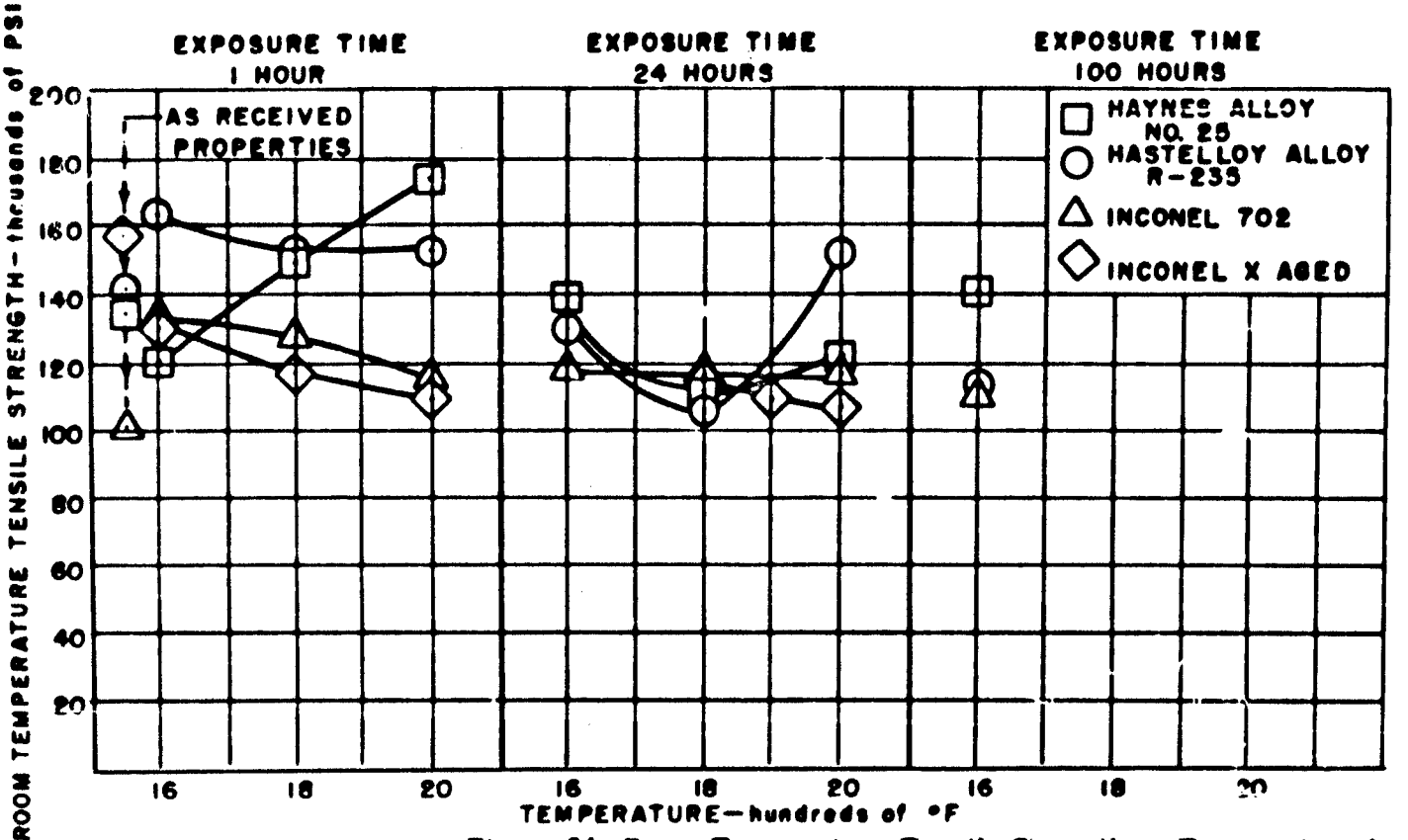

Figure 24. Room Temperature Tensile Strength vs Temperature for Various Exposure Times — Argon Atmosphere

sarily lowered by an amount proportional to the depth of intergranular oxidation. On an absolute strength basis, Haynes Alloy 25 has substantially the same room temperature tensile properties after a one-hour exposure to air at 2000°F as it has at room temperature without such exposure. This is true even though local areas of intergranular oxidation penetrated the cross-sectional area of the test samples by 17.5 per cent. The material does become more brittle, as evidenced by a decrease in its ductility, from approximately 19 per cent to 9 per cent. Considering only room temperature strength after exposure to elevated temperatures, Haynes Alloy 25 appears to be superior to any alloy tested to date after exposure to 1800°F for 24 hours, and exposure to 2000°F for one hour. The room temperature strength of this alloy shows no appreciable deterioration in strength after exposure to an inert atmosphere for at least 100 hours at 2000°F. Typical data for these observations are shown in Figures 23, 24, and 25.

Short-time tensile tests at 1600°F after exposure to air at 1600°F for periods up to 100 hours show the three alloys tested to have strength at these temperatures in excess of originally estimated design requirement values. Short-time tensile strengths at higher temperatures, after exposure to air at such elevated temperatures for periods of time up to 100 hours, are in progress.

It is believed that sufficient test information has been gained during this study period to again affirm the basic premise that metallic materials are available for the manufacture of required outer wall panels. The variation of properties with both time and temp-

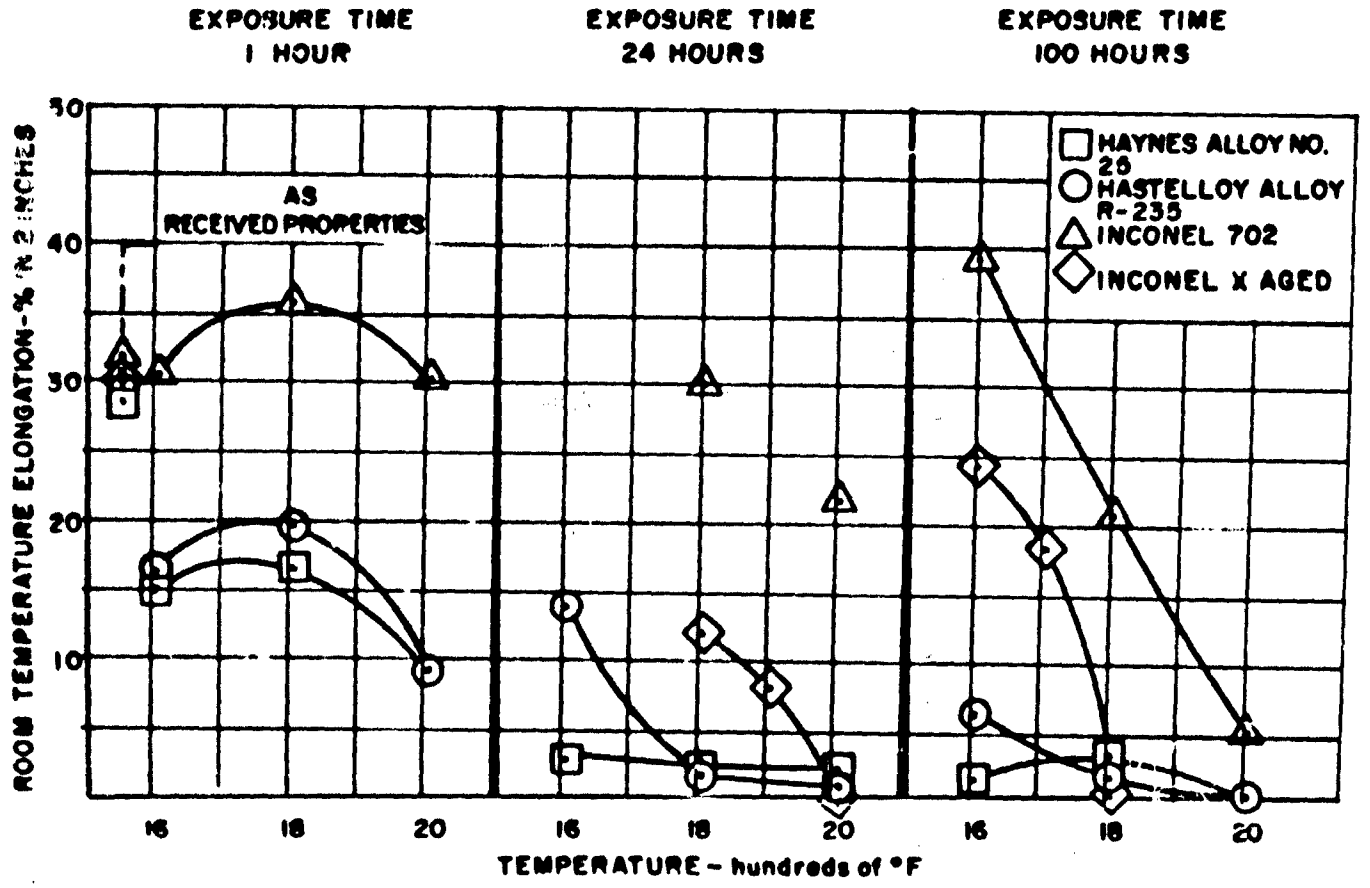

Figure 25. Room Temperature Elongation vs Temperature for Various Exposure Times — Air Atmosphere

erature and the knowledge that all panels will not be subjected to the same time-temperature-load environment leads to the comment that more than one metallic material may be used ultimately for the preparation of these panels for the Brass Bell vehicle.

Exposure of test samples at elevated temperatures in a protective atmosphere indicates that the relative efficiency of the panels may be increased by protecting the alloys from oxidation by the use of special coatings.

b. Protective Coatings for Metals

It was shown in exploratory testing in the previous study period that the Ferro Corporation coating XS-169G offered Inconel X limited protection against air oxidation at an arbitrary test temperature of 2000°F for one hour.

Five ceramic and three metallic types of coatings were evaluated simultaneously during the current study period to determine their suitability as protective coatings for 5-mil-thick Inconel X foil. The metallic coatings appear to be superior to the ceramic ones. Evaluation was based on oxidation resistance, thermal shock resistance, adherence, and flexibility tests. The tests were simple and for screening purposes.

Chromalloy Type SA, a metallic diffusion-type coating, was found to be the most promising coating. It offered excellent oxidation resistance to Inconel X at temperatures up to 2200°F for 100 hours as judged by examination of photomicrographs and flexibility tests. A comparison of Figures 26, 27, and 28 illustrates its effectiveness. Enlargements of photomicrographs of etched specimens indicate that the coating composition and interfacial constituents were altered by exposure at temperatures of 1500 to 2000°F. The nature of these changes and their effects on the mechanical strength of coating Inconel X will be investigated.

There appears to be no inherent limitation to the size or shape of structural elements that can be coated by the Chromalloy Type SA process. A preliminary test conducted in the laboratory affirmed that it is possible to spotweld through the coated metal. Effects of welding and brazing on the oxidation resistance of the base metal remains to be investigated.

It is believed the metallic-type coatings tested will be suitable for protecting other super-alloys against catastrophic oxidative deterioration.

c. Ceramics

A study was initiated to select ceramics for fabrication of low-density sandwich constructions. These structures might be used in place of sections of metallic outer walls in regions where temperatures of approximately 1800 to 2500°F may be encountered. Major emphasis was given to determining the availability of porous core materials for use between solid skins.

Pittsburgh-Corning Corporation's research variety of 19-pounds-per-cubic-foot density Foamsil shows promise for use as a core material for limited temperature and strength applications. The material has a fine-pore structure and noninterconnecting cells. Its room temperature compressive and modulus of rupture strengths are 620 and 328 psi, respectively. The modulus of rupture at 1500°F is 270 psi. Measurements are being performed at higher temperatures. Where higher strength at elevated temperatures is required for core materials, and where heavier materials will not cause a severe design penalty, porous alumina is being considered. The modulus of rupture of an 88-pound-per-cubic-foot density, 50 per cent porous alumina is 2040 psi. Its strength was 2440 psi when coated with 30-mil-thick skins of 10 per cent porous aluminum oxide.

6. MATERIALS FOR THERMAL INSULATION

The work in the previous study period included a general review of insulants, pre-

Figure 26. Photomicrographs Showing Oxidation Resistance of Uncoated Inconel X at Test Temperatures of 1500°F and 2000°F

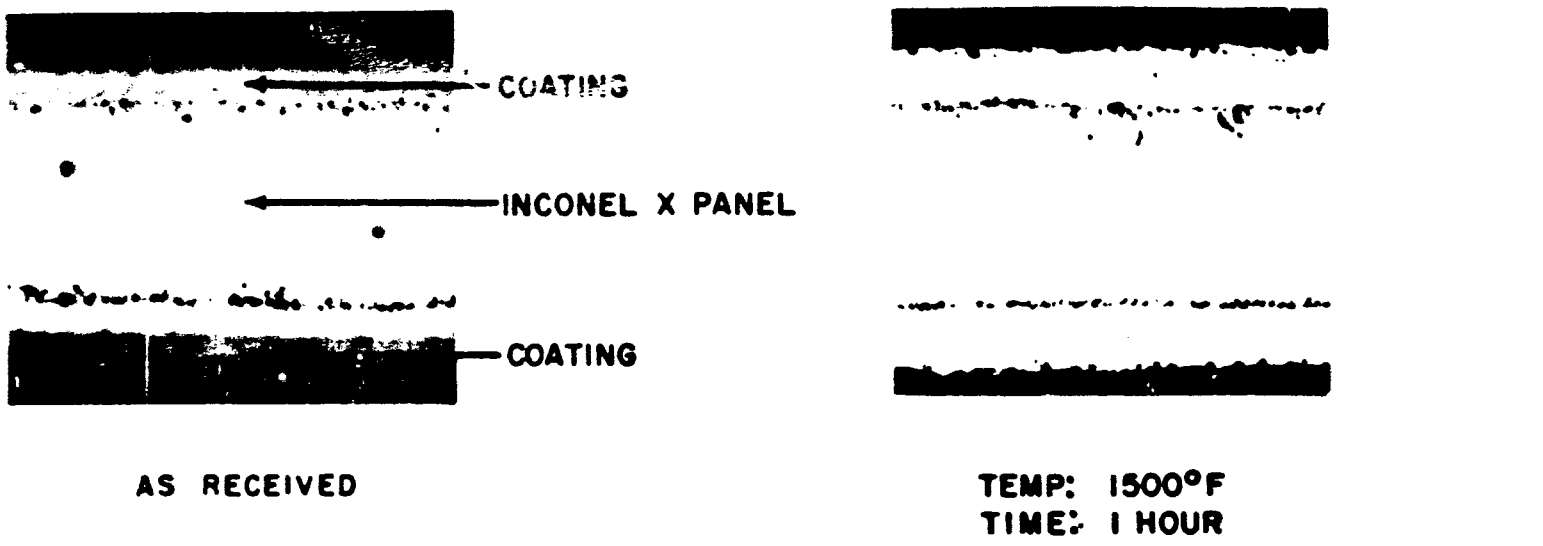

Figure 27. Photomicrographs Showing Oxidation Resistance of Chromalloy Type SA Coating on Inconel X at Test Temperatures of 1500°F and 2000°F

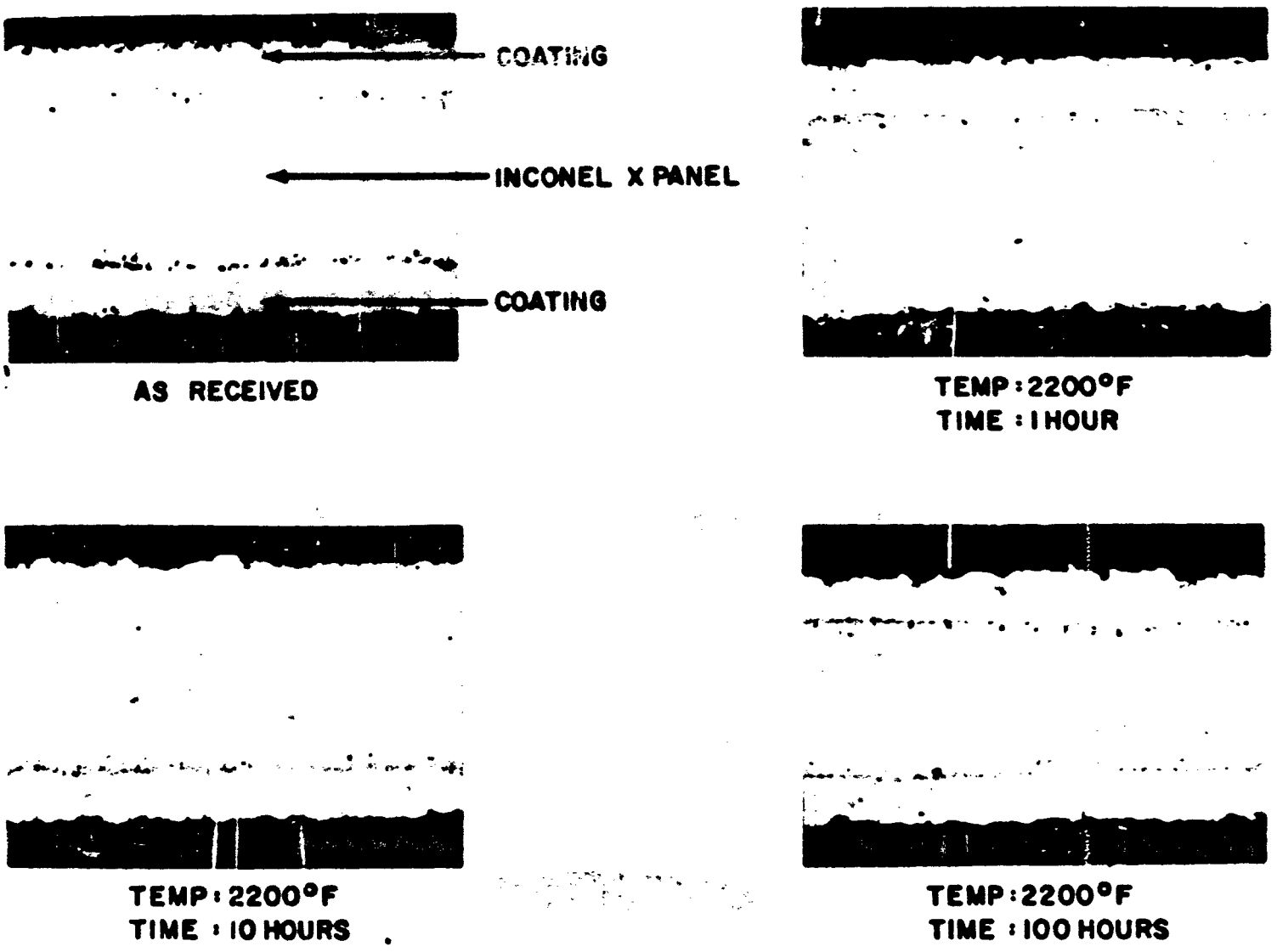

Figure 28. Photomicrographs Showing Oxidation Resistance of Chromalloy Type SA Coating on Inconel X at Test Temperatures of 2200° F

SECRET

liminary tests to determine the effect of heat-soaking of fibrous insulants, and the effect of vibration at room temperature on the insulants before and after heat-soaking.

During the current study period, the resistance of selected fibrous insulants to vibration at temperatures of 1800 to 2000°F for 48 hours was determined. The tests simulated anticipated service conditions by exposing one face of the vibrating insulant to a radiant heat source. No attempt was made to cool the outer face of the insulant, and equilibrium temperatures of 800 to 1000°F were noted. Nominal 3-pounds-per-cubic-foot density Kaowool, Micro-Quartz (formerly Q-Felt), Thermoflex RF-300, and Fiberfrax XSW-1 were tested. Thermoflex RF-300 appeared to be the most promising insulant, since it showed minor shrinkage and no observed deterioration.

A proposal solicited from the Babcock and Wilcox Company for the development of an improved insulant having greater resiliency and strength for "tie-down" purposes was reviewed and considered unacceptable for the following reasons:

a. The proposed research program was based almost entirely upon the assumption that a metallic coating of the fibers of the insulant would yield a more resilient blanket. However, the special metal coating which would be operable under the vibration and temperature "target" requirements was not known and had to be selected.

b. The proposal did not suggest alternate avenues of research and development which might reasonably lead to products fulfilling target requirements.

In discussions with a number of manufacturers of insulation materials, moreover, agreements were reached whereby (and not under subcontract) these manufacturers would submit new development in very high-temperature insulants for evaluation by Bell Aircraft.

7. MATERIALS FOR COOLANT TUBE BONDING

Materials for joining the coolant tubes to the primary structure were investigated; namely, a highly heat-conductive, thermosetting, structural adhesive, and a heat-conductive, nonsetting-type sealant. Major emphasis during this study period was given to the first approach.

Smooth On Manufacturing Company's "Metalset A4", a highly metal-filled room-temperature-setting epoxy resin, was the only adhesive studied that showed promise of meeting the heat transfer and strength requirements for this application. Standard tensile shear tests of aluminum-to-magnesium bonded sheets indicated the adhesive to have adequate strength at room temperature (approximately 2000 psi before post-curing, 2900 psi after post-curing). Its thermal conductivity is reported to be 24 BTU per hour-square foot-°F per inch. However, this value has not been verified as yet, but will be measured in a recently acquired Fitch Conductivity Apparatus. The tensile shear strength of Metalset A4 will also be investigated at temperatures up to 250°F.

8. COOLING SYSTEM FOR PRIMARY STRUCTURE

Tests of the cooling system for the primary structure were conducted on a complete element of double-wall construction. In this way, the cooling system was evaluated under the steady-state heat transfer characteristics of the construction and under more closely simulated conditions than in previous tests. Tests were also conducted on a magnesium honeycomb sandwich element representing the primary structure in order to determine the temperature gradients through the sandwich, and to evaluate adequacy and heat transfer characteristics of two methods of coolant-tube attachment to the primary structure.

The former tests were conducted by placing a 16 x 24-inch section of the double-wall construction described in Figures 8a and 8d, incorporating a closed-cycle ethylene glycol-water cooling system, in front of the Harper Furnace (Figure 29). (See Reference 7 for a description of the Harper Furnace.) Constant average temperatures from 1375 to 1700°F were maintained on the outer wall for extended periods of time, during which the temperature rise of the coolant mass was measured as it passed through the primary structure. The over-all heat conductance of the construction was thus determined for each outer wall temperature. Temperature gradients in the primary structure element were surveyed between coolant passages and at outer wall support points. Additional experimentation was made to determine the reduction in heat transfer to the cooling system by increasing the thickness of insulation between the walls and by insulating the outer wall support structure from the primary structure. The results of these tests are presented in Figure 30.

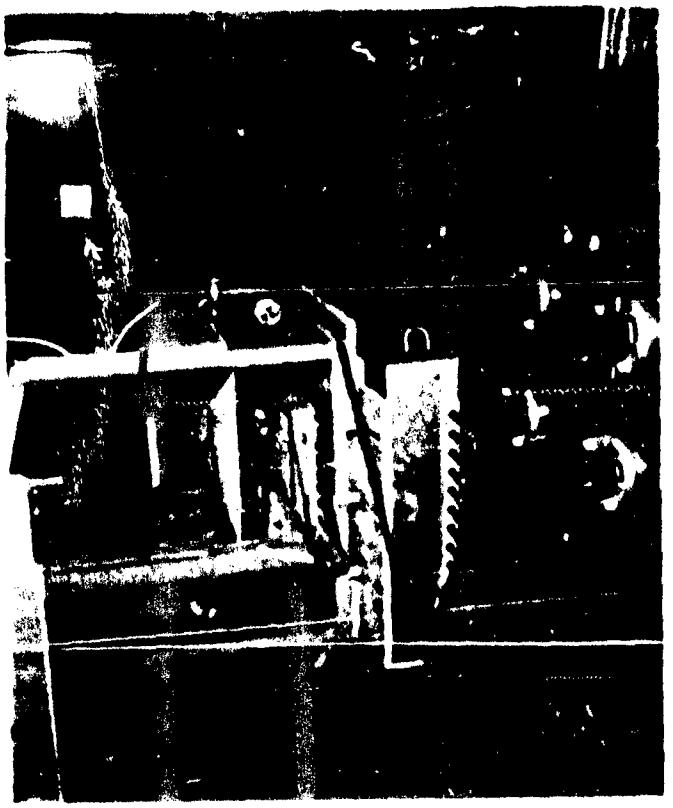

Figure 29. Set-Up for Primary Cooling System Test of Double-Wall Construction Using the Harper Furnace as a Radiation Source

The cooling system tests involving an element of the primary structure only were conducted in the Bell-constructed "Hot Box", in which calculated heat flux rates can be applied (Figure 31). In one experiment, 3/8-inch diameter aluminum tubes, which had been partially flattened for greater contact area, were bonded to the magnesium sandwich with an aluminum-filled epoxy resin. Due to the high heat transfer resistance of the resin, thermal stresses were introduced in excess of the shear strength and ductility of the bond, resulting in failure of the bond. In the other experiment, the coolant tubes were held in place by clips, and a colloidal copper compound applied at the facing surface. This method proved to be satisfactory. A small temperature gradient existed between the tubes and the adjacent magnesium sandwich face; moreover, negligible gradients existed between the two faces of the sandwich element.

9. ETHYLENE JET

In order to satisfy the desire to duplicate, in a single test of double-wall construction, the correct aerodynamic and thermal environment as well as load conditions, an element of the construction was tested late in this period in the Ethylene Jet at the NACA Wallops Island facility. The type of flow and the noise level within the flow emanating from this jet are more severe than the aerodynamic and thermal environment to which the vehicle would be subjected. However, for reasons mentioned later, the outer wall panels tested were reduced to a four-inch width. However, a test in this tunnel would serve to indicate, depending upon when failure of the specimen occurred, the resistance of double-wall construction to supersonic flow under the combined conditions of a high noise level environment, thermal shock, and high equilibrium temperature conditions. Certainly, if failure did not occur below an outer wall temperature of approximately 1600°F, the temperature above which the current test panels would have little strength, the test

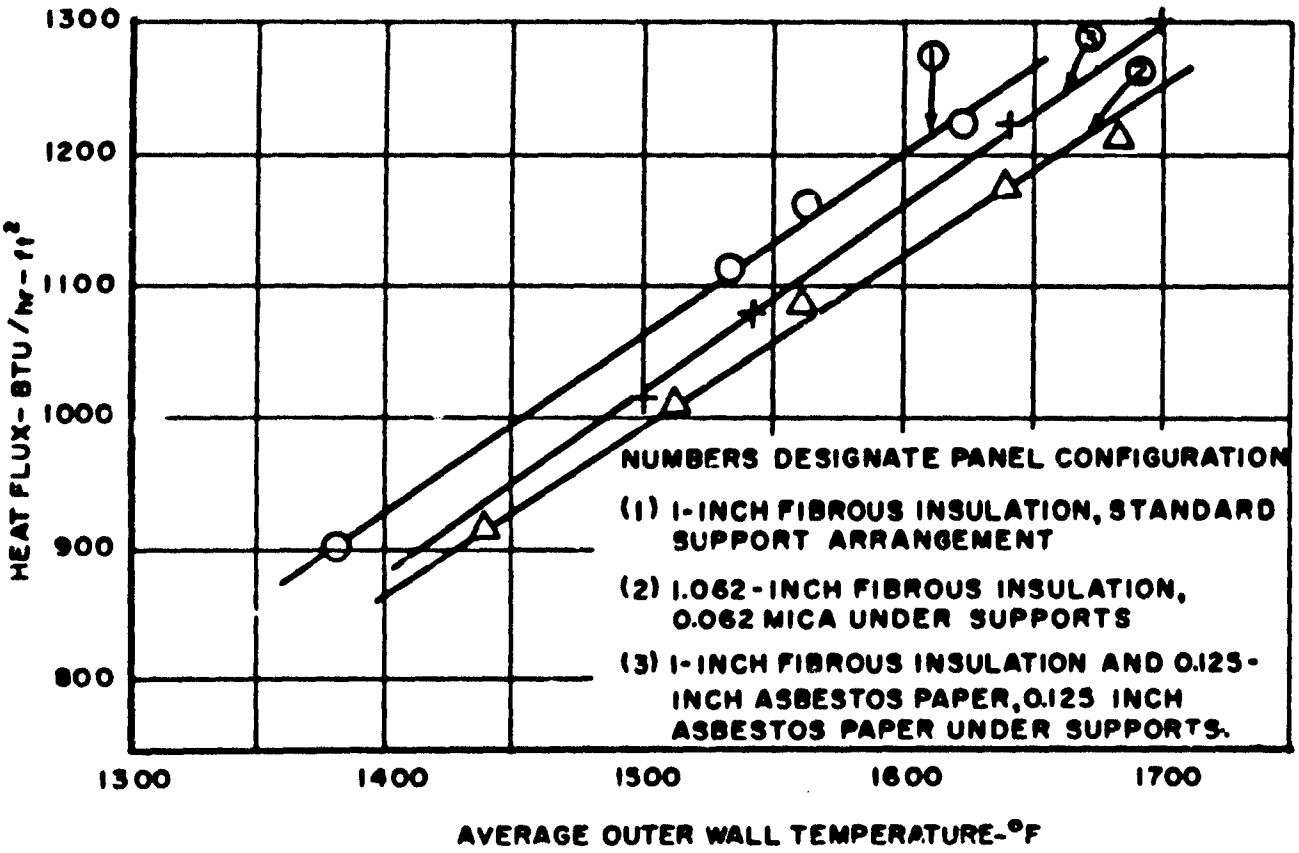

Figure 30. Heat Flux Removed by Cooling System vs Average Outer Wall Equilibrium Temperature

Figure 31. Set-Up for Primary Cooling System Test of Element of Primary Structure Using "Hot Box" Heat Source

would be most significant. The ethylene jet would also permit determining whether the panel expansion joints and gaps between the retainer plates would produce local "hot-spots". Since the composition of the jet is oxidizing, such "hot-spots" would be revealed positively by examining the specimen after test.

Stagnation temperature surveys of the 12-inch exit throat of the ethylene jet showed a marked temperature gradient from the center of the jet to the sides of 500 to 800°F, depending upon the stagnation temperature. For this reason, the specimen was constructed of two bays of three 4 x 4-inch panels of the configuration shown in Figures 8c and 8e. The retainer strips and the outer-wall support structure were located at the centerline of the specimen as shown in Figure 32. Fibrous insulation was also installed. In order to diminish the extreme thermal shock which the jet could impose upon a cold specimen, the specimen was preheated before insertion into the jet stream. Instrumentation consisted of 24 thermocouples located throughout the outer wall panels and on the center retainer strips, particularly to measure temperature gradients in the retainer strips and in the areas of the expansion joints.

The test conditions to which the specimen was subjected are shown in Table V. In all tests, the tunnel operated at Mach 2.0, and the pressure in the jet stream was atmospheric. The equilibrium temperature was measured in the center of each of the first outer wall panels, and thereby represents an average "spanwise" panel temperature; the equilibrium temperature of the center retaining strips should have been about 50°F higher at a stagnation temperature of 1400°F, and 100°F higher at 2150°F.

The specimen survived three runs. In the third run, the tunnel stagnation temperature and outer wall equilibrium temperatures were 2100°F and 1525°F, respectively. The length of tunnel running time per test was 10

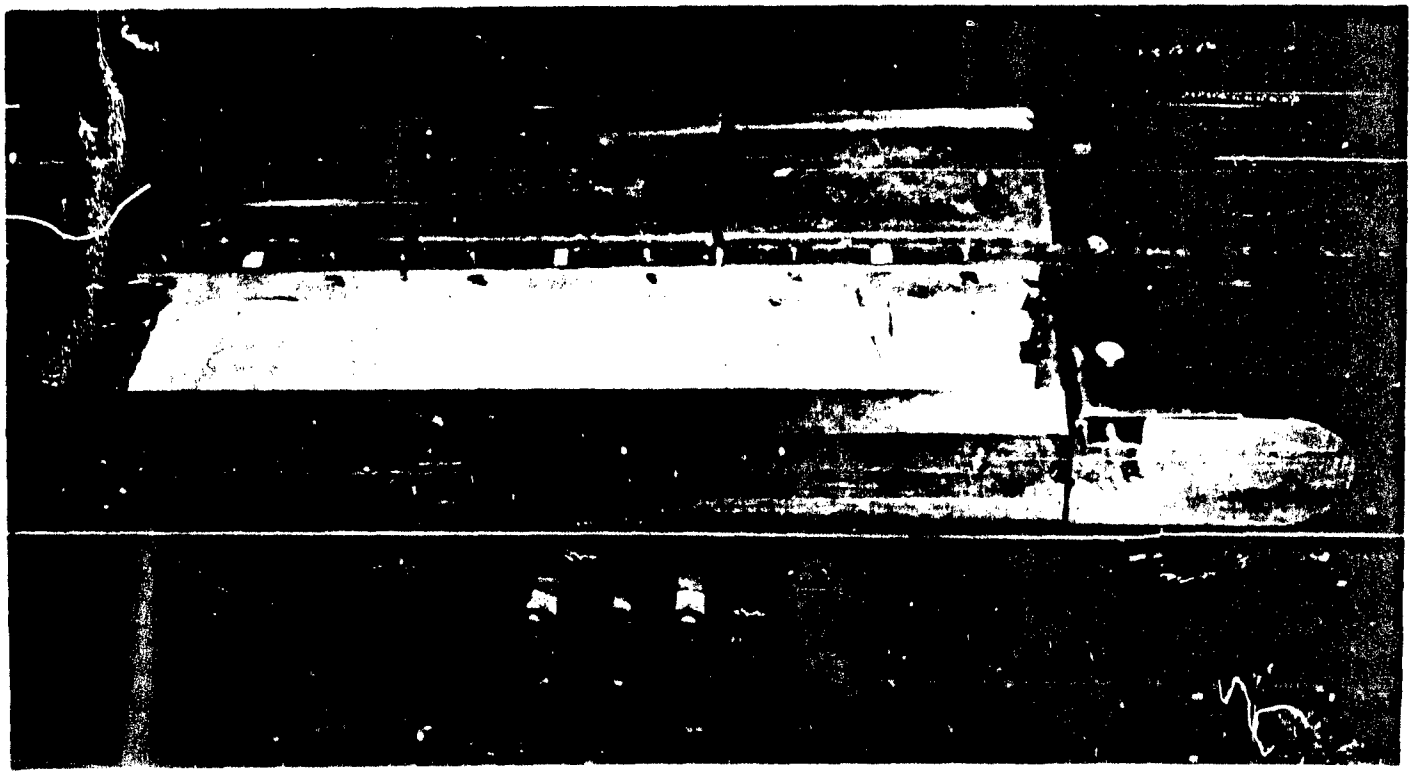

Figure 32. Specimen Used in NACA Ethylene Jet Test (One Length of Outer Wall Panel Removed)

TABLE V. ETHYLENE-JET TEST CONDITIONS

1.	Test Run No.	1	2	3	4
2.	Tunnel Stagnation Temperature (°F)	1650	2000	2100	2450
3.	Panel Temp. in First Panels (Reference Temperature)				
	Preheat (°F)	1093	1420	1085	1578
	Equilibrium (°F)	1278	1528	1525	1965
4.	Panel Heating Rates (After Insertion of Specimen in Tunnel)				
	Initial	37.5	40.5	225	236
	Average	18.5	10.7	43.5	107
5.	Max. Skin Temperature (°F) (Other than Reference Temperature)	1225	1580	1530	1778
6.	Max. Retainer Temperature (°F)	1205	1533	1450	1783
7.	Max. Expansion Joint Temperature (°F)	1034	1564	1530	1928
8.	Time in Jet (seconds)	10	10.1	10.1	3.6

seconds. From a brief and expedited survey of temperatures in the areas of the retainer strips and expansion joints, it was found that the leading edges of the retainer strips showed about 140°F rise over the temperature in the remaining length, and that the area of the expansion joints was the same or less than in the central panel. The specimen was examined following each test for local oxidation, and no indications of such were found. The specimen heating rate in Test Run No. 3 was much greater than the calculated Brass Bell rates. The specimen failed during the fourth run when the typical equilibrium temperature of the panel was 1750°F (one of the first panels reached 1965°F), a temperature at which this configuration of outer wall construction has negligible strength. When the high-speed photographs taken of the specimen during the test are developed and made available, the manner in which the panel failed will be determined and analyzed.

D. TEST RESULTS - "HOT-SPOT" AREAS

As discussed in Section B, the approach to structural design for hot-spot areas, such as the wing leading edge, has included investigations of cooling with liquid metals, and "temperature-resistant" designs. Supporting tests were performed on a sodium evaporative-cooling loop and on the strength and oxidation resistance of certain refractory materials.

The purpose and objectives of the tests, and design implications of the results, are contained in Section B. The present section contains brief descriptions of the test set-ups, equipment, instrumentation together with the procedures employed, and pertinent results.

1. LIQUID METAL COOLING SYSTEM

During the present period, tests were conducted under subcontract by the MSA Re-

search Corporation, on a sodium evaporative-cooling loop constructed during the previous study period, and described in Reference 7. This loop used an existing furnace through which sodium was circulated by an electromagnetic pump, at a pressure between 4 and 20 psi, depending on the test. The sodium left the furnace at approximately 1400°F, passing through a flow-restricting orifice into a low-pressure evaporator. Under the low pressure, some of the sodium evaporated and the vapor was passed through a wire mesh separator to remove unevaporated liquid, and then through an exhaust nozzle. The vapor was collected and condensed, while the unevaporated sodium was recirculated.

The system was operated for a total of 650 hours, with 180 hours of operation at maximum temperatures between 1100°F and 1400°F. Operating characteristics were observed, and pressure and flow data applicable to the design of the expansion orifice and the exhaust system were obtained.

Performance of the wire mesh separator was shown to be particularly satisfactory. Measured values of sodium condensate agreed with values calculated from temperature rise and flow rate through the furnace, within experimental error. Inspection of the interior of the loop, following the completion of testing, showed only traces of corrosion and erosion, with no evidence of blocking due to mass transfer.

The loop was subsequently modified for operation at a higher temperature (1600°F),

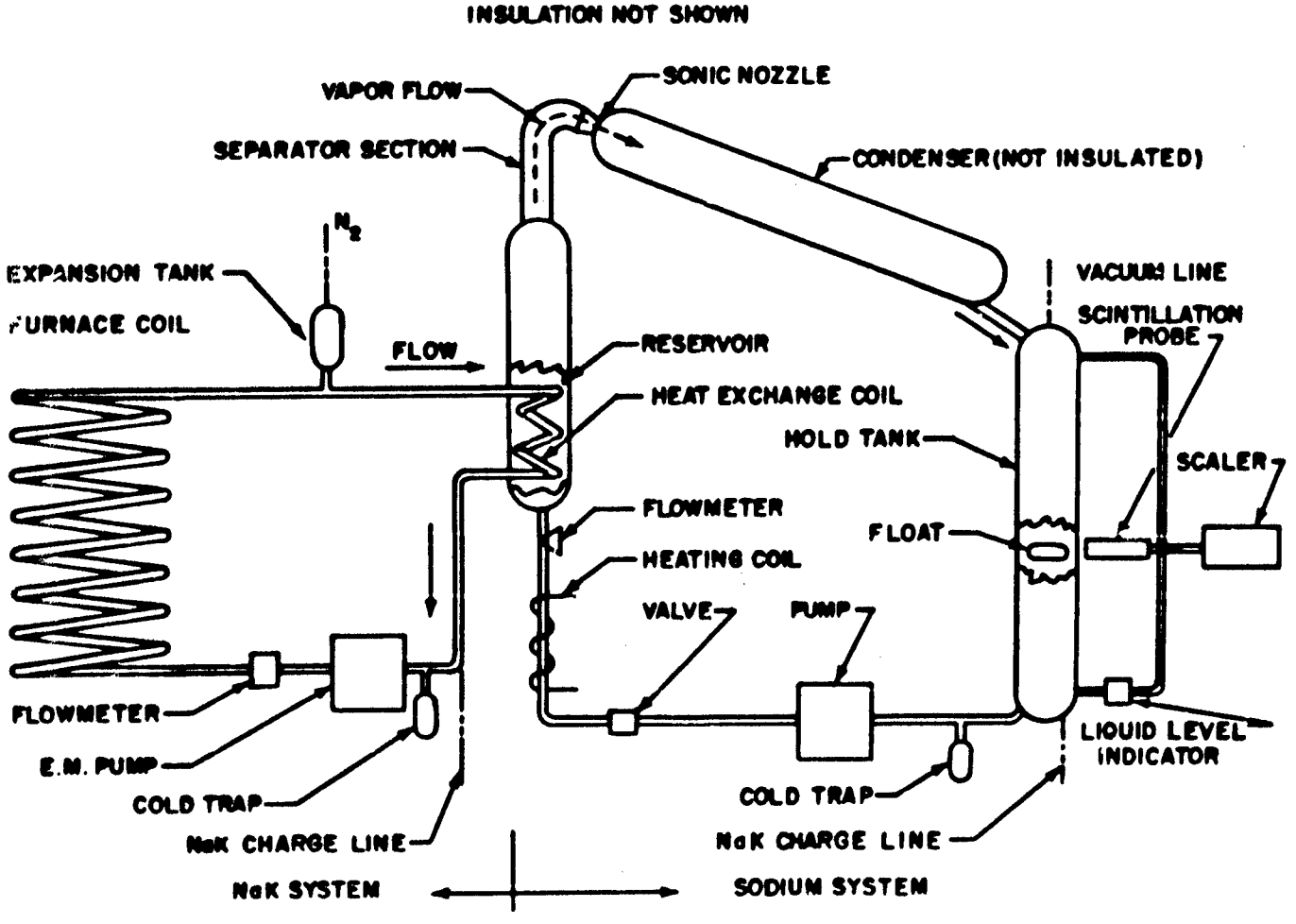

Figure 33. Schematic of Closed-Cycle NaK-Sodium Evaporative Cooling Test Loop

by replacing the furnace coil with a coil fabricated from Hastalloy X. The loop was also changed from an open to a closed cycle by removal of the flow-restricting orifice and by introducing a tubular heat exchange into the evaporator. An explanation of open and closed systems is given in Reference 7. This heat exchanger formed part of the closed circuit through the pump and furnace and was filled with NaK as the heat transfer fluid. Sodium was again used as the evaporating material, and initial runs were made without a wire mesh separator, as part of a program to find the minimum mesh requirements. A diagram of the modified system is shown in Figure 33.

Procurement delays and operational difficulties have prevented obtaining quantitive data to date. Limited operation has indicated excessive carry-over, which may have been due to the absence of a liquid-vapor separator or to violent boiling which gave rise to loud noises similar to "water hammer". Failure of a tube in the sodium system, while the sodium was at approximately 1200°F resulted in a typical nonflaming sodium fire. The loop was not damaged by the fire, but the cause of the tube failure has not been determined to date. While the tube failure is being repaired, the heat exchanger coil will be modified in an attempt to reduce the violence of boiling, and a wire mesh liquid-vapor separator will be added. This phase of the MSAR program will be continued.

In addition to the testing described above, five tests were conducted by MSAR to determine whether air would enter a container from which sodium vapor was being exhausted, and, if so, what effects would result. The test was representative of the system in that nitrogen gas was used over the sodium and the shut-down condition was reproduced. It can be expected that maximum opportunity for air entry exists when vapor production stops.

Tests were conducted at atmospheric pressure and at the sodium boiling temperature of 1620°F, using the set-up shown schematically in Figure 34. The sodium was heated under the protection of nitrogen gas which exhausted

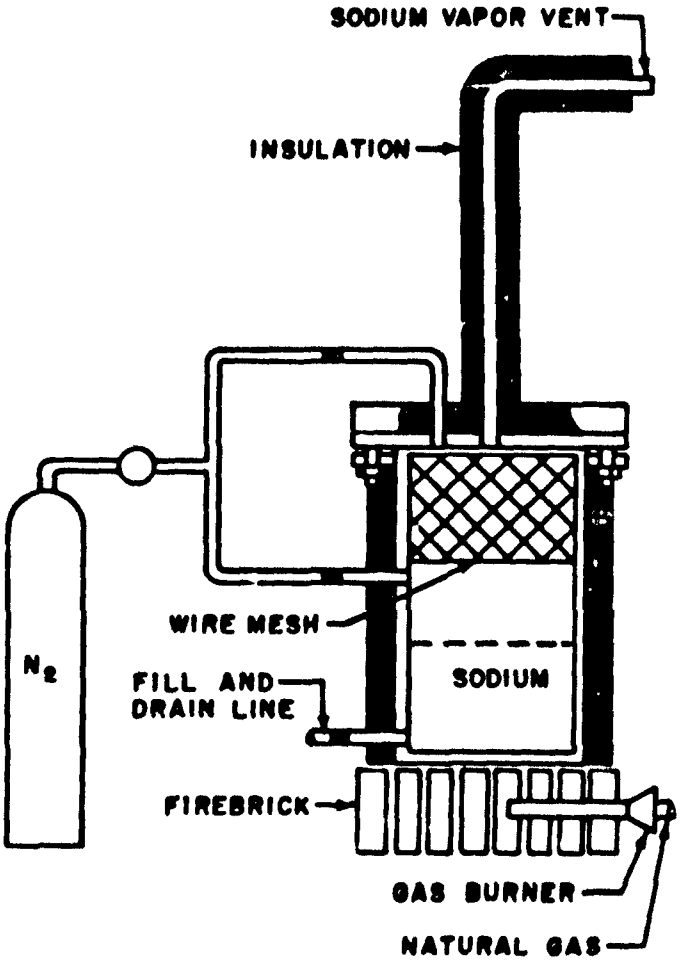

Figure 34. Schematic of Air Entry Test Apparatus

through the sodium vapor vent line. At about 900°F traces of white smoke (Na_2O) were observed exhausting from the vent, and, when boiling was reached, the production of smoke became greater. At violent boiling conditions, with high vapor velocities in the vent line, liquid sodium was carried over and visible yellow flames were observed in addition to the white smoke. This occurred both with and without a wire mesh separator. Since the wall of the vent line was below 1000°F, a portion of the carry-over is believed to be sodium vapor which condensed on the wall. In all cases Na_2O was found within the vent line and reservoir at the completion of a run; in one case, the vent line was found to be plugged. Oxidation of the sodium was not self-sustaining and stopped almost instantly as the system began to cool.

2. REFRACTORY MATERIALS FOR "HOT-SPOT" AREAS

Tests were continued on a number of selected high-temperature materials which may be useful as refractories for hot-spot areas (temperatures in excess of 2500°F). As noted in a previous report (Reference 4), most of the high-melting-point materials have mechanical, thermal, or chemical properties which make them unsuitable for some of these applications. Although no material is presently available which will meet the target requirements for all hot-spot areas, test data establishing useful life temperatures for available materials are imperative. The following refractory materials were, therefore, screened for rate of oxidation at 2800°F under a controlled oxygen flow of one liter per minute: zirconium carbide (ZrC), with a melting point of about 5700°F; tantalum carbide (TaC), with a melting point of about 6000°F; a refractory body consisting of 90 per cent silicon carbide and 10 per cent boron carbide (SiC-B_4C); a refractory body consisting of 80 per cent tantalum carbide and 20 per cent zirconium carbide (ZrC-TaC), with a melting point of about 7000°F; recrystallized silicon carbide (SiC); and AGR grade graphite coated with silicon carbide. The SiC-B_4C body exhibited the best oxidation resistance based on weight change and weight of CO_2 collected per unit of surface area after 3 hours exposure at a test temperature of about 2800°F (0.0016 gram CO_2 per square centimeter surface). More detailed data for the materials tested are given in Table VI. Weight of CO_2 collected per square centimeter of surface area for the SiC-B_4C body and recrystallized SiC is plotted in Figure 35 as a function of exposure time. The silicon carbide-coated graphite deteriorated by oxidation of the graphite through a limited number of pinholes in the 5-mil-thick coating. The other materials tested oxidized at a rate causing catastrophic deterioration.

The following materials were tested qualitatively for oxidation resistance in an oxyacetylene furnace at temperatures to 3700°F: a refractory body consisting of 75 per cent magnesia and 25 per cent zirconia (MgO-ZrO_2); a zirconium carbide body (ZrC); and KT silicon carbide. Little or no change was noted in the KT body after 10 minutes exposure at 3700°F; however, the body deteriorated quite extensively after 85 minutes exposure. Based on this limited test, the MgO-ZrO_2 body does not show much promise for application in hot-spot areas. The ZrC formed a nonadhering scale on its surface after exposure to elevated temperatures (3275 to 3450°F).

The quantitative oxidation resistance of SiC-B_4C systems will be evaluated at temperatures approaching 4000°F with equipment being assembled.

Modulus of rupture tests were conducted at room temperature and at temperatures up to 2700°F at Bell and, under subcontract, at Alfred University on Carborundum's KT (aluminum-modified) No. 3 research silicon carbide body and on a number of zirconia bodies. The modified KT body had an average modulus of rupture strength of about 12,000 psi at 2700°F after a one-hour soak at that temperature. KT (aluminum-modified) No. 3 silicon carbide was fabricated in an attempt to obtain commercially producible silicon carbide possessing a modulus of rupture approaching that of the best hot pressed variety prepared on a laboratory scale by Alfred University (70,000 psi at 2500°F). The Norton Company has advised at the writing of this report they can make pieces up to 9 inches diameter, 6 inches long of hot pressed aluminum-modified silicon carbide in accord with processing developed at Alfred University. This will be investigated in the immediate future. At a test temperature of 1500°F and after a 3-minute soak at that temperature, the best of the zirconia bodies tested had an average modulus of rupture strength of 3300 psi. Table VII gives the results of modulus of rupture tests on the KT (aluminum-modified) silicon carbide body at room temperature, 1500°F, 2000°F, 2400°F, 2600°F, and 2700°F after a 3-minute soak at temperature and a one-hour soak at temperature.

E. TEST EQUIPMENT INVESTIGATIONS

The problem of structural testing of high-speed airplanes, where large and variable

TABLE VI. OXIDATION RESISTANCE OF VARIOUS REFRACTORY BODIES

Material	ZrC	TaC	SiC-B_4C	ZrC-TaC	Recrystal-lized SiC	AGR Graphite Coated With SiC
Surface area (cm^2)	18.0114	9.2162	15.8097	4.2393	33.0965	21.1900
Volume (cm^3)	4.2118	1.5755	3.0090	0.5739	6.4359	7.4287
Weight (grams)	24.0208	17.9954	9.1089	5.5541	16.2308	13.3738
Apparent density (grams/cm^3)	5.7032	11.4218	3.0272	9.6774	2.5219	1.8003
Apparent porosity (%)	6.24	14.59	0.3556	18.12	20.71	8.54
Theoretical density of non-porous material (grams/cm^3)	6.0828	13.3729	3.0380	11.8190	3.1806	1.9684
Weight after acid wash (grams)	24.0191	17.9950	9.1075	5.5529	16.2141	13.3697
Loss of weight from wash cycle (grams)	0.0017	0.0004	0.0014	0.0012	0.0167	0.0041
Weight before heat treatment (grams)	24.0191	17.9950	9.1075	5.5529	16.2141	13.3697
Weight after heat treatment (grams)	yellow powder	Gray fused mass	9.1149	Buff colored fused mass	16.5733	13.1146
Gain in weight (grams) after 3 hours exposure	Decom-posed	Decom-posed	0.0074	Decomposed	0.3592	0.2551 (loss)
Average temperature of furnace (°F)	2870	2800	2840	2810	2820	2810
Weight of CO_2 produced (grams)	7.4614	3.4499	0.0259	1.1110	0.1697	0.9865
Theoretical weight of CO_2 producible (grams)	10.2400	4.1057	(7.2493(B_4C) (10.0030(SiC)	(1.2669(TaC) (2.3673(ZnC)	17.8084	14.6843
Percent of theoretical CO_2 actually produced	72.87	84.03	(0.36(B_4C) (0.26(SiC)	(87.69(TaC) (46.93(ZrC)	0.95	6.72

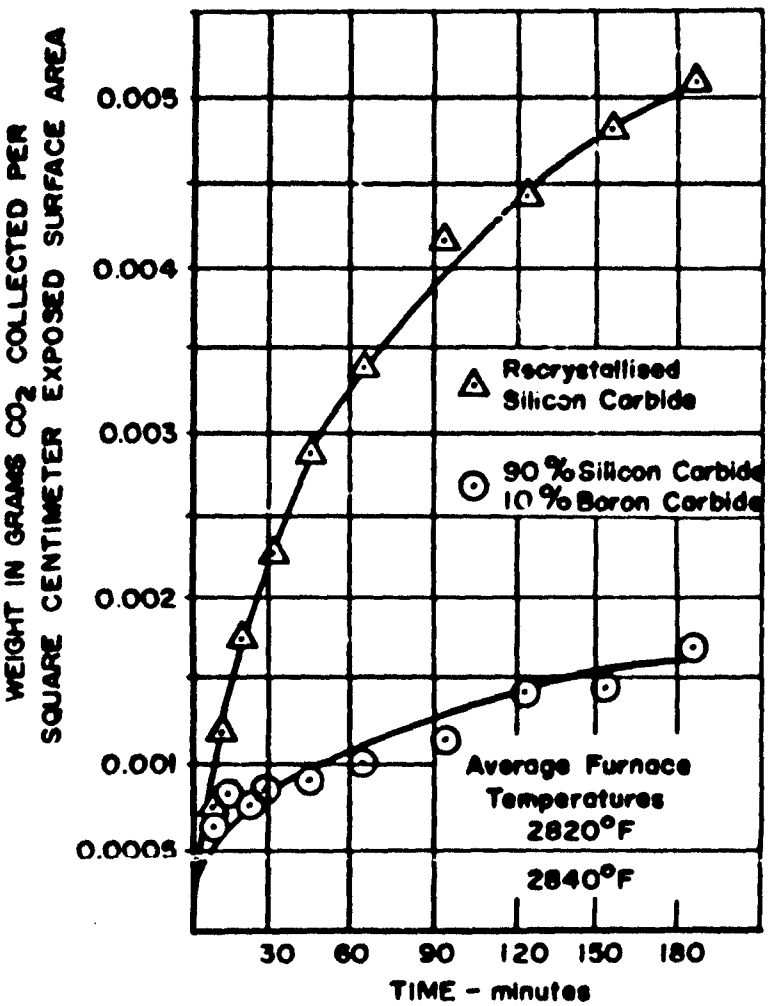

Figure 35. Weight of CO_2 Collected Per Unit Area vs Time

quantities of heat must be applied in addition to loads, is generally recognized. The problem could be acute with the present vehicle, but the use of double-wall construction eliminates the need for exposing the entire vehicle to heat and load simultaneously. Tests in which full-intensity heating must be applied will be confined to small areas of panels, and hot-spot areas such as the wing leading edge. The severe heating conditions at the leading edge still introduce testing problems, particularly if full-scale prototype testing is considered. Outer wall panel testing is difficult where combined heating, loading, and flow effects are required. In anticipation of such test facility requirements, studies were conducted on heat sources for leading edge testing and on the use of a rocket motor for panel and materials tests.

1. HEAT SOURCES FOR "HOT-SPOT" AREAS

Possible schemes for obtaining high intensity heating over a large area for long periods of time are:

a. High-temperature radiating elements.

b. High-temperature gas streams.

TABLE VII. MODULUS OF RUPTURE TESTS PERFORMED AT ALFRED UNIVERSITY ON CARBORUNDUM "KT" (ALUMINUM-MODIFIED SILICON CARBIDE NO. 3

Number of Specimens	Time (minutes)	Temperature (°F)	Modulus of Rupture (psi)	Remarks
6	-	80	17,700 to 32,100	One specimen had off-center break
2	3	1500	14,400 to 17,000	
4	60	1500	8500 to 17,900	One specimen had flaw in X-section. Another specimen had an off-center break.
2	3	2000	9500 to 15,100	
4	60	2000	8300 to 22,000	One specimen had a flaw in X-section
2	3	2400	6300 to 9200	
4	60	2400	9200 to 13,200	
2	3	2600	7600 to 10,700	
4	60	2000	3500 to 10,800	The specimen whose modulus was 3500 psi had large flaw in X-section
2	3	2700	8700 to 10,400	
4	60	2700	9300 to 17,200	One specimen had off-center break.

c. Condensation of liquid metal vapors.

d. Direct electrical resistance.

e. Electromagnetic induction.

One type of radiant heat source was investigated previously in Reference 4, and it was found that material limitations on element temperatures introduced very bulky insulation, to achieve the required heat input to a liquid-metal-cooled leading edge. Transformer requirements made the cost of this system very large.

Gas heating has been reviewed briefly during the present period by a contact with the Silas Corporation of America. This company expressed the belief that the heat inputs could be achieved using turbulent jet burners with gaseous fuels. Claims were made that gas heating offers lower initial, operating, and maintenance costs than electrical heating.

No studies were made of metal condensation or resistance-heating schemes, but a study of induction heating for a liquid-metal-cooled leading edge was conducted on a consulting basis by Roger W. Sampson of Florida University. This study (Reference 10) considered symmetrically and unsymmetrically heated tubes of various materials, with simulation of flux intensity and distribution. Work coil and loop designs, control, instrumentation, power, and coolant requirements were considered. It was concluded that induction heating

could be used satisfactorily, and for a leading edge specimen six feet long, the Air Force-owned equipment at the University of Florida would be suitable. No consideration has been given to the use of induction heating for testing a temperature-resistant leading edge.

Choice of a heating system is premature until all systems have been examined. The availability of induction heating equipment for preliminary testing is attractive, but the cost of the prototype test unit must eventually be the deciding factor.

2. ROCKET MOTOR AS A HEAT SOURCE

Interest in a rocket motor as a heat source was generated by the availability, at Bell Aircraft, of a surplus motor, and a test stand. This unit will provide a test section 15 inches in diameter with a flow velocity of 5000 to 6000 feet per second and a maximum stagnation temperature of 4000°F.

A facility of this type would be used for the reproduction of high-temperature and supersonic flow conditions simultaneously. Tests in which such conditions are required are:

a. Flutter tests, at elevated temperature, of outer wall panels.

b. Tests of outer wall panels for local hot-spots.

c. Erosion tests.

d. Oxidation tests under high-velocity, rather than static, conditions.

e. Tests of transpiration cooling.

So far as is known, the only existing facilities capable of producing temperature and velocity conditions comparable with those mentioned above, and also accepting large specimens, are at Redstone Arsenal and the Pilotless Aircraft Research Division of the NACA.

The investigation demonstrated that, by a simple modification, the motor could be operated on a mixture of hydrogen peroxide and JP-4. This arrangement permits wide variation of flow conditions during a run so that a range of heating rates typical of Brass Bell boost flight could be reproduced. It was also evident from the investigation that high noise levels might exist in the jet, to the extent that tests of sheet metal structural components would become fatigue and vibration tests. In particular, panel flutter tests would be very doubtful value.

Contact was made with Redstone Arsenal where a similar facility is used, principally for materials and nose cone testing. The Redstone motor gives much higher pressures in the test section, so that it would be less suitable for reproducing the conditions of hypersonic glide flight. Redstone personnel emphasized the high cost of this type of operation and suggested, for economy, a small motor for materials tests to operate from the same fuel supply and control equipment.

Some estimates have been made of the cost of setting up and operating a facility such as described above. These costs are large, so that an investigation is required of other methods for conducting the tests mentioned earlier, before conclusions can be drawn.

VI Aerodynamic Research

SECRET

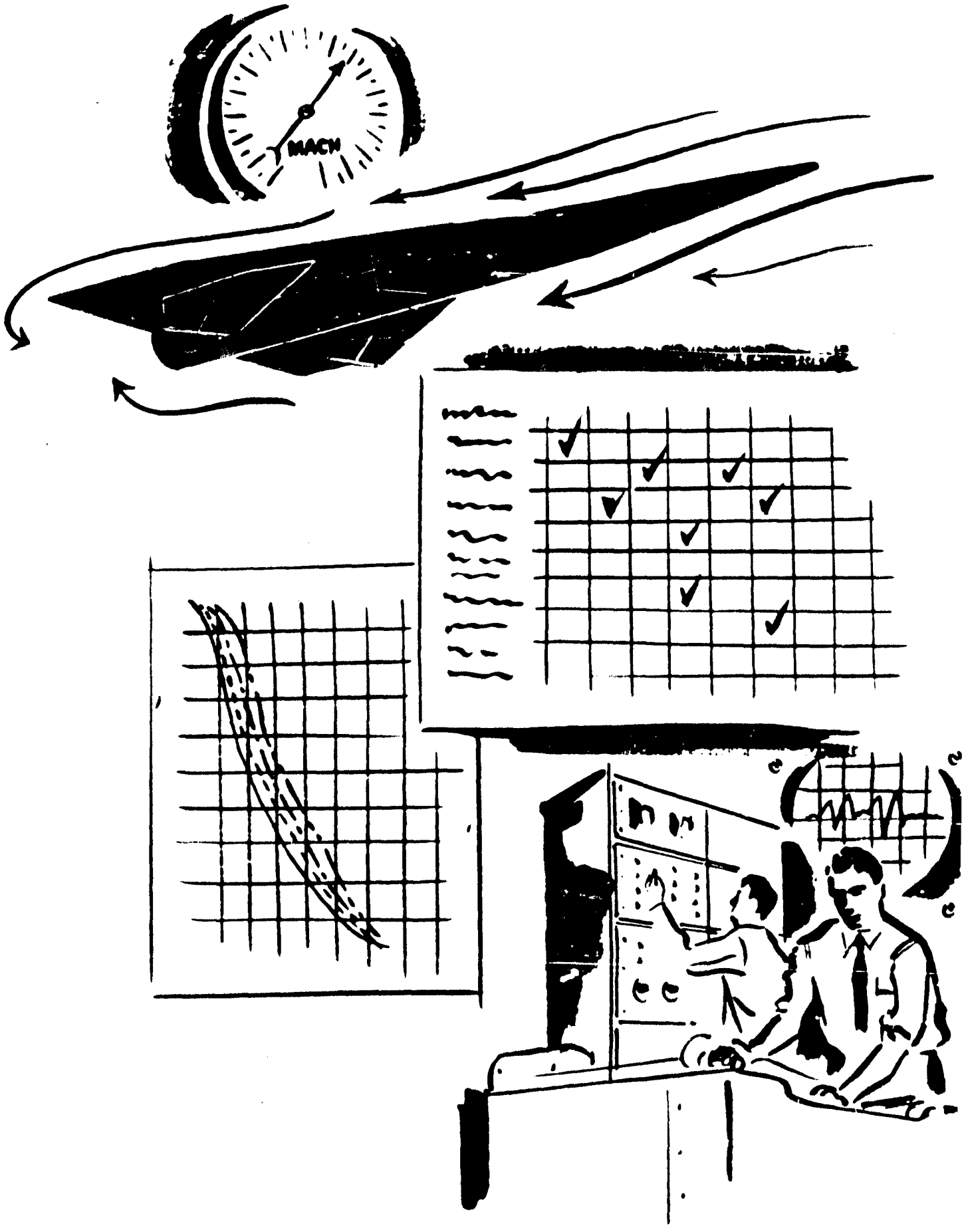
MACH

The course followed in the aerodynamic research program during this period concentrated on conducting experimental and analytical investigations of hypersonic flow. The intent was to determine the nature and extent of hypersonic low-density phenomena as they affect the aerodynamics of a boost-glide reconnaissance vehicle, and also to examine the real gas nature of air at the extreme temperatures expected during flight.

The results of this work are separated into experimental and analytical studies. Although the basic experimental programs are closely related to theoretical investigations, they are presented separately for clarity. In addition to the experimental programs, analytical studies of the effects of a hypersonic flight environment on the photographic and radar reconnaissance systems were made; these results are also discussed separately. The possibility of aircraft surface deterioration arising from several probable causes was also investigated and is presented herein. The information in this section is reported in detail in Reference 11.

A. EXPERIMENTAL PROGRAMS

The experimental investigations undertaken in this contract period are elements of a continuing large program designed to increase the basic knowledge of aerodynamic phenomena pertinent to the design of hypersonic glide vehicles. The initiation of individual test programs is governed considerably by the availability of suitable facilities. Therefore, in some cases a program cannot be completed in the same contract period in which it was started.

The experimental programs discussed herein are separated into those which have been completed to the point that test data are available, and those which have been contracted for, but not finished as of this writing. Investigations which have been initiated in the preceding contract period and completed in the current period are included in the first category.

1. COMPLETED PROGRAMS

a. Delta Wing Studies

The results of the delta wing exploratory studies completed in the past period were extended with further pressure distribution measurements in the Princeton University Hypersonic Helium Tunnel on 60° and 30° apex angle delta wings. These tests were conducted through a range of angles of attack at Mach ≈ 13.

The test data are presented in References 12 and 13. Briefly, these results show good agreement with theory at zero angle of attack, but show increasing error as the angle of attack increases. An example of the pressures obtained over the 30° apex wing is shown in Figure 36. The predicted values based on viscous-inviscid interaction theory are shown also for comparison. As noted, the theory agrees reasonably well with the measured values at zero angle of attack, but larger deviations are found at higher angles of attack. This discrepancy indicates that other phenomena, not adequately described by two-

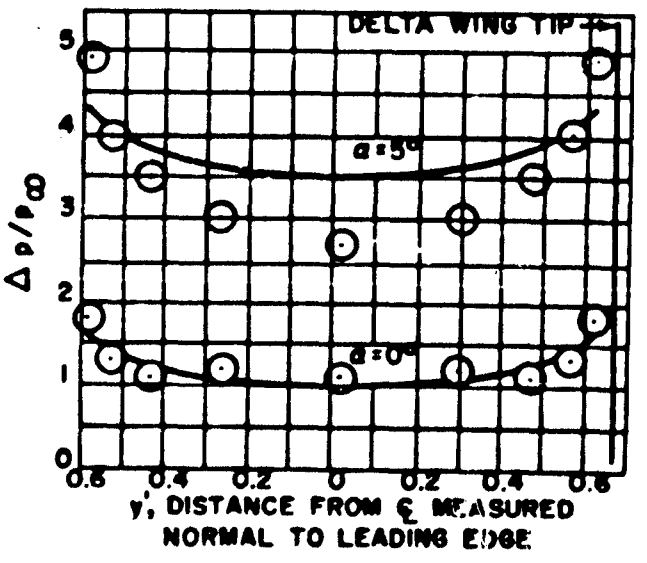

Figure 36 Pressure Distribution on Delta Wing in Hypersonic Flow at Angle of Attack

dimensional viscous-inviscid interaction theory, may be dominating the flow. Additional experiments are required to obtain a fuller understanding of this effect.

b. Wing-body Studies

An exploratory study of basic wings mounted on conical bodies was completed in the Princeton University Hypersonic Helium Tunnel at Mach ≈ 13. Pressure distributions and flow indications were obtained over straight and swept wings, and sharp and blunt-nosed cones in and out of the presence of each other at zero angle of attack. The purpose of these tests was to obtain some knowledge of the interactions between simple basic shapes at hypersonic speeds.

The results of these tests, which are reported on in Reference 14 show large interference effects between wings and bodies. In general, the presence of the wings increased the pressure around the body, with the largest changes occurring near the wing. The body pressure changes due to the unswept wing were larger than for the swept wing.

The data also show that both bodies induced positive pressures on the wings, with the largest increments occurring near the wing-body junction. The unswept wing was affected more than the swept, and the sharp-nosed body produced the largest interference.

An example of the unusual flow is shown in Figure 37, which is a photograph of the model during test with oil traces indicating the general direction of flow. This phenomenon is not explained at present in view of the many mechanisms involved. However, the experiment indicates that unusually large effects can be expected, and that further studies of this type are in order.

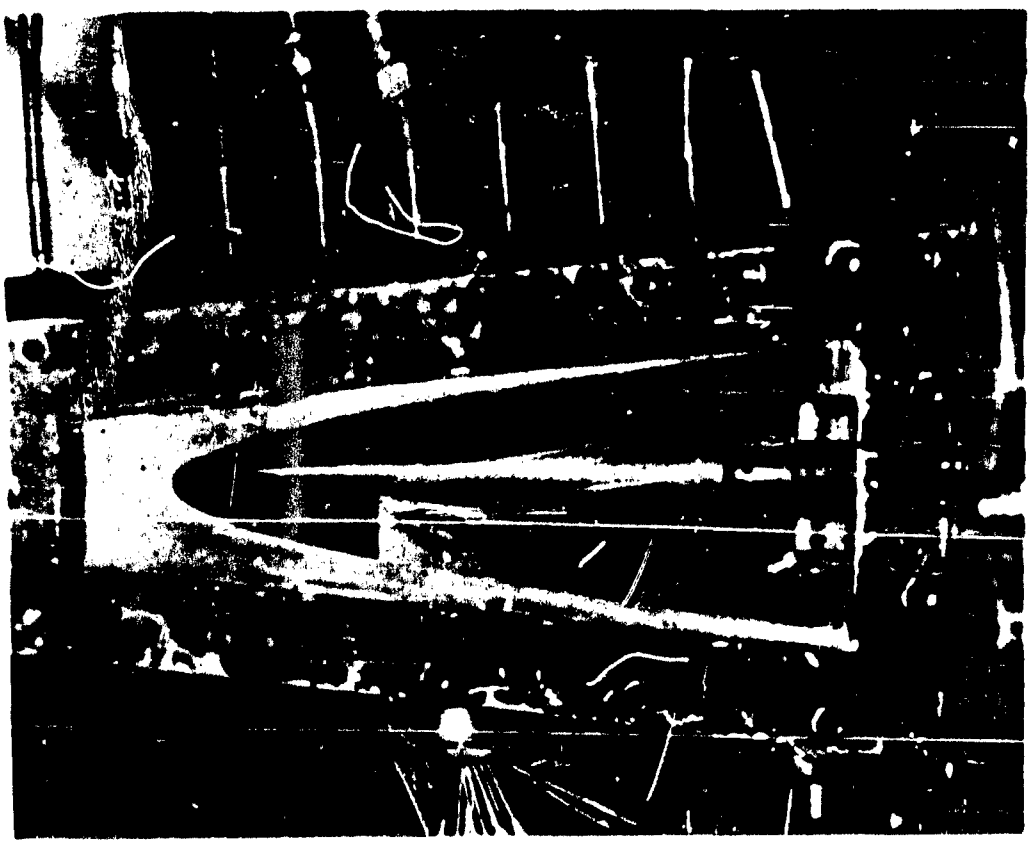

Figure 37. Wing-Body Flow Study at Princeton University

c. Low-Density Tests

Pressure distribution measurements were made in the University of California low-density wind tunnel on blunt-nosed flat plates and cones at Mach ≈ 6 and very low Reynolds numbers. The general objective of these tests was to learn more about the relative importance of inviscid interaction, viscous interaction, and possible noncontinuum effects, such as slip, on pressure distribution.

The test data results are published in References 15 and 16. Some of the lower Reynolds number data are shown in Figure 38 where reasonably good correlation with Lees' strong interaction theory is noted. Correlation of the higher Reynolds number data is found with an empirical relation. In the region of the nose of the sharp wedges, the measured pressures are lower than would be predicted by no slip conditions, indicating that slip effects may be occurring.

The results of the blunt cone tests generally are in good agreement with the modified newtonian theory in the nose region (Figure 39), and with the Kopal values on the conical portions. No significant viscous interaction or noncontinuum effects on pressures for these conditions was noted.

d. Swept Wing Studies

Pressure distribution measurements over hemispherical nose, flat plate wings with 45° and 60° sweepback were made in the Princeton University Hypersonic Helium Tunnel at Mach ≈ 13. The 60° wing was also tested at Mach ≈ 19. In addition to the pressure measurements, indications of flow separation were obtained by means of oil traces. These tests were conducted in order to determine the nature of flow for evaluation of the effect of sweepback in reducing drag and aerodynamic heating.

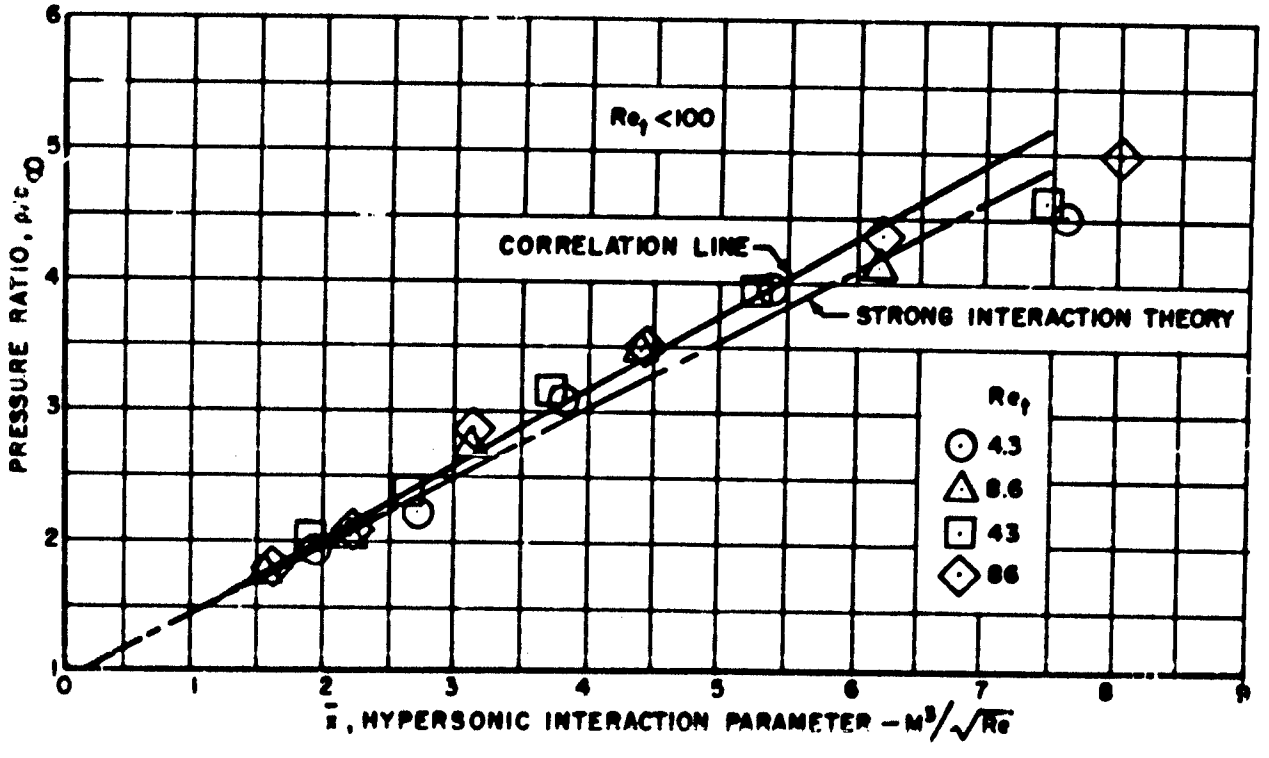

Figure 38. Induced Pressures on a Flat Plate

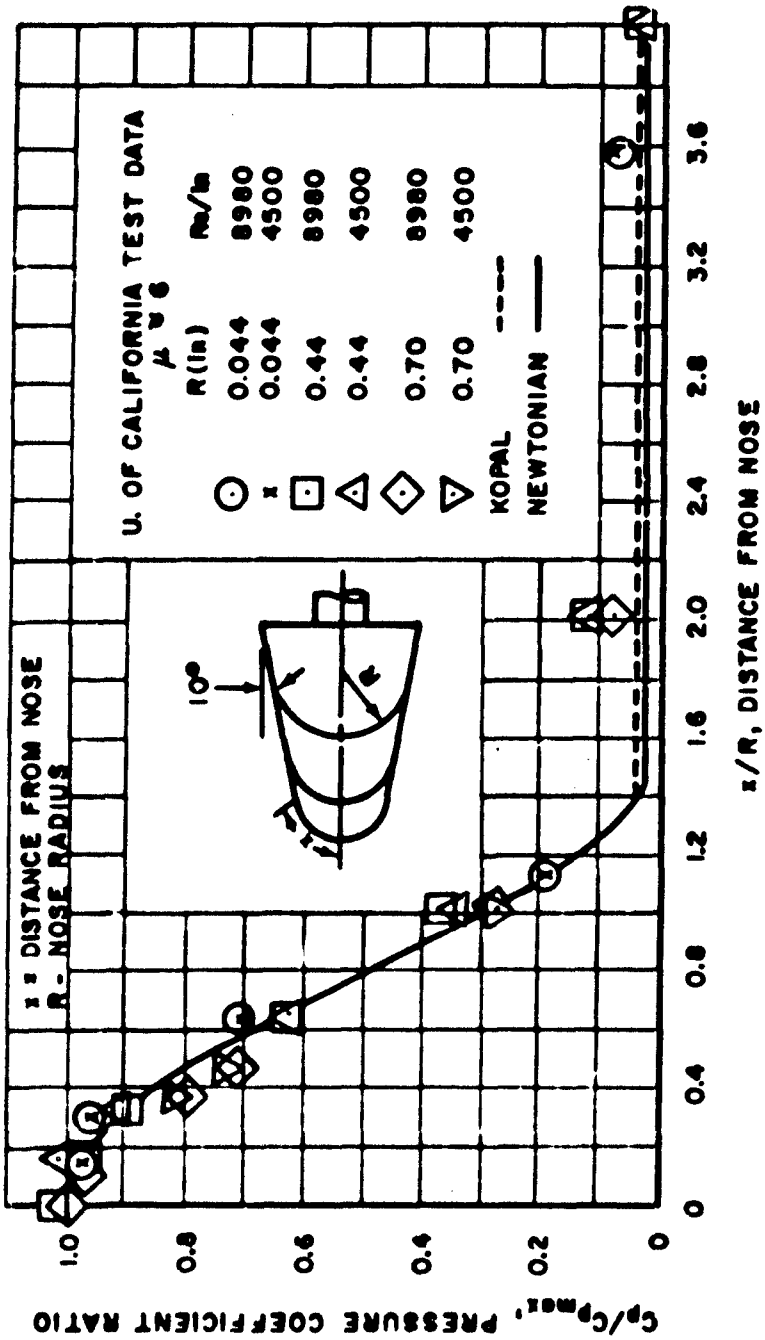

Figure 39. Surface Pressure Distribution, 10° Nose Cone Angle

Test results are presented in Reference 17 for the 45° wing, and the remaining results are in the process of being published. The pressures for both wings at Mach ≈ 13 correlate very well with blast wave theory (Figures 40 and 41). However, the Mach ≈ 19 data (preliminary) do not agree by a considerable margin (Figure 41). This unusual result is being investigated further.

c. Real Air Flow Phenomena

A program to investigate hypersonic low-density flow phenomena on basic two-dimensional shapes was conducted in the AEDC Hot-Shot I test facility. These tests were made to obtain pressure and heat transfer data under conditions which correctly simulate the high-speed, high-altitude portion of the Brass Bell flight regime. Simple wedge and round-nosed models were tested at zero sweep. The wedge model was also tested at 45° sweep. In addition, an extensible nose bar was tested in conjunction with the round-nosed model.

The test data have been published in Reference 18, and are currently being analyzed. The pressures measured over the wedge-plate model at Mach ≈ 15 are shown in Figure 42 together with the theoretical values assuming equilibrium composition and frozen flow. Figure 43 illustrates a comparison of theory with the measured heat transfer rates.

Instrumentation difficulties associated with the models and sensors precludes positive conclusions to be drawn from these data. Additional testing in this facility is desired, and it is believed that with the use of plastic models, certain probable instrumentation errors may be reduced. This possibility is currently being investigated.

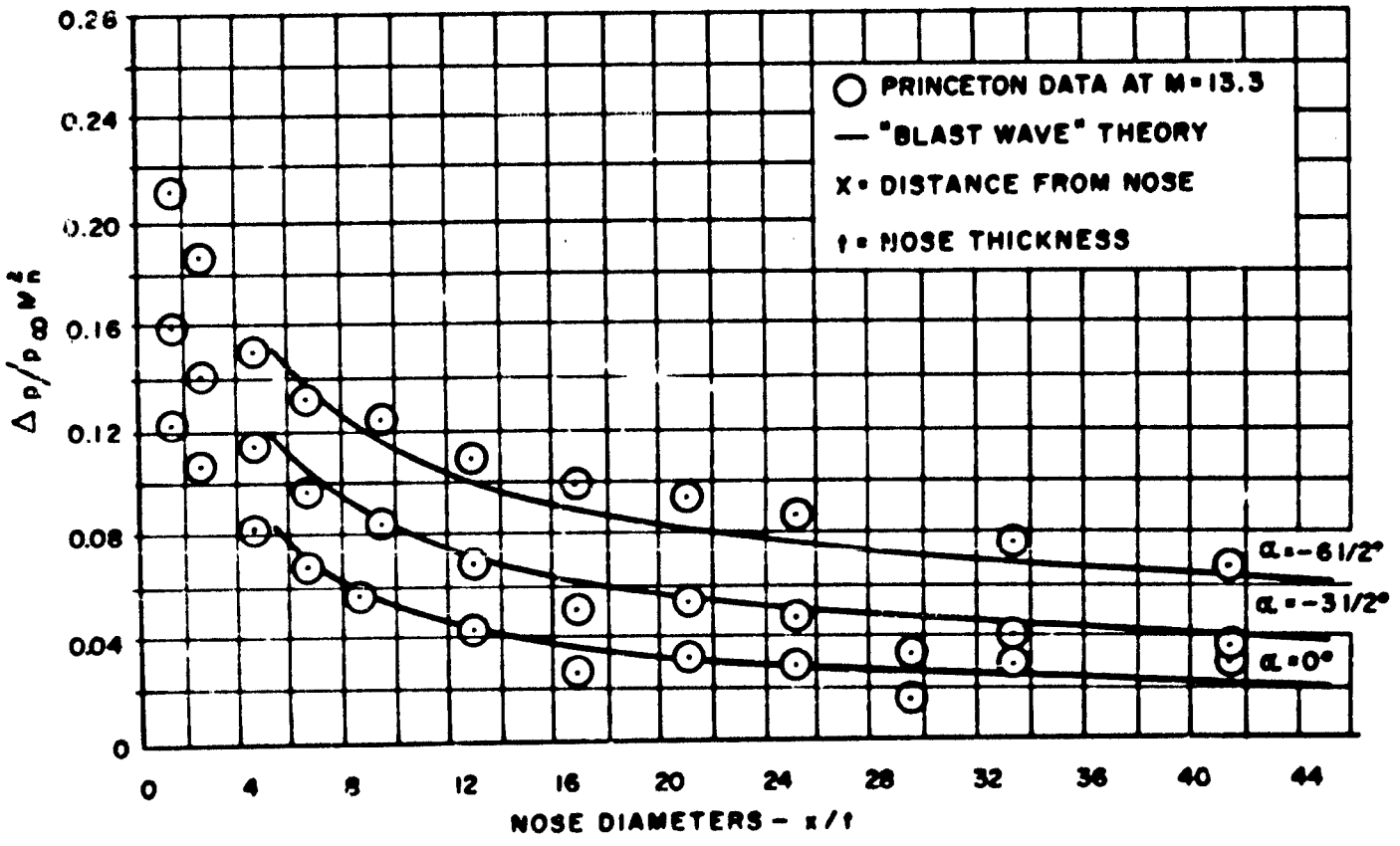

Figure 40. Pressure Distribution on 45° Sweptback Wing at Angle of Attack

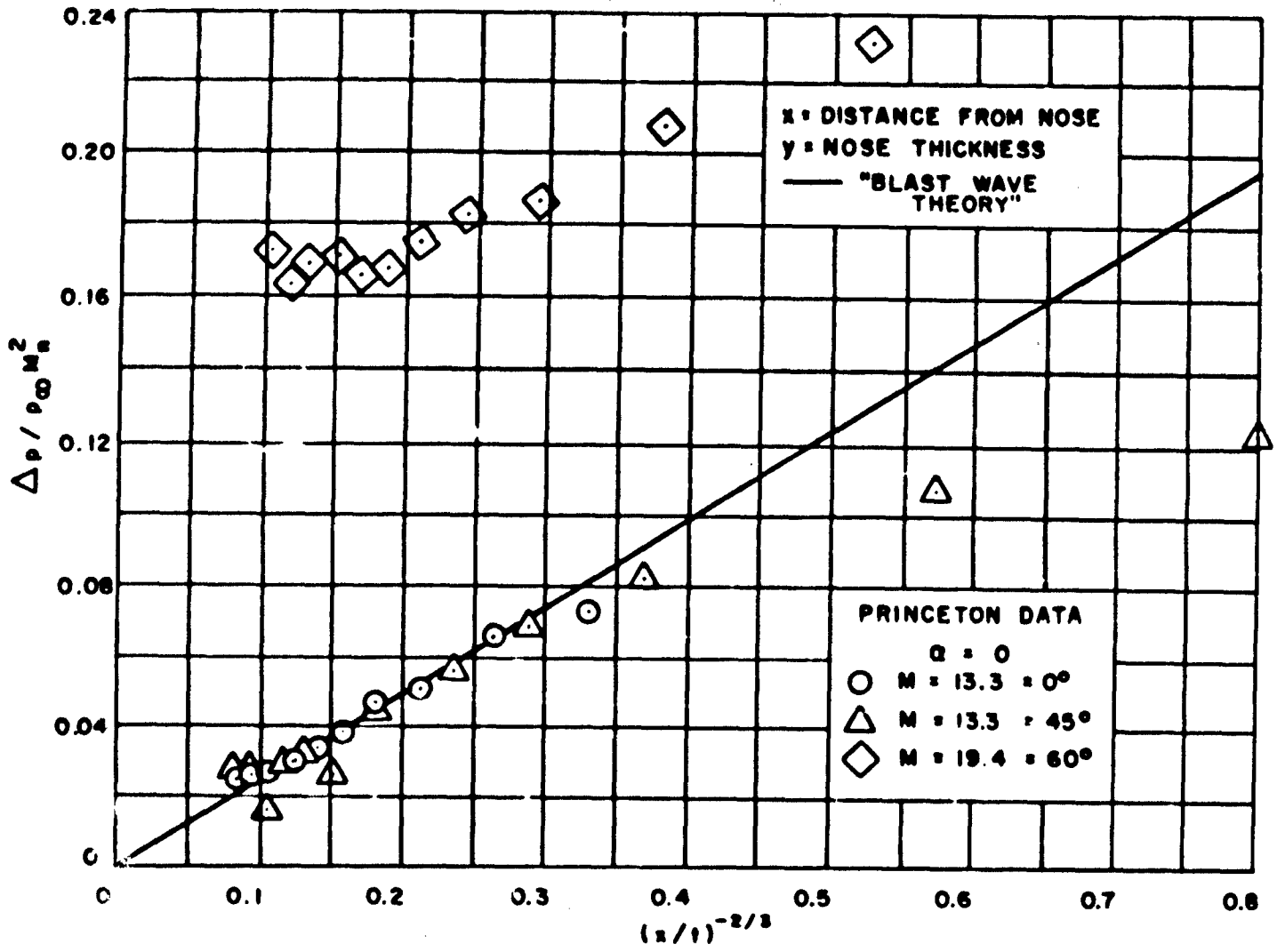

Figure 41. Pressure Distribution on Sweptback Wings in Hypersonic Flow

2. INCOMPLETE PROGRAMS

a. Cold Air Tests

A study of the flow over a 60° apex angle delta wing and a hemispherical nose flat plate at angle of attack is being conducted in the Ohio State University hypersonic wind tunnel at Mach ≈ 13. This program involves pressure distribution tests similar to some of those already completed in the Princeton University helium tunnel. The purpose is to obtain wind tunnel data using air as the medium to compare with the results obtained in helium. It is expected that this program will be completed by December 1957.

b. Free Flight Tests

NACA/PARD is planning a series of tests designed to extend their high Mach number heat transfer test programs to higher altitudes and lower Reynolds numbers. In addition, attempts will be made to simulate the relatively steady flight conditions of hypersonic glide vehicles with flat-topped trajectories.

The first of three models will provide pressure and temperature data on a hemisphere-tipped cone of 15° half angle. The other two tests will be directed towards the study of heating associated with wing-body combinations. Bell Aircraft's participation in this

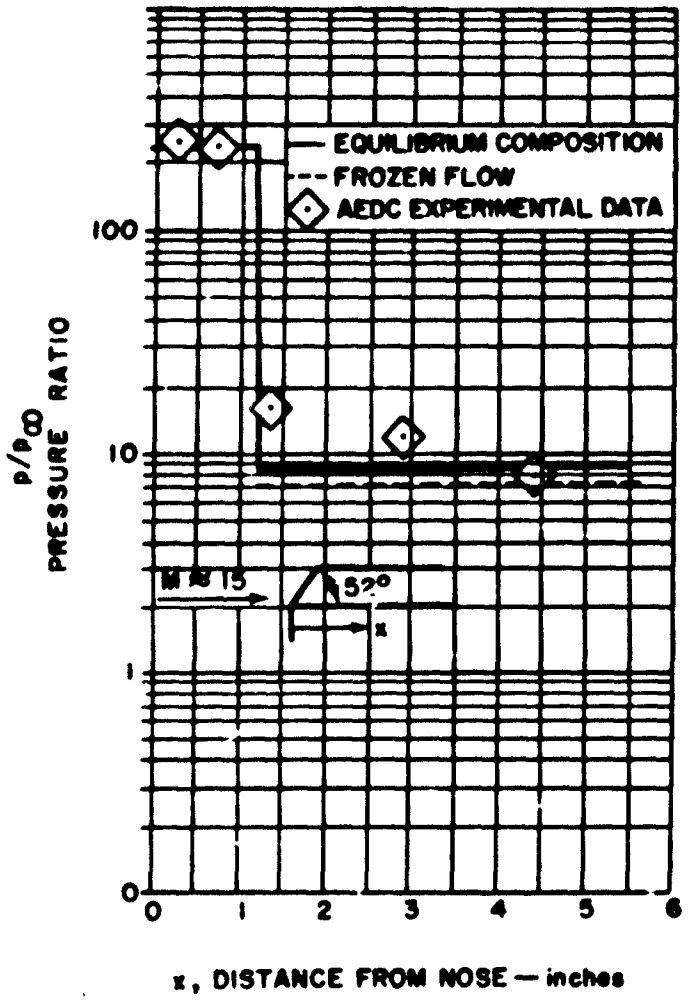

Figure 42. Pressure Distribution on Wedge-Plate Combination

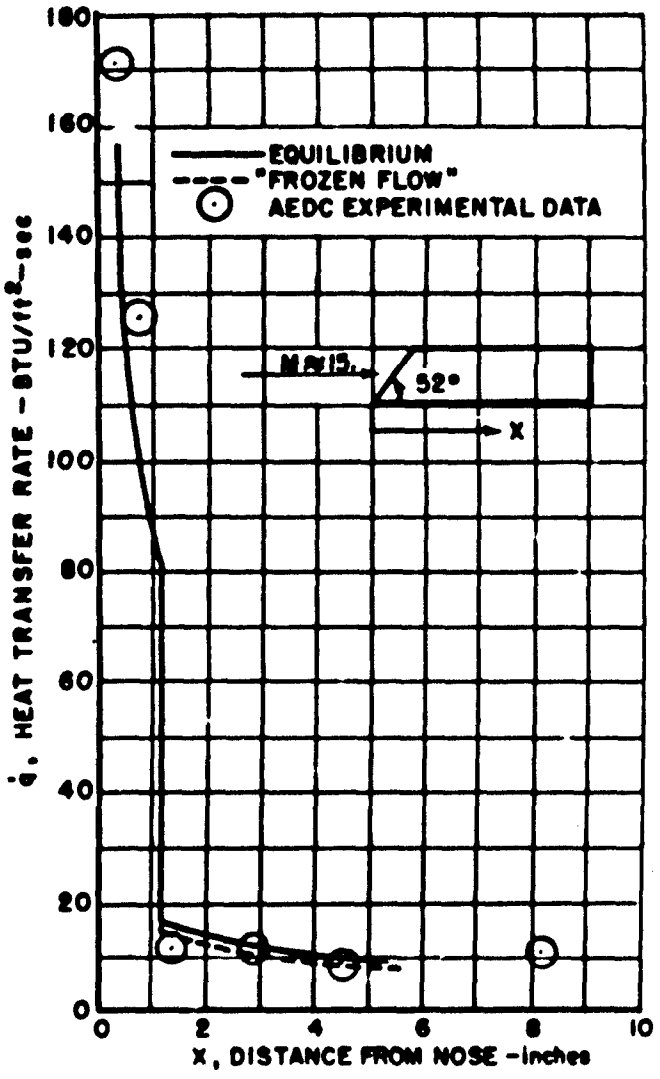

Figure 43. Heat Transfer Rate for a Gas in Thermal Equilibrium

program involves the purchase of the third-stage boosters of the four-stage test vehicles; these are expected to achieve Mach 12 at about 170,000 feet.

The first flight is tentatively scheduled for December 1957 and the last in April 1958.

c. Configuration Tests

Hypersonic tests of configurations of the Brass Bell type are scheduled for the NACA/Langley 11-inch Hypersonic Wind Tunnel in December 1957. The primary objective of this program is to obtain basic aerodynamic force and moment data on complete configurations and some knowledge of the interference effects between components.

Models have been designed and are currently being fabricated which complement a rather extensive NACA test program of hypersonic configurations at Mach numbers of 10 and 7.

d. Hypersonic Flap Tests

Previous tests of a simple flap model conducted in the Princeton University Hypersonic Helium Tunnel at Mach ≈ 13 indicated large effects which warranted a con-

tinuation of this study (Reference 19). Therefore, another test program was evolved for the same facility to obtain a further knowledge of shock wave-boundary layer interaction in the region of a deflected flap by means of pressure measurements and flow observations.

This program is currently in progress, and is expected to be completed by December 1957.

e. Flow in a Corner

The previous test results of wing-body combinations discussed in Paragraph VI-A-1-b indicated that the flow phenomena are quite complex. Therefore, in order to obtain a better understanding of this effect, a simple set of experiments was conceived which essentially idealizes the wing-body juncture problem. That is, the flow in a streamwise juncture, formed by two flat plates normal to each other, will be studied with the aid of measured pressures and oil traces. The tests will be conducted at Mach ≈ 13 and zero angle of attack in the Princeton University Hypersonic Helium Tunnel in the near future. The test results are expected to be available before December 1957.

f. Blunted Delta Wing Tests

The exploratory wind tunnel tests of delta wings discussed in Paragraph VI-A-1-a were primarily on relatively sharp leading edges which produced flows largely dominated by the viscous-inviscid interaction effect. In order to increase the knowledge of delta wings in hypersonic flow, additional testing of such wings with blunt leading edges was initiated. The purpose is to produce flows which are dominated by strong shock systems, i.e., the blunt nose effect.

A 60° apex delta wing will be tested at angle of attack in the helium wind tunnel at Princeton University at Mach ≈ 13. Pressure distributions will be measured and oil traces observed. These tests are expected to be completed by December 1957.

g. Nonequilibrium Effects

Many of the aerodynamic phenomena associated with high-speed, low-density conditions are susceptible to nonequilibrium effects of a real gas. In particular, heat transfer phenomena and visible radiation may be dominated by the reaction processes of air at high temperatures. In order to obtain an understanding of the basic mechanisms involved, a program was initiated with the Cornell Aeronautical Laboratory to study the approach to thermodynamic equilibrium in pure nitrogen, oxygen, and air. Optical measurements of density gradients obtained in shock tubes are characteristic of the type of experiments contemplated. The detailed experiments will be guided by concurrent theoretical analyses.

This program is expected to be completed to the limit of the available funds by November 1957; an estimated additional six months of effort would complete the program in full.

h. Real Air Tests

To further increase the knowledge of hypersonic real air flow as related to aerodynamic heating, boundary layer, and separation phenomena, a combined theoretical and experimental program was initiated with the Cornell Aeronautical Laboratory. This program involves testing basic aerodynamic shapes in hypersonic shock tunnels. It is expected that these results will allow a correlation of high-temperature data with those obtained in other facilities.

This program is partially funded to November 1957. An additional six months of effort is estimated to be required for completion.

B. AERODYNAMIC HEATING

One primary objective of the theoretical and experimental program in hypersonic gasdynamics which has been maintained as part

of the Brass Bell study program is to obtain accurate methods for predicting the aerodynamic heating at any part of a hypersonic aircraft.

An essential prerequisite for this work is a thorough knowledge and understanding of hypersonic flow phenomena and the physical behavior of air at high temperatures where it dissociates, ionizes, and, in general, behaves as a reacting mixture of molecular, atomic, and ionic species (quite different from its behavior at temperatures associated with the lower supersonic speeds). This realization provides background for the recognition and delineation of problems, as well as a basis for the evaluation of the simplifying approximations inherent in any tractable flow theory, which, in turn, is the basis for any practical analytical method.

Progress in this area is currently inhibited by, among other things, the paucity of experimental information on basic physical data for the behavior of air at high temperatures, and also on hypersonic flows over configurations with full simulation of all significant parameters. This information is needed to provide a basis for the theoretical flow models as well as a check on the accuracy of prediction of the methods developed. In the past few years, however, considerable progress has been made by research workers, both in the theoretical work underlying the prediction of aerodynamic heating and in the technique of experimentation in hypersonic high-temperature flow.

Accurate methods now exist for determining the heat transfer to two-dimensional and axially symmetric bodies, and to swept wings; in particular, the critical heating areas. Spot checks have been made for comparison with the predictions of aerodynamic heating in the Brass Bell design studies. These checks showed that the latter procedures have conservative (i.e., high) estimates of the heating. Thus the demonstration that the aerodynamic heating of Brass Bell can be handled structurally is based on conservative estimates of the heating in critical areas, so that this aspect of the Brass Bell feasibility is reaffirmed by the present studies.

1. EQUILIBRIUM HEATING RATES

Two advanced methods, proposed by Lees, and Fay and Riddill, for predicting the aerodynamic heating of simple two-dimensional and axially symmetric bodies, assuming thermal equilibrium, show fairly good correlation with experimental data. The theoretical analysis underlying these methods was carefully checked, and two simplifying assumptions were generalized. The implications of these studies to practical problems are illustrated.

The results of a study of stagnation-point heating on a swept wing, taking into account real gas effects, are also summarized. Essentially, the results show a lower reduction of heating with sweepback than predicted on the basis of ideal gas theory.

a. Laminar Boundary Layer with Pressure Gradient

An analysis of a laminar boundary layer with a prescribed external pressure gradient produced by the "blunt nose effect" was made with regard to aerodynamic heating. The results show that, although the heating rate is strongly dependent on the local pressure level, it is not very sensitive to the pressure gradient for the case of a cooled wall.

Figure 44 illustrates the effect of a blunt leading edge on the equilibrium heat transfer downstream of the leading edge. At the shoulder of a hemicylindrical section, the heating rates, considering the blunt nose effect, are higher than the corresponding values predicted by Newtonian methods. This difference vanishes for this example at about 20 nose diameters aft of the leading edge. Thus, it can be seen that neglecting the blunt nose effect in certain cases can produce relatively large local errors in the predicted heat transfer rates. It should be noted, however, that the largest errors do not occur in the critical, or highest heating regions.

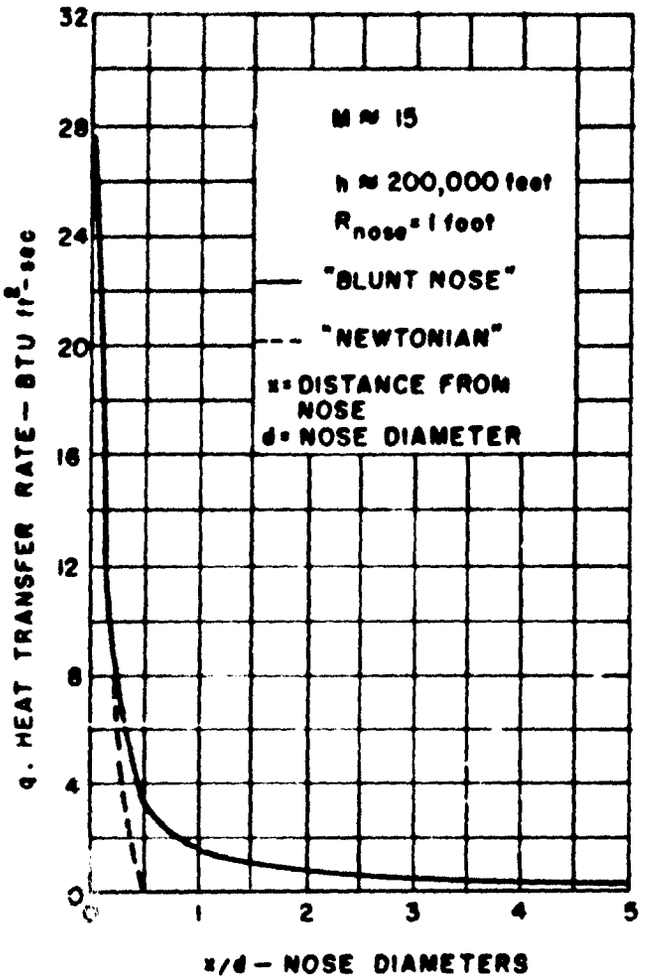

Figure 44. Theoretical Influence of "Blunt Nose Effect" on Heat Transfer Rate

b. Dependence on Transport Properties

In any solution of the boundary layer equations, such as for heating rates, a fundamental question arises as to the appropriate values of the transport properties to be employed in the calculations. The values of these properties for dissociated and ionized air and their variations at the high temperatures attained in the boundary layer are not accurately known, although this basic and difficult problem is, and has been, the subject of considerable research, primarily theoretical.

In order to obtain some insight into the way various equally plausible variations of transport properties could affect the theoretical predictions of aerodynamic heating, two current viscosity-temperature laws were considered. The linear viscosity law as proposed by Chapman and Rubesin and the Sutherland viscosity law were employed in comparing heat transfer rates computed at arbitrary points, including the stagnation region.

The results of this study indicate that the Chapman-Rubesin law results in about 10 per cent larger predicted heat transfer rates than the Sutherland variation. Although general conclusions regarding the dependence of heat transfer on viscosity cannot be drawn from this work, it does point out the need for a good knowledge of the viscosity parameter when precise values of heat transfer rates are required.

c. Sweptback Wings at Hypersonic Speeds

It is always desirable, from an aerodynamic drag viewpoint, to be able to utilize slender bodies with very sharp leading edges. At hypersonic speeds, however, all bodies must be "blunt nosed" to some extent in order to reduce the heat transfer rates to manageable proportions and to allow for internal heat conduction. It is apparent, from physical considerations, that the use of wing sweepback will reduce these large heating rates and thus allow the use of thin, low-drag shapes. The question arises as to how to predict the heat transfer over a swept wing with a blunted nose. This problem which has also been studied by others, is discussed in some detail in Reference 11.

The practical result of this study is summarized in Figure 45, which indicates the reduction in heating rate due to sweepback as predicted by methods based on an ideal gas and a real gas in thermodynamic equilibrium. As shown, significant differences appear at the larger sweepback angles, which indicates the possible inaccuracies that may result when ideal gas, small sweepback concepts are extrapolated to cases involving large sweepbacks and real gases.

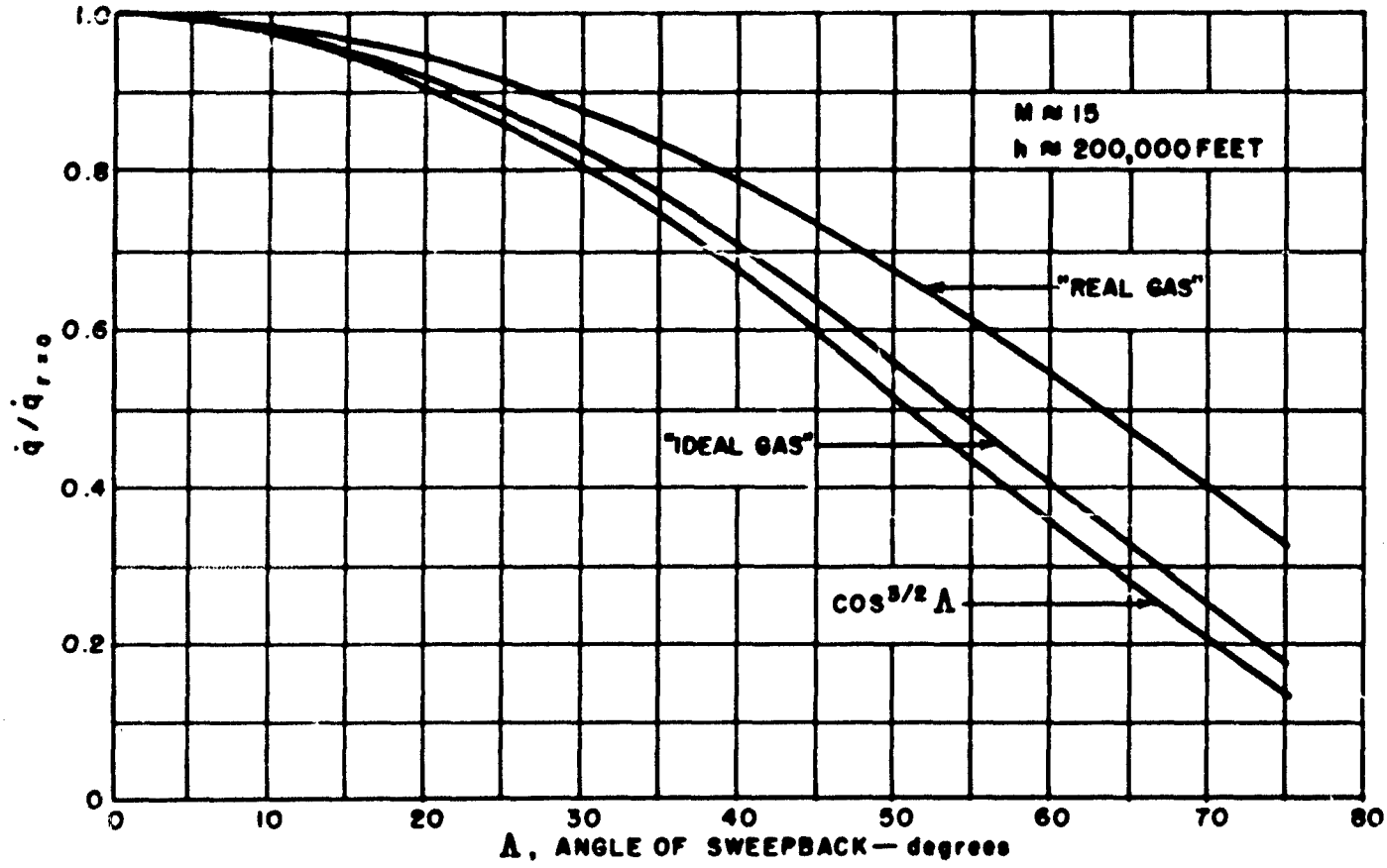

Figure 45. Effect of Sweepback on Local Heat Transfer Rate

2. NONEQUILIBRIUM HEATING RATES

Preliminary considerations show that it is quite likely that the flow field produced by Brass Bell at the higher (Mach number and altitude) portion of its flight path may be in thermal nonequilibrium. A theoretical investigation of the nonequilibrium case, paralleling and extending previous work, is reported in detail in Reference 11. The practical implications of this work are presented here.

An estimate of the important nonequilibrium effects on the heat transfer at any point in the nose region of a blunt-nosed, unyawed, axisymmetric body was extracted from the results of Fay and Riddell. The ratio of heating rates for nonequilibrium conditions to corresponding equilibrium conditions is shown to depend on the catalytic effect of the wall and the reaction rate models assumed to represent the dissociation process in the gas.

a. Stagnation Region

At the present time, three different reaction rate laws have been proposed (Hirschfelder, Logan, and Davidson). The effect of these laws on the heating rates at the stagnation region of a one-foot radius hemispherical-nosed body was investigated for a flight condition corresponding to Mach 15 at 200,000 feet altitude. These results show that, for this condition, a catalytic surface has a negligible effect on the heat transfer rates; they are only slightly greater than the equilibrium rates. The use of a noncatalytic surface, however, can significantly reduce the heat transfer, depending on the reaction rate law chosen. For the present example, the use of the Davidson law predicts that the heat

transfer rate will be reduced by a factor of 3.6 with the use of surface "poisoning", whereas the Logan rate predicts a negligible reduction with a noncatalytic surface. On the basis of recent limited experimental evidence, it appears that the Davidson rate is definitely too slow. For the given example, the effects of surface "poisoning" on the heat transfer rate would, therefore, be nearer those predicted on the basis of the Logan rate model.

b. Local Regions

The heat transfer rates for areas aft of the stagnation region were estimated approximately for the three rate laws and the same flight condition of Mach 15 at 200,000 feet. The variation of the heat transfer rate with distance for the catalytic surface was found to be negligible. The noncatalytic surface case, however, shows that the faster reaction rate laws can lead to a significant reduction of local heat transfer rates as a consequence of the larger local pressure drops around the vehicle. The slower Davidson rate exhibits only a slight decrease in local heat transfer, since most of the available reduction due to surface "poisoning" in this case has occurred at the stagnation point.

It can be concluded, on the basis of the Logan rate law, that surface "poisoning" will produce a significant reduction (approximately 50 per cent of the equilibrium value for this case) of heat transfer downstream of the stagnation point.

c. Effect of Flight Condition

To obtain an appreciation of the effect of changing altitude-freestream flight Mach number conditions on the nonequilibrium heat transfer to a noncatalytic surface, the ratio

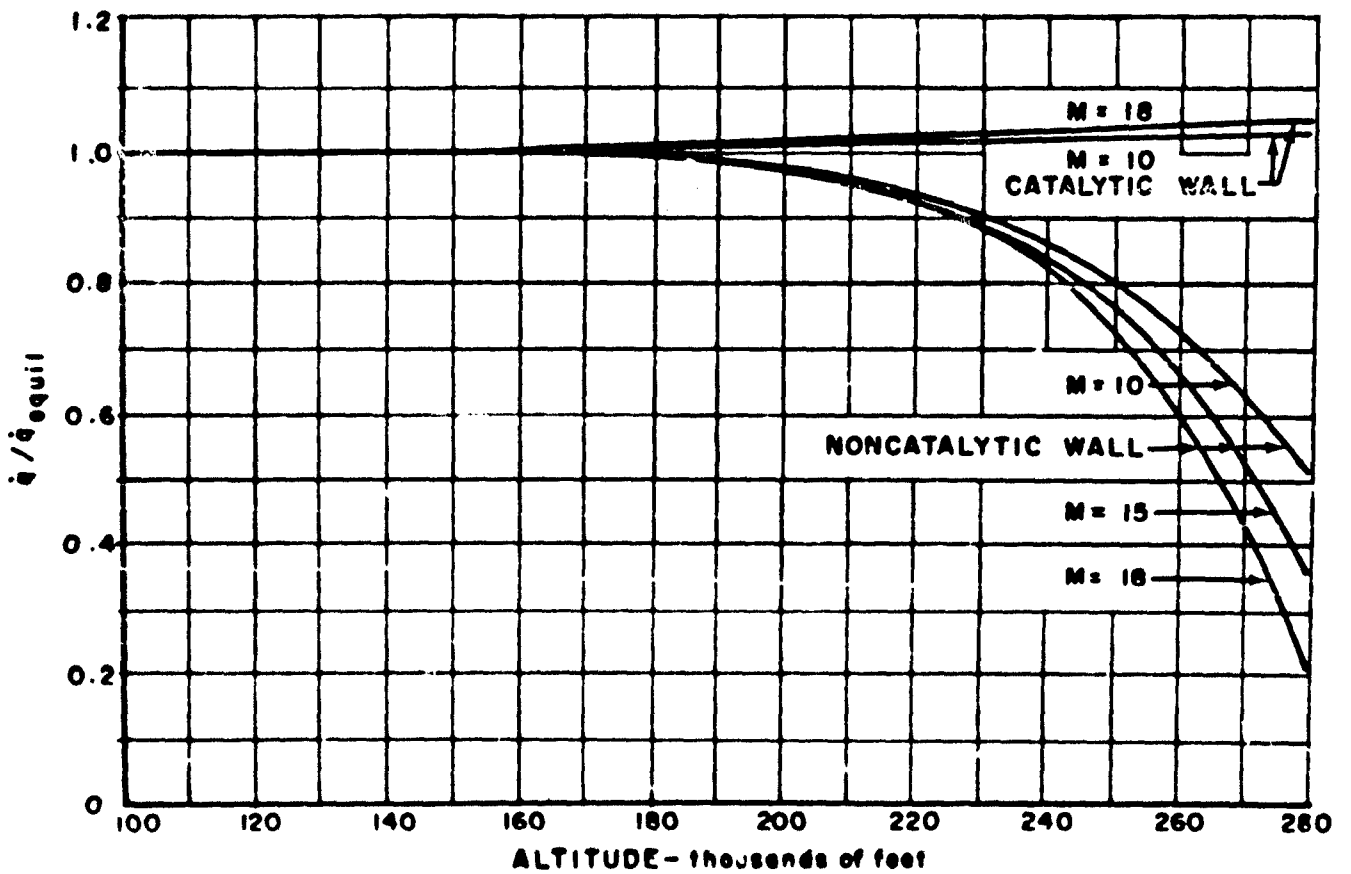

Figure 46. Nonequilibrium Stagnation Point Heat Transfer Variation with Flight Condition

(q/q_{equil}) was calculated as a function of altitude for several different Mach values, based on the Logan Rate Law. The results are given in Figure 46. At sufficiently higher altitudes (above 200,000 feet at Mach 15, for example), the surface heat transfer can be significantly reduced by the use of wall "poisoning" even for the faster reaction rate models.

C. ENVIRONMENTAL CONDITIONS FOR VISUAL RECONNAISSANCE AT HYPERSONIC SPEEDS

The problem of visual or photographic reconnaissance from a hypersonic aircraft is complicated by the fact that the human eye or the camera is in an environment quite different from that which prevails at rest on the ground. The various aerodynamic phenomena which could conceivably affect the light gathered by the camera, particularly those which are possible only in hypersonic flight, are brought out and evaluated herein. These are categorized into two major areas; i.e., those associated with changes of the refractive index of air, and those associated with the emission of radiant energy in the visible portion of the spectrum. The results obtained on the basis of the best theoretical and experimental information available show that the practical use of a camera or any other optical device on Brass Bell is possible, but will be limited to selected regions of the visible spectrum where the interaction of the incoming light with optically active high-temperature air in the boundary layer is a minimum.

In the following paragraphs, the influence and importance of each effect in either distorting the light field or in producing extraneous masking background light is discussed qualitatively and quantitatively, and the practical measures which can be taken in each case to minimize any undesirable effects are indicated.

1. REFRACTION OF LIGHT WAVES

A body moving at hypersonic speeds produces a shock pattern with its associated sharp density gradients in the surrounding air. The question thus arises as to the extent of refraction of light waves coming in through this shock pattern to a camera located on the body.

Immediately adjacent to a moving body, there is also a thin boundary layer where the state parameters velocity V, temperature T, and density ρ change rapidly from their values on the body to their extreme values. This boundary layer of highly heated air could conceivably affect light rays coming into a camera in the vehicle in several ways also. One is by refraction of the rays due to the large density variation in this layer, whether the flow in the boundary layer is laminar or turbulent. Frequency selective refraction will also occur where the highly heated air in the boundary layer has absorption lines and bands in the visible part of the spectrum.

a. Refraction by Shock Waves

The shock pattern in the neighborhood of the camera is due to the conical shock off the nose of the body, softened by expansions from the shoulder (cone-cylinder joint) of the body, and the shock off the leading edge of the wing. These patterns were computed for conditions corresponding to two points on the Brass Bell flight path (Mach 8, and Mach 15), and the results were presented in detail in Reference 9. Essentially, it has shown that the angle between the incident light to the camera (located near the rear of the body) and the shock wave is always less than 60 degrees. Corresponding deviation of incoming light rays was shown to be in the order of 0.003 degree. Although some design changes have occurred which would affect these calculations slightly, it is expected that the resultant deviations will still be negligible for all flight conditions.

b. Refraction by Density Gradient in Boundary Layer

A simple order-of-magnitude argument was used in Reference 9 which demonstrated that the refraction of light by the boundary layer density gradient is very small at altitudes

above 100,000 feet (less than 0.0001 degree). This small value is essentially due to the low air density where the index of refraction is very close to that in a vacuum. A re-evaluation of this result in the light of the latest information resulted in the same conclusions; i.e., this effect is negligible.

c. The Index of Refraction at Elevated Temperatures

The path of a light ray as it passes through an optical medium (air) is completely specified by the spatial (and temporal) variation of the index of refraction and the position and direction of the ray as it enters the medium. The mathematical description of this statement is contained implicitly in the fundamental equation of geometrical optics. The only quantity in the equation which depends on the properties of the medium is the index of refraction. At low temperatures, the index of refraction is essentially a function of the air density. At high temperatures the problem is more complex; the refractive index is a function both of temperature of the medium and of the light frequency. A detailed discussion of this expression and its implications is given in Reference 11. The essential features of the argument followed there and the results obtained are:

(1) At high temperatures, absorption lines and bands appear in the visible part of the spectrum of air, as differentiated from a continuous, essentially zero, absorption at room temperatures.

(2) The magnitude of the refractive index is changed by these new absorption processes and it becomes frequency sensitive (dispersion).

(3) The greatest changes in the value of the index are in the neighborhood of the line or band.

(4) The greatest change in index for conditions significant for the Brass Bell vehicle is given by a typical calculation as $n - 1 = 0.00012$.

The results obtained lead to the conclusion that the dispersion effects of high-temperature air must be considered in any detailed study of maximum resolution.

2. RADIATION

The highly heated and partially dissociated and ionized air in the boundary layer surrounding a hypersonic vehicle emits radiant energy in the visible part of the spectrum. If this flux of radiant energy is very small compared to the luminous flux arriving at the vehicle from photographic objects, the visual reconnaissance capability of the aircraft will be unimpaired. Conversely, if the intensity of light in the boundary layer is large compared to the intensity of light arriving from the object, visual reconnaissance is not feasible. For the intermediate case, visual or photographic reconnaissance will be possible but with some degradation in clarity which must be evaluated (Section XI).

At the present time, the flow quantities V, ρ, and T in the boundary layer for the flight conditions of interest to Brass Bell can be obtained by considerable computational labor, on the basis of reasonably accurate theories now available. The accurate prediction of the intensity and distribution of the luminous radiation from an element of air at a given uniform temperature and density, however, requires relatively detailed information concerning the composition of highly heated air. This is particularly true with respect to the minor constituents whose formation and break-up are accompanied in the atomic picture by electronic transitions which produce radiation in the visible and near infrared part of the spectrum. The exact stage of an element of air in the boundary layer at a given point and under given external conditions depends on the history of the particle, starting with its passage through the shock wave. This brings in the

question of whether complete thermodynamic equilibrium of all components exists, or, if not, as is the more probable case for the conditions of interest, what is the actual composition of the air at a specific point in the flow pattern? The current state of the art does not permit such precise predictions to be made.

It is possible to demonstrate, however, the general nature of the problem of boundary layer luminosity and to delineate the conditions where it could be significant, by presenting some characteristic numerical calculations. This has been done in Reference 11 for the significant radiating processes. A brief description of this work is presented in the following paragraphs.

a. Equilibrium Radiation

The visible radiation emitted by the highly heated boundary layer is produced by only a very small fraction of the molecules in the air in the temperature and density range of interest to Brass Bell. The radiation due to the recombination of electrons with oxygen atoms to form the negative oxygen ion is expected to be the significant process, since the characteristic time for this mechanism is small enough to make equilibrium calculations meaningful. Although equilibrium calculations would show that the formation of nitrogen dioxide from nitric oxide and oxygen atoms produces a larger luminous flux, this process is too slow to be effective.

The results of the calculations, the bound-free transition of O^- only, are given in Table VIII for a 5-centimeter slab of air at various densities and temperatures. These values represent the luminous flux received at the surface of the slab in the spectral region between 5000A° and 6000A° in lumens per square centimeter. Previous estimates of these phenomena (Reference 19) are slightly different than the present ones, due to the use of more recent values of the concentration of oxygen atoms and electrons.

The values given in Table VIII must be compared with a typical value of 5×10^{-3} lumens per square centimeter representing the intensity of the light from the terrain. The boundary layer temperatures at the camera station are estimated to be less than 3000°K and the thickness of the maximum temperature layer about 5 centimeters at most, so that the intensity of light from the terrain is approximately 10 times larger than the intensity of the background light from the boundary layer.

It was shown previously in Reference 9 that visible radiation will emanate in the region of the body nose due to the local high temperature of the air. This is only significant in the region near the nose, however, and will not affect cameras located in positions aft.

b. Nonequilibrium Radiation

The general concept of nonequilibrium radiation can be demonstrated as follows. Consider the time history of a given element of fluid as it passes through a strong normal shock. At time t = zero, the air is suddenly

TABLE VIII. LUMINOUS FLUX FROM EQUILIBRIUM RADIATION

Temperature K	(lumens per square centimeter) ρ/ρ_0 (where ρ_0 = sea level density)			
	10^{-1}	10^{-2}	10^{-3}	10^{-4}
5000	1.89×10^{-1}	3.76×10^{-1}	6.79×10^{-3}	1.16×10^{-4}
4000	7.50×10^{-1}	2.20×10^{-2}	4.41×10^{-4}	7.54×10^{-6}
3000	8.70×10^{-4}	7.22×10^{-5}	3.42×10^{-6}	1.22×10^{-7}

heated by compression as it passes through the shock and, as a result, it is put into a new thermodynamic state defined by T, ρ , and V. The actual mechanism of the emission process requires a characteristic time, τ . Therefore, the radiation is not emitted until the fluid element has traveled a distance $d = V\tau$ from the shock front.

The time τ for a given radiation process can be computed from radiation theory, and the approximate velocity V can be calculated from the flow equations. The nonequilibrium radiation problem is significant in those cases where the distance is of the order of a characteristic vehicle length, L. The distance, d, for the reaction ($NO + O \rightarrow NO_2 + h_\nu$) is given in Table IX for several typical flight considerations.

The calculated distances, d, of Table IX are at least an order of magnitude larger than the vehicle length, leading to the conclusion that this process is definitely not in equilibrium and will not contribute to the background radiation at the camera station.

c. Other Radiation Phenomena

A possibility exists, which cannot be completely discounted at the present time, that oxidizer particles of the highly heated nose or skin will flake off or be eroded off by the high velocity air stream and, glowing and emitting visible radiation, be carried downstream over the camera field of vision. Preliminary tests have shown that flaking is unlikely with the metals currently being considered for the structural skin. Furthermore, microscopically thin ceramic or metallic coatings which will not oxidize or sublimate into the outside air exist and can be used if necessary. The possibility of the skin at a temperature of the order of 2000°F vaporizing slightly into the boundary layer and providing a luminous source has been recognized, and an experimental program to study the existence and extent of this phenomenon has been outlined for future investigation.

3. FUTURE STUDIES

The studies which have been completed at this time show that optical reconnaissance is feasible with a Brass Bell vehicle. The basis for showing that the refraction effect would not be significant for a reasonable choice of camera location and a usable portion of the visible spectrum is very firm. In conjunction with the radiation studies, however, it must be kept in mind that the theory involves many assumptions which must be verified by further

TABLE IX. CHARACTERISTIC DISTANCES FOR NONEQUILIBRIUM RADIATION

Altitude (feet)	Mach Number	d (feet)
120,000	10	4.61×10^5
	12	8.15×10^4
	14	8.50×10^4
	16	1.03×10^5
180,000	10	1.44×10^6
	12	5.97×10^5
	14	8.70×10^5
	16	9.98×10^5
	17	1.05×10^6

experimental studies or flight tests to supplement the available experimental information on radiation. The numerical calculations are sensitive to small concentrations of particular species of molecules, and consequently the validity of these results can only be established when the concentrations can be confidently predicted with accuracy. The problem of predicting the concentrations is made difficult by the labor involved for the required accuracy for the equilibrium case, and by the lack of reliable basic information on recombination rates for the nonequilibrium case.

Specific experimental and theoretical programs to obtain the required basic information underlying the prediction of visible radiation from the boundary layer have been delineated and are presented in Reference 11. A program to obtain, among other things, accurate values of recombination rates for the various processes occurring in air throughout a range of temperatures and densities of interest for Brass Bell consideration, has already been initiated and is currently being conducted at Cornell Aeronautical Laboratory under the present Brass Bell contract.

D. ENVIRONMENTAL CONDITIONS FOR RADAR RECONNAISSANCE

The use of electromagnetic radiation in the radar frequencies for communication and reconnaissance by Brass Bell will be subject to interference by the environment of a highly heated boundary layer, where this layer plays a similar role to that outlined in the preceding section on visual reconnaissance. The properties of the air in the boundary layer no longer resemble its properties at room or ambient temperatures. In particular, the concentrations of free electrons and oxygen atoms produced in the highly heated air are large enough to provide strong interactions with radar waves.

Two types of interactions have been investigated and found to be important. The first is the interaction of the electromagnetic wave (radar frequencies) with free electrons. This interaction refracts or, in the limiting case, reflects the wave as it enters an ionized layer. The second interaction is the frequency continuous absorption of the electromagnetic wave associated with the free-free transition of an electron in the neighborhood of an oxygen atom. There may be a number of absorption bands in the radar spectrum which are the result of molecular transitions, but these were not given priority for investigation during the current study period, since, in practice, they can be avoided by a judicious choice of radar frequency. These questions must be investigated ultimately, however, because of their effect on ferret reconnaissance.

1. EQUILIBRIUM CONDITIONS

a. Refraction and Reflection of Electromagnetic Radiation

The gross aspects of the interaction of the radar waves with the free electrons in the boundary layer is studied by considering the index of refraction, n, of an electron gas which is shown to be a function of the critical frequency of magneto-ionic theory. When the frequency of an electromagnetic wave incident on an ionized layer of gas is less than the critical frequency for the layer, the wave is reflected by it. The value of the critical frequency for air at various temperatures and densities can be computed on the basis of the equilibrium concentrations of electrons. Table X gives the results of this type of calculation; here the critical wave length in centimeters is tabulated for a range of temperatures, T, and density ratios, ρ/ρ_0, where ρ_0 = sea level density of air. The equilibrium concentrations of electrons used in these calculations were obtained from the (calculated) values given in Reference 20.

It is noted that the critical wave length is very temperature dependent and only slightly density dependent; dependence on layer thickness is also small. Typical conditions in the boundary layer of the Brass Bell vehicle several feet downstream of the nose for flight at Mach 15 are that the maximum temperature is less than 3000°K and $\rho/\rho_0 < 10^{-4}$. Hence, it is seen from Table X that, on the assumption of equilibrium electron concentration, radar

TABLE X. CRITICAL WAVELENGTHS FOR ELECTRON REFLECTION (cm)

T(°K)	ρ/ρ_0			
	1	10^{-1}	10^{-2}	10^{-3}
3000	11.4	20.4	37.2	72.5
4000	0.96	1.04	3.90	9.25
5000	0.23	0.51	1.18	8.90
6000	0.10	0.22	1.65	1.23
7000	0.05	0.12	0.26	0.52
8000	0.03	0.07	0.13	0.24

wave lengths smaller than about 20 cm will not be totally reflected, although they will be refracted to some extent. The amount of refraction is dependent on the wave length and the angle of incidence of the incoming wave to the antenna. This must be determined for a given case by a more detailed method than the gross study given herein.

b. Absorption of Electromagnetic Radiation

The absorption of electromagnetic waves by the free-free transitions of electrons in the field of atoms or molecules becomes important in the frequency range characteristic of radar systems. This absorption process is continuous in nature and is frequency dependent. The absorption coefficient can be calculated and used for quantitative predictions of the transmission of radar waves through a layer of high-temperature air, taking into account the effects of induced emission. The practical significance of the free-free absorption can be demonstrated with a few sample calculations. The percent of transmission of a 2-cm wave (K-band) through a 5-centimeter slab of air at a temperature, T, and a density ratio, ρ/ρ_0 is given in Table XI for some representative values of these parameters.

The boundary layer conditions during the flight of Brass Bell are not expected to exceed 3000°K, with densities between 10^{-1} and 10^{-2} of the sea level value. Therefore, Table XI indicates that some attenuation of the radar signal may occur, but the magnitude of this effect cannot be definitely established at this time.

TABLE XI. PER CENT TRANSMISSION OF A 2-CENTIMETER WAVE THROUGH A 5-CENTIMETER HEATED AIR LAYER

T (°K)	ρ/ρ_0			
	1	10^{-1}	10^{-2}	10^{-3}
3000	0.01	36.8	92.1	99.6
4000	0.01	0.01	0.01	57.4
5000	0.01	0.01	0.01	0.37
6000	0.01	0.01	0.01	0.01

2. NONEQUILIBRIUM CONSIDERATIONS

The discussion in the previous section was based on the assumption that the concentrations of electrons, oxygen atoms, etc., in the boundary layer are approximately equal to the equilibrium values. The validity of this assumption can only be established when the characteristic times for the electron recombination mechanisms, oxygen dissociation processes, etc., can be shown to be small compared with the characteristic flow time. The characteristic times for radiative recombination of electrons are discussed in Reference 11, but a great deal more work is required to complete the investigation of all the processes which can be important in nonequilibrium flow problems. The concentration of each molecular species in the boundary layer is determined by a large number of competing reactions (radiative and nonradiative). The fact that one (say, radiative recombination) process is slow does not mean that the products of this reaction are not in equilibrium; a nonradiative three-body process may be fast enough to maintain equilibrium. On the other hand, a fast reaction may involve reactants which are products of slow reactions only; consequently, it will not be an important process. Quantitative statements about the effects of nonequilibrium flows must be based on a complete knowledge of the detailed reactions, which at the present time is not available.

E. INTERACTION OF AIRCRAFT SURFACE WITH ENVIRONMENT

It is conceivable that the surface of a vehicle moving at hypervelocities through the upper atmosphere can suffer deterioration due to several possible causes. A thorough experimental investigation of the extent and practical importance of each anticipated phenomenon is not possible, since the various phenomena are not amenable to adequate simulation in the laboratory at the present time. These phenomena and their effect can thus only be estimated by an extrapolation — guided by theory — of the very little information available from closely related experiments.

It was estimated that the most important potential causes of surface damage to the Brass Bell vehicle are pitting or penetration by micrometeoric impacts, erosion due to surface sputtering, erosion due to chemically-induced scaling of the surface metal, and possible ignition of the metal surface. Each of these phenomena are discussed and quantitative estimates of these effects are given.

1. IMPACT WITH MICROMETEORS

The limited amount of information available at this time about the size and density distribution of micrometeors in the atmosphere must necessarily make any deductions regarding their interaction with the surface of the vehicle highly speculative. Previous estimates had to be revised because very recent information from upper atmosphere rocket firings gives an estimate of micrometeoric density in the atmosphere several orders of magnitude greater than the previously accepted density.

Micrometeors enter the earth's atmosphere with velocities ranging from 36,000 to 240,000 feet per second. Unlike the larger meteors, micrometeors slow down because of collisions in the rarefied atmosphere. At about 230,000 feet, the micrometeors lose their high entry velocity and slowly settle to the ground, taking from one to seven days to fall. Below this altitude, therefore, one need not consider the high velocity of entry into the earth's atmosphere, but need only consider the velocity of the flight vehicle in the interaction between the micrometeor and the skin of vehicle.

Recent rocket soundings have been undertaken to determine the density of micrometeoric dust by measuring the rate of meteor impacts with the rocket vehicle (Reference 21). Results of these early findings indicate a number density of micrometeors of one per 10 cubic meters, with diameters ranging between 10 and 50 microns, and density and composition unknown.

Damage to the skin of a vehicle by an individual micrometeor will depend primarily upon several factors; the impact momentum of

the meteor relative to the vehicle, the size and composition of the meteor, and the skin material. Damage will depend also upon the structure of the meteor; e.g., "feathery" meteorites honeycombed with holes, meteors with a high iron content, or stony meteors. A discussion of this point, however, is quite speculative at this time.

Results of available laboratory tests on damage due to high-velocity particles impinging upon targets of various materials do not give a completely satisfactory basis for predicting damage due to meteors, since full simulation of particle size and velocity have not been attained. However, an indicative trend may be obtained by using the results obtained from steel pellets impinging upon a steel target (Reference 22). For a value of V = 18,000 feet per second for the velocity of the vehicle (impact velocity), it is seen that for steel impacts upon steel, the depth of penetration is approximately 3 particle diameters. For a 50-micron diameter meteorite, this penetration amounts to 0.006 inch.

A consideration of the interaction between the shockwave and the micrometeor shows that the depth of penetration-particle diameter ratio is not significantly altered for the velocities of interest. That is, particles in the order of 50 microns will affect a body moving at M ≈ 10 and preceded by a shock wave essentially as much as they would in the idealized case of no shock wave interaction.

For a vehicle traveling at 18,000 feet per second through a micrometeoric concentration of one particle per 10 cubic meters as given by the latest data, the impact rate is about 50 hits per second per square foot of frontal area. Thus, the frequency of impact and the damage per impact indicate that the micrometeor problem may be severe. It is emphasized again, however, that (1) the damage results given above are based upon laboratory data where complete simulation was not possible, and (2) knowledge regarding the composition and specific gravity of micrometeors is far from adequate.

It is expected that more experimental data providing the basis for the estimates of micrometeoric concentration in the atmosphere will become available from sounding rocket firings scheduled during the current IGY program. Also, the problems of firing particles of less than 0.005 inch in diameter in the laboratory are being solved, so that reliable penetration data should also be available in the next year or two.

2. SURFACE EROSION

a. Sputtering

Sputtering is the name given to the phenomena of a gas atom moving at high speed which strikes the skin of the vehicle with sufficient kinetic energy to remove an atom of the skin material. Two distinct types of sputtering mechanisms were investigated previously (Reference 19). These were the bombardment of the metal skin by fast moving neutral atoms with sufficient kinetic energy to remove an atom from the metal lattice, and the bombardment by ions in the surrounding air accelerated by a potential difference between the metal lattice and the source of the ions. It was considered at that time that sputtering would not be a significant factor for Brass Bell. Since no basically new information has become available, this conclusion is still considered valid.

b. Chemically Induced Scaling

A limited amount of work has been done on oxide scale formation on materials at elevated temperatures, and this under static rather than dynamic conditions. Thus, there is no adequate basis upon which to evaluate the possibility or extent of oxide formation and scaling on the Brass Bell skin.

The thickness of scale formed in the absence of surface cracks is roughly proportional to the square root of the time, the principal mechanism being the diffusion of lattice vacancies between oxide and metal. High shear flows, turbulence, and impinge-

ment of small particles can cause greatly increased oxidation attack on metal surfaces, since the oxide coating will be continuously removed, leaving virgin metal continuously exposed to further oxidation attack. Reference 23 shows that the amount of scale formed depends somewhat on the composition of the alloy, but no predictions were made as a result of this work. Indications are, however, that oxide scale can be effectively inhibited by proper alloying.

The question of whether or not oxide formation and scaling occurs, and whether it is important for suitable skin material, like Haynes alloys, must await experimental investigation where the high skin temperature, the oxidizing atmosphere, and the shearing stresses are all simulated. Facilities for making these tests, such as Rollo (Cornell Aeronautical Laboratory) and various proposed modifications of plasma jets and high-intensity arcs are being built and will shortly be available.

3. SURFACE IGNITION

The possibility of combustion of the skin should be considered, since many structura' materials react with oxygen or even nitrogen with the evolution of heat. However, a thorough study is not possible at this time because relatively little basic work has been done in this field that can be applied to hypersonic conditions.

While the fundamental principles underlying ignition are relatively simple and some preliminary experiments are available for relatively slow cold flows, it is extremely difficult to extrapolate these data to hypersonic conditions. For example, ignition depends on the rate of change of heat transfer. Since heat transfer predictions are extremely complex at hypersonic speeds, the rates of changes are even more so.

An understanding of the theory of ignition and combustion, however, allows setting forth guiding principles which tend to minimize the probability of encountering these phenomena during flight. These involve selecting the conditions which (1) raise the ignition temperature of the surface material above the temperature of the body, and (2) result in a higher rate of change of heat loss with surface temperature than the rate of change of heat input with surface temperature, so that the equilibrium temperature is stable.

Factors which tend to raise the ignition temperature are:

a. High thermal conductivity and high emissivity.

b. Low heat of reaction.

c. A slow reaction rate due to a high activation energy and a thick protective film.

The rate of change of heat loss with respect to surface temperature relative to the rate of change of heat input can be increased by selecting a material with a strong temperature dependence of thermal conductivity and emissivity, and having both a low heat of reaction and a low activation energy. Except for the low heat of reactions, the requirements are conflicting.

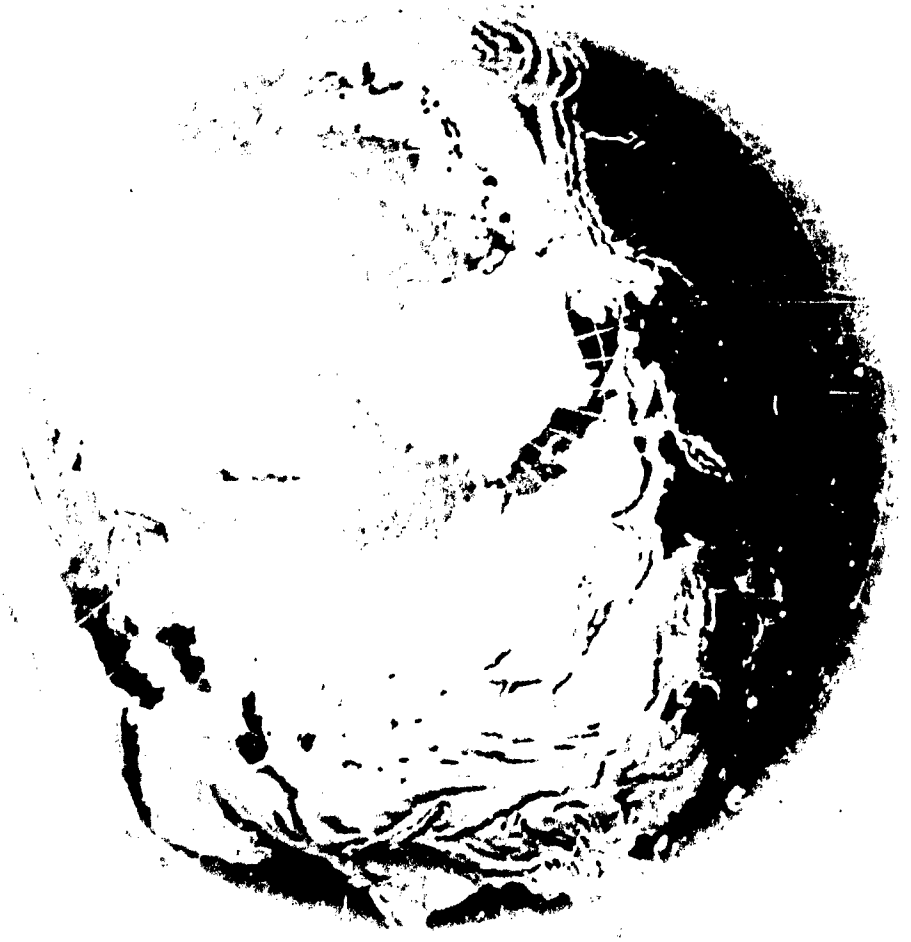

VII Navigation

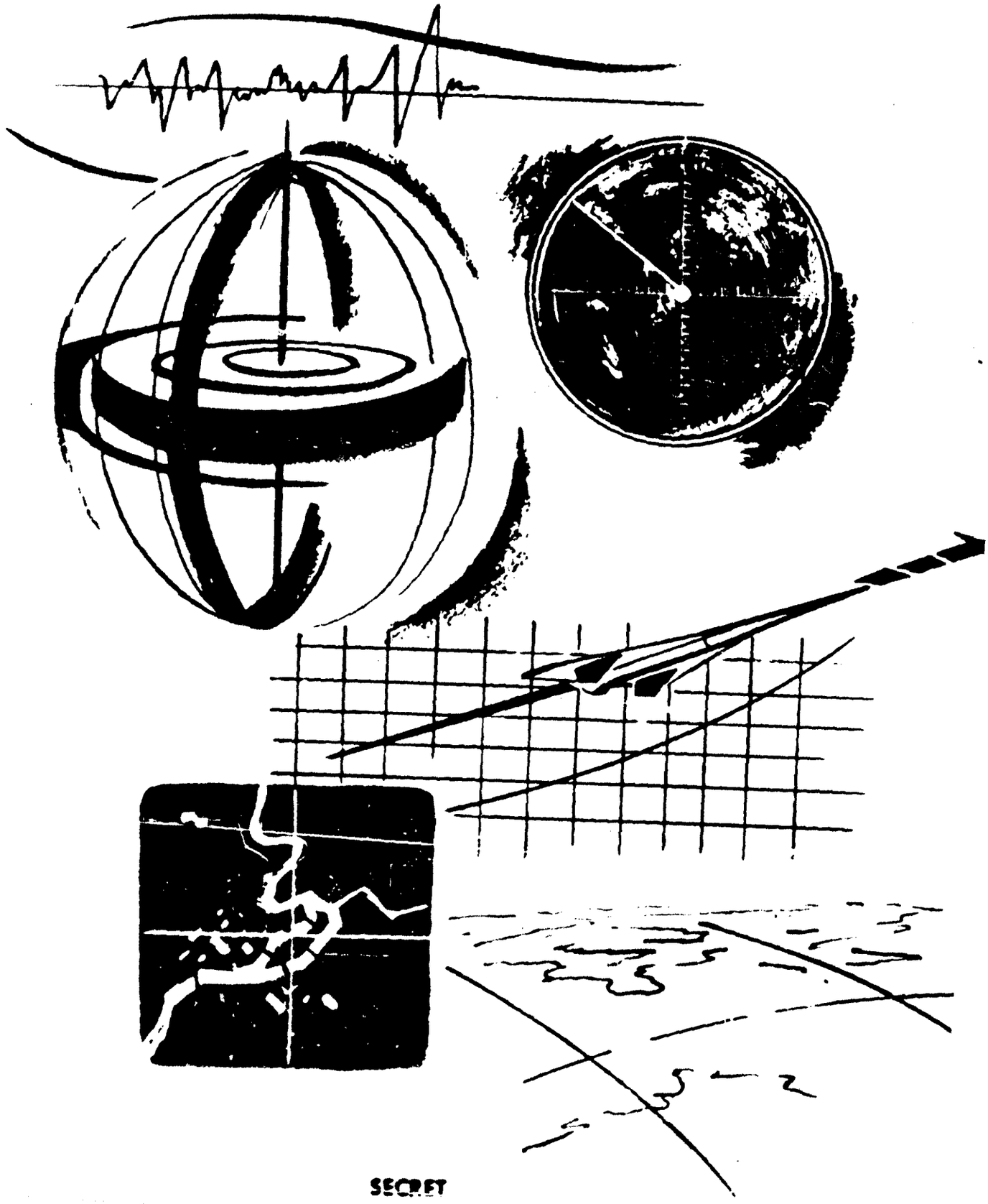

The broad purpose of the navigation system studies conducted during this period (reported in detail in Reference 24) was to extend the preliminary system analysis performed during the previous period and reported in Reference 25.

In detail this study covered:

A. Selection of error equations

B. Vertical channel analysis

C. Horizontal channel analysis

D. The effects of components dynamics

E. Digital computer performance

F. Review of over-all system configuration.

This particular study was restricted to a consideration of the navigational requirements only and did not include the many associated tie-in problems. The effort was concentrated on determining major effects unique to the environment caused by use in a hypersonic vehicle rather than on design details. These studies were applied only to the system described in Reference 25, and no examination was made at this time of other possible system configurations.

A. SELECTION OF ERROR EQUATIONS

During previous studies (Reference 25), the differential equations for platform tilt, velocity, and position errors were derived for various source errors. These derivations were based on the assumption of all-analog computation. Since many of the computations required in the Brass Bell navigation system will be performed by a digital computer, the system was again analyzed, but as a sampled-data system.

The purpose of this study was to compare the results obtained originally for an analog instrumentation (solutions of differential equations) and the corresponding results calculated when digital computations are performed (solutions of difference equations).

The results of this study indicated that the additional errors due to the introduction of a digital computer into the Schuler loops are, for a sampling period of less than 0.1 second:

Platform tilt	1×10^{-4} minutes of arc
Velocity	1×10^{-3} feet per second
Position	3 feet

This analysis assumed no errors in the digital computer itself. These effects will be treated separately as computer errors. The conclusion that can be drawn from this study is that even though digital computations are used, the system can be treated on a linear basis, greatly simplifying the analytical work.

B. VERTICAL CHANNEL ANALYSIS

Previous estimates of the accuracy of vertical channel information for accelerometer compensation and the computation of earth's radius were based on the use of average values. However, considering an inertial vertical instrumentation, the major contribution of uncertainties in the vertical instrumentation to horizontal position errors occur during the early portion of flight when the vehicle velocity is high. At this time, vertical errors are small. Thus, it is more realistic to consider the entire instrumentation, including the effects of cross-coupling between the horizontal and vertical channels. This method permits the specification of a vertical instrumentation that has errors increasing with time rather than average values.

At a time of 3200 seconds, the errors in horizontal position as a function of inaccuracies in the vertical instrumentation are.

For acceleration errors — 2.0×10^8 feet per g

For velocity errors — 8.5×10^3 feet per feet per second

For initial platform tilt — 22.5×10^3 feet per minute

Assuming an allowable horizontal position error of 3000 feet for each source, the resulting instrumentation accuracies for a pure inertial vertical channel are:

Acceleration - 1.5×10^{-5} g

Velocity 0.35 feet per second

Initial Platform Tilt - 0.13 min. of arc

Although these requirements are not too different from the horizontal channel, some means of supplementing the vertical channel would still be desirable.

Several possible sources of external references to supplement the inertial vertical instrumentations are as follows:

a. Radar altimeter

b. Atmospheric measurements

c. Programmed reference data

d. Doppler radar

A radar altimeter gives an indication of altitude above terrain to a reasonable degree of accuracy. However, to be useful to the navigation system, a terrain correction and the ellipticity of the earth must be programmed in to achieve the desired radius vector. Vertical velocity information can be obtained from a radar altimeter by averaging over a finite time interval. Good terrain information must be programmed into the system, and appropriate sampling times, based on the terrain variations, must be employed to obtain the desired accuracies. An important consideration to be noted is that, for all possible flight paths, certain regions exist where terrain information is accurately known and either small in value or with minute variations. Thus, with a system making corrections at discrete intervals over these known regions, the use of a radar altimeter appears practical.

At first glance, the possibility of obtaining vertical information from atmospheric measurements appears to be undesirable because of the difficulty of measuring the atmosphere at high speeds and correlating these measurements to height. However, the vertical information obtainable from an inertial instrumentation is of relatively high accuracy during the early portion of flight. This information could possibly be used to calibrate an air data system. Additional experimental work would be required to verify this possibility.

The fact that the average requirements for vertical velocity and position accuracies represent about 5 to 10 per cent of both the maximum vertical velocity and the change of altitude during the glide, introduces the possibility of obtaining this information from a program of the glide path. Again, this requires an analysis of how accurately the glide path can be predicted.

The use of a Doppler radar does not appear to offer a satisfactory solution.

The optimum method of inserting external vertical information into the inertial instrumentation varies from a discrete insertion of an altitude signal used only to correct vertical position, to a continuous introduction of vertical information where the steady state velocity and altitude measurement is obtained from the external reference and the transient information from the inertial reference.

Figure 47 shows in block diagram form a system using discrete corrections of both velocity and position. To establish the advantage of this system against one using only position correction, an analog computer evaluation of the error equations was performed. It was assumed that no errors existed in the reference information and that the forcing error source was due to a bias error in the vertical

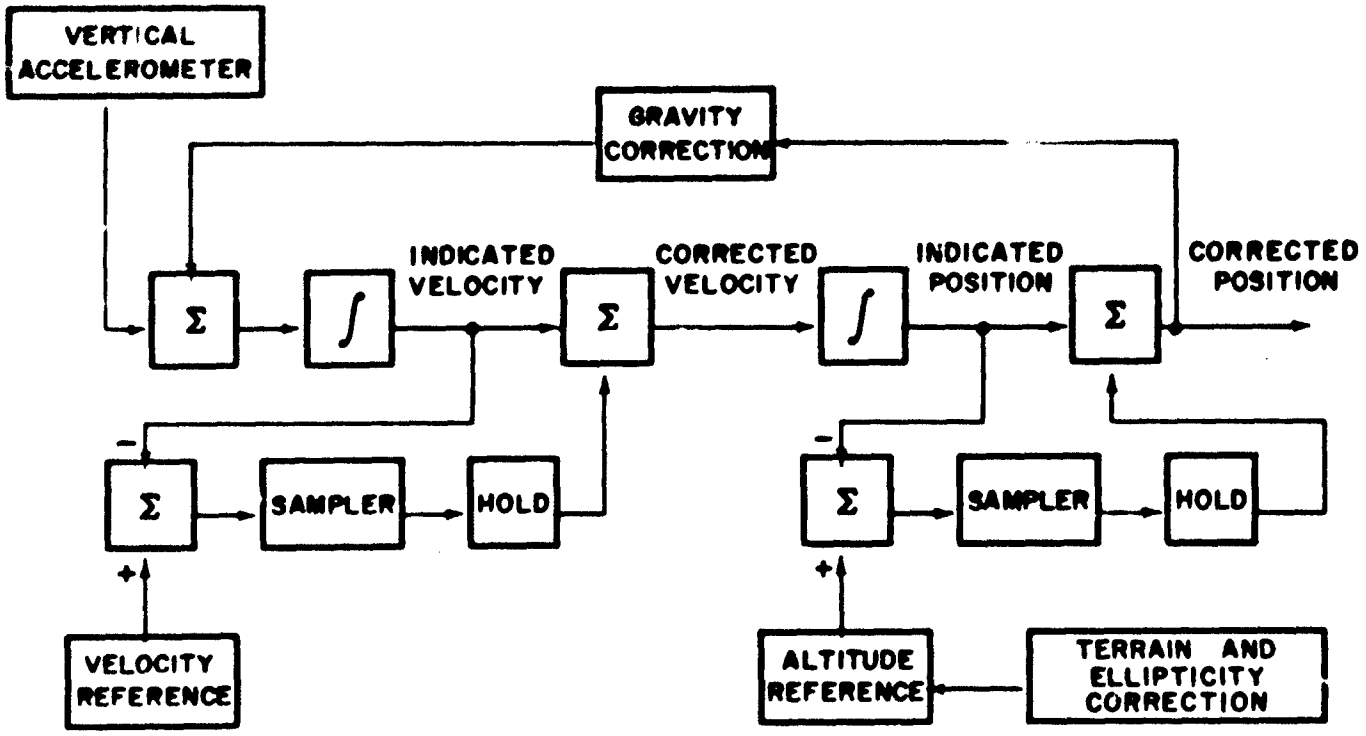

Figure 47. Inertial Vertical Instrumentation with Discrete Velocity and Position Corrections

accelerometer of 7.6×10^{-5} g. The resulting horizontal position error at the end of flight is 15,000 feet for a pure inertial vertical instrumentation, 12,000 feet if only a position correction was made at the halfway point, and 4000 feet if both a position and velocity correction were made at the halfway point.

The decision as to which scheme to use to supplement the inertial instrumentation must await the evaluation of all the various sources of error in the vertical channel. Of primary interest are the errors associated with the vertical position and velocity reference and the terrain program. The places at which the fixes are to be made can be selected such that the probable terrain errors are low.

Since a radar altimeter will probably be required to provide image motion compensation for the photographic equipment, this can also be used to provide the external reference required for the navigation system.

C. HORIZONTAL CHANNEL ANALYSIS

1. CROSS COUPLING

One of the major objectives of this study was the evaluation of the effects of cross-coupling between channels occurring when the true coordinate system and the coordinates indicated by the system instrumentation are not coincident.

The generalized equations denoting the cross-coupling terms were derived and listed in Reference 24. Since it was determined that this system could be treated as if it were analog instrumentation, the evaluation of these equations was performed using the analog computer.

To simplify the original analysis it was assumed that the equator of the navigation coordinate system was coincident with the earth's

equator, and that the true flight path was along the equator. Coupling between the vertical and horizontal channels was not considered as having been studied as part of the vertical channel analysis. These assumptions permit a simplification of the analysis in that the coupling of the longitudinal equations and the lateral and azimuth angle equations is eliminated.

To determine the effects of mass unbalance and anisoelasticity, two possible orientations of the gyros with respect to the X, Y, Z coordinates were assumed as shown in Figure 48. For the mission selected a_x is very near zero and terms containing it can be neglected. For the cases studied, the major effect of cross coupling in the horizontal channels is the

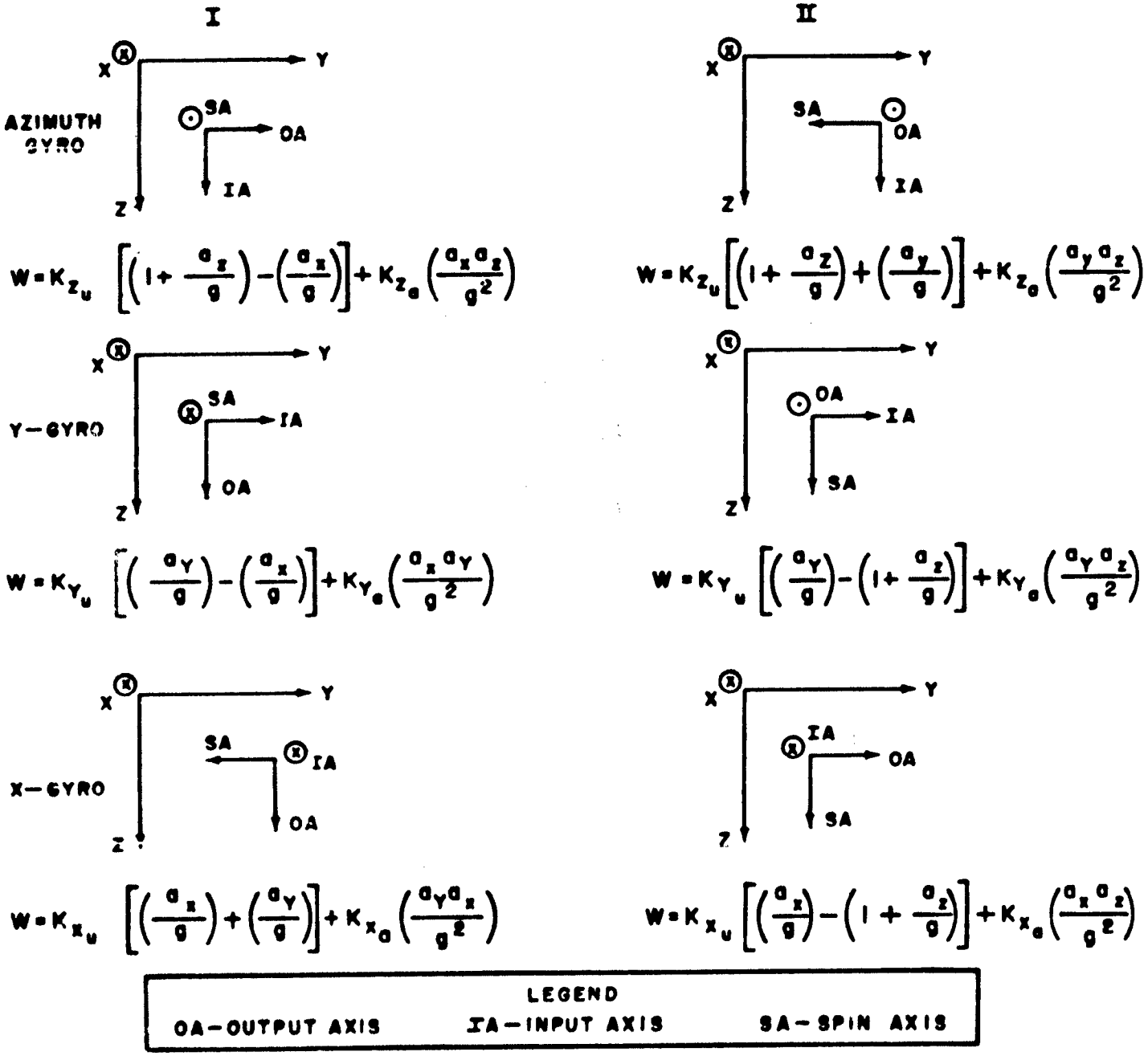

Figure 48. Possible Gyro Orientation and Resulting Drift Rate

TABLE XII. COMPARISON OF COUPLED AND UNCOUPLED ANALYSIS

Error Type	Value	Position Error (ft) at end of Flight			
		Longitudinal		Lateral	
		Uncoupled	Coupled	Uncoupled	Coupled
Acceleration	5×10^{-5}g	3000	3000	2950	3000
Random Gyro Drift					
X-Gyro	0.01°/hr	3400	3250	-	-
Y-Gyro	0.01°/hr	-	-	3350	2750
Azimuth Gyro	0.01°/hr	-	-	0	1500
Gyro Mass Unbalance					
X-Gyro Pos. I	0.02°/hr/g	1350	1100	-	-
X-Gyro Pos. II	0.02°/hr/g	2350	2200	-	-
Y-Gyro Pos. I	0.02°/hr/g	-	-	1350	250
Y-Gyro Pos. II	0.02°/hr/g	-	-	2350	2000
Azimuth Gyro. Pos I	0.02°/hr/g	-	-	0	650
Gyro Anisoelasticity					
Y-Gyro Pos. II	0.02°/hr/g^2	-	-	1200	600
Azimuth Gyro Pos. II	0.02°/hr/g^2	-	-	0	1500
Accelerometer Scale Factor	5×10^{-5}	150	70	-	-
Drive Scale Factor	7.3×10^{-5}	3500	3600	-	-
Initial Platform Misalignment					
X-tilt	0.17 min of arc	2180	2040	-	-
Y-tilt	0.17 min of arc	-	-	2000	1100
Z-tilt	0.17 min of arc	-	-	0	3350

introduction of terms in the y-tilt and azimuth rate equations that are functions of the vehicle velocity and dependent upon azimuth and y-tilt errors, respectively. The comparison of the resulting horizontal position errors for both the coupled and uncoupled analyses are shown in Table XII for the various types of source errors. The small difference occurring in the longitudinal errors is the effect of using a variable Schuler frequency in the coupled analysis rather than an average value as previously used.

Detailed results of this study appear in Reference 1, and the resulting RMS position errors are shown in Figures 49 and 50. These curves are based on gyro orientation according to Position I shown on Figure 48. Thus, there are no terms included for gyro anisoelasticity. The effects of gyros operating under a vibration environment has not been evaluated as yet. These results, including coupling, are not significantly different from the uncoupled analysis presented in Reference 24.

The effect of a great circle flight other than along the equator introduces additional

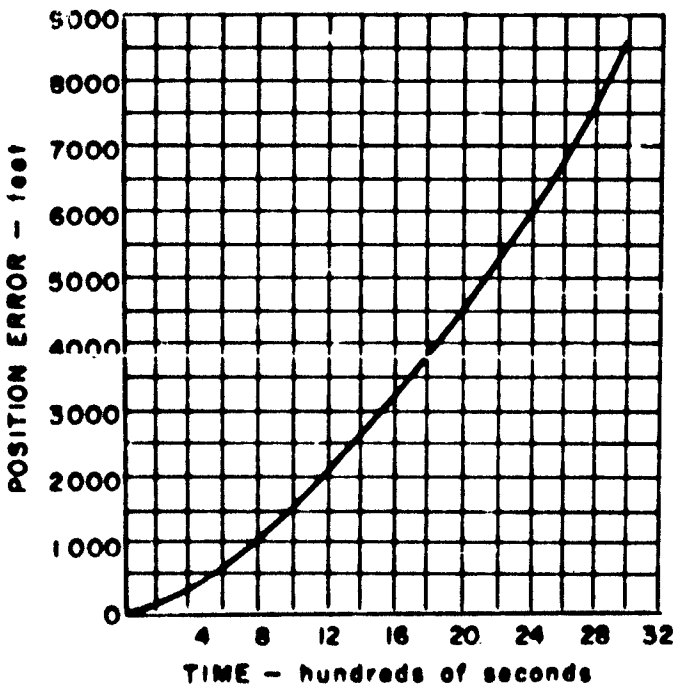

Figure 49. RMS Longitudinal Position Error

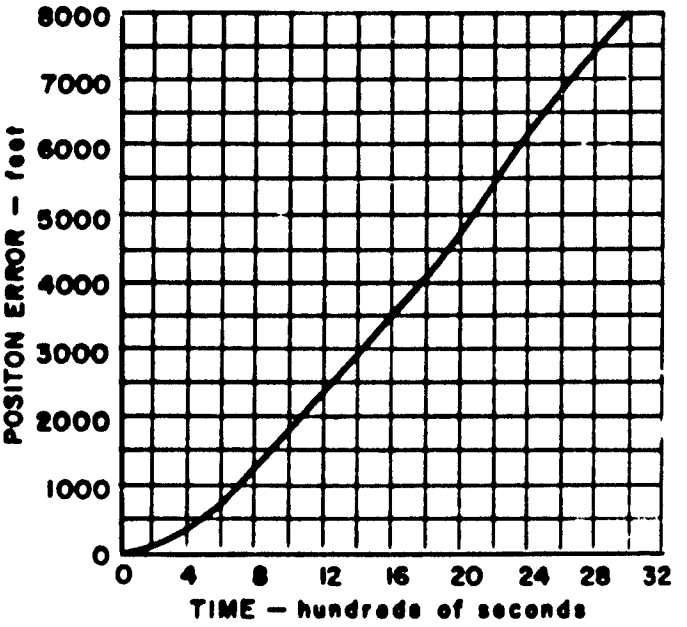

Figure 50. Lateral Position Error

cross-coupling terms that are a function of the earth's rate. However, because of the high velocity of the vehicle, they are less than 10 per cent of the forcing functions studied for the simplified case. Their additional effect on system accuracy should be relatively insignificant.

For non-great circle flight where $\dot{a}_z$ can no longer be considered zero, additional coupling terms must be considered. Scale factors errors will also occur in the lateral channel, and the mass unbalance and anisoelastic gyro drift equations will include additional terms. However, with the lateral deviation limited to 500 nautical miles from the great circle and heading angles off the great circle no greater than 30 degrees, no major new sources of error exist and the position error curves obtained for great circle flight are not altered appreciably.

2. DIFFERENTIAL POSITION ERRORS

One of the important functions of a reconnaissance system is its ability to determine the distances between two points over which the flight occurs.

Figures 51 and 52 show the accuracy attainable in determining the distances between

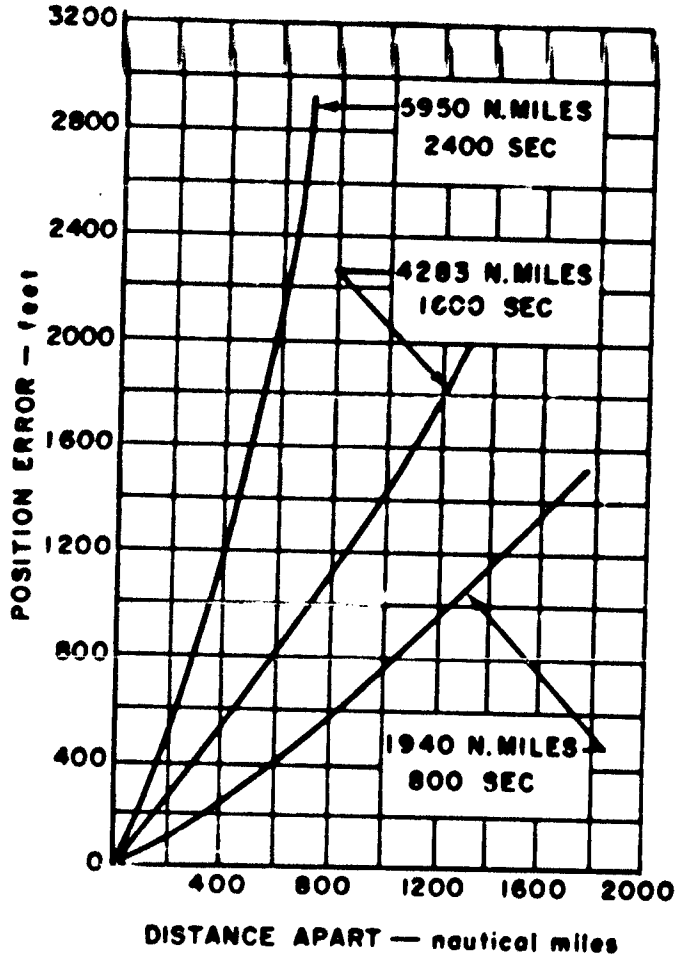

Figure 51. Longitudinal Errors Between Two Points

two points by subtracting the total positions of the points as indicated by the navigation system. Three curves are shown for the location of the first point, corresponding to times of 800, 1600, and 2400 seconds after take-off. These curves are based on the fact that, over small time intervals, the position error due to any individual error source is perfectly correlated.

D. EFFECTS OF COMPONENT DYNAMICS

The effects of instrumentation dynamics are most important during the boost phase of flight when the input parameters are changing rapidly. The effect of the boost profile on gyro performance has been considered previously under mass unbalance and anisoelasticity. The

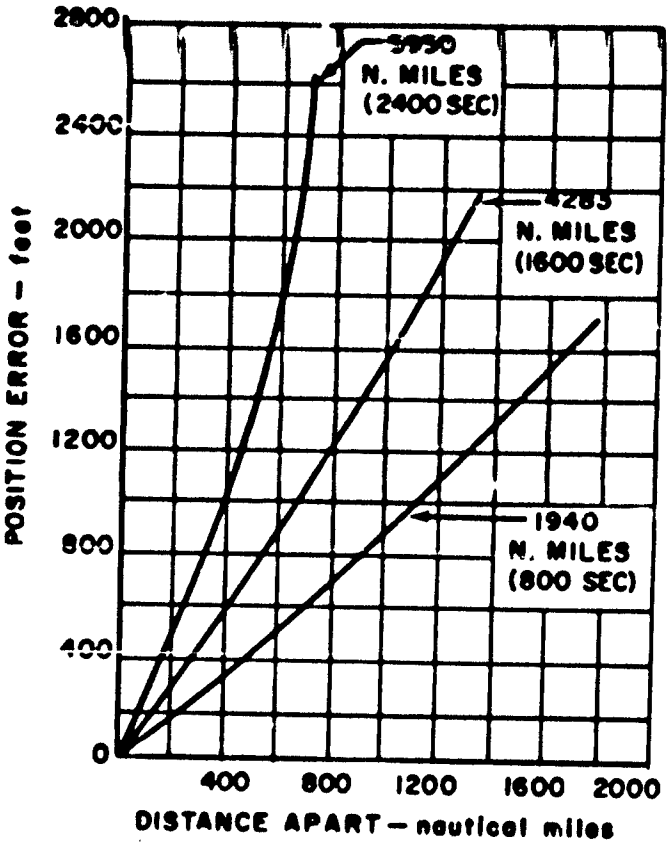

Figure 52. Lateral Errors Between Two Points

purpose of this study was mainly concerned with the dynamics of the accelerometers.

The results of this study indicate that, for existing instrumentation design, the natural frequency of an accelerometer is essentially determined by the maximum allowable cross-coupling error. For the accelerometers required for this system, this error results in a natural frequency in the order of 2800 radians per second, which is the same order of magnitude obtainable for existing accelerometers. With a damping factor in the order of 0.4 to 0.7, the errors introduced by the accelerometer's inability to follow the boost profile exactly were found to be insignificant.

A study was made to determine the effect of platform vibration isolators on the input accelerations. Results indicated that with an isolator having a natural frequency as low as 10 radians per second, the errors that occurred were negligible. The effect of platform vibra-

tion isolators on the accuracy of the attitude information measured by the platform presents a much more serious problem, and additional investigations are necessary to determine the adequacy of these data as an attitude reference for flight control. To perform this analysis, the expected vibration spectrum must be available in order to specify isolator requirements for a given set of instruments.

Based on the assumed flight profile during the boost and a 0.5-foot per second maximum allowable velocity error at the start of glide, the required accelerometer sampling rates were determined to be 180 per second and 195 per second for a computer using, respectively, trapezoidal and rectangular integration techniques. It should be mentioned that these are maximums, and in the practical case should be lower.

E. DIGITAL COMPUTER PERFORMANCE

A study was performed to determine the suitability of a fixed-increment type of computer for the Brass Bell navigation system. Originally it was estimated that some form of programmed flight profile augmentation would be required during the boost phase of flight.

These studies indicated that, based on the use of an integrating accelerometer with outputs quantized to a value of 0.5 foot per second, a fixed increment computer with (+1, 0, -1) size increments and a 128 per second iteration rate would be capable of the following performance.

1. Scaling error	- 145 feet
2. Time base error	- 733 feet
3. Scale Factor error	- 750 feet

If an accelerometer were used, the required iteration rate would be 256 per second.

The most significant errors contributed by the digital computer are the scale factor or quantization errors that are dependent on the incremental computations. The ability to follow a fast changing quantity and the minimizing of quantization errors requires an increased iteration rate. Thus, it is recommended to perform only the position integration by fixed incremental techniques, and the integration of acceleration with full binary words to avoid unreasonably high iteration rates.

F. REVIEW OF OVER-ALL SYSTEM CONFIGURATION

As a result of this study, a review was made of certain details of the system configuration proposed in Reference 24. In general, no significant changes were found to be necessary. Certain additional considerations pertinent to this system were found as a result of this study.

The gyros could be oriented as shown in column I of Figure 48, thereby minimizing the effects of mass unbalance and anisoelasticity for constant acceleration inputs.

An integrating accelerometer is recommended for this application because of present-day problems connected with accurately converting analog acceleration data into digital form.

Self-leveling of the platform using the accelerometers partially eliminates the errors associated with accelerometer bias uncertainties.

Although certain cross-coupling effects were found to be of some significance, their consideration did not result in any major change in system performance.

After more detailed study, a review of the component specifications listed in Reference 24 showed that the assumed values were conservative and some improvement in the over-all system performance could be obtained by assuming improved accuracy figures for:

a. Accelerometer compensation

b. Drive scale factor

c. Geocentric scale factor

d. Earth's rate compensation

e. Position integrator

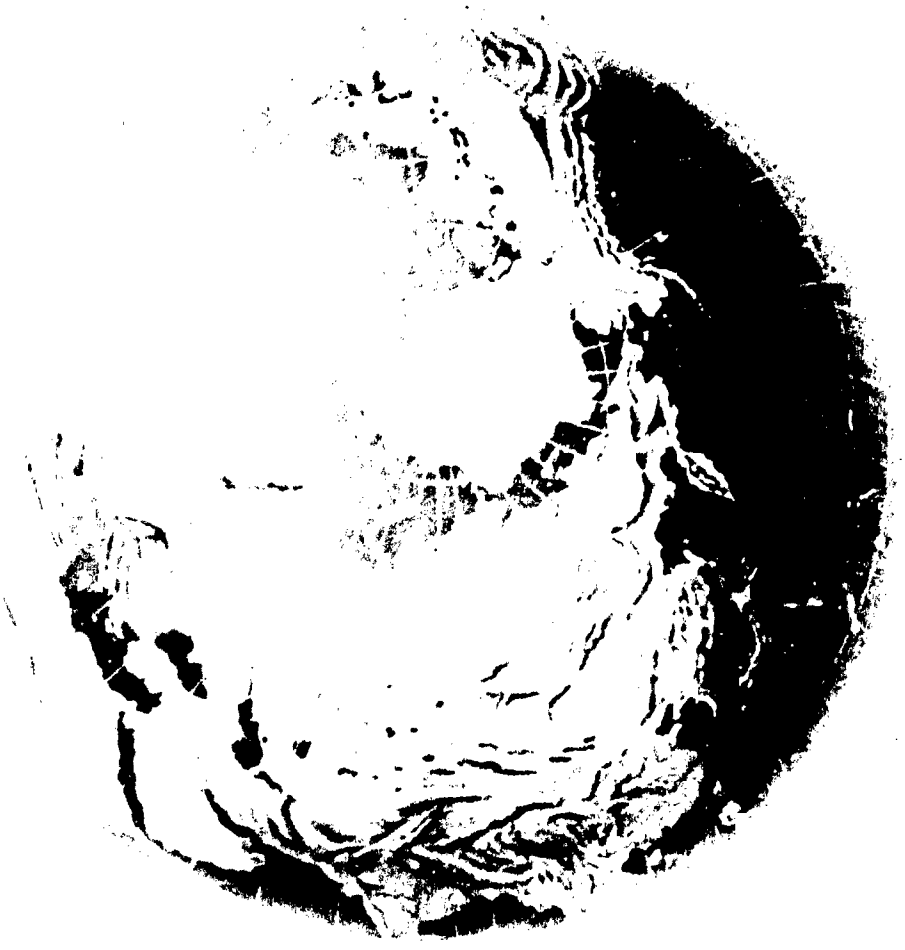

VIII Control

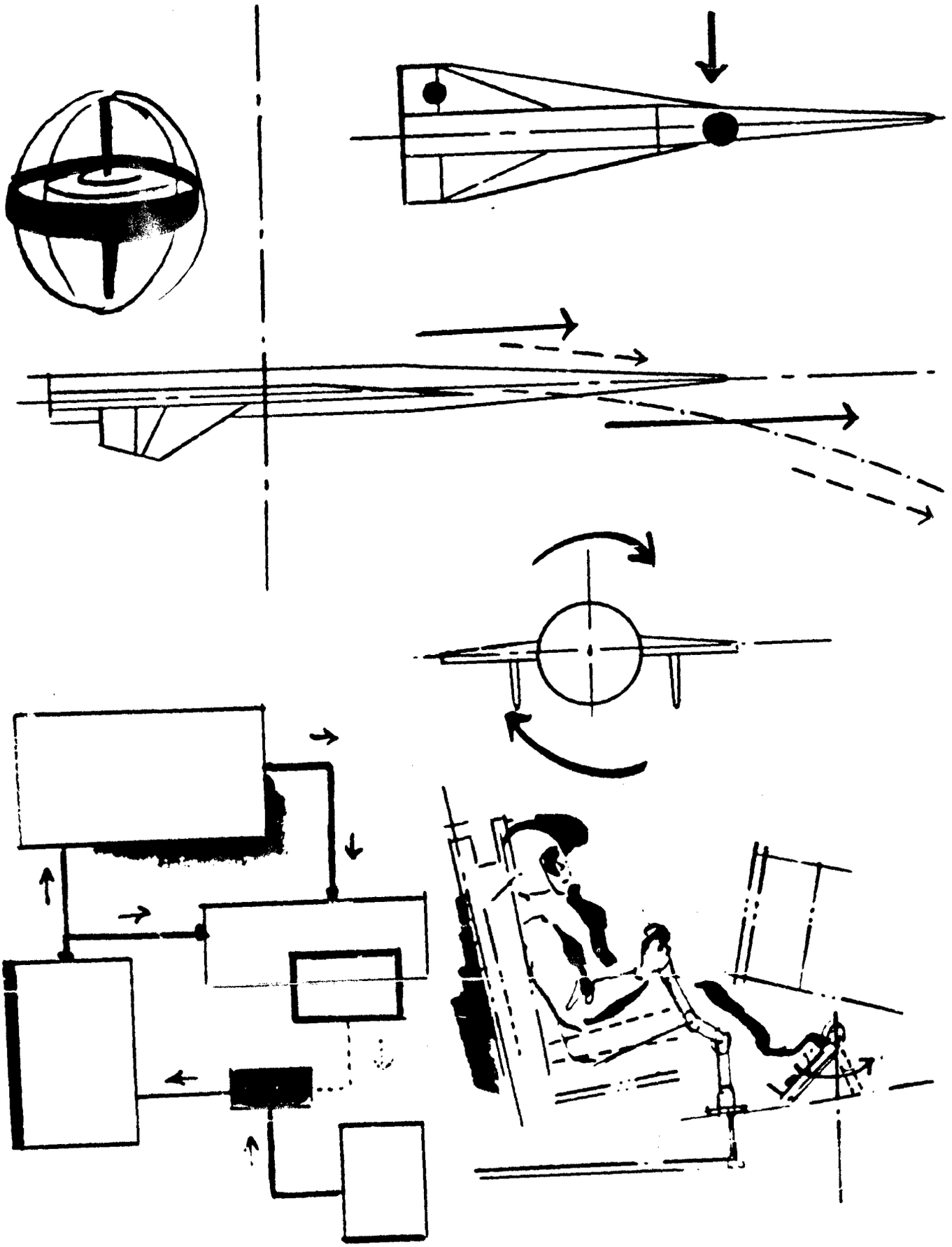

The effort in the area of flight control during this period has been a continuation of the studies reported in Reference 26.

These studies, reported in detail in Reference 27, have been limited to the following analyses pertaining to the airplane automatic flight control system.

A. Pitch Attitude Stabilization

B. Glide Path Control for Maximum Range

C. Yaw Stabilization and Turn Coordination

A. PITCH ATTITUDE STABILIZATION

Although the aerodynamic and aeroelastic characteristics of the Brass Bell airplane are not firmly established, an analysis of the autopilot was made to uncover any special control problems that might occur with the airframe and to permit a resolution of many of the autopilot problems which can only be done after a detailed analysis. An important objective of this study was to effect a comparison of reaction control systems with conventional aerodynamic controls.

During these studies, a conservative design approach was taken insofar as the aerodynamic characteristics were selected for the case of maximum static instability. (Angle of attack at trim assumed zero.) In the actual case, it is expected that, at trim conditions, positive static stability will exist. This belief was not investigated at the present time, and will be the subject of future studies.

There were five major objectives of this study:

a. To establish performance figures for attitude stabilization.

b. To compare the use of reaction controls and aerodynamic surfaces.

c. To establish the accuracy of attitude control.

d. To establish preliminary performance specifications.

e. To determine and point out those aspects of the structural and aerodynamic design that may preclude a practical autopilot design.

1. ATTITUDE STABILIZATION

Two criteria exist for establishing the performance of an autopilot for a statically unstable airframe. First, a minimum gain is required to overcome the unstable moments; and second, consideration of the aeroelastic characteristics and the dynamics of the autopilot components establishes a maximum gain.

Because of the low aerodynamic damping existing during hypersonic flight conditions, artificial damping must be provided. Theoretically, the damping signal could be obtained from rate gyros or passive networks operating on the attitude signal. However, consideration of the use of the inertial platform of the navigation system as an attitude reference and the bending characteristics of the airframe makes the use of rate gyros most desirable. Considerably more freedom is available in locating the rate gyros rather than the inertial platform in a position favorable to the bending modes.

Based on the existing aerodynamic and aeroelastic data, the maximum and minimum autopilot gains together with a recommended setting were determined as a function of altitude as shown in Figure 53. These data are for a system using aerodynamic control surfaces. Since the required gain of 5 at 180,000 feet is greater than usually employed for flight control systems, some problems may exist due to unwanted control surface oscillations caused by internal autopilot noise or control surface inertia feedback.

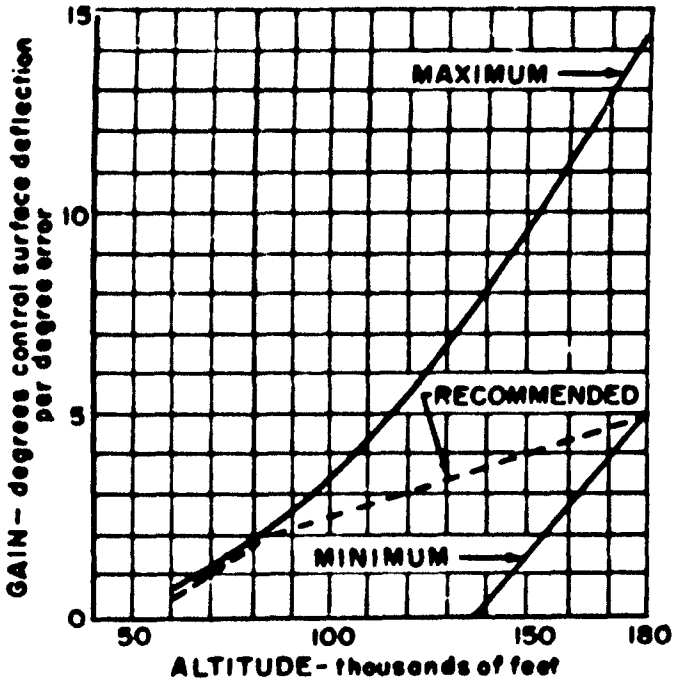

Figure 53. System Pitch Autopilot Gain Variations

Autopilot noise, which exists for both aerodynamic and reaction control systems, can be controlled by careful design. Control surface inertia feedback is unique to aerodynamic controls and represents a major limitation to operation at high autopilot gains. A study was made of this problem, and the results indicated that, for the existing control surface configuration, poor stability characteristics were present at frequencies in the region of the natural frequency of the actuator loop.

An analysis of the actuator loop indicated that a stable loop could be attained, having a loop gain of 20 and a natural frequency of 70 radians per second. Although it is desirable to have the natural frequency as high as possible, practical design limitations are imposed by the mechanical parts. A further restriction must be imposed on the actuator loop in that its natural frequency must not coincide with the natural frequencies of the body bending modes.

As a part of this study, the effect of certain of the system nonlinearities was investigated, particularly nonlinear aerodynamic moment curves and control surface position and velocity limits. The results of this study indicated that a control surface position limit of 15 degrees and a velocity limit of 30 degrees per second would be required to provide adequate stability.

2. COMPARISON OF AERODYNAMIC AND REACTION CONTROLS

According to studies conducted by the NACA, reaction control is required when the dynamic pressure is below a figure in the range of 2.5 to 10 pounds per square foot. However, for Brass Bell, the minimum expected dynamic pressure is in the order of 250 pounds per square foot. Thus, a comparison between the two methods of control was made on the basis of efficiency in terms of monopropellant weight to provide thrust for reaction control and hydraulic power for aerodynamic surfaces. To provide a comparison, the parameters of each system were selected to give equivalent responses. The disturbing forces were assumed to be caused by gusts, and a study was conducted to establish a suitable gust power spectrum.

The results of this study are shown in Figure 54 in terms of the ratio of monopropellant consumption for reaction controls to consumption for aerodynamic control. It should be noted that the major power requirement for the aerodynamic control system is established by leakage flow conditions. Elimination of this leakage would increase the ratio shown in Figure 54 by an order of magnitude.

It is thus apparent that aerodynamic controls are by far more efficient and, therefore, despite the problems connected with operation at high autopilot gains due to control surface inertia coupling, reaction controls are not recommended for Brass Bell.

3. ACCURACY OF ATTITUDE CONTROL

Based on the autopilot parameters and the gust power spectrum established during this study, preliminary calculations indicate the standard deviation of the attitude error will

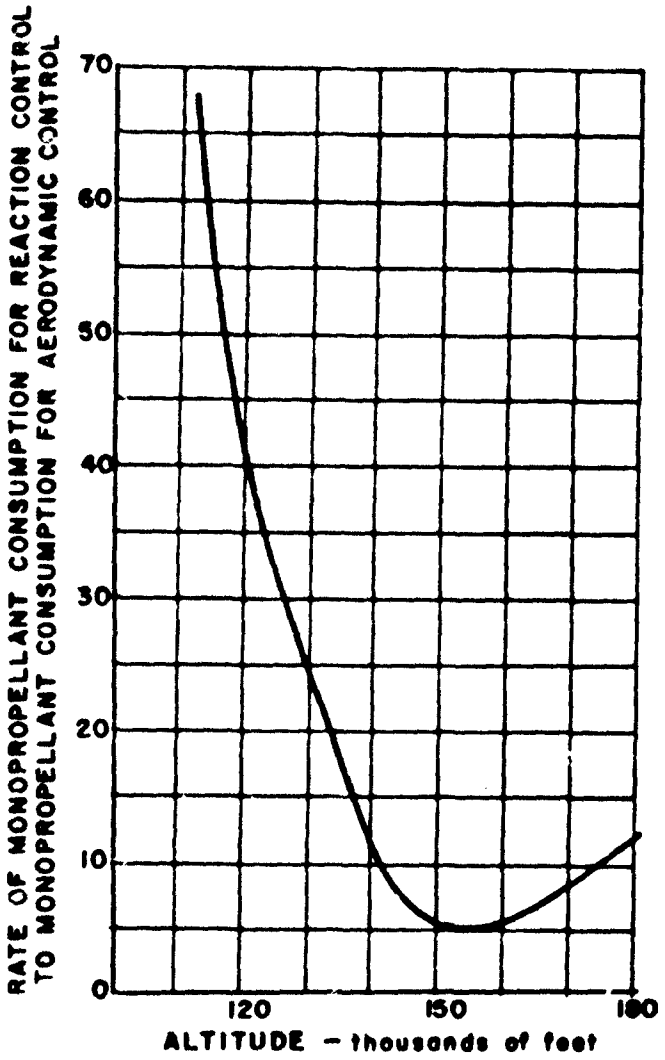

Figure 54. Relative Efficiency of Reaction and Aerodynamic Controls

not exceed 0.1 degree for altitudes above 100,000 feet.

However, before it can be determined that stabilization of the airframe alone will provide an adequate platform for the reconnaissance sensors, the gust power spectrum must be defined with a greater degree of confidence.

4. PRELIMINARY PERFORMANCE SPECIFICATIONS

A detailed list of the preliminary pitch autopilot performance specifications is in Reference 27. Of these the most important ones are:

a. Autopilot static gain and damping must be varied as a function of altitude.

b. A rate gyro must be used for damping and located at a position defined by consideration of the bending modes.

c. The control surfaces should have a position travel of at least ±15 degrees with a velocity greater than 30 degrees per second.

d. The natural frequency of the actuator loop should not coincide with any of the natural frequencies associated with the bending modes and should be at least 70 radians per second.

5. AERODYNAMIC AND AEROELASTIC DESIGN CONSIDERATIONS

Although aerodynamic control surfaces are recommended for Brass Bell, the results of this study have indicated the over-all stability characteristics are marginal for the presently defined configuration.

However, in the spirit of the design philosophy of the present control system studies, it is important to point out the following design trends that will tend to improve the performance of the automatic control system.

a. Increased static stability of the airframe.

b. Increased rigidity of the airframe.

c. The establishment of a more favorable mass balance of the control surface about the hinge line.

B. GLIDE PATH CONTROL

Previous studies had assumed that if the lift-to-drag ratio was maximized, maximum glide range would be achieved. An instrumentation capable of providing this control

was described in Reference 26. However, this instrumentation was rather complex and, further, some doubt existed as to whether maximum lift-to-drag represented the optimum condition for glide range control. Therefore a study was initiated to:

1. Determine rigorously the required flight path control to obtain maximum glide range.

2. Find the best compromise between ease of instrumentation and range penalty based on the theoretical maximum range.

The results of this study indicated that:

1. Flight path control by maximizing the lift-to-drag ratio results in only a 0.1 per cent reduction of the theoretical maximum range.

2. Flight path control by commanding a constant angle of attack results in a 0.3 per cent reduction of the range attainable for maximum lift-to-drag ratio control.

3. The flight paths obtained had a considerable long-period oscillation whose damping could be improved by adding a signal proportional to acceleration. Since a corresponding reduction of range occurs, the desirability of damping the phugoid will have to be evaluated in more detail.

C. YAW STABILIZATION AND TURN COORDINATION

During this period, an analysis similar to the one performed for the pitch channel was initiated for the yaw automatic control system.

The present concept of control for the Brass Bell airplane is to accomplish lateral manuvering by rolling the aircraft and utilizing the rotated lift vector as the generating force of the turn. Therefore, the yaw control system, in addition to providing directional stability, must also provide turn coordination. The definition of a coordinated turn is that all aerodynamic forces in the yaw plane and normal to the longitudinal axis of the aircraft are zero.

From these definitions, it can be seen that lateral control of the aircraft requires the integrated action of the pitch, roll, and yaw control systems. The pitch attitude control system must provide the proper lifting forces to maintain the desired vertical plane flight path and to generate the required turning rate. Roll attitude control accomplishes the rotation of the lift vector. The yaw control system maintains the angle of side slip at zero to give turn coordination.

To determine the control requirements, the expressions describing the forces and velocities acting on the airframe were derived for the condition where coordination exists. Certain simplifying assumptions were made for this preliminary analysis. These do not change the basic equations derived other than the addition of certain terms. Their consideration will be part of future analyses. These equations show that, for the case studied (coordinated turn in a horizontal plane), rotational rates exist about the aircraft yaw and pitch axes. On the basis of these conditions, possible schemes can be considered for achieving the desired control.

The most obvious method of control is to actually measure the forces in the yaw plane and null them. An accelerometer can be used for this purpose. As was the case in pitch, a rate gyro is necessary to supplement the low inherent damping of the airframe. Since in the steady state during a coordinate turn, an angular velocity exists about the yaw axis, it will be necessary to either compute out this rate or to eliminate it from the rate gyro indication with the use of a high-pass filter. A similar procedure is required for the rate gyro in the pitch instrumentation. A block diagram of this yaw control system is shown in Figure 55.

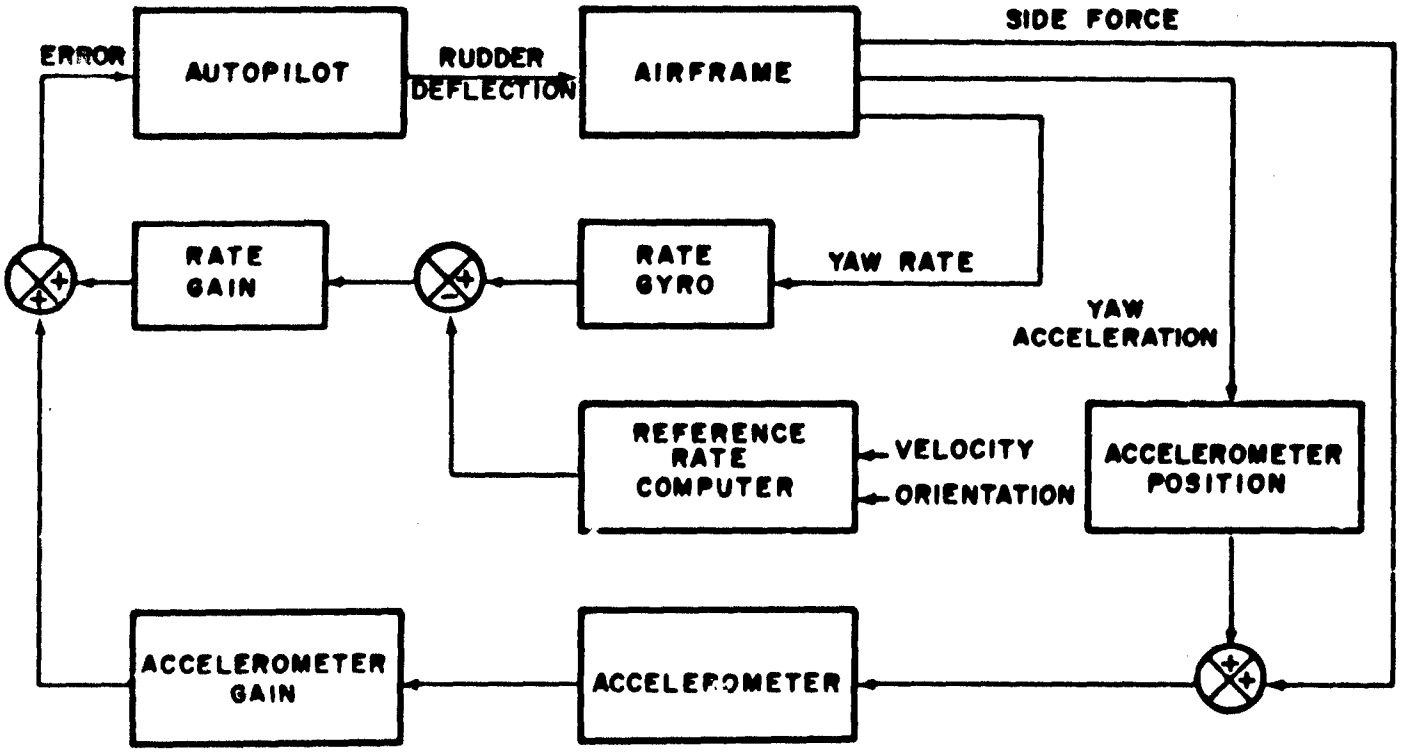

Figure 55. Yaw Control System with Accelerometer for Turn Coordination

Another possibility that exists is shown in Figure 56. This system is based on the fact, given the orientation and velocity of the aircraft, the conditions for turn coordination can then be specified by a turning rate about the aircraft pitch and yaw axes. Since rate gyros are used in both axes for artificial damping, the desired control can be achieved by commanding computed turning rates. Since no direct measurement is made of the miscoordination in this system, it may be expected to be less precise than the system using an accelerometer.

Detailed analyses have begun, but have not been completed for the system shown in Figure 55. No analysis has been performed as yet on the other system.

Although the bending characteristics were not available, a general statement can be made concerning their effects on this system. An accelerometer tends to amplify the bending effects at high frequencies and can create serious stability problems, requiring care in selecting adequate filters or places for the physical location of the accelerometers.

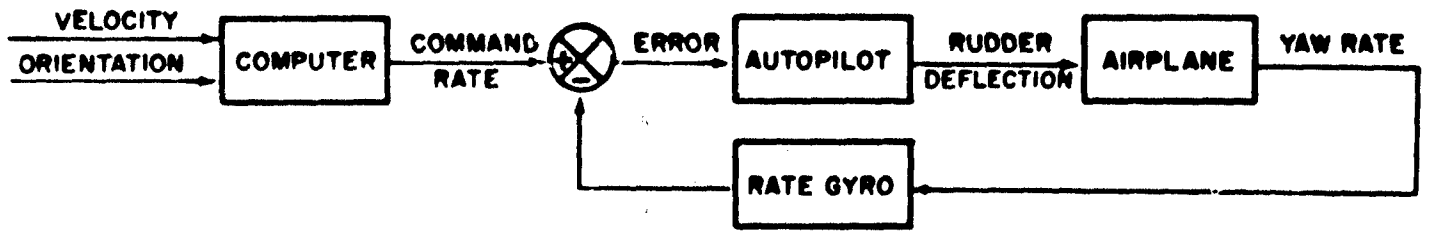

Figure 56. Yaw Control System — Calibrated Turn

The use of a linear accelerometer introduces another consideration into the stability analysis. If the accelerometer is not mounted on the cg of the aircraft, it will sense a component of angular acceleration; the sense and magnitude of which is a function of where it is located relative to the cg. Analyses show that, to achieve stability for this application, the accelerometer should be mounted forward of the cg.

This study has proceeded to the point of determining system performance as a function of accelerometer position and acceleration and rate gyro gain. Future work necessary to complete this preliminary analysis includes determination of:

1. The performance required.
2. Practical design limitations on loop gains.
3. The effect of airframe bending.
4. The effect of major system nonlinearities.
5. Parameter variations as a function of flight conditions.

The alternate method of control shown in Figure 56, as well as others, should also be evaluated in order to achieve an optimum solution.

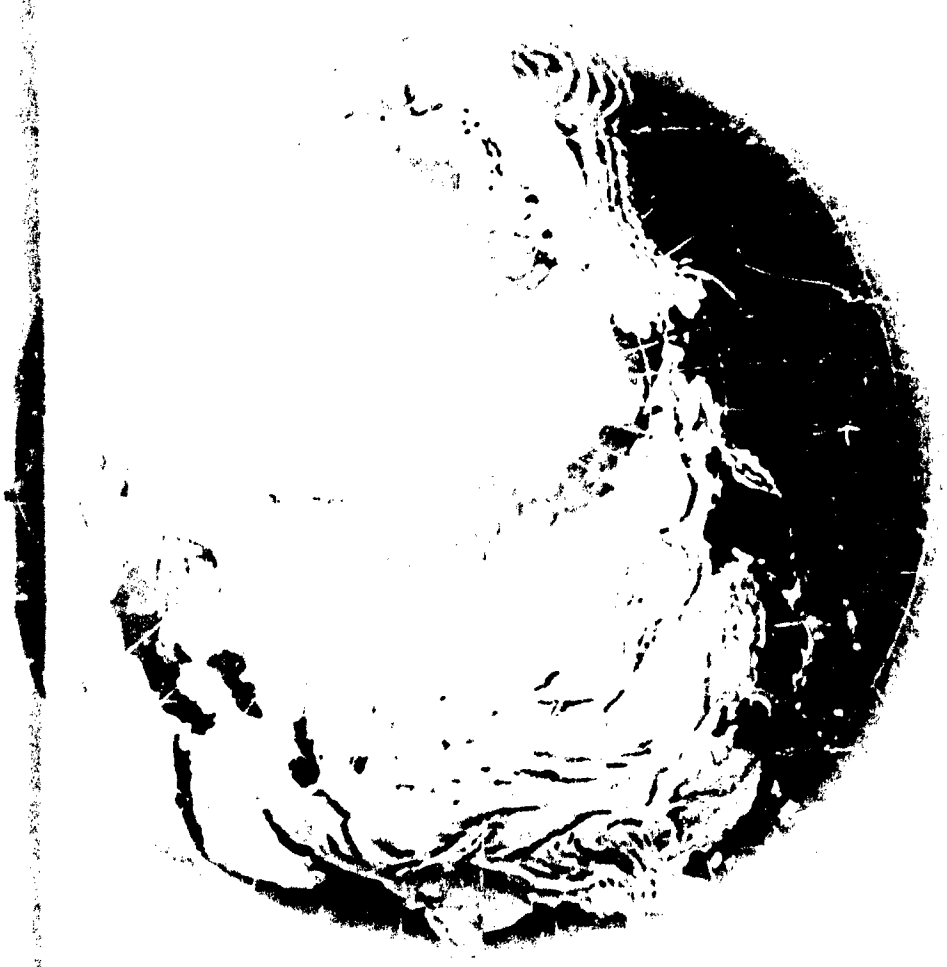

IX Radar

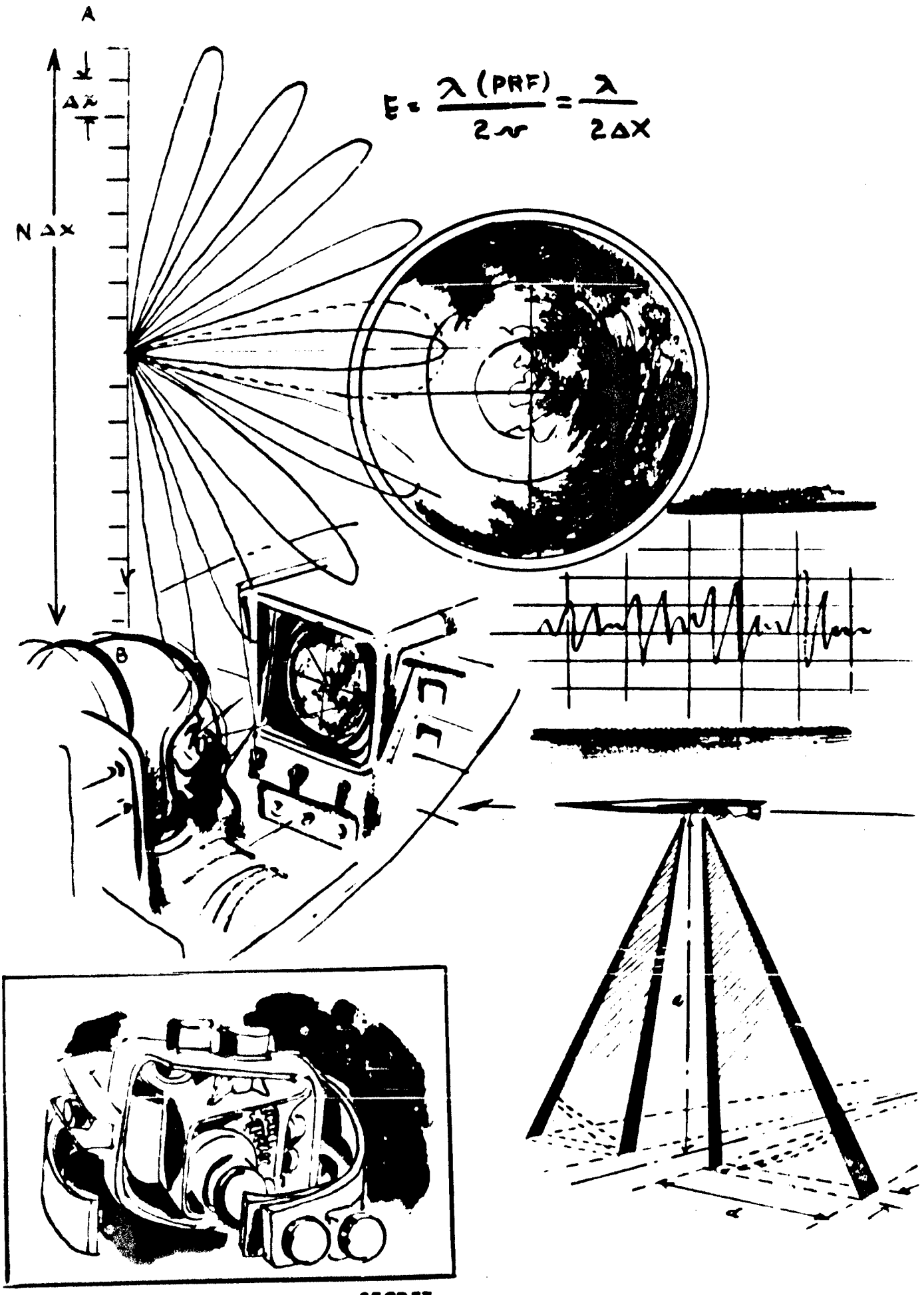
A
Δx
N Δx
$E = \frac{\lambda (PRF)}{2v} = \frac{\lambda}{2\Delta X}$
B

A radar capable of achieving 100 feet resolution in both range and azimuth in a vehicle traveling at speeds of 10,000 to 18,000 feet per second and at altitudes in the range of 100,000 to 180,000 feet is required. Range coverage of 10 nautical miles to 60 nautical miles on either side of the aircraft is also believed necessary for maximum usefulness of the system. Therefore, a study has been in effect to determine the special problems imposed by the Brass Bell environment, both internal and external, and to explore all possibilities for radar reconnaissance. It has been the conclusion of previous studies that only a velocity-scanned, side-looking radar is practical for radar reconnaissance in Brass Bell. It has also been previously concluded, that to meet the desired resolution capability, the techniques associated with coherent Doppler reconnaissance radars are necessary. A possible design for such a radar had been proposed.

The present study phase began with efforts directed toward a more exact analysis of the operation of a previously proposed radar, since the existence of discrepancies had been discovered. It became evident that the proposed design did actually present ambiguous information. Therefore, a more general investigation of the radar problem was initiated.

High resolution is obtained in a coherent Doppler reconnaissance radar because the outputs from a succession of pulse transmissions are combined in a manner similar to the way the outputs of a linear antenna array are combined. Such systems are characterized by the presence of side lobes which present ambiguous azimuth information. The angular distance to these ambiguous lobes is proportional to array spacing or, for a coherent Doppler system, to the pulse repetition frequency. By making the PRF large enough (array spacing small), the angular distance to an ambiguous lobe becomes large enough so that it can be attenuated by the pattern characteristic of the individual element. However, if the PRF is increased, a new type of ambiguity appears. Returns from targets at different ranges within the coverage area are received simultaneously.

Thus, the problem of designing a coherent Doppler radar for Brass Bell is one of increasing the PRF without introducing the resultant range ambiguity. Methods of distinguishing overlapping range returns must be found.

A. PULSE-CODED SYSTEMS

Three coding schemes have been investigated which appear to have useful properties. These are:

1. Chirp coding.
2. Random binary phase coding within the pulse.
3. Random binary phase coding of a sequence of successive pulses, at the PRF rate.

The chirp system, which is now under development by Bell Telephone Laboratories under contract AF33(616)-2847, is a technique for generating a long pulse of wide bandwidth to combine the features of high resolution and high average power. The operation is based on the principle of matched filters. In the Bell Laboratories system, a coding filter network which has a time delay characteristic which varies linearly with time is used. If such a filter is fed a short pulse, the output will be a long pulse whose frequency varies linearly with time. This pulse is then amplified and transmitted. Upon return, the long pulse is fed into an inverse network to recreate the short pulse necessary for range resolution. For purposes of Brass Bell, several coding filters would be required. A block diagram of such a system is shown in Figure 57. By performing the heterodyning shown, it is possible to use similar filters for coding and decoding.

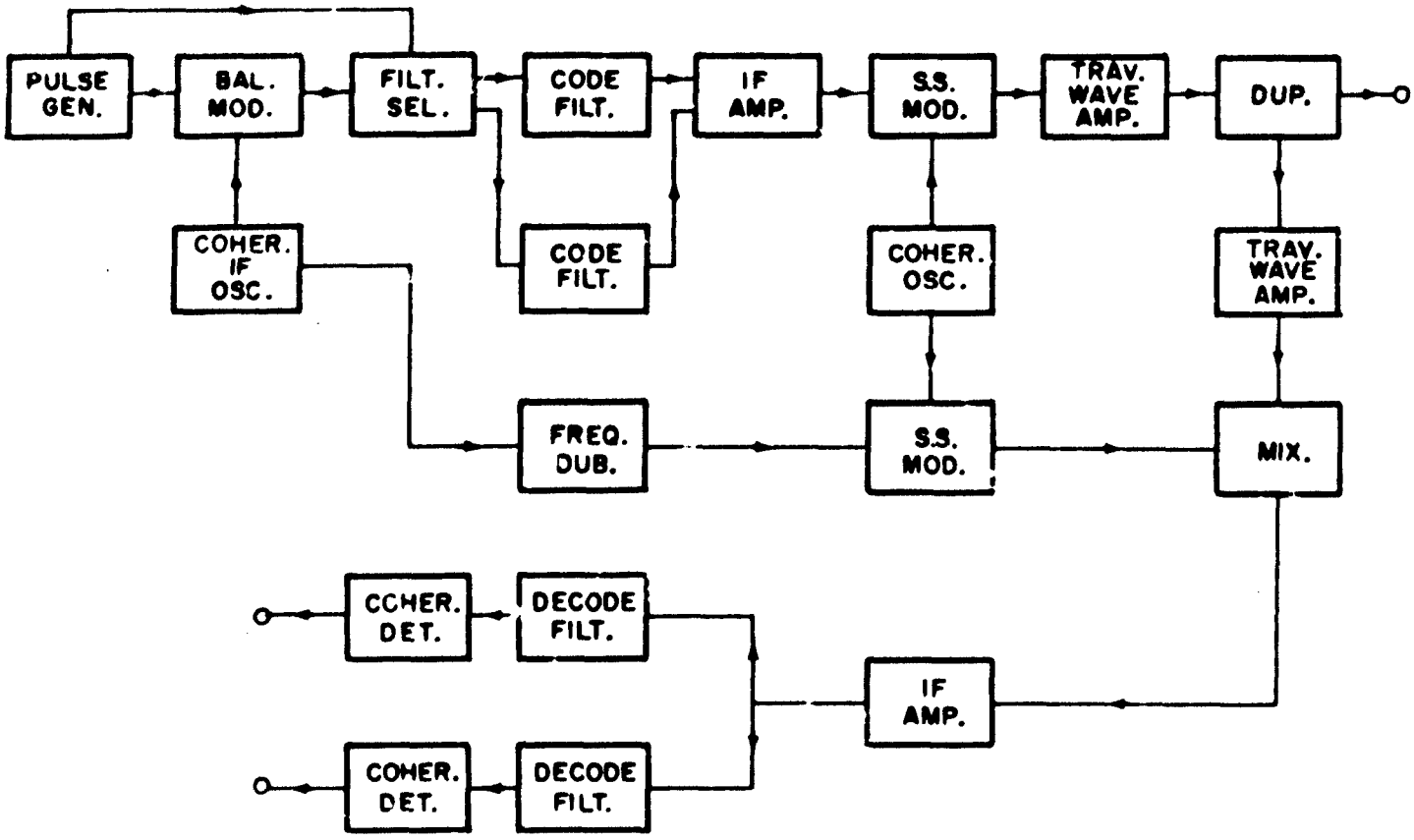

Figure 57. Chirp System

The mathematics involved in attempting to synthesize the required filter network are quite complex, and considerable study should be made to determine limitations of this method. It is quite obvious that the required filter network will be very complicated. For example, the Chirp System of Bell Telephone Laboratories consists of 80 cascaded bridged T-networks. From the theoretically ideal standpoint, this system is attractive, but practical limitations may limit its use to two different codes.

Random binary phasing coding is similar in principle of operation to the Chirp System, but provides for a different manner of generating codes. The individual random binary pulse phase coding system creates a long pulse from each short r-f pulse of duration τ by means of a coder delay line which has N taps separated a distance, τ, to create an N-pulse or N-position code. The coding consists of a random combination of the taps into two groups. The polarity of one group is reversed and the outputs of all taps are then added. Although the grouping of the taps are random-like, each group contains an equal number of pulses.

If a code pulse of amplitude, E, and width, $N\tau$, is passed through the decoder in a reverse direction, the output will consist of a decoded pulse of amplitude, NE, with a random-like distribution of smaller pulses symmetrical about the center for a length $(N-1)\tau$ on each side of the decoder pulse. These small pulses can be called decoder noise and are similar in effect to antenna side lobes except for their random nature.

In general, the larger the number of code positions, the smaller the noise level relative to the decoded pulse. Two point targets separated by less than $N\tau$ but more than τ will not interfere with each other except for an increase in the decoder noise level in the region where the noise of each overlaps, provided processing is linear. Thus, although the transmitted pulse

has a duration N τ, the radar range resolution is the resolution obtained by transmitting a pulse of width τ. In regions where the density of targets is high, it is necessary to take special care in the selection of the code in order to keep decoder noise level low, since each target will contribute to the over-all noise.

Another method of random binary phase coding consists of taking N consecutive short pulses each separated by the PRF period and inverting the phase in a random-like manner. This phase inversion is repeated each N pulses, where N is the number of pulses in the Doppler summation. Thus, the N consecutive returns of any point target will contain a random binary phase distribution. Decoding consists of re-inverting the returns of each main bang to one common phase. During decoding of one particular main bang, the returns of some other main bang will receive a random re-inversion. Thus, range ambiguous returns will still contain a random phase distribution which will have a small value after being summed during processing. For this system, as in those described above, it is necessary to select a random-like sequence so that the noise introduced by ambiguous signals within the antenna beam will be small. The code would probably have to be selected by a cut and try process. The pulse-coding schemes discussed have high rejection ratios for isolated point targets. However, the transmitted waveform necessary to increase the rejection ratio also increases the number of undesired targets which can contribute to the over-all noise. Since the actual noise level is dependent on the number of undesired targets, the over-all signal-to-noise ratio tends to be small in regions where target density is high. For example, the rejection ratio in chirp coding or binary phase coding is proportional to pulse length. However, the number of noise returns from undesired targets is also proportional to the pulse length, i.e., within each pulse there are many resolvable elements, each of which contributes some noise. Therefore, it appears that these systems are usable only where the target density is low and where the requirement for high resolution is not as important.

It should be noted that the calculations of signal-to-noise ratio have been made on a statistical basis and give a result for the average noise waveform. The low signal-to-noise ratios indicate that a "statistical radar" will operate marginally. However, there may be particular noise-like codes which give rejection ratios much greater than the average. The low signal-to-noise ratio calculated would tend to indicate that these particular codes are hard to find, and, indeed, have not been found thus far. Therefore, although it cannot be concluded that the solution of the Brass Bell ambiguity problem is theoretically impossible, it appears to be very difficult practically.

B. MULTI-LOBED ANTENNA SYSTEMS

In the previous discussion, systems were investigated wherein the transmitted signal was modified so as to minimize the effects of ambiguities. Another approach is to shape the antenna pattern so that it does not illuminate any ambiguous targets. For example, the range ambiguities can be avoided if second-time-around echoes are attenuated by means of the cut-off characteristics of the vertical pattern of the antenna. To obtain complete coverage, several vertical lobes are required, each illuminating a strip on the ground. An antenna analysis has indicated that vertical apertures on the order of 2.5 to 3.0 feet would be necessary for each lobe. This limits the number possible because of space limitations within the aircraft. Use of separate frequencies would ease the aperture size requirements because the two-way antenna pattern is used to provide attenuation instead of the one-way pattern. This is achieved at the expense of duplications of the transmitter equipment.

C. OTHER POSSIBLE APPROACHES

In the search for usable systems, many which were suggested as possible workable solutions were not found to be practical. These are enumerated below:

1. CW noise modulation systems

2. Two-frequency simultaneous transmission

3. Pulsed systems utilizing a noise-modulated PRF

D. COMPROMISE SOLUTION

Consideration was given to what might be accomplished if some of the requirements specified for the radar system were released.

A simplification can be provided if only one vertical lobe is utilized in conjunction with an antenna having a horizontal aperture of about 17 feet. Such a system would provide coverage out to about 35 nautical miles maximum ground range, and would work only for speeds below about 15,000 feet per second.

E. RECOMMENDATIONS

Further investigation of the coded pulse schemes should be made to determine whether suitable binary codes can be found. Rejection ratios on the order of 40 db are believed necessary.

The chirp technique needs to be examined more fully to determine whether suitable filters necessary for coding can be built on a practical basis. Present filters are very complicated. It is not known whether filters, which can generate arbitrary codes, can be constructed. The use of techniques similar to side-lobe rejection in antennas is possible in this system, and it should be determined whether suitable rejection ratios can be obtained by these means.

Consideration should be given to making available space for larger antenna apertures in the Brass Bell airplane. The use of larger antennas allows the use of a lower PRF and, hence, eases the design. On an over-all systems basis the trade-offs between vehicle velocity and radar complexity should be determined, since it is apparent that at reduced speeds the desired radar performance is more easily achieved.

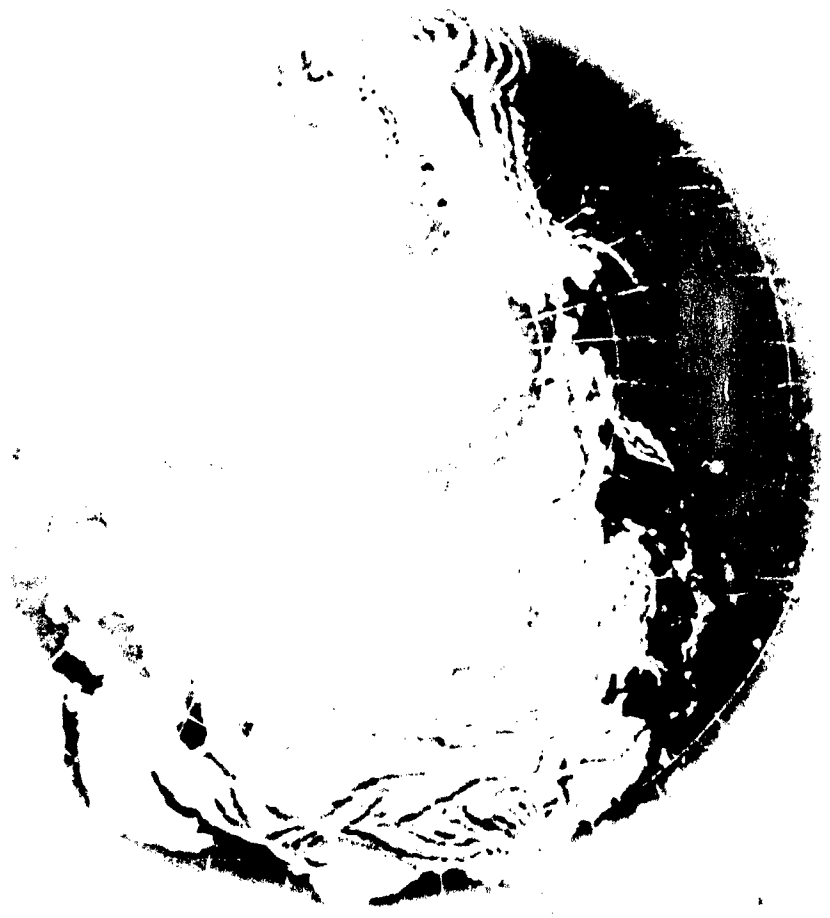

X Ferret

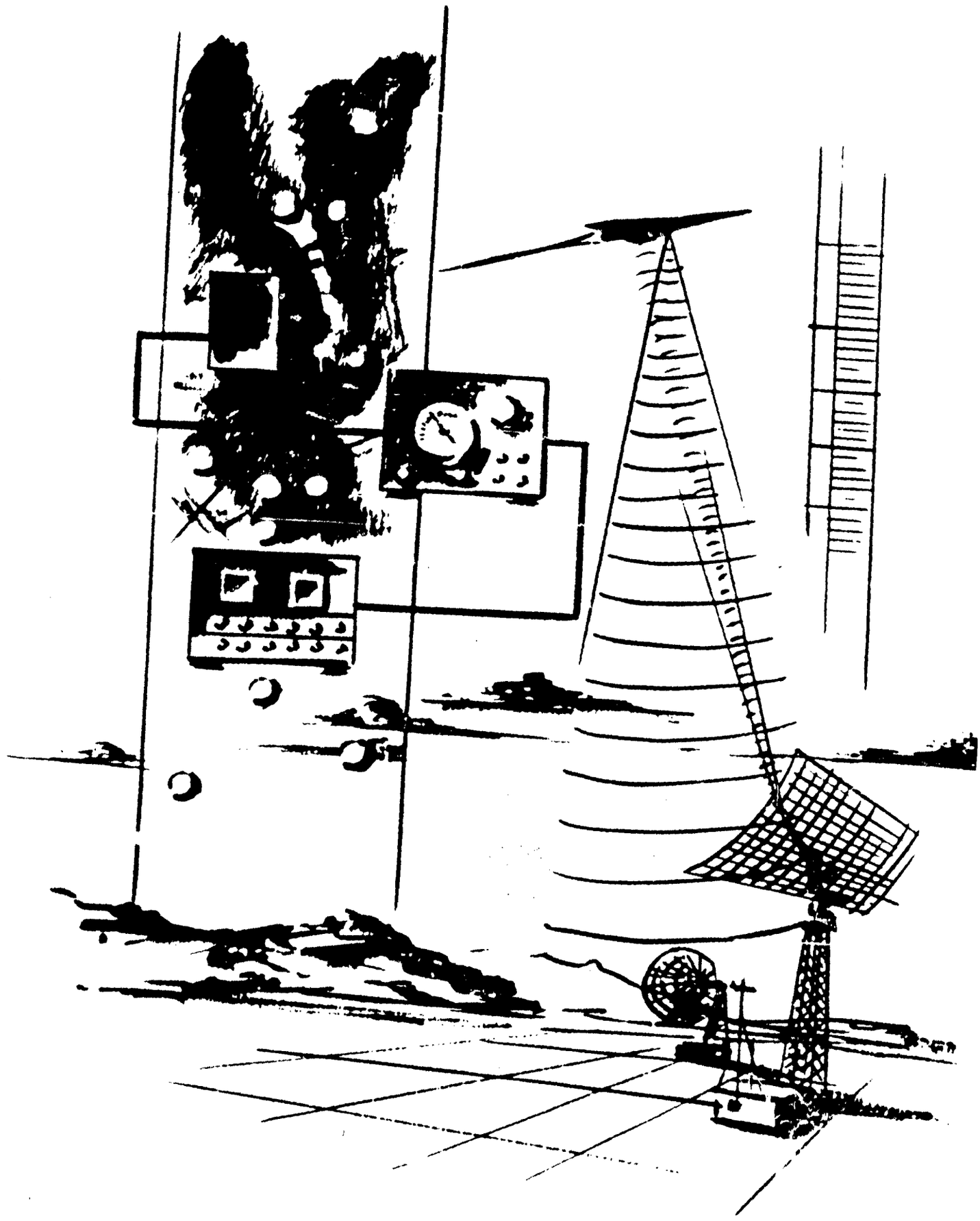

A. GENERAL

The ferret system investigation was limited chiefly to an extension of the 850 to 40,000 mc system described in Reference 28 to the 100 to the 850 mc range. Details of the investigation can be found in Reference 3. In general, it was found that the approach to the ferret problem used in the earlier study applies to the added frequency range and that most of the techniques recommended also apply.

B. SIGNAL SOURCES

Analysis of available information on the number of signals which might be expected from pulsed radars in this frequency range indicates that the frequency density (radars per megacycle) will probably be much lower than is the case in the microwave bands (L, S, and X-bands). Therefore, it will not be necessary to use very narrow receiver bandwidths to separate the pulsed radar.

A major source of signals to be considered in the design of ferret equipment is the so-called "CW Radars", most of which use some form of modulation, and some of which use very long pulses in addition to modulation. Included in this class are all radars having duty cycles appreciably longer than conventional radars. One of the most important of such radars is the anti-ICBM radar. The proposed system should have the ability to detect, locate, and perform technical analysis on such signals.

Although the ferret system will not be required to gather data on television stations, it will be required to gather data on other signals (such as radars) in the frequency ranges used by television stations. There is danger that, since the television stations are so numerous and since each station uses a very wide frequency range, they may mask the signals it is desired to investigate. Fortunately, a TV station will not effectively mask other signals everywhere in its channel, since the sideband power level is 40 to 50 db below the picture carrier level. Narrow-band scanning receivers such as those proposed will be able to receive other signals in the channel under the proper conditions. Flight tests in conventional aircraft in the United States will be necessary to determine receiver threshold adjustments which will make such reception possible.

Other signals such as IFF, communication, navigation, etc., will be present in this frequency range also. Techniques for bundling data which are presently utilized in low-frequency electronic intelligence being performed from the ground may perhaps be utilized for airborne systems also.

C. RECEIVERS

The ferret system proposed for the 850 mc to 40,000 mc frequency range uses receivers that scan in frequency and are wide open in direction. The same techniques, except for direction finding, are suitable for the frequency extension. The ability of scanning receivers to intercept CW signals is a more important advantage in the lower frequency region than it was in the original frequency range.

The width of the bands covered by the receivers will be limited to about one octave by the practical problem of antenna design. Therefore, it is proposed to cover the 100 to 850 mc frequency range in the three bands shown in Table XIII. The frequency ranges chosen were selected in order to concentrate certain television bands into a single ferret band. They represent a compromise between the desire to provide maximum separation of the signals, while minimizing the frequency range lost to TV stations, versus the expected requirements as regards pulse width and PRF of the pulsed signals to be present.

Using these bands, the minimum PRF that can be measured in band 2 is inconsistent with the expected PRF of anti-ICBM radars (30 to

BELL Aircraft CORPORATION

TABLE XIII

FREQUENCY RANGES FOR LOW-FREQUENCY FERRET SYSTEM BANDS

Band No.	Frequency Range (mc)	KC per Channel	No. of Channels	Minimum Pulse Width (usec)	Time per Channel (ms)	Minimum PRF (pulses/sec)	Pulse Sensitivity (dbm)	Video Bandwidth (cycles)	Noise Bandwidth (cycles)	CW Sensitivity (dbm)
1	100-225	250	500	4	20	100	105	50	3536	124
2	225-450	500	450	2	22.2	90	102	45	4743	123
3	450-850	500	800	2	12.5	160	102	80	6325	122

50 pulses per second). Techniques for modifying the system to accept such PRF's are presented in Reference 3.

The possible CW sensitivities, using a post-detector filtering technique, are also shown in Table XIII. However, it is more significant to compute the power a CW source must have in order to be detected at maximum range. If the narrowest possible bandwidths (Table XIII) are used, the minimum power signal that can be received varies from 4 mw at 100 mc to 0.5 watts at 850 mc. Here again, flight testing may prove useful in selecting and designing the equipment.

D. DIRECTION FINDING

The 850 mc to 40,000 mc ferret system uses five antenna beams, each approximately 24° wide on each side of the airplane to determine direction of the incoming signal. Unfortunately, antennas designed to provide the same characteristics below 850 mc, as are specified in the high-frequency part of the ferret system, would be too large to carry in the airplane. The direction-finding techniques for this portion of the spectrum must therefore be modified.

Techniques considered to provide direction-finding information include amplitude comparison, phase comparison, and narrow beam systems. At the present time, the last-mentioned system seems best suited for this particular function. Instead of using several antennas, the use of a single slotted antenna for each band has been suggested. The angle between the center of the beam and the axis of the array can be varied by controlling the relative phase, or delay, of the slots. Since only one dimension of the array need be large, use of such antennas may be feasible from an installation standpoint.

E. OTHER CHANGES

There will also have to be changes made in other parts of the system to accommodate the increased frequency range. For example, the PRF circuits will have to measure lower PRF's and the pulse width measuring circuits wider pulses. Changes of this nature are easily made and will have very little effect on the over-all system.

It was stated in Reference 28 that the low-frequency ferret could probable not be incorporated in the same airplane with the high-frequency ferret. This conclusion was based on the volume required for the antennas. If slot arrays can be used for the low-frequency direction-finding antennas, this conclusion is no longer valid, and it seems likely that the entire proposed frequency range (100 mc to 40,000 mc) can be covered in one airplane. If this is done, the increase in physical requirements for the combined system would be less than the increase in number of bands (37.5 per cent), since most of the data handling part of this system is common to both the low-frequency and high-frequency receivers.

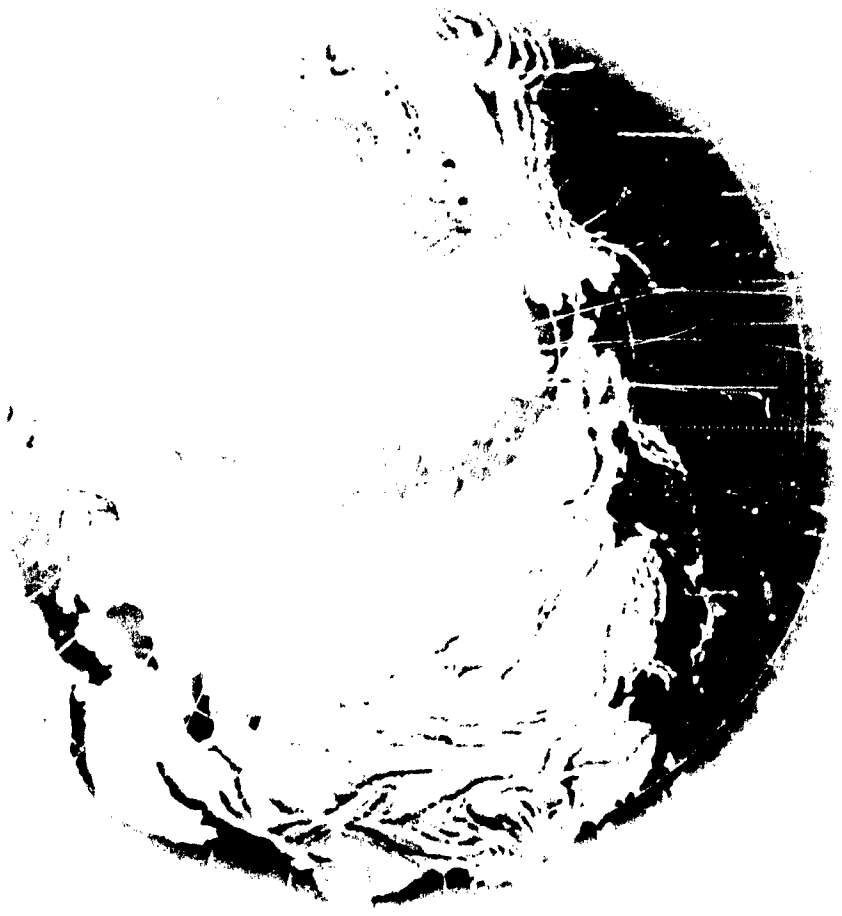

XI Photographic

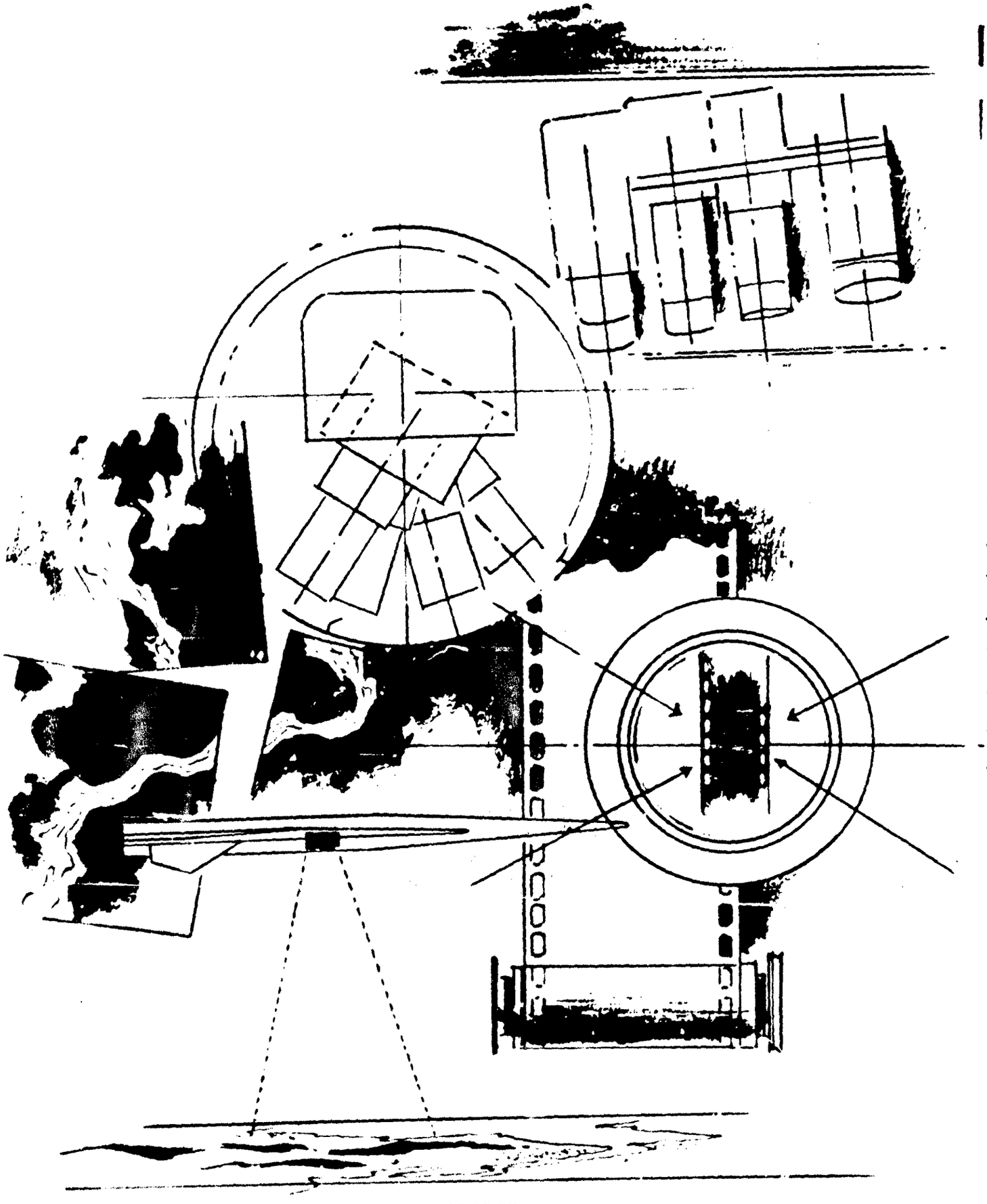

This phase of the Brass Bell program has been devoted to preparation for specific experimental work in the area of photoreconnaissance under very high altitude hypersonic conditions (Reference 29). It has been found that the state-of-the-art progression of vehicle performance in terms of velocity and altitude has not been reflected in an equal progression of investigation of the corresponding reconnaissance equipment environment, and that current efforts are directed primarily at the supersonic rather than hypersonic regime.

Application of the Terrain, Operational, and Technical objective reconnaissance missions (recognition of 20-foot, 5-foot, and 1-foot objects, respectively) to Brass Bell characteristics required revision of the previous MX-2276 results, which were based on 118P design objectives. The camera size necessary for the one-foot requirement suggested application of the diffraction-limited, or perfect, lens approach, using Kodak Aerecon (S.O. 1121 series) and Micro File film types to arrive at the smallest installable camera capable of the desired performance. This analysis demonstrated the influence of camera aperture diameter, restricted by photo window installation and fuselage diameter, on resolution limits and on the motion during exposure recordable by the system.

This method, based on Boston University experimental data, shows that use of Aerecon film at 150,000 feet allows no smaller than 2.1 and 11.25-foot vertical focal lengths for the recognition of 20 and 5-foot low contrast objects, respectively. One-foot low-contrast objects require uninstallable focal lengths between 45 and 50 feet, depending on aperture diameter, if Aerecon is used. The use of Micro File emulsion requires not less than a 13.0-foot focal length for borderline recognition of one-foot low-contrast objects, with the Terrain and Operational missions requiring focal lengths no smaller than 0.6 feet and 2.4 feet, respectively. Optimum vertical focal lengths and conditions of use are plotted in Figure 58.

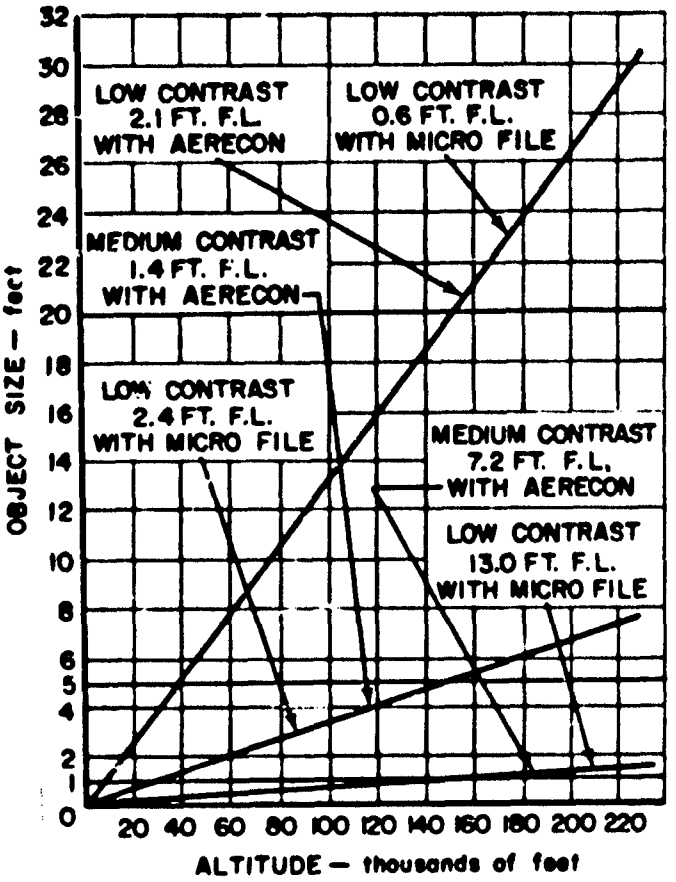

Figure 58. Object Recognition Potential for Diffraction — Limited, Installable Camera Systems Under Various Contrast Conditions and with Film Indicated

Experiments by Eastman Kodak Research Laboratories have shown that, with imperfect IMC, focal length in excess of an optimum value provides no additional information with a given film. For example at 158,000 feet with perfect IMC, a 328-inch f/16 system using Pan X film will record a 9-inch object on the ground. A one per cent IMC error does not allow less than a 23-inch object to be recorded, and focal lengths in excess of 139 inches is superfluous.

Kodak Research Laboratories studies of the accuracy of measurement of photographic images indicate that, at 150,000 feet altitude, measurement of a one-foot object to 5 per cent accuracy requires a 52.2-foot focal length Aerecon system or a 10.4-foot Micro File system, using normal image densities.

The analogy of atmospheric haze effects to those of aerodynamic luminosity from the boundary layer and/or shock wave has been used to predict the effects of photographic contrast reduction from this source. A luminosity value of 1450 foot-lamberts brightness places the apparent contrast threshold at 0.07 in the low terrain contrast range and 0.020 in the high-contrast areas. Aerodynamic calculations described in Reference 11 place the aerodynamic luminosity brightness in the 0.5 foot-lambert region, which is insignificant. An experimental laboratory and free flight program is planned to confirm or correct these calculations.

Normal aerodynamic refraction from boundary layer and shock waves has not been investigated in further detail because of the low air densities predicted. The possibility of refraction anomalies in air resulting from the appearance of absorption lines and bands under high-temperature conditions has been raised and requires further experimental work (Reference 11).

Preliminary calculations, based on a black body peaking at 1800°F (maximum skin temperature), show the photographically visible glow from fused silica photo windows will be at a brightness of 229 foot-lamberts, equivalent to a 5 per cent atmospheric haze condition. Heat transfer characteristics of fused silica, leading to the temperatures incident on camera equipment, are being investigated by Corning Glass to indicate the necessity of optical or mechanical heat control to maintain camera performance.

Interim results of the Aerial Reconnaissance Laboratory High Acuity program demonstrate the capabilities of carefully controlled optical and mechanical components of an airborne photographic system in obtaining resolution approaching the diffraction-limited condition. Continuation of this work should contribute greatly to the improvement of equipment necessary to meet performance objectives of the Brass Bell.

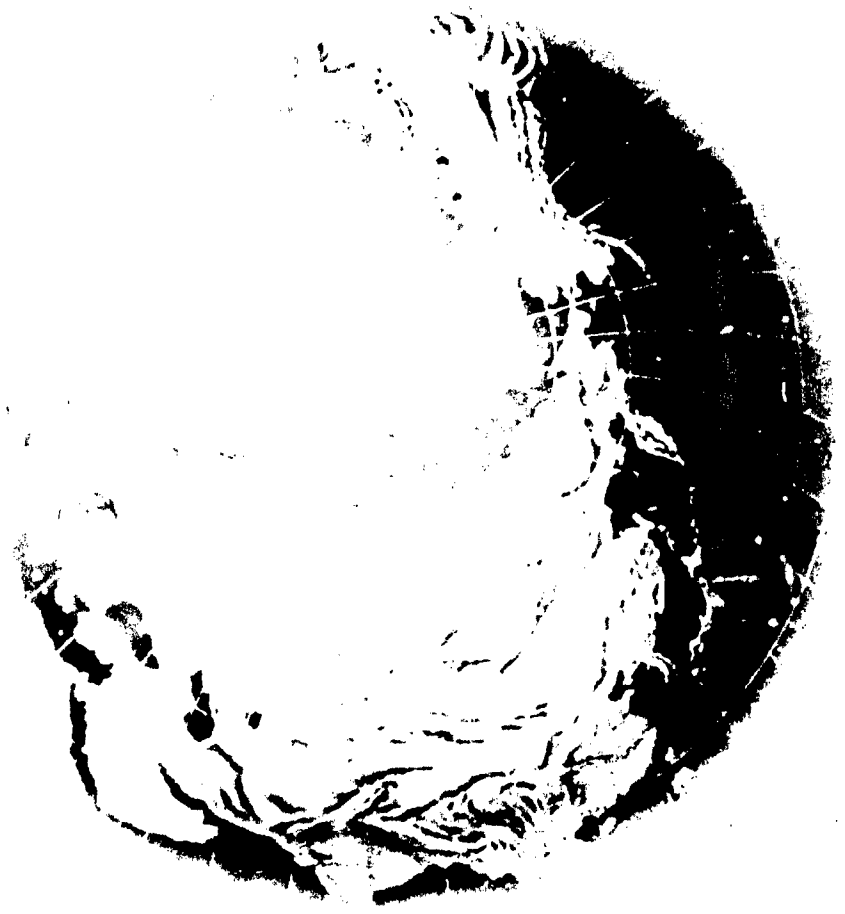

XII Human Factors

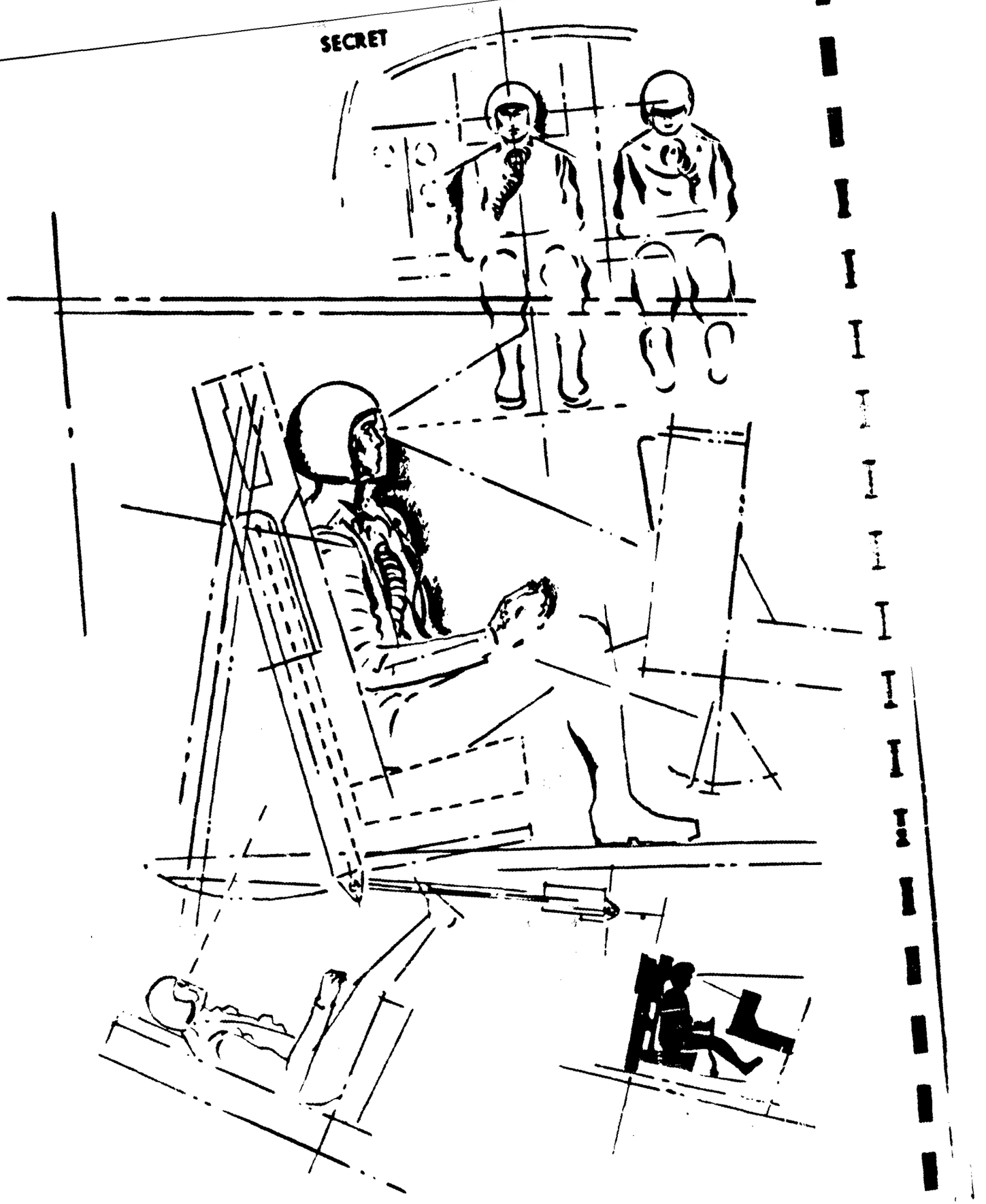

A. GENERAL

During the present study period, the overall crew task analysis has been expanded and completed to a degree compatible with the detail of the various systems involved. In addition, specific tasks and the equipment required for their accomplishment have been investigated in some detail. One of these tasks is that of monitoring the progress of the airplane by means of external visual or radar references. It has been determined that two optical viewing systems will be necessary, a vertical viewing system for the high-speed, cruise portion of the flight and a system looking forward and down for let-down, approach, and landing. The vertical system would be primarily for use by the navigator-observer, while the landing system would be primarily for use by the pilot. The vertical system has been investigated in some detail.

B. VERTICAL VIEWING SYSTEM

The design considerations for the vertical systems have been investigated, using optical systems with various angles of coverage. The systems considered all utilize negative distortion in order to obtain wide-angle coverage without extremely large optics or screen presentation. This distortion is such that near the nadir, distortion is minimized, but the distortion increases as the extremes of the area viewed are approached. At the present time, a 160-degree system, i.e., a system which allows observation of a 160-degree cone centered on the aircraft nadir, is considered most suitable.

Figure 59 illustrates the effects of this type of distortion. The photograph in this figure was taken at 30,000 feet over Middletown, Connecticut. This photograph, which has a 73° 44' lateral field of view, was made by swinging a strip camera through an arc from horizon to horizon. The area covered is a function of the secant of the observer's angle of view from the vertical. The light area on the accompanying map illustrates the area covered by the photograph. This figure illustrates the fact that many checkpoints can be recognized and utilized even though they are appreciably distorted at the extremes of the picture. At the same time, the area around the nadir can be used for a more precise information or position comparison.

The 160-degree system described above has the following characteristics from 180,000 feet. An object 168 nautical miles ahead would appear in the display and move at a rate of 0.25 degree per second until approximately 90 miles from the nadir. From this point on, the apparent motion will accelerate to a maximum of approximately 5.7 degrees per second at the nadir. The motion rate will then decrease until the object passes from view 168 nautical miles behind. The maximum time in view (which will occur for objects located on the line of flight diameter of the presentation) from this altitude will be 114 seconds at a velocity of 18,000 feet per second.

C. VERTICAL VIEWING SYSTEM DISPLAY

The 360-degree azimuth coverage required for this display, dictates that the display area should be circular. Previous studies have been based upon providing three 10 or 12-inch-diameter displays (radar, map, and visual) for the navigator-observer. By combining these into a single unit upon which any of the three presentations may be displayed at any time, the diameter may be increased to 18 inches. This increased diameter should make possible an increase in central magnification to approximately 8X as compared with 5X for a 12-inch screen.

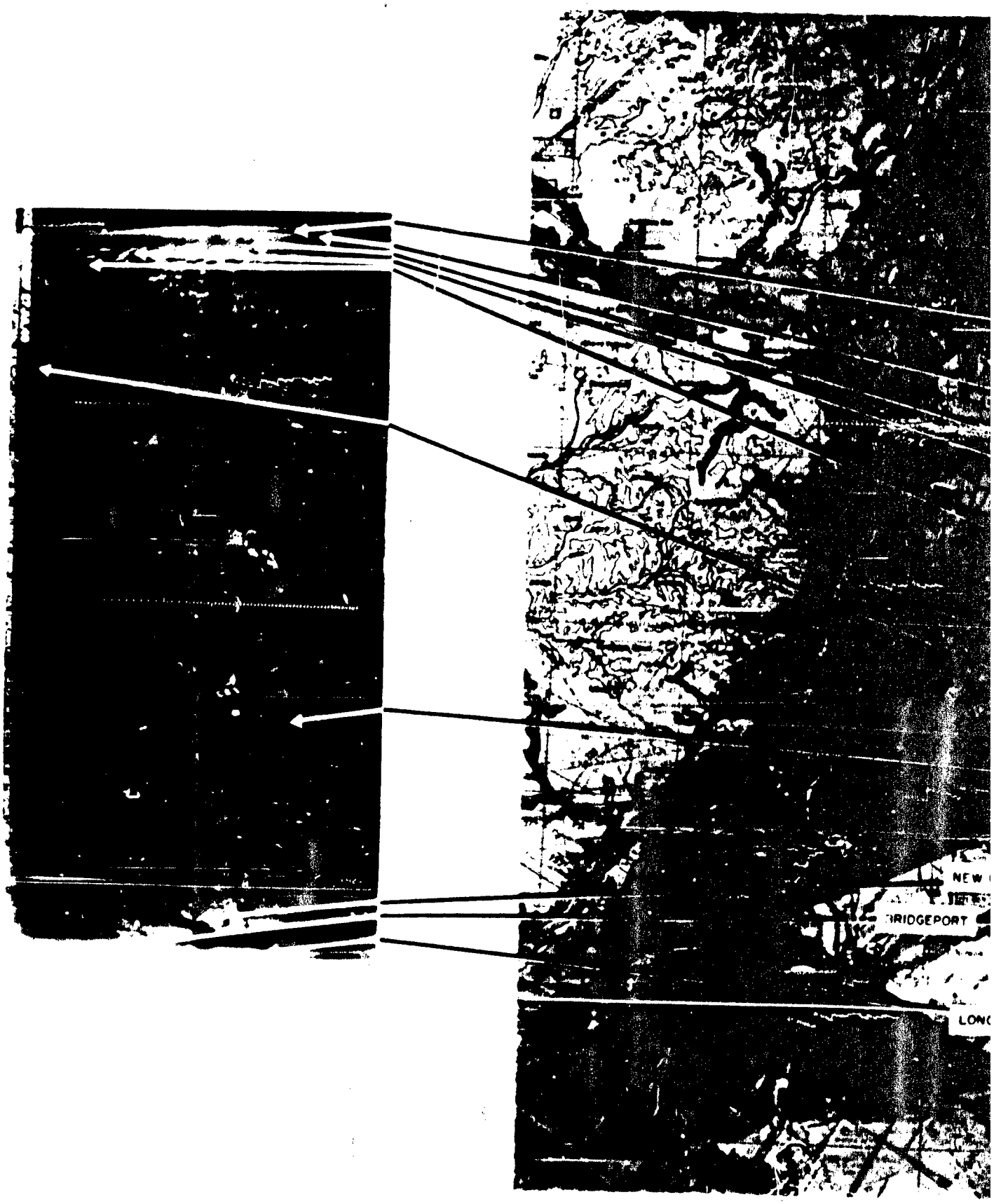
NEW
BRIDGEPORT
LONG

Figure 59. Fore and Aft Section of High-Altitude Periscopic View

D. RADAR DISPLAY

There is some question as to whether or not the cockpit radar display must be capable of providing the detail which the reconnaissance radar is capable of obtaining. It is doubtful that the crew will require this much detailed information to perform their tasks. It appears that an 18-inch display would provide this capability, provided the smallest spot size presently attainable is incorporated in the system.

E. COMBINED DISPLAY

The combination of the radar, optical, and map displays into a single unit upon which any of the three presentations could be displayed has several attributes from a human factor standpoint. One of the problems involved is that, in order to provide the same scale (hence, distortion) for all three, it would be necessary to provide a system which would distort the map and radar presentations in the same manner that the vertical viewing system distorts the terrain. This technique is more advantageous than rectifying the vertical system distortion, because of the larger field of view thus made possible on a fixed-size display medium. Systems which appear feasible and will provide the necessary distortion have been devised.

Utilizing the same screen (or other medium) for both radar and visual displays would facilitate examination of checkpoints using both systems. Since the visual system looks ahead while the radar does not, an object entering the optical field of view could be observed and an estimation of where it would enter the radar field of view could be made. This same object could be observed as it traveled through the radar field of view.

With the combined display, the relative position of each object would remain fixed (within error limits) as the navigator-observer switched his sensor presentation. This would minimize reaction time required for focusing the eye and re-identification of an object as compared with a side-by-side display.

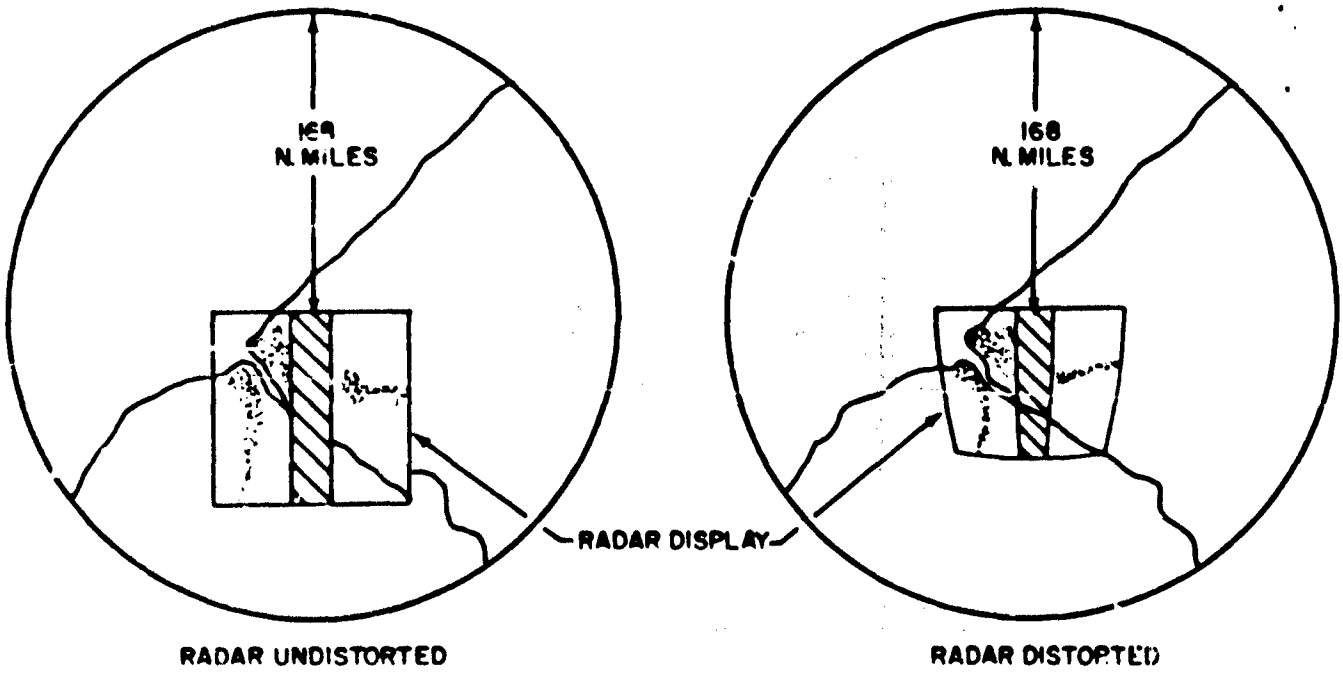

Figure 60. Radar and Vertical Viewing System Projection on Single Screen

Figure 60 illustrates the relative positions of the distorted and undistorted radar display upon either the distorted visual or map display. The center of the circular display area would be the aircraft nadir. The much greater field of view obtainable with the distorted visual system is very apparent from this figure.

F. WEIGHTLESSNESS

During the cruise portion of the flight, the crew will be subjected to normal g forces varying from approximately 0.5g at initiation of cruise to 1.0g at flight termination. The effects of g reductions of this magnitude may well be limited to sensomotor accommodation only, and produce no ill effects at all. The results of tests at the School of Aviation Medicine indicate that, in persons subjected to nearly zero gravity (less than 0.1 g) for very short times, the effects varied from sickness to enjoyment, depending upon the individual. These tests suggest that an immediate solution to the problem lies in the selection of personnel who are not adversely affected by this phenomenon. If additional solutions become available as a result of further testing, these may also be utilized.

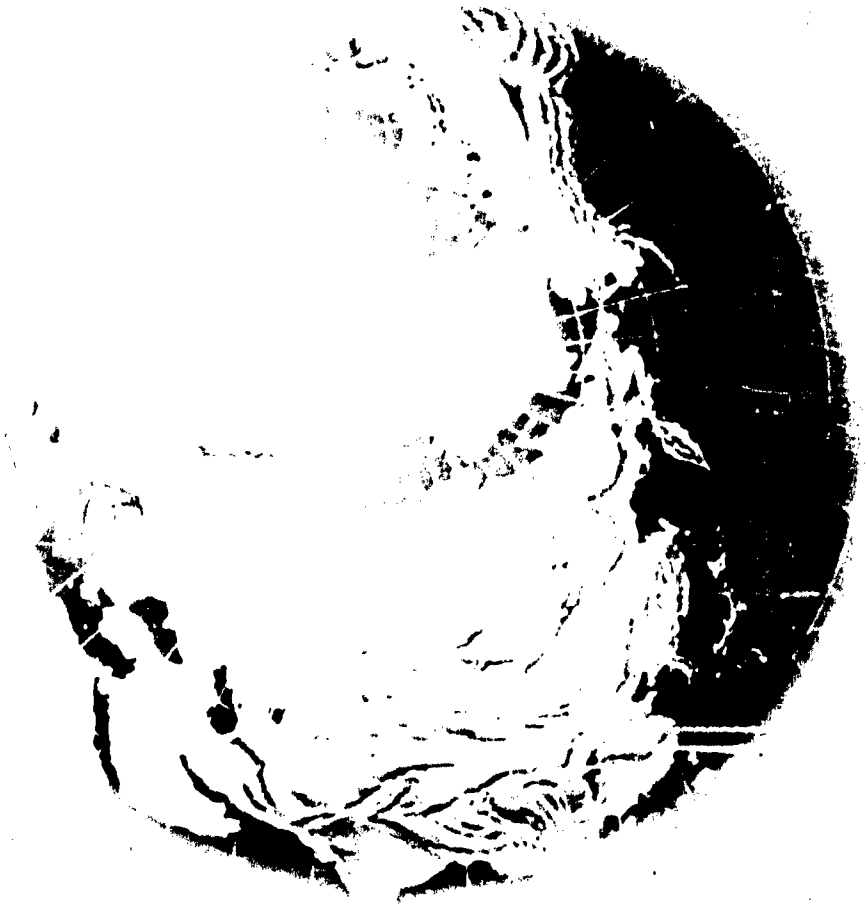

XIII Ground Support

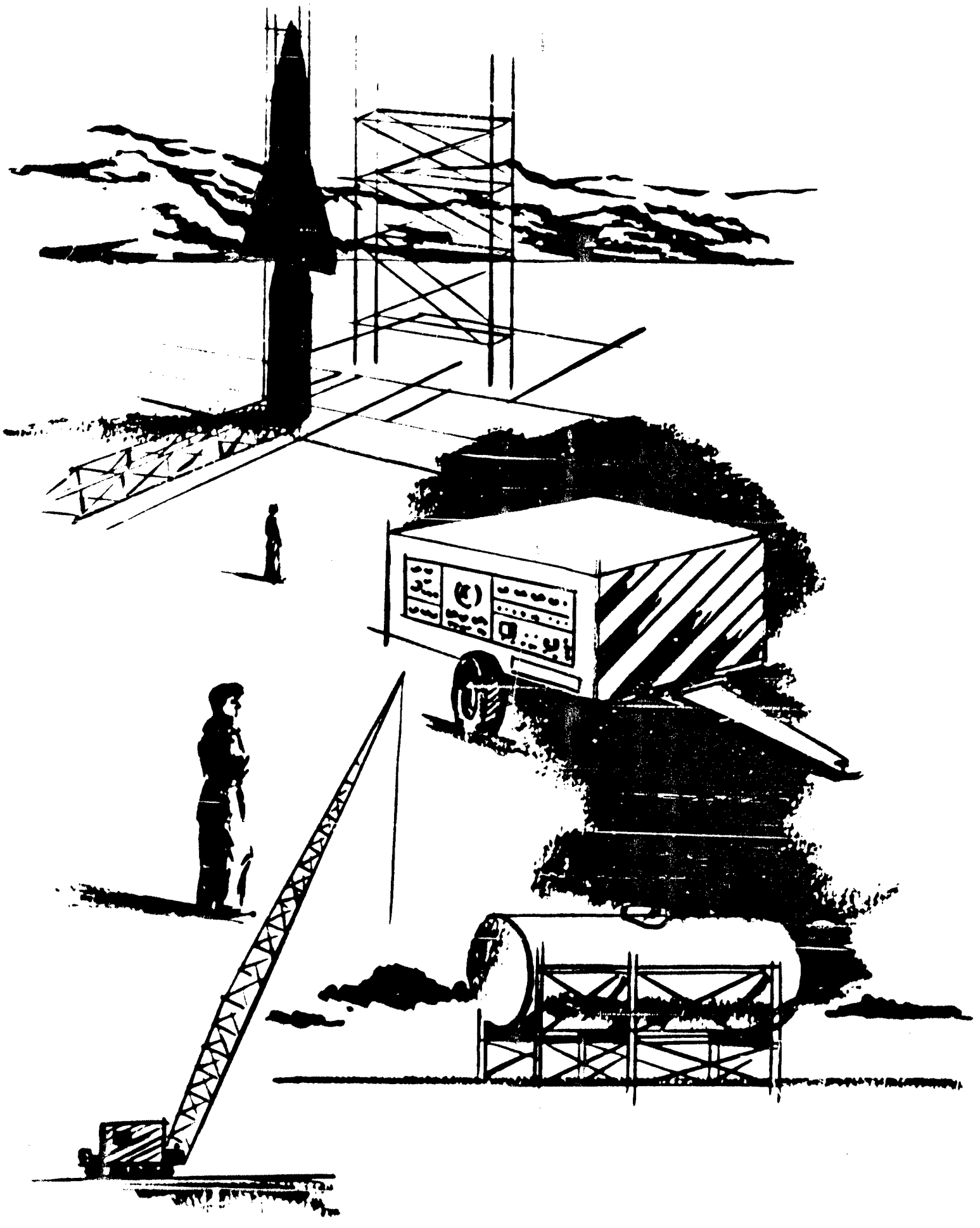

A. GENERAL

An integrated ground support program entails consideration of all development sequences associated with the weapon system. The areas discussed in this section are those which appear to involve unusual or significant problems.

B. NEW DEVELOPMENTS

1. ROCKET ENGINE TEST FACILITY

To insure the high reliability required of a rocket-powered, manned aircraft, it is evident that a large number of static powerplant firings will be required. Therefore, a test facility which permits large numbers of powerplant hot firings, coupled with extensive system tests, must be provided. Figure 61 shows the major features of a rocket test facility, including underground propellant storage tanks. Since high energy propellants such as fluorine and ammonia or hydrazine, may be required, particular attention must be given to their logistics and to their handling and storage peculiarities. Fluorine production, for example, requires large plants for a limited output (10 tons per day from a six-acre plant). One full-duration flight of the Brass Bell system using fluorine in both stages will consume about 46 tons of liquid fluorine. From these figures, it is evident that large storage facilities must be provided at the usage points. These can then be supplied by remotely located generating plants which operate full time.

Ammonia or hydrazine present fewer problems, since their physical properties are well known. Large quantities are presently produced, and they are less toxic and corrosive.

With the increase in feasibility of high-impulse, long-burning solid propellants, many of the liquid-propellant rocket problems could be obviated. Present trends in solids indicate the possibility of mixing and casting the grain at the test site. This would not only solve the toxicity and corrosion problems, but would also eliminate the necessity of transporting a large fragile booster from assembly plant to test facility.

2. SUBSYSTEM CHECKOUT

Other systems checked out at the rocket engine test facility will include the cooling system, and all internal subsystems. Operation of the ferret, radar, and photographic subsystems will be monitored during test firings and serviced by standard instruments. The nose and leading edge cooling systems will require some unusual servicing techniques, however. Two such cooling systems are proposed for Brass Bell. The first utilizes the high heat of vaporization of a liquid metal such as lithium. The second depends on the high heat capacity of compressed hydrogen. Figure 62 shows the schematic for a lithium ground supply and flushing scheme to be used for charging, removing, and cleaning the liquid metal system. All of the components, with the exception of the flushing system and the power supply, will be mounted on a single vehicle for mobility and handling ease.

Considerable work has been done at Bell Aircraft on a liquid hydrogen-fueled airplane. The pertinent conclusions reached from this work are: (1) transportation in the quantities required (707 pounds per flight) is feasible; (2) production of liquid hydrogen from the raw material should be done at the point of usage, if outside of the zone of interior as in an operational Brass Bell site; and (3) economical production schemes using portable units can be available for the Brass Bell operational period.

C. TRANSPORATION

Transportation of the Brass Bell stages from the assembly plant to the test site will be

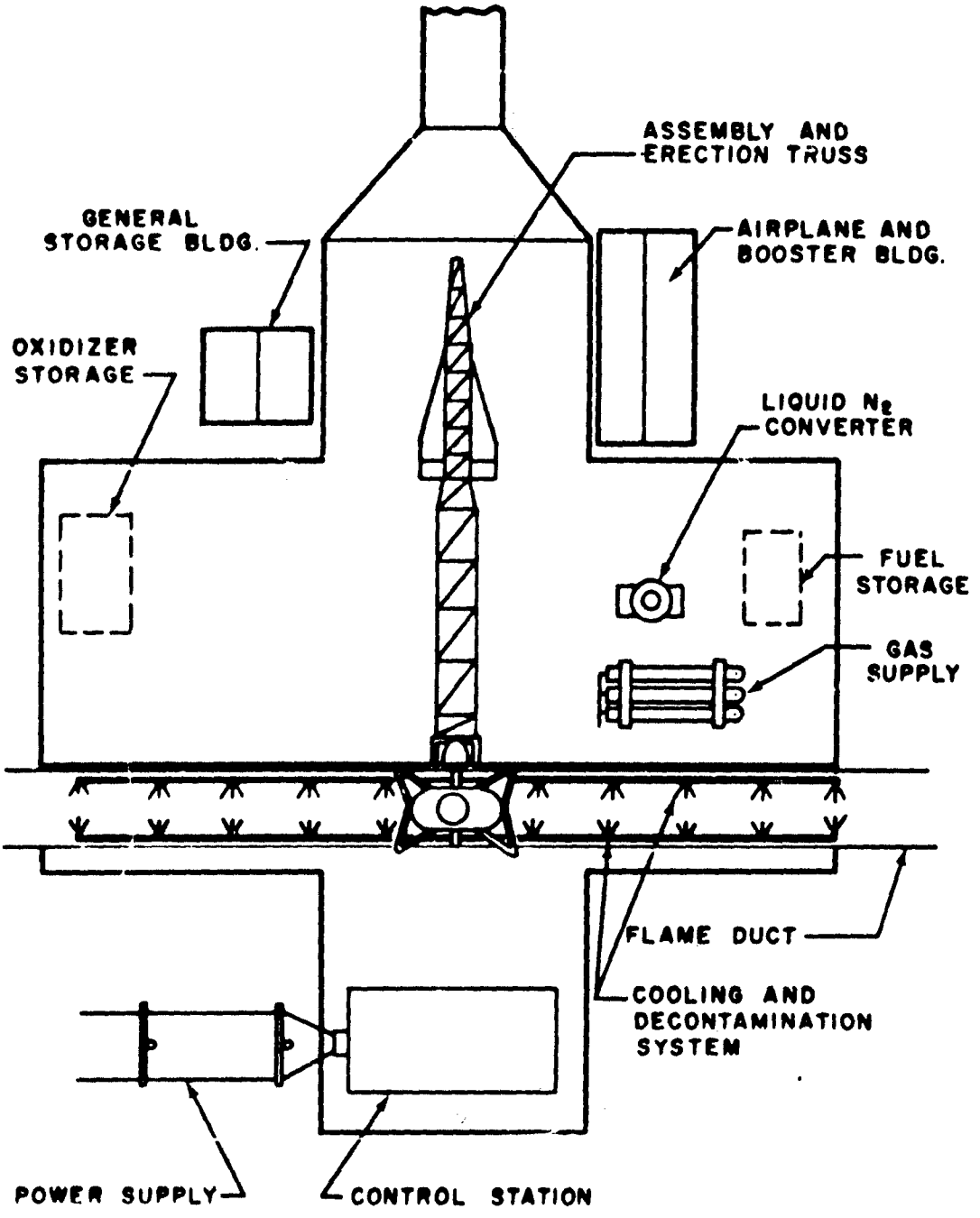

Figure 61. Rocket Test Facility

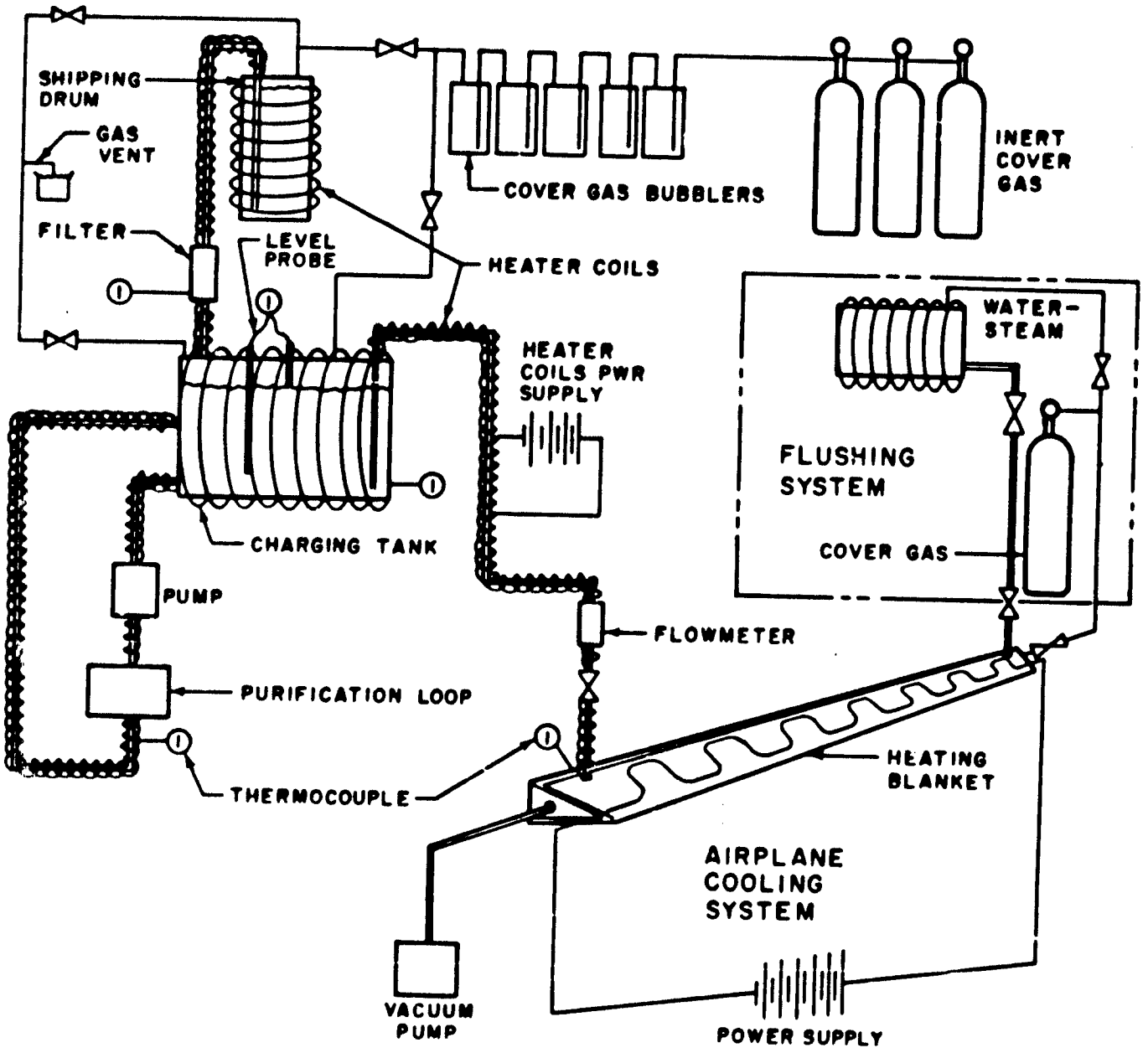

Figure 62. Liquid Metal Supply System

accomplished by either C-133A cargo aircraft, railroad flatcar, tractor and semi-trailer, or cargo ship. The wings and vertical tail of the final stage must be removed, and many of the more delicate subsystem components will be shipped uninstalled in the airframe.

D. TRAINING

Extensive use of ground simulators and aids and particular emphasis on crew education in the fields of aerodynamics, flight mechanics, propulsion, and navigation will form the basic training philosophy. Supplementing this ground school training will be transitional flight training from modified operational aircraft to a final stage Brass Bell airplane dropped from a carrier, and later to vertical take-offs using all stages. Flights incorporating en-route navigation and reconnaissance problems will follow.

E. ORGANIZATION

Figure 63 shows a typical organizational breakdown for the Brass Bell Reconnaissance System operating in conjunction with a SAC bombardment group. The bombardment vehicle could be either an advanced ICBM or a manned rocket-powered hypersonic glide bomber similar to Brass Bell, possibly with global capabilities.

It is assumed in this figure that the nine bomber take-off sites are supplied with intelligence information from three reconnaissance sites. If information from a continuous surveillance type of mission is required, the 1:3 ratio may be unconservative. On the other hand, if intelligence requiring less numerous flights is desired, the ratio may be high.

The Brass Bell take-off sites are serviced through a support facility where sufficient components and spares are kept in ready storage, and where checkout and trouble-shooting equipment is available. The depot level will include equipment and supplies sufficient for the anticipated requirements of the serviced units as well as management of the propellant production and supply schemes.

F. TAKE-OFF SITE COMPARISON

Two types of take-off sites were investigated, each of which utilizes large propellant storage facilities.

1. A system composed of fully mobile service units attached to an existing Air Force bomber base.

2. A completely independent underground operation.

These types represent distinctly different reconnaissance site concepts. The first has the features of economy, minimum reaction time, and close group support at the expense of high vulnerability due to close association with a prime target. The second scheme represents a costly means of achieving a high degree of base hardening, but provides long operational life expectancy.

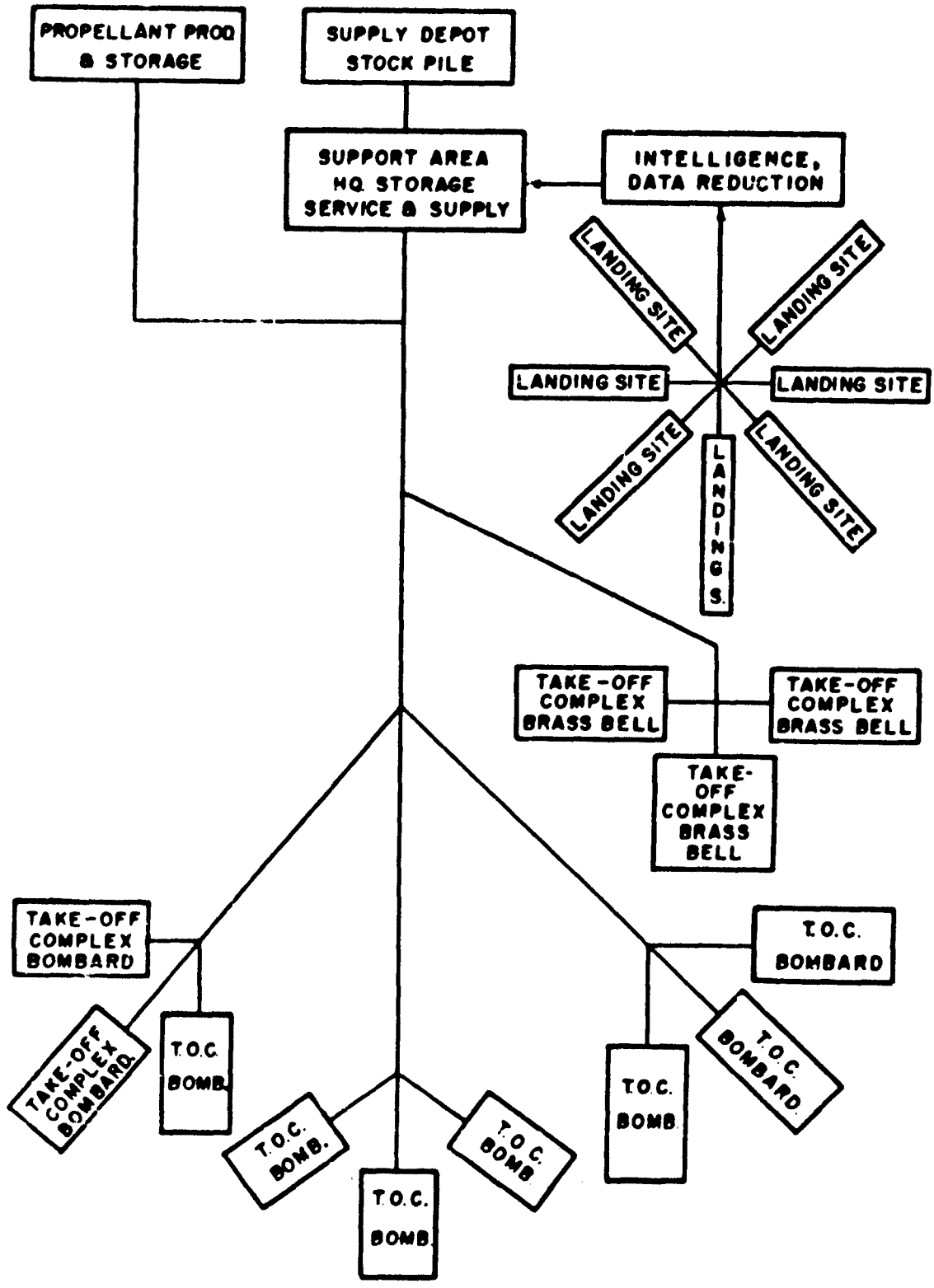

Figure 63. Organization

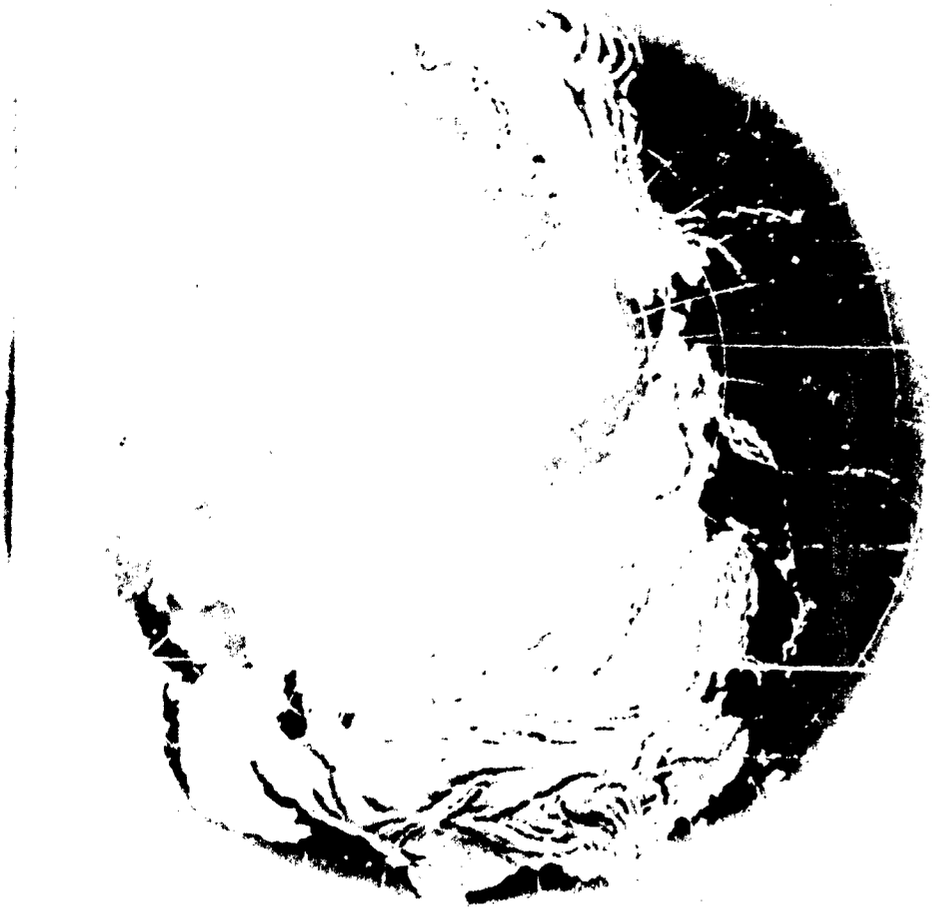

XIV Conclusions

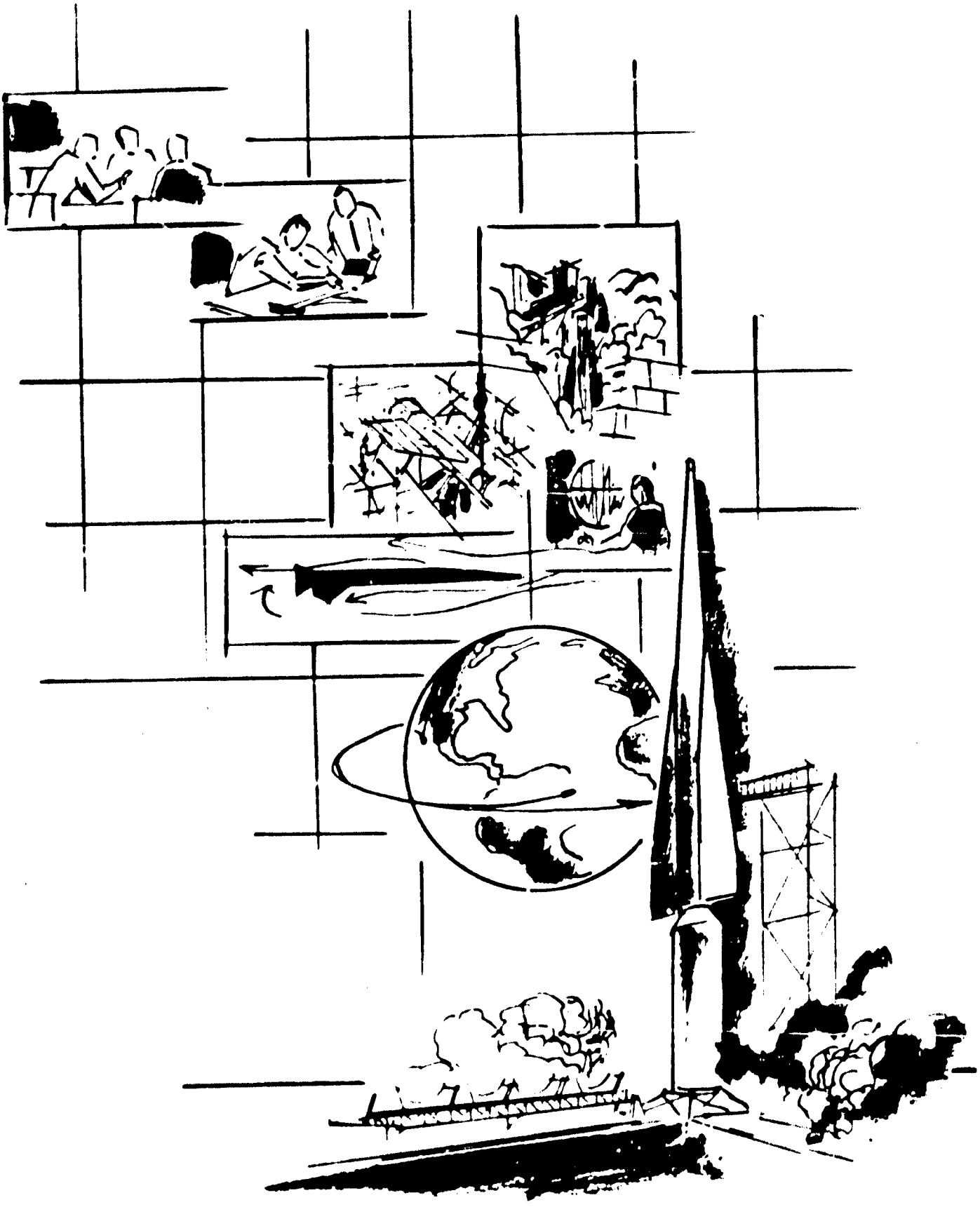

As a result of this study, the following conclusions have been drawn. Some of these conclusions, which were reached in earlier studies, but have been substantiated as a result of the present studies, are repeated.

A. The performance objectives stated in the current contract can be achieved with a manned, hypersonic, glide aircraft which is boosted to the necessary initial speeds and altitudes by two stages of boost. A typical configuration would weigh in the order of 190,000 pounds. The final stage is launched to an altitude of approximately 170,000 feet and a velocity of 18,000 feet per second; during the mission it glides down to an altitude of approximately 100,000 feet and a velocity of 4000 feet per second. During this glide it attains a range of 5500 nautical miles.

B. The desired photographic capabilities (resolvable surface dimensions of 20 feet, 5 feet, and 1 foot) can be obtained by photographic techniques which are known today. In order to achieve the one-foot capability, in the case of low-contrast objects, with a system compatible with space available in the airplane, the use of a system utilizing Micro-File emulsion will be required. A total of three interchangeable camera installations will be required.

C. Analysis of radar techniques for resolving ground dimensions of 100 feet or less, achieving the area coverage desired, and maintaining a small antenna length give results which indicate marginal operation. Techniques for compromise solutions have been determined, but the selection of a recommended technique has not been made.

D. Ferret systems capable of operating from this vehicle and performing both radar order of battle and technical intelligence missions over the frequency range from 100 to 40,000 megacycles can be developed. The systems recommended utilize frequency scanning with superheterodyne receivers. Only two interchangeable installations will be required, one for each type of ferret mission.

E. An inertial navigation system can provide the necessary accuracy and information for stabilization of both the vehicle and the reconnaissance equipment. To achieve the accuracy and flexibility required by the one-foot photographic resolution requirement, some means of improving the navigation system performance may be necessary.

F. The feasibility of double-wall construction has been demonstrated in wind-tunnel and thermal tests; and designs which show advantages from a producibility standpoint have evolved.

G. Tests of metallic materials show promise for raising the present temperature limit of double-wall construction from 1600°F to 1800°F; limited tests of ceramic sandwiches indicate the possibility of raising the limit to 2500°F.

H. Continued tests of a representative liquid sodium evaporative system shows this approach to the absorption of heat from the hot-spot areas to be satisfactory.

I. The use of hydrogen as a coolant and the results of designs, analyses, and tests of refractory materials show promise as alternative methods of handling hot-spot areas.

J. The results of aerodynamic research efforts have increased the confidence factor significantly with respect to hypersonic glide feasibility. In particular, the aerodynamic heating predictions have shown excellent correlation with free-flight data.

K. A further understanding of the environmental effects of hypersonic flight on the reconnaissance sensors have been achieved. Indications thus far are that no unavoidable problems are to be expected.

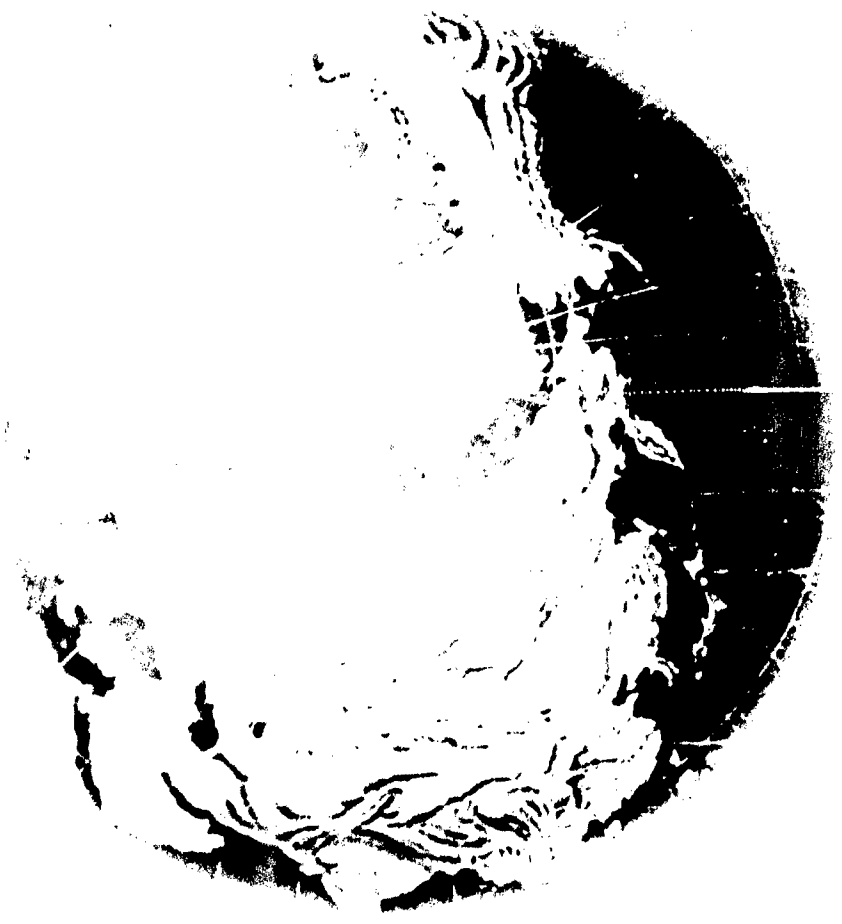

XV Recommendations

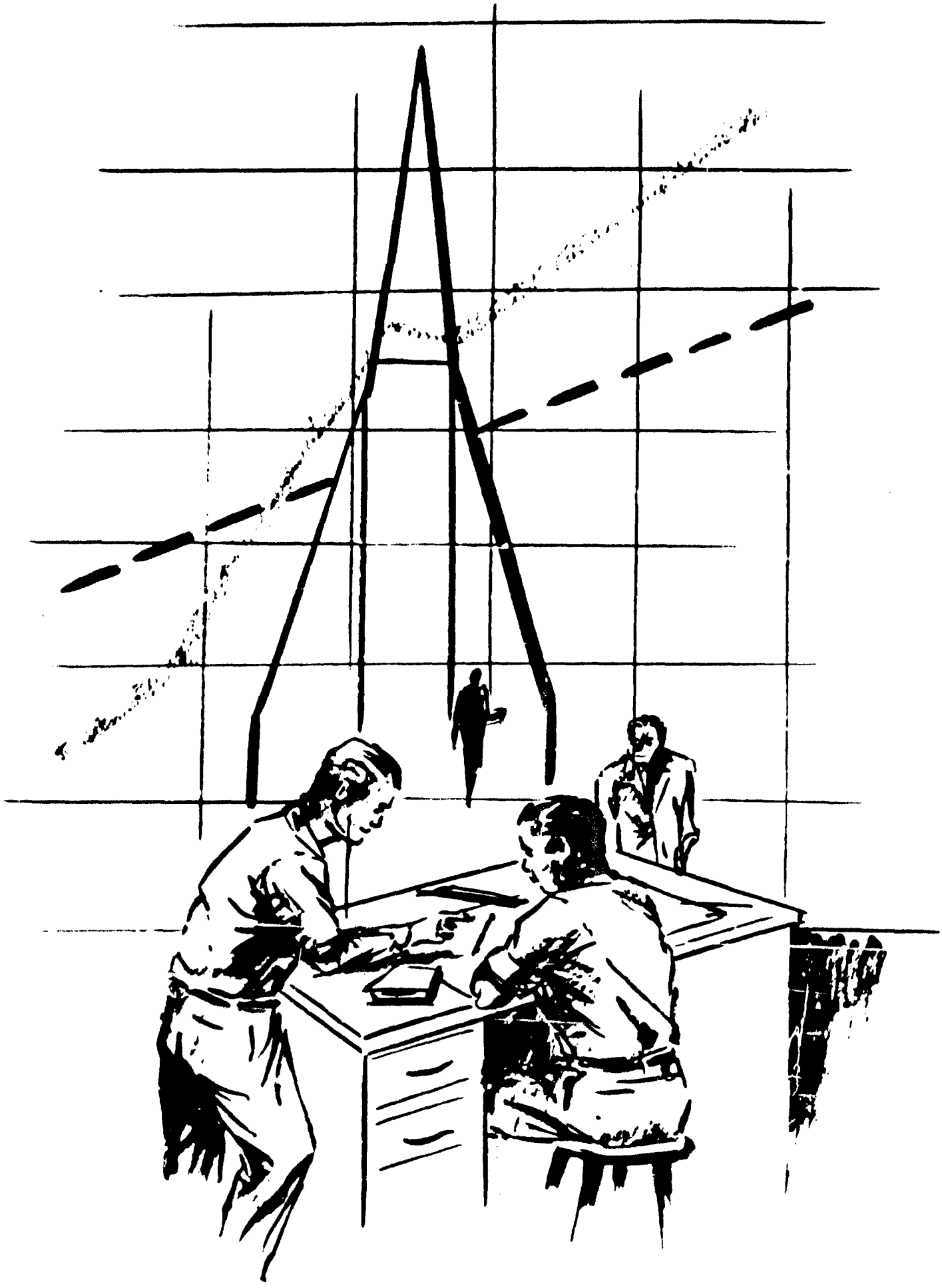

Reference 1 presents a detailed recommended program for the next year on Brass Bell. Some of the major items presented in the reference are:

A. Design of the weapon system should be established in the form of a preliminary configuration. This should include incorporation of test results and subsystem developments.

B. The experimental program should be expanded:

1. The airplane configuration should be tested throughout the complete speed range, subsonic, transonic, supersonic, and hypersonic.

2. Hypersonic flow phenomena should receive continued effort; special consideration should be given to the state of the air immediately surrounding the vehicle in the region of the reconnaissance sensors.

3. Refinement of the double-wall design should continue.

4. Tests of the three techniques (hydrogen, liquid metal, refractory) for handling the hot-spot areas should continue until a selection of the best technique can be made.

C. Subsystem component evaluation should be initiated where the subsystem has been defined to this extent. When the subsystem has not been defined satisfactorily, over-all system analysis should continue.

D. Analysis of the mission function, utilization of reconnaissance data, and the integration of reconnaissance information should be considered in more detail.

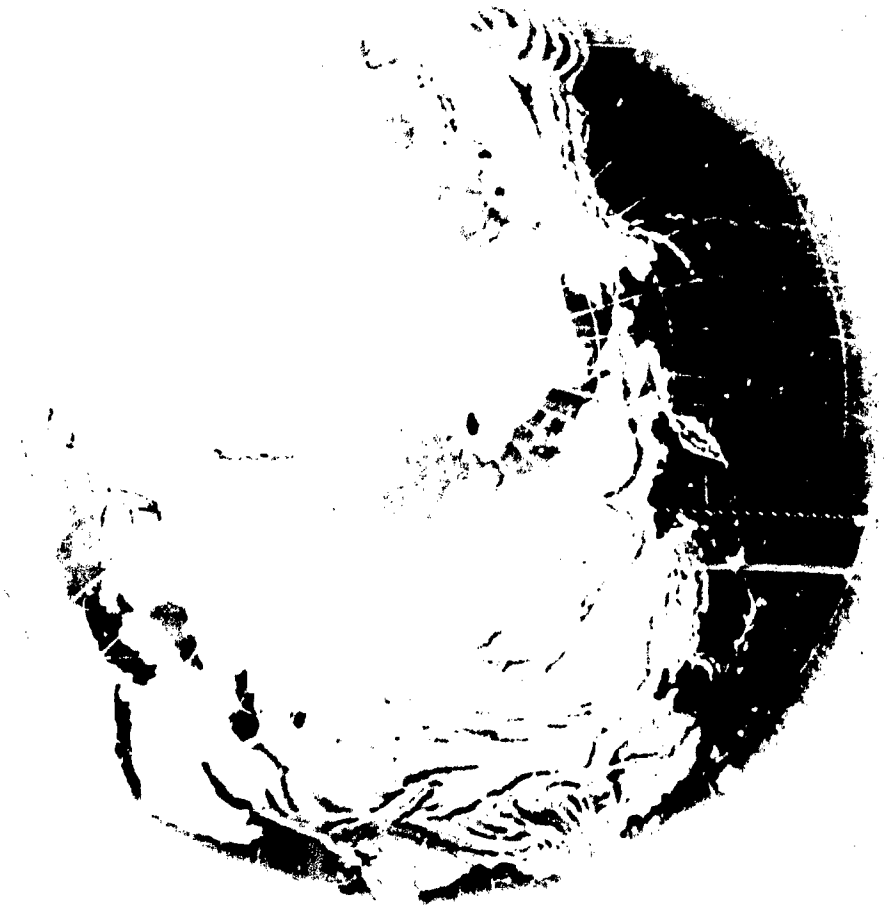

XVI References


SECRET

1. Brass Bell Reconnaissance Aircraft Weapon System – Program Plan (Supplemental Agreement No. 5). Bell Aircraft Corporation Report No. D143-945-047, dated 1 August 1957.

2. Photography Symposium – U. S. Air Force ARDC Report No. C-6-18847, dated 19-20 July 1956.

3. Brass Bell Reconnaissance Aircraft Weapon System – Weapon System. Bell Aircraft Corporation Report No. D143-945-054, dated 31 August 1957.

4. MX-2276 Reconnaissance Aircraft Weapon System – Structures. Bell Aircraft Corporation Report No. D143-945-025, dated 1 December 1955.

5. Brass Bell Reconnaissance Aircraft Weapon System – Structures. Bell Aircraft Corporation Report No. D143-945-037, dated 29 October 1956.

6. Brass Bell Reconnaissance Aircraft Weapon System – Structures. Bell Aircraft Corporation Report No. D143-945-050, dated 31 August 1957.

7. Brass Bell Reconnaissance Aircraft Weapon System – Summary Report. Bell Aircraft Corporation Report No. D143-945-039, dated 29 October 1956.

8. MX-2276 Advanced Strategic Weapon System – Aerodynamics. Bell Aircraft Corporation Report No. D143-945-012, dated 29 April 1955.

9. MX-2276 Reconnaissance Aircraft Weapon System – Aerodynamics. Bell Aircraft Report No. D143-945-024, dated 1 December 1955.

10. Test Equipment Investigation – Induction Heating for Leading Edge Testing. Prepared by R. W. Sampson, Consultant, Bell Aircraft Corporation Report No. D143-941-027, dated 5 June 1957.

11. Brass Bell Reconnaissance Aircraft Weapon System – Aerodynamic Research. Bell Aircraft Corporation Report No. D143-945-049, dated 31 August 1957.

12. An Exploratory Study of a Delta Wing at Hypersonic Speeds – Part II: Further Detailed Studies of the Pressure Distribution at Angles of Attack: 60° Included Angle Delta with a Blunted Leading Edge. Prepared by Princeton University. Bell Aircraft Corporation Report No. D143-978-006, dated December 1956.

13. An Exploratory Study of a Delta Wing at Hypersonic Speeds. Part III: Pressure Distribution Studies on a 30° Included Angle Delta Wing at Angles of Attack. Prepared by Princeton University. Bell Aircraft Corporation Report No. D143-978-009, dated 26 March 1957.

14. An Exploratory Investigation of Wing Body Interference at Hypersonic Speeds – Part I: Preliminary Results at Zero Angle of Attack. Prepared by Princeton University. Bell Aircraft Corporation Report No. D143-978-007, dated February 1957.

15. Induced Pressure on Flat Plates in Hypersonic Low Density Flow. Prepared by University of California. Bell Aircraft Corporation Report No. D143-978-008, dated 25 January 1957.

16. Pressure Distributions on Blunt-Nosed Cones in Hypersonic Low Density Flow. Prepared by University of California. Bell Aircraft Corporation Report No. D143-978-010, dated 30 April 1957.

17. The Effect of Sweep Back Angle on the Pressure Distribution of a Blunt Flat Plate at Hypersonic Speeds. Part I: Studies of a Hemicylindrical Leading Edge Flat Plate at Angles of Attack = 45° and M = 13.3. Prepared by Princeton University. Bell Aircraft Corporation Report No. D143-978-001, dated 7 June 1957.

18. W. N. MacDermott, et al Pressure and Heat Transfer Measurements on Three Two-Dimensional Models for the Brass Bell Project. Arnold Engineering Development Center, Preliminary Data Report AEDC-GDF-F-PDR-2, dated July 1957.

19. Brass Bell Reconnaissance Aircraft Weapon System – Aerodynamics Research. Bell Aircraft Corporation Report No. D143-945-034, dated 29 October 1956.

20. Logan, J. G. Jr. and Treavor, C. E.: Tables of Thermodynamic Properties for Air from 3000°K. Cornell Aeronautical Laboratory Report AD-1052-A-2, dated June 1956.

21. Dubin, M. – Air Force Cambridge Research Center – Private Communication.

22. Huth, J.: Thompson, J.: and Valkenburg, U.: "Some New Data on High Speed Impact Phenomena" ASME Paper 56-A-15 Applied Mechanics Divisions, dated November 1956.

23. Day, M. J. and Smith, G. V.: Ind. and Eng. Chem., Vol. 35, No. 10, October 1943.

24. Brass Bell Reconnaissance Aircraft Weapon System – Navigation. General Electric Company Report R57-APS83, dated 20 August 1957.

25. Brass Bell Reconnaissance Aircraft Weapon System – Navigation. General Electric Company Report R56-A0161, dated 31 October 1956.

26. Brass Bell Reconnaissance Aircraft Weapon System – Flight Control. Bell Aircraft Corporation Report No. D143-945-035, dated 29 October 1956.

27. Brass Bell Reconnaissance Aircraft Weapon System — Flight Control. Bell Aircraft Corporation Report No. D143-945-051, dated 31 August 1957.

28. Brass Bell Reconnaissance Aircraft Weapon System — Ferret. Airborne Instruments Laboratory Report AIL 3887-1, dated 31 October 1956.

29. Brass Bell Reconnaissance Aircraft Weapon System — Photographic System. Bell Aircraft Corporation Report No. D143-945-053, dated 31 August 1957.

30. Brass Bell Reconnaissance Aircraft Weapon System — System Design. Bell Aircraft Corporation Report No. D143-945-038, dated 29 October 1956.

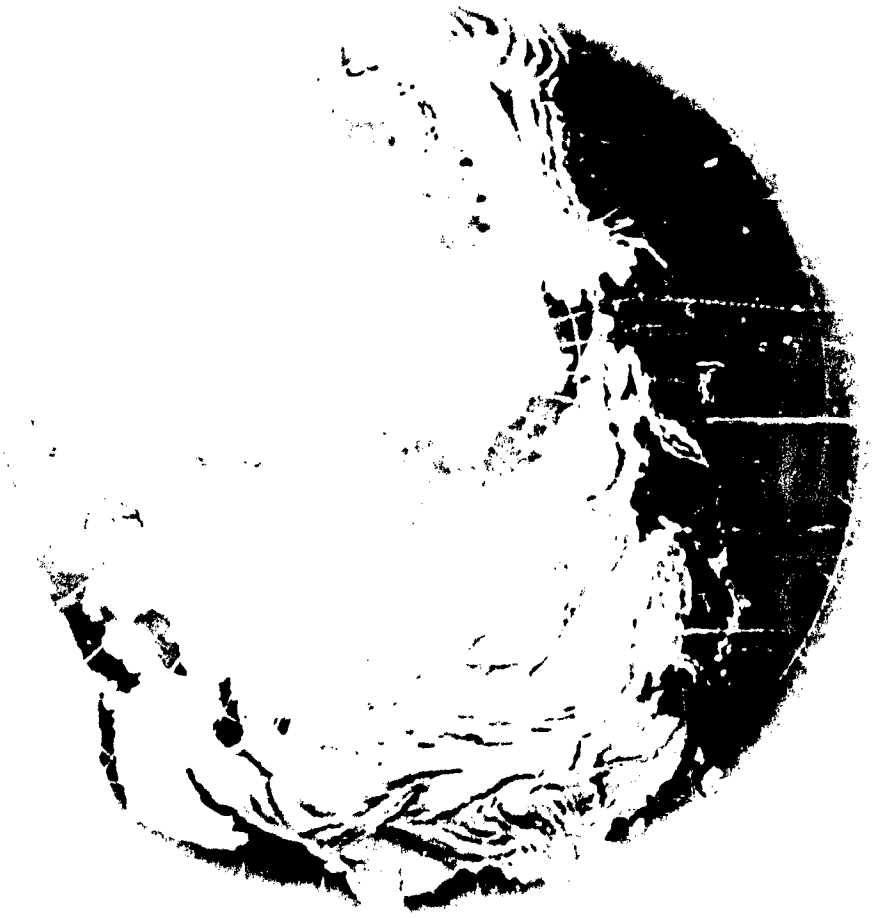

Appendix

The following reports, published by the Bell Aircraft Corporation, contain the results of previous investigations of rocket-boosted hypersonic weapon systems performed under USAF as well as corporate sponsorship.

Report No.		Title	Date	
S-13077	BOMI	Long-Range Strategic Weapon System (Brochure)		
D143-945-010	BOMI	Strategic Weapon System — Preliminary Design		
D143-945-011	MX-2276	Advanced Strategic Weapon System — Interim Technical Report	15 July	1953
D143-945-012	MX-2276	Advanced Strategic Weapon System — Aerodynamics	29 April	1955
D143-945-013	MX-2276	Advanced Strategic Weapon System — Structures	29 April	1955
D143-945-014	MX-2276	Advanced Strategic Weapon System — Preliminary Global System Study	29 April	1955
D143-945-015	MX-2276	Advanced Strategic Weapon System — Radar	29 April	1955
D143-945-016	MX-2276	Advanced Strategic Weapon System — Navigation and Control	29 April	1955
D143-945-017	MX-2276	Advanced Strategic Weapon System — Propulsion	29 April	1955
D143-945-018	MX-2276	Advanced Strategic Weapon System — Final Summary Report	29 April	1955
D143-945-019	MX-2276	Advanced Strategic Weapon System — Program Plan	31 March	1955
D143-945-020	MX-2276	Configuration Study — Design Analysis	25 May	1955
D143-945-021	MX-2276	Configuration Study — Structural Analysis	25 May	1955
D143-945-022	MX-2276	Configuration Study — Aerodynamic Analysis	25 May	1955
D143-945-023	MX-2276	Advanced Strategic Weapon System	August	1955
D143-945-024	MX-2276	Reconnaissance Aircraft Weapon System — Aerodynamics	1 December	1955

BELL Aircraft CORPORATION

Report No.		Title	Date
D143-945-025	MX-2276	Reconnaissance Aircraft Weapon System — Structures	1 December 1955
D143-945-026	MX-2276	Reconnaissance Aircraft Weapon System — Navigation and Control	1 December 1955
D143-945-027	MX-2276	Reconnaissance Aircraft Weapon System — System Design	1 December 1955
D143-945-028	MX-2276	Reconnaissance Aircraft Weapon System — Photographic Subsystem	1 December 1955
D143-945-029	MX-2276	Reconnaissance Aircraft Weapon System — Summary Report	1 December 1955
D143-945-030	MX-2276	Advanced Strategic Weapon System Supplementary Report	1 December 1955
D143-945-031		Proposed Ames Supersonic Tunnel Tests of Double-Wall Construction	29 October 1956
D143-945-032	Brass Bell	Reconnaissance Aircraft Weapon System — Proposed Plan	2 July 1956
D143-945-033	Brass Bell	Reconnaissance Aircraft Weapon System — Aerodynamics Design Vol. I and II	29 October 1956
D143-945-034	Brass Bell	Reconnaissance Aircraft Weapon System — Aerodynamics Research	29 October 1956
D143-945-035	Brass Bell	Reconnaissance Aircraft Weapon System — Flight Control	29 October 1956
D143-945-036	Brass Bell	Reconnaissance Aircraft Weapon System — Radar	29 October 1956
D143-945-037	Brass Bell	Reconnaissance Aircraft Weapon System — Structures	29 October 1956
D143-945-038	Brass Bell	Reconnaissance Aircraft Weapon System — System Design	29 October 1956
D143-945-039	Brass Bell	Reconnaissance Aircraft Weapon System — Summary Report	29 October 1956

Report No.		Title	Date
D143-945-041	Brass Bell	Reconnaissance Aircraft Weapon System — Electrical System	29 October 1956
D143-945-043	Brass Bell	Reconnaissance Aircraft Weapon System — Program Plan	1 March 1957
D143-945-047	Brass Bell	Reconnaissance Aircraft Weapon System — Program	1 August 1957
D143-945-048	Brass Bell	Reconnaissance Aircraft Weapon System — Briefing (Brochure)	1 July 1957
D143-941-001	Brass Bell	Criteria and Loads	29 October 1956
D143-941-002	Design Study	Liquid Metal Cooling Systems for "Hot Spots"	29 October 1956
D143-941-003	Design Study	Secondary Structure	29 October 1956
D143-941-004	Design Study	Outer-Wall Panels and Insulants for Primary Structure	29 October 1956
D143-941-005	Design Study	Auxiliary Power from Aerodynamic Heating	29 October 1956
D143-941-006	Design Study	Water Cooling System for Primary Structure	29 October 1956
D143-941-007	Design Study	Primary Structure	29 October 1956
D143-941-008	Study of Ground Winds, Gusts and Wind Shears		29 October 1956
D143-941-009	Study of Acoustic Loadings		29 October 1956
D143-941-010	Test Results -	Thermal and Wind Tunnel Double-Wall Construction	29 October 1956
D143-941-011	Test Results -	Cooling System for Primary Structure	29 October 1956
D143-941-012	Test Results -	Internal Airflow in Double-Wall Construction	29 October 1956
D143-941-013	Test Program Plans - Structures		29 October 1956
D143-941-014	Test Results and Test Program Plans - Materials		29 October 1956
D143-941-015	Test Results and Test Program Plans -	Liquid Metal Cooling System Prepared by the Callery Chemical Company, Callery, Pennsylvania	31 October 1956
D143-941-016	Load and Stress Analysis of Ames Wind Tunnel Model		29 March 1957

Report No.	Title	Date
D143-941-017	Test Results - Liquid Metal Coolant Prepared by the MSA Research Corporation Callery, Pennsylvania	21 March 1957
D143-984-001	Work Statement - Information for Materials Program Covering Coatings, Insulants and High Temperature Resistant Materials	29 October 1956
D143-978-001	Preliminary Study of the Flow over a Blunt Flat Plate at Various Angles of Attack at M = 13.3. Part 1: Studies of Flat and Hemicylindrical Leading Edges — Prepared by Princeton University	15 May 1956
D143-978-002	An Exploratory Study of a Delta Wing at Hypersonic Speeds — Prepared by Princeton University	10 June 1956
D143-978-003	A Preliminary Study of the Effect of Sweep Back Angle of Shock Shape of Hypersonic Speeds — Prepared by Princeton University	29 June 1956
D143-978-004	A Study of a Blunt Flat Plate Trailing Edge Flap Interaction at Hypersonic Speeds — Prepared by Princeton University	9 July 1956
D143-978-005	Preliminary Study of the Flow over a Blunt Flat Plate at Various Angles of Attack — Prepared by Princeton University	1 October 1956
D143-978-006	An Exploratory Study of a Delta Wing at Hypersonic Speeds — Prepared by Princeton University	1 December 1956
D143-978-007	An Exploratory Investigation of Wing Body Interference at Hypersonic Speeds - Prepared by Princeton University	February 1957
D143-978-008	Induced Pressures on Flat Plates in Hypersonic Low Density Flow — Prepared by University of California	25 January 1957
GE Report R56AO161	Brass Bell — Reconnaissance Aircraft Weapon System — Navigation	31 October 1956
CAI Report 1725	Brass Bell — Reconnaissance Aircraft Weapon System — Photographic Analysis	31 October 1956
AIL Report 3887-1	Brass Bell — Reconnaissance Aircraft Weapon System — Ferret	31 October 1956
PRA Report 56-16	Brass Bell — Reconnaissance Aircraft Weapon System — Human Factors	31 October 1956

The following reports published by Bell Aircraft Corporation on the designated subcontractors contain the results of the present study.

D143-945-049	Brass Bell	Reconnaissance Aircraft Weapon System — Aerodynamic Research	31 August	1957
D143-945-050	Brass Bell	Reconnaissance Aircraft Weapon System — Structures	31 August	1957
D143-945-051	Brass Bell	Reconnaissance Aircraft Weapon System — Flight Control	31 August	1957
D143-945-052	Brass Bell	Reconnaissance Aircraft Weapon System — Radar	31 August	1957
D143-945-053	Brass Bell	Reconnaissance Aircraft Weapon System — Photographic System	31 August	1957
D143-945-054	Brass Bell	Reconnaissance Aircraft Weapon System — Weapon System	31 August	1957
D143-945-055	Brass Bell	Reconnaissance Aircraft Weapon System — Summary Report	31 August	1957
D143-978-009	An Exploratory Study of a Delta Wing at Hypersonic Speeds, Part III: Pressure Distribution Studies on a 30° Included Angle Delta Wing at Angles of Attack. Princeton University Report		31 August	1957
D143-978-010	Pressure Distributions on Blunt Nosed Cones in Hypersonic Low Density Flow — University of California Report		31 August	1957
D143-978-011	The Effect of Sweepback Angle on the Pressure Distribution of a Blunt Flat Plate at Hypersonic Speeds, Part II: Studies of a Hemicylindrical Leading Edge Flat Plate at Angle of Attack = 45° and M = 13.3 — Princeton University Report		31 August	1957
D143-941-018	Brass Bell	Reconnaissance Aircraft Weapon System — Test Results - Strength, Thermal, Vibration and Noise — Double Wall Construction	31 August	1957
D143-941-019	Brass Bell	Reconnaissance Aircraft Weapon System — Cooling System of Double-Wall Construction	31 August	1957
D143-941-020	Brass Bell	Reconnaissance Aircraft Weapon System — Internal Air Flow in Double-Wall Construction	31 August	1957

Report No.		Title	Date	
D143-941-022	Brass Bell	Reconnaissance Aircraft Weapon System — Outer Wall Materials	31 August	1957
D143-941-023	Brass Bell	Reconnaissance Aircraft Weapon System — Thermal Insulants and Cooling Tube Bonding Materials	31 August	1957
D143-941-024	Brass Bell	Reconnaissance Aircraft Weapon System — Test Results Refractory Materials for Hot Spot Areas	31 August	1957
D143-941-025	Brass Bell	Reconnaissance Aircraft Weapon System — Design Studies and Test Results Leading Edge Cooling System Prepared by MSA Research Corp. for Bell Aircraft Corporation	31 August	1957
D143-941-027	Test Equipment Investigation — Induction Heating for Leading Edge Testing — Prepared for Bell Aircraft Corporation by R. W. Sampson, Consultant		31 August	1957
R57-APS 83	Brass Bell	Reconnaissance Weapon System Navigation, Part II General Electric Company Report	31 August	1957
2606-3-T	A Study of the Hypersonic Laminar Boundary Layer with Dissociation, Part I — University of Michigan Report		31 August	1957